Studying Thermomorphogenesis using the bio-active small molecule Heatin

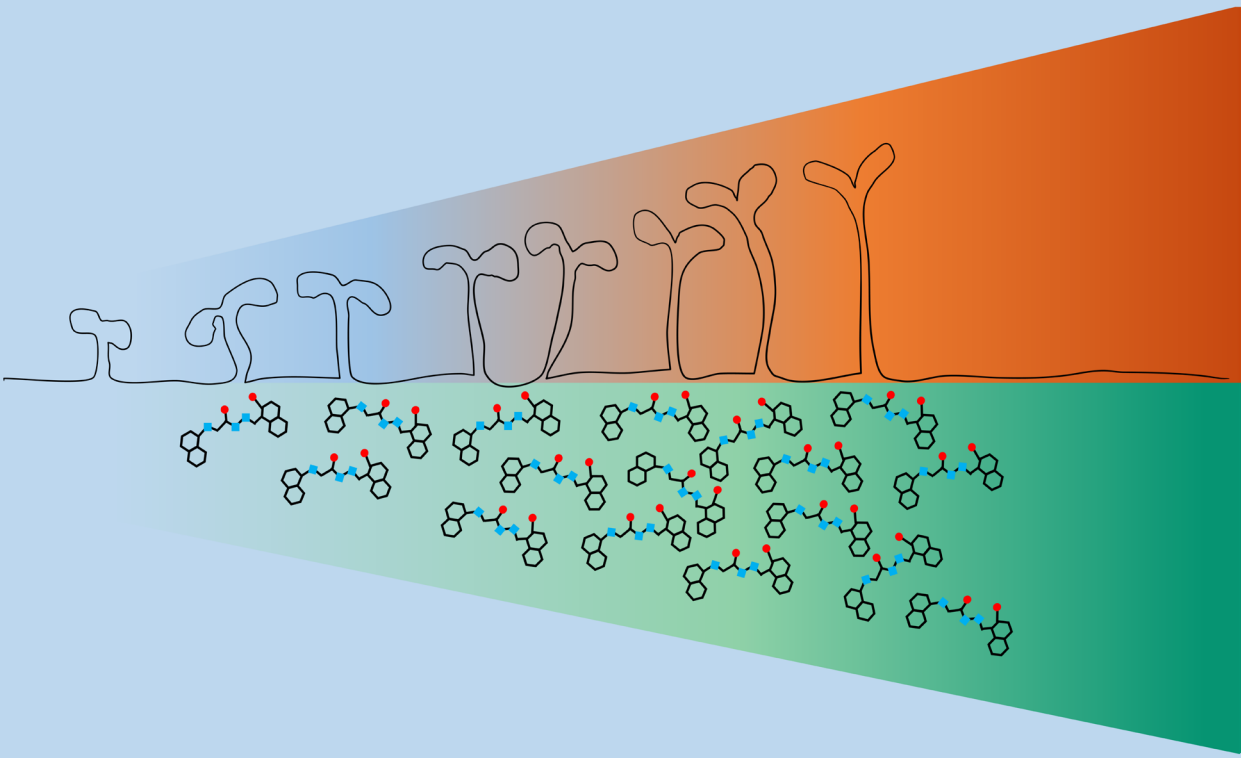

Lennard van der Woude

Studying thermomorphogenesis using the bio-active small molecule Heatin

Lennard Casper van der Woude

ISBN 978-94-6380-216-1

Layout: ProefschriftMaken, www.proefschriftmaken.nl
Printed by: ProefschriftMaken, www.proefschriftmaken.nl

Studying thermomorphogenesis using the bio-active small molecule Heatin

Studie van thermomorfogenese middels het bioactieve kleine molecuul Heatin
(met een samenvatting in het Nederlands)

Proefschrift

ter verkrijging van de graad van doctor aan de Universiteit Utrecht op gezag van de rector magnificus, prof.dr. H.R.B.M. Kummeling, ingevolge het besluit van het college voor promoties in het openbaar te verdedigen op maandag 25 maart 2019 des ochtends te 10.30 uur

door

Lennard Casper van der Woude
geboren op 19 december 1988 te Rotterdam

Promotor: Prof. dr. J.C.M. Smeekens
Copromotor: Dr. M. van Zanten

Dit proefschrift werd (mede) mogelijk gemaakt met financiële steun van:

De Nederlandse Organisatie voor Wetenschappelijk Onderzoek (NWO) en BEJO Zaden B.V.: *Graduateschool Uitgangsmaterialen* grant NWO#831.13.002

De Nederlandse organisatie voor gezondheidsonderzoek en zorginnovatie (ZonMw): Enabling Technology Hotel grants #435002019 en #435003004

Table of Contents

CHAPTER 1

General Introduction

Lennard van der Woude[1] | Sjef Smeekens[1] | Martijn van Zanten[1]

[1] Molecular Plant Physiology, Institute of Environmental Biology, Utrecht University, the Netherlands

Climate adapted crop varieties can be developed through breeding

The Earth's climate is currently undergoing rapid changes, mostly due to an increase in atmospheric concentrations of heat-trapping gasses (greenhouse gasses), such as carbon dioxide. Atmospheric carbon dioxide levels have been on the rise since the industrial revolution, and average global temperatures are increasing since the middle of the last century[1,2]. Projections of future climate change, based on an estimated doubling of greenhouse gas concentrations, foresee a further increase in global average temperature on the short-term in the range of 1 to 2.5 degrees Celsius and a long-term equilibrium between 1.5 and 4.5 degrees Celsius increase[3,4].

Effects of climate change on plant life are already evident. For example, shifts in the timing of flowering have been observed for plants in their natural habitat[5,6]. Additionally, shifts in the geographical distributions of species have been observed towards colder higher altitudes or more northward, where temperatures approximate the pre-climate change environment[7,8].

As in nature, climate change also affects crop plants in agricultural settings. Next to flowering time, changes in *e.g.* plant morphology, viability and seed set are observed[9–12]. Climate change therefore poses challenges for future food security. Most worrisome, models of global production of staple crops predict a major decrease in crop yields in from 2030 onward[10,13–15], which is incompatible with the need to feed a growing world population. In addition, crop quality and therefore market value is affected by climate change[15–18].

Breeding of novel thermo-tolerant crop varieties that grow and produce optimally in a warmer climate potentially ameliorate negative effects of climate change on crop production[16,19–21]. Such climate-adapted next-generation crop varieties can be developed via traditional breeding approaches for varieties with optimal performance in warm temperature conditions. Next generation knowledge-based breeding techniques can be implemented to speed-up the introduction of adapted varieties[22,23]. However, the genetic – and thereby phenotypic – window in thermotolerance traits is surprisingly limited in the germplasm of several crops[24]. Already small perturbations in the genetics underlying development result in a sub optimally operating developmental system. Moreover, breeding efforts focussed on generating high-yielding compact plant varieties with synchronized phenology, which could have resulted in an unintended breeding against responsiveness to environmental cues, and therefore erosion of genetic variation that can be tapped in the breeding process. A better understanding of the precise traits that are affected by high temperature, and the underlying orchestrating molecular networks is urgently needed to allow for efficient and knowledge-based breeding of thermotolerant crop varieties that maintain productivity under the regime of projected global climate warming[25].

Plant thermomorphogenesis

Plants can respond to changes as small a one or two degrees Celsius[26–28] over the range of naturally occurring temperatures[29]. Extreme high or low (stress) temperatures typically induce survival mechanisms, *e.g.* cellular protection mechanisms to avoid lethal damage. These tolerance mechanisms often result in growth cessation and are not further discussed here. However, within the ambient temperature range, in between the cold and heat stress ranges, plants continuously acclimate with the aim of maintaining optimal growth under suboptimal conditions[28]. This involves many physiological processes, such as photosynthesis[30], membrane fluidity[31], immunity[32,33] and the circadian clock[28,34,35]. However, for the model plant *Arabidopsis thaliana*, one of the most visible adaptations to changes in ambient temperature is the striking change in plant architecture (**Fig. 1.1**). For Arabidopsis, the ambient range is more or less defined as being between ~10 and ~30 degrees, where no survival stress markers are observed. The set of architectural adaptations in the high ambient temperature ranges is collectively called thermomorphogenesis, and consists of among others hypocotyl elongation in seedlings[36], petiole (leaf stalk) elongation in leaves[37] and hyponastic (upward) leaf movement[38] (**Fig. 1.1**). In the past decade, thermomorphogenesis has quickly became a topic of interest and is now intensively studied by many labs[37,39–43], yet still poorly understood.

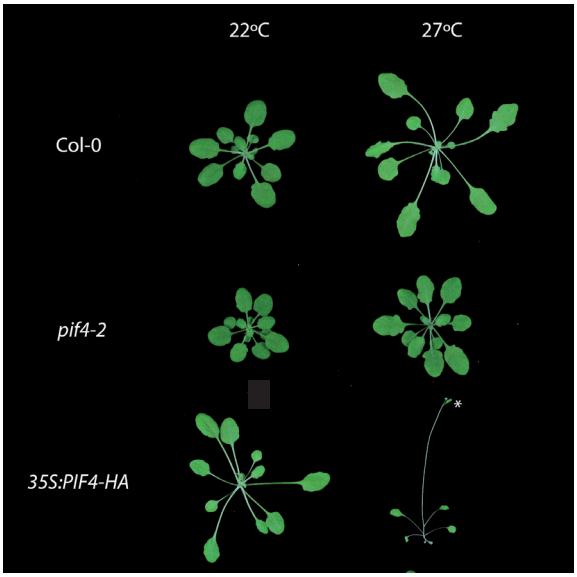

Figure 1.1: Thermomorphogenesis phenotypes in Arabidopsis.

Photos of representative adult rosettes plants grown at 22°C or 27°C. Col-0 WT displays the characteristic open rosette structure, whereas the pif4-2 knock out mutant does not respond to the increased temperature. Overexpression of PIF4 by the 35S promoter results in constitutive thermomorphogenesis, and hypersensitivity to temperature. The asterix indicates a flower bud.

Physiological relevance of thermomorphogenesis

Thermomorphogenesis results in an open rosette structure (**Fig. 1.1**). It has been proposed that this stimulates the plant's evaporative cooling capacity[36,44] and reduces the influx of heat by decreasing the surface (smaller leaves), separation of organs (elongation growth) and reducing the light interception angle (hyponasty)[38]. Thus, thermomorphogenesis is considered a cooling-down strategy. Indeed, plants with the open structure typical for thermomorphogenesis appear cooler than plants with a compact rosette, when growing at the same temperature[44] (**Fig. 1.2**). Modelling of the effects of thermomorphogenesis on plants evaporative cooling capacity under different temperatures confirmed that these adaptations lead to cooler plants under warm conditions and are additive, *i.e.* cooling by hyponasty is only efficient when also the petioles elongate[45]. This is due mainly to the separation of different leaves and the subsequent reduction of the formation of thick stagnant air (boundary) layer with high humidity around the leaves, thereby stimulating efficient evaporation of water via stomata. Therefore, these simulations and experiments assume well-watered conditions as responses to high temperature under water limiting conditions are partly distinct[46].

In the context of thermomorphogenesis, it is worth mentioning that shading by neighbouring plants triggers similar elongation and hyponastic responses in Arabidopsis and other species, in a process called the shade avoidance response. Thermomorphogenesis and shade avoidance can act synergistic, but can also contradict each other. For example, when temperatures are low in winter, plants do not elongate even if they are shaded by neighbouring plants. This prevents photodamage of the plants when the photon influx cannot be efficiently processed by the photosynthesis machinery due to the low temperature[47].

Temperature sensing

In addition to a phenotypic resemblance, the molecular signalling mechanisms controlling thermomorphogenesis overlap with those mediating the shade avoidance responses. Most strikingly, recently the red/far-red light receptor protein Phytochrome B (PhyB) has also been assigned a temperature sensory function[42,43] (**Fig. 1.3A**). PhyB forms active, nuclear localized, homo-dimers in response to red light that supress elongation growth by inhibiting activation of genes driving this response. PhyB reverts to inactive homo-dimers in the cytosol under far-red light (canopy shade). In addition to this response to red/far-red, PhyB is inactivated in a temperature-dependent manner in darkness (dark reversion)[48]. In cool temperatures, the reversion is slow. Therefore, active nuclear localized PhyB retains suppression of elongation growth long into the night. When temperatures rise, the speed of PhyB deactivation is increased, relieving its indirect suppression of elongation growth genes and elongation growth is triggered. Additionally, mutant analyses show that other Phytochrome family members also contribute to the suppression of elongation growth under low temperatures[49]. Nevertheless, the high temperature transcriptome of wild type plants overlaps only partly with quintuple *phy* mutant plants, suggesting that other molecular temperature sensory events and signalling pathways exist in plants[49].

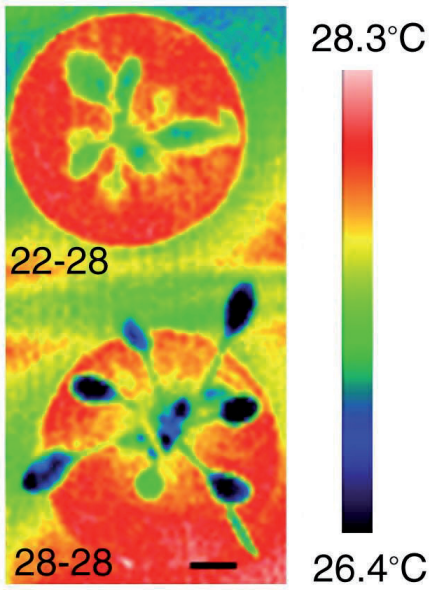

Figure 1.2: Thermal images of Arabidopsis rosettes growing at 28°C, with different pre-growth conditions.

The top panel shows a plant pre-grown at 22°C, thus not showing thermomorphogenesis. The bottom panel shows a plant pre-grown at 28°C that shows thermomorphogenesis. Bar represent 1 centimeter. Adapted from Crawford *et al.*, 2012, with permission under licence #4418780222341 between Elsevier and Utrecht University.

On the molecular level, active PhyB dimers inhibits positive regulators of elongation growth. Specifically, the proteasomal degradation of PHYTOCHROME INTERACTING FACTOR (PIF) transcription factors is stimulated by active PhyB[50] (**Fig. 1.3A**). Additionally, PhyB might interact with PIFs to inhibit their transcriptional activator activity non-destructively, or bind competitively to G-box promoter elements[51]. Among the PIF transcription factor family, PIF4 has been shown to be an essential hub for thermomorphogenesis[37], integrating other environmental signals as well[52–55]. Accordingly, loss of function of PIF4 results in a lack of temperature response of architecture[37] and defence modulation[32]. *PIF4* gene expression and PIF4 protein stability are enhanced by high temperatures. As a result, PIF4 is able to bind promoters of auxin biosynthesis genes and stimulate their expression, which is required for the induction of thermomorphogenesis[39,56] (**Fig. 1.3B**). In accordance with the signalling pathway where PIF4 promotes high temperature signals into increased auxin biosynthesis, overexpression of *PIF4* leads to an exaggerated thermomorphogenesis phenotype already under control conditions (**Fig. 1.1**). Additionally, absence of high temperature elongation growth in the *pif4-2* mutant background can be rescued by applying the synthetic auxin Picloram[56].

Temperature-dependent auxin biosynthesis

Biosynthesis of the endogenous auxin indole-3-acetic acid (IAA) occurs via a metabolic pathway that converts chorismate in several enzymatic steps into L-tryptophan (TRP)[57]. Subsequently, TRP is metabolized via three semi-parallel pathways containing several different intermediates into IAA[59] (**Fig. 1.3B**). High temperature-induced PIF4 stimulates IAA biosynthesis by direct binding to, and stimulation of expression of the auxin biosynthesis genes *YUCCA8* (*YUC8*)[39] and *TRYPTOPHAN AMINOTRANSFERASE OF ARABIDOPSIS1 (TAA1)*[56]. *YUC8* and *TAA1* function in the dominant of the three alternative auxin biosynthesis pathways, where TRP is converted into indole-3-pyruvic acid (IPyA) by TAA1, and subsequently into bioactive IAA by YUC8[59]. Indeed, exaggerated elongation growth of *PIF4* overexpressor lines could be partially suppressed by a *yuc8* knockout mutation[39].

Additionally, PIF4 directly binds and induces the expression of the cytochrome P450 family member *CYP79B2*[56]. *CYP79B2* functions in a *Brassicaceae*-specific parallel pathway where it converts TRP into indole-3-acetaldoxime (IAOx)[60]. IAOx is subsequently converted into indole-3-acetonitrile (IAN) by CYP71A1 and then hydrolyzed by Nitrilase proteins into bioactive IAA[61]. This alternative IAA biosynthesis pathway involving IAN and Nitrilases has also been implicated in metabolism of defense-related compounds[62,63]. Recently it has been proposed that the IAN-dependent auxin biosynthesis pathway functions specifically in balancing growth and defense responses[63]. A third IAA biosynthesis pathway has been described that involves the intermediate indole-3-acetamide, however this pathway has as of yet not been implicated in temperature responsive growth[64].

Temperature-dependent auxin signalling

On the structural level, auxin (IAA) acts as a 'molecular glue' between its receptor protein complex, the ubiquitin ligase SKP1/CULLIN/F-BOX (SCF)$^{TIR1/AFB}$ complex, and AUXIN/INDOLE-3-ACETIC ACID (AUX/IAA) proteins[65,66] (**Fig. 1.3B**). In the receptor complex, the F-Box protein subunit functions as receptor in binding auxin and the AUX/IAA proteins[65]. In Arabidopsis, six F-Box auxin receptor proteins are known; TIR1 and AFB1 to AFB5. The interaction between the SCF complex, auxin and AUX/IAA proteins leads to polyubiquitination of the AUX/IAA proteins, causing their proteasomal degradation[67]. In addition to stimulating the biosynthesis of IAA, high temperature also stimulates auxin sensitivity via HEAT SHOCK PROTEIN 90 (HSP90) mediated stabilisation of TIR1, thereby further stimulating AUX/IAA protein degradation [40] (**Fig. 1.3B**).

AUX/IAA proteins form a family of 29 members in Arabidopsis that supress the transcriptional activating activity of AUXIN RESPONSE FACTOR (ARF) transcription factors. ARFs themselves form a family of 23 members in Arabidopsis[68]. AUX/IAA degradation releases their inhibition on the ARFs[69], resulting in transcription of downstream ARF-targeted genes. One major challenge facing the unravelling of any auxin driven process is to identify the specific TIR1/AFB, AUX/IAA and ARF proteins that contribute

to the response under investigation, as there exists substantial redundancy between the functions of the different proteins[66,70,71]. Specifically, which TIR1/AFB contributes to degradation of which AUX/IAAs to relieve particular ARFs under high temperature conditions is not well understood. Although *ARF6* has been implicated in general *PIF4*-dependent hypocotyl elongation[72], *arf6* mutants remain responsive to high temperature-induced elongation growth (our unpublished observation). Additionally, In response to temperature induced auxin stimulation , the transcription of *AUX/IAA 19* and *29* is enhanced at warm temperatures in a PIF dependent manner[52,73]. This acts as a feedback mechanism, ensuring the transcriptional response – and downstream responses - are tempered. Additional control in the thermomorphogenesis signalling network comes via a positive feedback loop between brassinosteroid signalling downstream of auxin, and *PIF4*. These control mechanisms likely allow for tight control of the elongation response to warm temperatures[74] balancing optimal acclimation against exaggerated elongation that could be detrimental.

Following auxin perception and ARF degradation, members of the *SMALL AUXIN UP RNA* (*SAUR*) are induced[75]. Especially the *SAUR19-24* family has been shown to function in thermomorphogenesis signalling[56] (**Fig. 1.3C**). For a long time the function of SAURs remained elusive, but recently the mechanism of action has been elucidated[76]. It was shown for SAUR19, as well as other family members, that they supress the activity of a PP2C-D phosphatase via a direct interaction. The inhibition of this phosphatase leads to increased phosphorylation of H^+-ATPases, allowing the binding of 14-3-3 protein and subsequent activation of the H^+ pump action[76]. Together, this results in a reduced pH in the apoplast and cell wall (**Fig. 1.3C**). Such a reduced apoplastic pH leads to cell elongation in a process referred to as the 'acid growth mechanism'[77]. Indeed, acidification of the apoplast is observed upon auxin application[78]. Cell wall modifying enzymes such as EXPANSINs present in the cell wall are activated by the reduced pH and modify the cell wall composition[79]. This leads to reduced rigidity of the cell wall. As the cell wall is continuously experiencing internal pressure exercised by turgor, the weakening of its rigidity results in an increased expansion of the cell. This effect on the cell level is coordinated across the elongating organ and leads to the characteristic elongation response at warm temperature conditions[78].

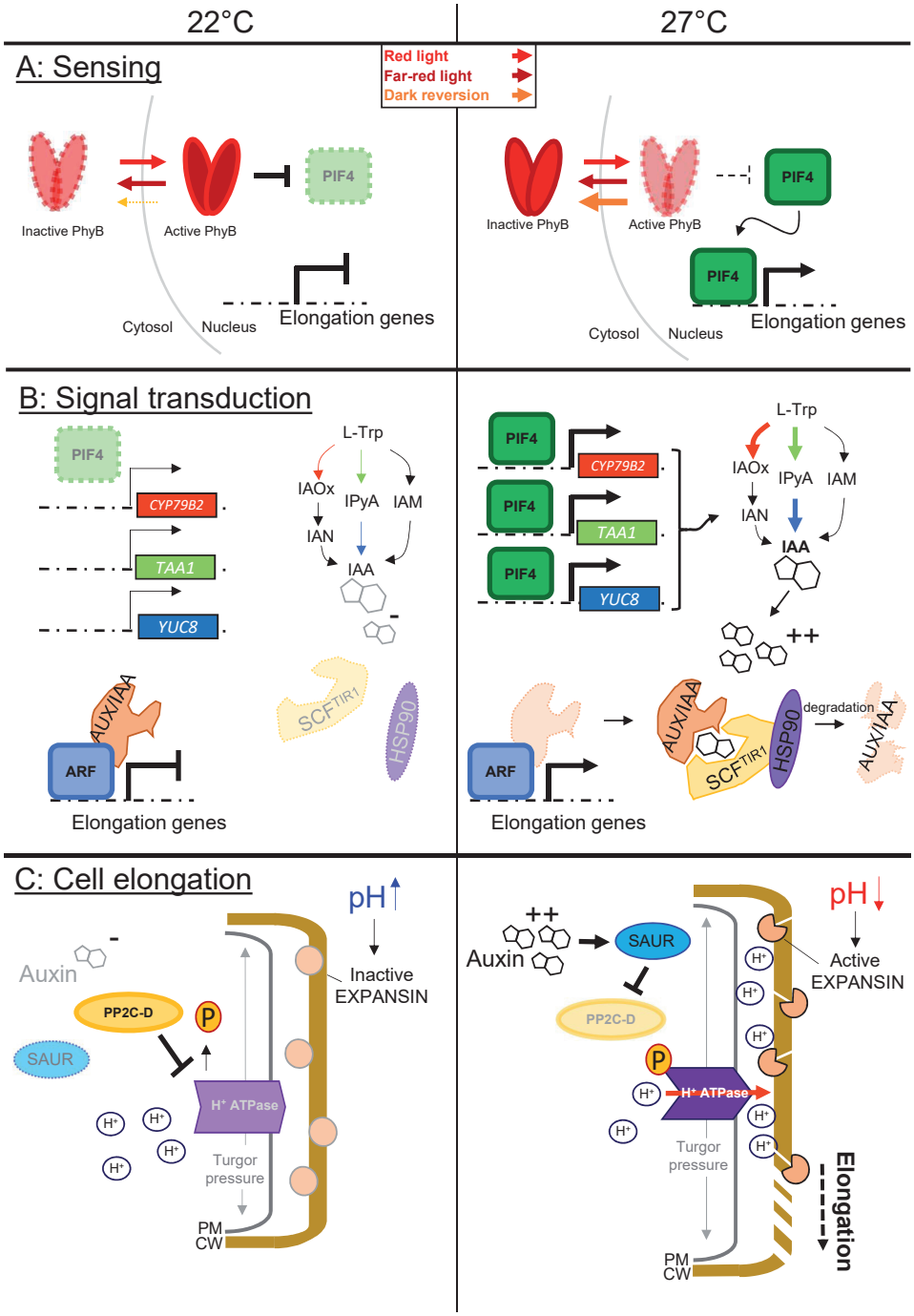

Figure 1.3: Schematic overview of temperature signaling and thermomorphogenesis regulation events relevant for this thesis.

(**A**) Red light-activated Phytochrome B (PhyB) is translocated to the nucleus, where it suppresses PIF4 activity (green block), thereby limiting elongation growth. Conversely, illumination by Far-red

light results in PhyB eviction from the nucleus, relieving PIF4 activity. At warm temperatures (27°C), the dark reversion of nuclear localized PIF4 is strongly enhanced, resulting in rapid PhyB eviction, relieve of PIF4 suppression and hence temperature-induced elongation growth. (**B**) Active PIF4 stimulates the expression of auxin biosynthesis genes (red, green and blue box, corresponding to steps in IAA biosynthesis indicated by the same color arrow), resulting in increased levels of the bioactive auxin IAA. Auxin acts as a molecular glue, facilitating the interaction between the SCF^{TIR1} protein complex (yellow shape) and repressive AUX/IAA proteins (orange shape), which leads to the degradation of the latter. This degradation relieves the suppression of ARFs transcription factors (blue block), allowing the activation of downstream signaling genes leading to elongation growth. Additionally, high temperature increases HSP90 (purple oval) levels, which stabilizes the TIR1 protein and increases auxin sensitivity. (**C**) At control temperature with low auxin levels, SAUR protein (blue oval) levels are low, resulting in active PP2C-D protein (yellow oval) de-phosphorylating (orange circle) and inactivating H^+-ATPases (purple arrow). The apoplastic pH remains relatively high, resulting in inactive EXPANSIN cell wall modifying enzymes (pink circles). When temperatures rise, auxin and SAUR protein levels increase, which results in inhibition of PP2C-D de-phosphorylation of H^+-ATPases. This results in active H^+-ATPases pumping protons out of the cell, to the apoplast. Consequently, the apoplastic pH drops, activating EXPANSINs, which results in weakening of the cell wall. Turgor pressure subsequently drives cell elongation, observed during thermomorphogenesis. In all panels; Light colored objects indicate inactivation and dashed lines indicate degradation. Differences in line thickness corresponds to the relative strength of response/effect.

Chemical genetics

Principles and successes of chemical genetics

In chemical genetics, small molecules are used to disrupt a biological system to study it in mechanistic (molecular and genetic) detail. Reverse chemical genetic studies aim to identify chemicals disturbing the function a known protein of interest and can for instance be of use when looking for novel a(nta)gonist to certain receptors, or identify novel tools to study a single protein.

Reverse chemical genetics has not been widely applied in plant science[80]. This contrasts with forward chemical genetics studies, that aim to identify chemicals causing desired effects or phenotypes, without knowing the molecular targets beforehand[80]. Forward chemical genetic approaches are conceptually similar to classical forward genetics approaches (mutant screenings) that uses mutations to disrupt a biological system, followed by identification and studying the mutations in detail[81] (**Fig. 1.4**).

In forward chemical genetic approaches, often a chemical library is initially screened for novel molecules that cause the desired effect or phenotype. Subsequently, by studying how the identified molecules exert their effects, more insight into the molecular regulation of the phenotype can be obtained.

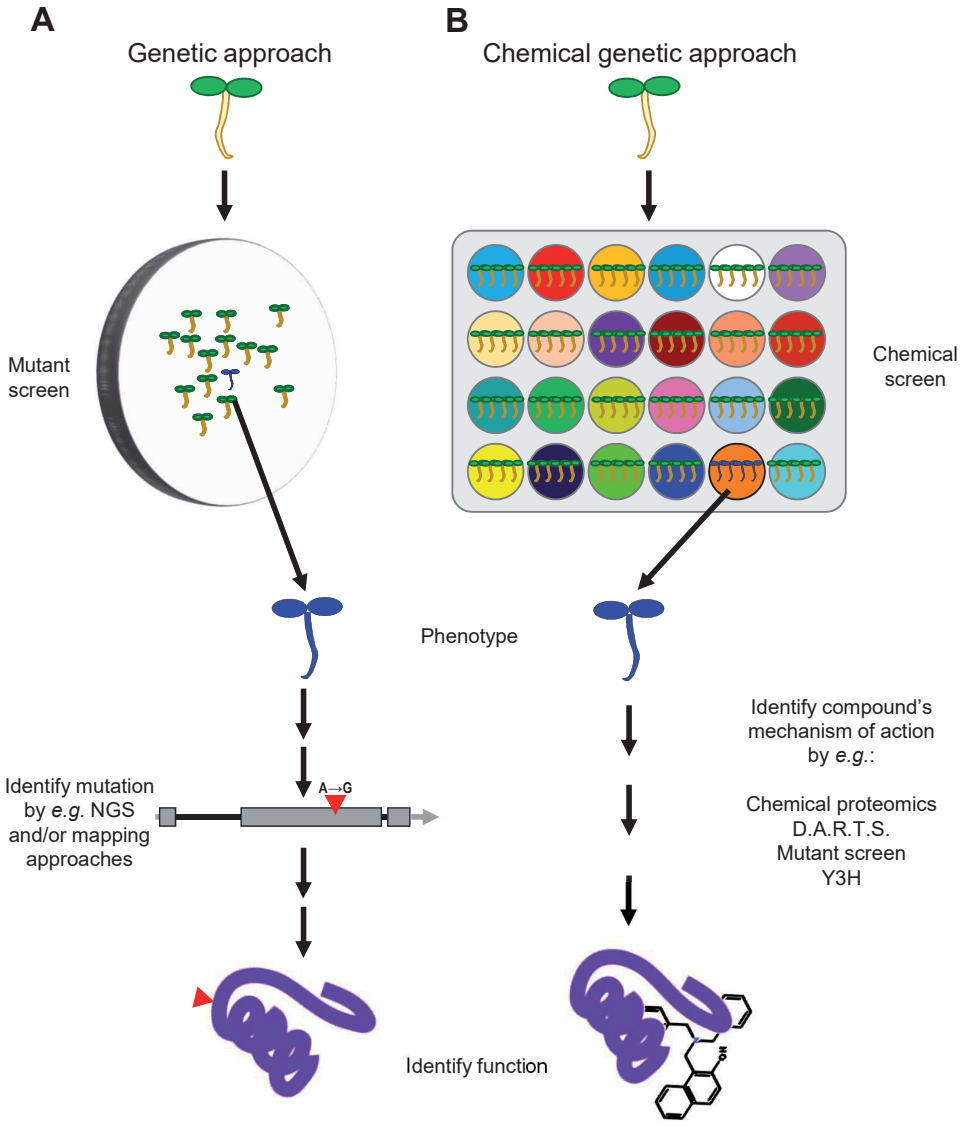

Figure 1.4: Comparison between classical genetic and chemical genetic approaches to identify genes involved in a biological process.

(**A**) Genetic approaches usually involve screening of a large population of mutagenized plants for a specific desired phenotype. Casual mutations in plants with phenotypes of interest are often identified by next generation sequencing (NGS) of a segregating population, and/or other mapping approaches. (**B**) Chemical genetic approaches involve the screening of chemical libraries for a desired phenotype. The mechanism of action of a compound that induces a phenotype of interest is elucidated by studying how the compound interacts with the plant's molecules *(e.g.* proteins). Often this relies on identification of the targeted proteins by methods such as Drug Affinity Responsive Target Stability (D.A.R.T.S.), Yeast-3-Hybrid (Y3H), chemical proteomics or a mutant screen for resistant plants. The identified targeted protein(s) provide insight on the molecular mechanism causative for the phenotype at hand. Adapted from McCourt and Desveaux (New Phytologist, 2009).

A major advantage of chemical genetics is that pharmacological application of identified compounds or their derivates can be directly applied to steer plant responsiveness or development. Perhaps not surprisingly, chemical genetics therefore has its roots in the pharmaceutical sciences where it is frequently used to identify targets of known drugs or identify novel potential drug molecules (drug discovery)[82]. In plant science, chemical genetics has been mainly applied and optimized to identify agrochemicals such as herbicides[83]. In recent years however, chemical genetics has gained popularity in fundamental studies into molecular signalling networks[84]. This is in part, because a major advantage of chemical genetics over classical genetics approaches is the possibility to overcome genetic redundancy[85]. This is because chemicals are not necessarily limited to affecting a single target protein, but can bind similar domains in different proteins in the same way simultaneously, while classical mutational studies typically investigate the effects of mutating one target at a time. As genetic redundancy is highly prevalent in plants (at least 50% of genes[86–88]), mutation phenotypes are often masked by gene family members taking over (part of) the mutated gene's function. A striking example is the compound Bikinin, which binds and inhibit the function of seven Glycogen synthase kinase 3 proteins at the same time[89]. Bikinin has turned-out to be a very useful tool in brassinosteroid signalling research, since knocking-down seven genes in one plant is a daunting task.

Many other examples of successful chemical biology studies can be found in the phytohormone signalling field[90]. This can be likely explained by the fact that these signalling cascades are sensitive to small molecules (*i.e.* phytohormones) by nature. One of the most striking discoveries following chemical genetics in the phytohormone field relates to the identification of the ABA receptor protein[91]. The small molecule pyrabactin was identified in a screen for germination inhibiting compounds. It was found to copy ABA signalling exclusively in seeds, and not in young seedlings. The pyrabactin receptor was then identified in a forward genetics mutant screen for pyrabactin resistance. In contrast to ABA, pyrabactin only bound one member of the ABA receptor protein family. Of note, in the many conducted classical genetics screenings for resistance against the endogenous phytohormone ABA, this receptor was never identified, due to genetic redundancy between the different ABA receptor protein family members. Chemical genetics screens aimed at other hormones (*e.g.* auxin[92–94] or brassinosteroids[89,95]) have also been successful in further unravelling of their respective biosynthesis and functioning[80,90].

Other major advantages of chemical genetics studies, next to overcoming redundancy, include possible tissue specificity of the compound, the possibility of local application and the possibility to apply compounds in the desired stage of plant development. The latter can be helpful in avoiding the problem of lethality that can occur when targeting genes by classical genetic approaches. Additionally, chemical compounds can be added or removed from a growth medium, allowing for tight control.

A characteristic forward chemical genetic strategy can be divided in different stages[96]. First, a screening assay is developed that allows for efficient and high throughput screening of chemicals. With this assay at hand, a library of chemicals is screened to identify novel molecules of interest. After confirming and validating the effects of the molecules, the mechanism of action of the molecules needs to be identified. This often involves testing for (genetic) interactions with known genes/molecular networks and investigating the relationship between the chemical's structure and the caused phenotype to identify different (non-)functional moieties in the structure; the so-called Structure-Activity Relationship (SAR). An important and challenging next step is then to identify direct (protein) target(s) of the identified molecules, followed by determining the mechanism of action of the compound in the biological system.

Compound identification by chemical genetic approaches

The success of chemical genetics screenings relies on the suitability of the assay to obtain as unambiguous results as possible in terms of hit-compounds[97]. In general, qualitative phenotypes are more suitable than subtler quantitative ones. As chemicals are costly and often only available in small volumes, screening assays are practically limited to small set-ups, often using seeds, pollen or young plants, or cell/tissue cultures[84]. Examples of frequently used assays are hypocotyl[89,92,95,98] or root growth[99,100] in Arabidopsis. To identify molecules that target certain cellular signalling pathways, reporter lines with Luciferase-tagged proteins are useful as they allow for efficient, automated and quantifiable measurements of the compound's effect[101].

The choice of chemical library will logically determine possible hits found and is therefore non-trivial. Ideally, a screen would encompass all possible chemical compounds; the full chemical space. As this is practically impossible, most large libraries aim to cover as wide a chemical space as possible, by using diverse starting building blocks to synthesize thousands of different compounds (combinatorial libraries)[102]. To increase the chance of containing bioactive molecules, most libraries contain compounds that adhere to Lipinski's rule of five[103], which allows for predicting the bioavailability of small molecules. As an alternative strategy to quantity, some chemical libraries focus on quality, *i.e.* solely containing proven bioactive compounds. These libraries are typically smaller, for example the LATCA[104] or Spectrum (http://www.msdiscovery.com/spectrum.html) libraries. Following the initial screening of the chemical library, a rescreening of the identified hits using chemicals from a different source (separate collection, vendor, or synthesized in house) is desirable, as it will identify false positive responses due to contamination or degradation products in the initial library. Altogether, a successful screening will lead to one or a limited number of reliable 'hit compounds' which can be the subject of further studies.

An important step following the compound discovery phase, is gaining understanding of the relationship between the molecular structure of the identified

compound and its bioactivity, by so-called Structure Activity Relation (SAR) studies. Typically, the effect of synthetic analogues of the hit compounds and its derivates/ building blocks will be tested for bioactivity using the same assay as used in the library screening. By doing so, the contribution of different hit compound moieties to bioactivity can be deduced and the minimal active structure can be assigned[105–107]. SAR studies can also lead to the identification of more potent chemicals, which may increase the range of observed phenotypes[108]. Additionally, SAR can identify inactive, so called 'dead' analogues[91], which can be used as accurate controls – and of course – helps in deducting what moiety or combination of moieties is required for the compounds' biological activity. Furthermore, moieties that are not required for bioactivity can be used for compound modification, without disturbing the bioactivity. For instance, such non-required moieties can be replaced by fluorescent probes to visualize the compound *in vivo* localization[109] , or moieties can be added that aid in later target identification stages, such as photo-reactive crosslinkers or mini-tags[110].

Mechanism of action identification; Receptor identification

When a hit compound, or its minimal active structure, is identified, the next step is to investigate how the compound causes its biological effects. For this, identification of the direct target molecule(s) and uncovering of the affected molecular pathways is often essential[111]. A commonly applied method for target pathway identification is to screen a mutagenized population for resistant, or oversensitive, plants followed by identification of the causal mutation(s). As described above, such a mutant screening method has been successfully applied to identify the target of the ABA analogue pyrabactin[91]. Another example is the uncovering of the pathway affected by the auxin analogue Sirtinol, where a mutant screen resulted in the isolation of genes functioning in the biosynthesis of an essential co-enzyme involved in the metabolic conversion of Sirtinol into an active auxin[93,105]. Advantages of such mutation-based strategies include the straightforward practical set-up, the lack of a need for a modified compound and the potential to discover factors in signalling pathways required for the compound's action, that are not necessarily directly affected by the compound. The latter is also a disadvantage as mutagenesis-based target discovery does not provide information about the receptive molecule(s) itself, which requires direct confirmation of receptive abilities of the identified proteins. Another disadvantage is that obtaining resistant mutants can be hampered by genetic redundancy, as mentioned before.

Several methods are available to identify the direct binding target(s) of a hit compound. One strategy is to form a covalent bond between the hit compound and the interacting proteins and subsequently analyse the identity of the tagged proteins. This strategy requires SAR knowledge to be able to modify the compound with a photoreactive covalent linker and a tag for purification of the protein, *e.g.* biotin. A proof of concept of this strategy in plants is provided by the identification of the BRI1 protein

as the BR receptor. A photoreactive linker-functionalized, biotinylated variant of BR was designed based on SAR studies and used to prove that BR interacted directly with BRI1[112]. A variation of this strategy uses mini-tags rather than larger, more disruptive tags such as biotin. Mini-tags are small inert modifications of a compound that can be 'clicked' to an isolatable tag after *in vivo* covalent linking to target proteins. This has the advantage that the chance of compromising the bioactivity and bioavailability of the compound by the tag is reduced. Proof of concept was obtained by demonstrating that this method could be used to covalently bind the small molecule protease inhibitor E-64 to its target proteases. These could be subsequently isolated and identified[110].

The afore-mentioned chemical proteomic methods rely on modification of the initial compound while ensuring bioactivity is retained in the tagged versions of the molecule. As this can be problematic, modification-free methods for target identification have also been developed. An example is Drug Affinity Responsive Target Stability (DARTS), which relies on the ability of a small molecule to stabilise its receptor and protect it against protease degradation[113]. To the best of our knowledge, as of yet no proof of concept studies of the successful application of DARTS in plants have been published.

Thesis Outline

In this thesis, a chemical genetic strategy is described that we employed to uncover molecular mechanisms mediating plant thermomorphogenesis.

Chapter 2 describes the results of a chemical compound library screening for molecules modulating thermomorphogenesis. 8360 compounds were tested on *pif4-2* mutant seedlings to identify molecules that can restore the compromised high temperature-induced hypocotyl elongation phenotype of the mutant under high temperature conditions. Initial candidate 'hit' compounds were rescreened and tested to what extent they displayed phenotypic similarities with Picloram treatment, a synthetic auxin that induces many side effects in addition to rescuing the *pif4-2* phenotype. The resulting selection of non-picloram-like compounds was tested over a range of concentrations, and the compound Heatin is presented as a hit compound that reliably phenocopies thermomorphogenesis by means of hypocotyl elongation in seedlings, already under control conditions in a manner distinct from picloram treatment.

In **Chapter 3**, investigations are presented into the mode of action of Heatin by additional phenotyping, reverse genetics and a detailed SAR study. We show that Heatin effects are restricted to the hypocotyl in seedlings. Additionally, Heatin induces thermomorphogenesis phenotypes in adult plants as well.

SAR analyses identified 1-aminomethyl-2-napthol as the active moiety of Heatin. Additionally, the SAR analyses point towards a similarity between Heatin and Sirtinol. Strikingly however, Sirtinol was identified as a compound inhibiting hypocotyl elongation in darkness. We demonstrate that Sirtinol derivatives induce hypocotyl elongation in the light as well, but at significantly lower concentrations. Moreover, we show that Sirtinol-resistant mutants are also Heatin resistant. Next, auxin receptor mutant seedlings are were found to be resistant to Heatin, yet no activation of the auxin reporter *DR5:LUC* or accumulation of free IAA could be detected. Our results suggest that Heatin-induced phenotypes depend on auxin signaling, but Heatin effects appear distinct from canonical auxin effects.

Using genome wide transcriptomics, proteomics and metabolomics, **Chapter 4** compares general temperature treatment with Heatin treatment. First, Heatin-induced growth dynamics is analyzed by time-lapse camera analyses. From this, an early and late sampling time point were identified for transcriptomic analyses. This experiment revealed that the effects of Heatin on the transcriptome is more specific than that of high temperature treatment. However, relevant overlap between Heatin and high temperature treatment exists, suggesting that Heatin is activating a specific part of the temperature signaling network controlling elongation growth. Genes are proposed that play a possible causal role in the Heatin and temperature signaling network leading to hypocotyl elongation. Strikingly, overlap between Heatin and temperature treatment on the proteome and metabolome levels were less apparent.

Chapter 5 describes a chemical proteomics approach to identify Heatin's molecular targets. Based on the SAR knowledge from chapter 3, a probe was designed and synthesized that was attached to magnetic beads. Using these Heatin-probe-covered beads, a pulldown was done with protein extracts from young Arabidopsis seedlings. Heatin was used to elute targets from the beads, leaving unspecific binding proteins behind. Statistical comparison between elute and on-bead samples reveals several protein families to be overrepresented in the elute fractions. Strikingly, the full NIT1-subfamily of proteins was identified as specific Heatin targets. Using *in vitro* enzymatic activity assays, it is shown that Heatin inhibits Nitrilase functioning. Additionally, *nit* mutant lines were found to be resistant to Heatin application, establishing Nitrilases as Heatin targets. As Nitrilases are implicated in auxin biosynthesis and Heatin-effects depend on auxin signalling, effects on auxin metabolism are assessed by measuring *in vivo* auxin biosynthesis pathway metabolite levels. This revealed a Heatin effect on IAN levels, that is absent in *nit* mutants, as well as a smaller, but still significant effect on IAA. The latter is possibly responsible for the increased hypocotyl elongation growth in response to Heatin treatment.

In **Chapter 6**, intra- and inter species variation in Heatin response is assessed. A Genome-Wide Association analyses using 360 Arabidopsis accessions reveals the existence of extensive natural genetic variation in the responsiveness to Heatin within the Arabidopsis germplasm, which in part is explained by a locus on chromosome 1. At the same locus, SNPs are located that have a strong but not significant association with the hypocotyl elongation response to high temperature and Picloram. Analysis of the effect of Heatin on various crop species indicated that the effects are restricted to *Brassicaceae* species. An in-depth analysis of white cabbage varieties adapted to grow under different climates revealed that strength of the thermomorphogenesis response of seedlings weakly correlates with the environment they were bred for. Surprisingly, no such correlation was found between Heatin responsiveness and the environment they were bred for.

CHAPTER 2

2

Identification of small chemical compounds that affect thermomorphogenesis in *Arabidopsis thaliana*

Lennard van der Woude[1,2] | Sjef Smeekens[1] | Stéphanie Robert[2] | Martijn van Zanten[1]

[1] Molecular Plant Physiology, Institute of Environmental Biology, Utrecht University, the Netherlands
[2] Umeå Plant Science Center, Swedish University of Agricultural Sciences, Sweden

Abstract

Global warming threatens food security in the coming century. Therefore, either thermotolerant varieties of important crop plants need to be bred, or alternative methods to maintain stable crop yields and quality must be developed. For both approaches fundamental knowledge is required on how plants sense temperature and how temperature signals are translated into relevant acclimation responses.

We performed a high-throughput chemical genetics screen to identify small molecule compounds that enhance thermomorphogenesis, *i.e.* temperature responsive growth, in the model plant *Arabidopsis thaliana*. Thermomorphogenesis includes, but is not restricted to, hyponasty (upward leaf movement), petiole elongation and hypocotyl elongation and depends on the transcription factor PHYTOCHROME INTERACTING FACTOR 4 (PIF4).

We used hypocotyl elongation as an efficient bioassay for the temperature acclimation response. 8360 initial compounds were screened for their ability to restore hypocotyl elongation, *i.e.* thermomorphogenesis, in the *pif4-2* mutant background. Based on the results of independent repeat experiments and exclusion of auxin-like compounds, nine compounds were identified that stimulate high temperature-induced hypocotyl elongation distinct from canonical auxin application, in a dose-dependent manner. These compounds can be employed to study the molecular mechanisms underlying thermomorphogenesis *in planta* and could be potentially applied directly on crops in agricultural settings.

Introduction

Imposed by their sessile nature, plants have evolved the ability to adjust their development and architecture to fit their environment[114]. Changes in ambient temperature, as small as 1°C, already have significant effects on plant development throughout the plant s life cycle by controlling the timing of major phase transitions such as germination and flowering[26]. Ambient temperature also has particular strong effects on various aspects of vegetative plant morphology and physiology including architecture, membrane fluidity, and circadian clock[29,41,115].

In the ambient temperature range, roughly between 10°C and 30°C, the model organism for molecular plant research *A. thaliana* compensates continuously for the effects caused by changing temperatures by a suite of adaptation to high ambient temperature together called thermomorphogenesis. Thermomorphogenetic acclimation includes hypocotyl elongation, hyponasty (upward leaf movement) and petiole elongation. The open rosette structure caused by these adaptations is proposed to allow for more efficient evaporative cooling due to improved airflow around the leaves and a reduction of the boundary air layer surrounding the leaves. Also, the plant moves its leaves away from the hot soil, into the cooler air[44,45], which simultaneously reduces influx from direct sunlight. Indeed, leaf temperature of Arabidopsis plants that were adapted to high temperature (28°C) was around 2°C lower than non-adapted (22°C pre-grown) plants, when placed at high temperature conditions[44]. If the high temperature conditions persist, plants secures offspring by initiating an early flowering response[116].

As even small changes in temperature are able to seriously affect plants, the projected rise in average global temperature during the present century is predicted to severely damage crops worldwide resulting in major yield losses[13]. Breeding of crops with enhanced thermotolerance or development of technological solutions that can help plants to better cope with rising temperatures, is therefore urgently needed[20]. This requires fundamental knowledge on how plants sense high temperature and transduce the signals to relevant acclimation responses[19,22]. Recent discoveries have provided insight into how ambient temperature information is integrated into developmental control[41,47].

Chromatin remodeling was shown to play an important role in integration of ambient temperature information[117]. Generally, temperature responsive genes contain the H2A.Z histone-variant close to the transcriptional start site. At the occurrence of high temperature, the H2A.Z occupancy on the nucleosomes is reduced, which allows differential accessibility of gene-specific *cis*-elements (promoters) for transcription factors, RNA Polymerase II and/or repressing protein binding. In this manner, the expression of over 2000 genes is (co-)regulated[117,118].

Recently, the light receptor Phytochrome B (PhyB) was shown to be a night-time thermo-sensor as well[42,43]. PhyB has previously been described as a red/far-red light sensor,

activating elongation growth in response to shade. Temperature was shown to affect PhyB in a similar manner as far red light, accelerating the natural decay of the activated proteins at night. This decay lifts PhyB's inhibition on downstream transcription factors that cause elongation growth[42,43].

Subsequent signaling pathways, downstream of temperature sensing, have also been uncovered[41,74]. The most commonly used system to systematically study thermomorphogenesis is the before-mentioned high ambient temperature-induced hypocotyl elongation in *A. thaliana*. This architectural adaptation to high temperature was shown to depend on the phytohormones auxin and brassinosteroids[36,39,56,74]. Biosynthesis of auxin, its transport and signaling are all necessary for high temperature-induced hypocotyl elongation. This was shown genetically, *e.g.* by testing auxin response defective mutants, auxin transport defective mutants and lines with altered auxin levels, as well as pharmacologically, using *e.g.* N-1-Naphthylphthalamic Acid (NPA), which blocks polar auxin transport[119,120] and Picloram, a synthetic auxin[66]. These compounds respectively inhibit and stimulate hypocotyl elongation at high temperature conditions[36,56].

The bHLH transcription factor *PIF4* is a major signaling hub required for high temperature-mediated architectural changes[37]. Picloram addition rescues the *pif4* mutant phenotype at warm temperatures, hence PIF4 functions upstream of auxin. Indeed, PIF4 directly regulates levels of auxin by binding to the promoter and controlling the expression of key auxin biosynthesis genes, *TRYPTOPHAN AMINOTRANSFERASE OF ARABIDOPSIS* (*TAA1*, also called *TRANSPORT INHIBITOR RESPONSE 2/TIR2*) and the *cytochrome P450s*, *CYP79B2*, and *CYP79B3* genes, as well as *YUCCA8* (*YUC8*) in a high temperature-dependent manner[39,56]. Downstream of auxin biosynthesis, the *shy2* mutant, an *IAA3* mutant, was shown to be able to suppress the elongation phenotype of the *35S::PIF4* overexpressor line, implying that IAA3 is involved in high temperature-dependent auxin signaling[39]. Additionally, members of the *SMALL AUXIN UPREGULATED RNA* (*SAUR*) gene family are involved in *PIF4*-dependent high temperature acclimation. Expression *of SAUR19-24* is higher at 28°C compared to 22°C, and this upregulation is almost completely lost in the *pif4* mutant[56]. In accordance with this finding, it was shown by genetic analyses that the *SAUR19-24* genes play a role in the cell expansion event that leads to hypocotyl elongation[76]. Recent findings moreover indicated that the SKP-Cullin-F-box^{TIR1} (SCF^{TIR1}) Ubiquitin ligase auxin receptor complex is stabilized under high temperature conditions, through HEAT SHOCK PROTEIN 90 binding[40]. Additionally, a key role for the brassinosteroid phytohormones has been demonstrated in a feedback loop involving PIF4 and IAA[74].

Despite this impressive progress in thermomorphogenesis research in recent years, current lack of comprehensive understanding on how temperature is perceived and translated into relevant acclimation responses, redundancy in temperature sensing and response mechanisms as well as the (passive) effects temperature has on almost every

process in the plant, hinders identification of associated factors and further unravelling of the signaling networks.

We therefore decided to pursue a chemical genetics approach to identify novel small molecules that affect thermomorphogenesis, with the aim of developing new tools to study the molecular networks that underlie temperature acclimation. The advantage of such a strategy is that the problems of genetic redundancy and embryonic lethality can be circumvented, which can severely hamper classical genetic knock-out approaches[87,91,121]. In chemical genetics, large libraries of small molecules are screened for induction of a phenotype of interest in the studied organism. The screening of chemical libraries for phenotypes is an established method to identify novel pharmaceutical drugs, but in plants this approach is not as widely applied yet[85]. Nevertheless, a notable example of a successful chemical genetic strategy is the identification of the highly redundant PYRABACTIN RESISTANCE 1 (PYR1) family of phytohormone Abscisic acid receptors[91].

In this project, a chemical compound library was screened for compounds that enhance thermomorphogenesis. More specifically, 8000 compounds of a diverse library of small aromatic compounds ('Laboratories for Chemical Biology Umeå (LCBU) Screening library' provided by Chembridge; www.chembridge.com) and 360 compounds previously found to be active in plants[122] were screened, to identify compounds that rescues impaired high temperature-induced hypocotyl elongation of the *pif4-2* mutant in *A. thaliana*. After initial screening, the effects of candidate compounds were confirmed and the dose-dependency was determined.

Because auxin is a potent inducer of thermomorphogenesis in the *pif4-2* mutant background[56], candidate compounds that were structurally related to auxins or caused classical auxin-like phenotypes were omitted from further analyses. Using these selection criteria, we were able to identify nine compounds that stimulate high temperature-induced hypocotyl elongation in manner distinct from canonical auxin application, in a dose-dependent manner. These compounds show potential to further unravel the molecular mechanistic basis of high ambient temperature sensing and signaling in plants. Moreover, these compounds – or their optimized analogous - can be used in the future to enhance acclimation in the field or greenhouse by directly applying the compound to important crops suffering from thermal stress.

Results

Chemical library screening; qualitative identification of novel compounds that induce thermomorphogenesis

With the goal of identifying small aromatic compounds that enhance thermomorphogenesis in *A. thaliana* seedlings, we developed a high-throughput screening protocol based on temperature-induced hypocotyl elongation, which is an established fast and reliable

thermomorphogenesis capacity assay[36,37,56,123,124]. 8000 compounds of the 17500 small aromatic compound LCBU screening library (Chembridge) and a 360 bio-active compound library[122] were tested for their ability to restore hypocotyl elongation at 28°C in the *pif4-2* mutant, which is defective for thermomorphogenesis[37,56] (**Fig. 2.1**). As controls, Col-0 wild type seedlings were grown in parallel on medium containing the solvent DMSO (positive control) and in the presence of the auxin transport inhibitor NPA (negative control). Additionally, *pif4-2* seedlings were grown on DMSO (negative control) and in the presence of the synthetic auxin Picloram (positive control), which restores hypocotyl elongation at high temperature conditions in this mutant[56] (**Fig. 2.2, S2.1**).

Since auxins are potent inducers of high temperature-induced hypocotyl elongation[36,56], we intended to exclude canonical auxinic compounds. Treatment with the synthetic auxin Picloram induces a typical phenotype with small, inward curved leaves, reduced root growth[125,126] and agravitropic growth (**Fig. S2.1**). As a first qualitative selection to omit auxinic chemicals, all compounds that resulted in a display of these typical phenotypes, in addition to hypocotyl elongation, were therefore excluded from further analyses (**Fig. S2.1**).

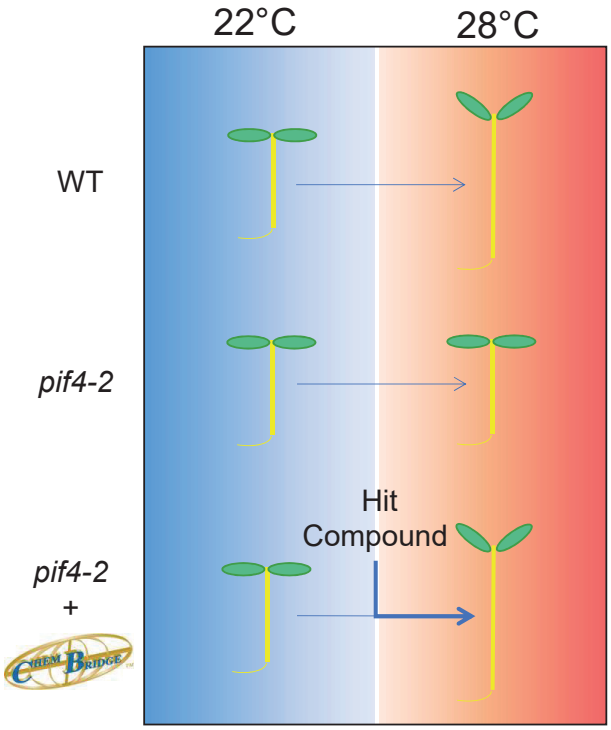

Figure 2.1:

Schematic representation of the screening setup. Hypothetical hit compounds are able to rescue the *pif4-2* mutant phenotype.

Based on initial visual selection, a total of 298 primary hit compounds were identified that restored hypocotyl elongation in the *pif4-2* mutant at warm temperatures (data not shown). Notably, this initial screening was performed under high temperature conditions. To confirm the initial hits and reduce the number of false positive hits, a validation experiment was performed using the identified 298 primary hit compounds. Plants were grown in the same experimental set-up, under high temperatures (28°C) and control conditions (22°C) and again visually screened. This classified 260 compounds as either false positives or auxinic and were omitted from further study. The remaining 38 compounds were visually confirmed to induce hypocotyl elongation in a manner distinct from canonical auxin application (data not shown).

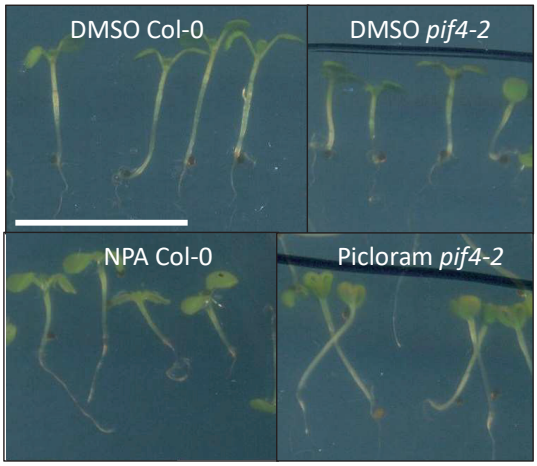

Figure 2.2:

Typical hypocotyl elongation phenotypes observed under high ambient temperature conditions. Indicated are added chemicals and genotype of seedlings. DMSO was used as solvent mock treatment, NPA and Picloram were added at a final concentration of 4.18µM. Seedlings were grown at 27°C for 9 days. Scale bar equals 1cm.

Quantitative confirmation of hit compound effects

To quantitatively confirm the 38 remaining candidate hit compounds and to further exclude compounds that resemble auxin treatment, the hypocotyl length validation experiment at 22°C and 27°C was repeated using fresh powder of 36 out of the 38 compounds, ordered from the Chembridge vendor. Two compounds were not available for follow up studies. Additionally, this experiment allowed us to exclude contaminations in the library that may have occurred due to repeated use for diverse screens. The effects of the compounds on Col-0 wildtype hypocotyls were quantified next to the effects in the *pif4-2* mutant background, to dissect between compounds that affected high temperature-induced hypocotyl elongation downstream or upstream of PIF4 signaling.

These quantitative hypocotyl length measurements allowed us to select 10 compounds (designated A-J) that had a high temperature-specific effect on hypocotyl length (**Table 2.1, Fig S2.2A**). An exception is compound D, which was selected for its strong enhancing effect on hypocotyl elongation, independent of temperature, without inducing a picloram-like phenotype. Six compounds enhanced hypocotyl elongation in both Col-0 and *pif4-2* (*i.e.* compounds A, B, C, D, E and G). Two compounds (*i.e.* compounds H and I), only had an effect on Col-0 in this experiment (**Fig S2.2A**).

In addition, the orientation of the seedling relative to the gravity vector was scored (gravitropism, **Fig S2.2B**), since agravitropism is associated with disturbance of auxin distribution and/or signaling in the plant[120,127] and is strongly induced by compounds like NPA and Picloram (**Fig. S2.1, S2.2**). Compound J consistently induced agravitropism to a level similar as Picloram (**Fig S2.2B**). This strongly suggests that this compound potentially enhanced hypocotyl elongation by acting as auxin homolog or interferes with auxin transport. Other compounds (*e.g.* D, E, F, and G) affected gravitropy to levels above background noise, but with large variety between replicates and to a lesser degree than Picloram or NPA (**Fig. S2.2B**)

Table 2.1: 10 chemicals selected after quantitative confirmation experiment.

Shown are the given compound ID, the Vendor ID at Hit2Lead.com the structure, generated chemical molweight and Partition coefficient cLogP. Data extracted from Hit2Lead.com chemical database.

Compound	Vendor ID	Structure	Chemical name	MW	cLogP
A	5156996	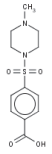	4-[(4-methyl-1-piperazinyl)sulfonyl]benzoic acid	284	-0.49
B	5685297	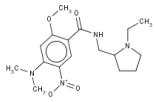	4-(dimethylamino)-N-[(1-ethyl-2-pyrrolidinyl) methyl]-2-methoxy-5-nitrobenzamide	350	2.68
C	5688969	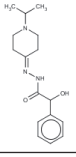	2-hydroxy-N′-(1-isopropyl-4-piperidinylidene)-2-phenylacetohydrazide	289	3.52
D	5713980	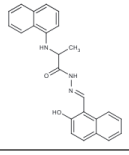	N′-[(2-hydroxy-1-naphthyl)methylene]-2-(1-naphthylamino)propanohydrazide	383	4.38

E	5364749	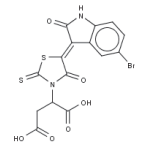	2-[5-(5-bromo-2-oxo-1,2-dihydro-3H-indol-3-ylidene)-4-oxo-2-thioxo-1,3-thiazolidin-3-yl] succinic acid	457	0.89
F	6148371	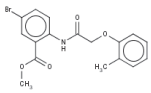	methyl 5-bromo-2-{[(2-methylphenoxy)acetyl] amino}benzoate	378	4.55
G	6131881	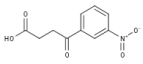	4-(3-nitrophenyl)-4-oxobutanoic acid	428	1.16
H	7674471	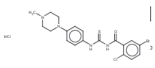	5-bromo-2-chloro-N-({[4-(4-methyl-1-piperazinyl) phenyl]amino}carbonothioyl)benzamide hydrochloride	504	2.963
I	7724721	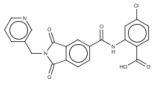	4-chloro-2-({[1,3-dioxo-2-(3-pyridinylmethyl)-2,3-dihydro-1H-isoindol-5-yl]carbonyl}amino) benzoic acid	436	3.997
J	7948967	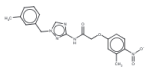	N-[1-(3-methylbenzyl)-1H-1,2,4-triazol-3-yl]-2-(3-methyl-4-nitrophenoxy)acetamide	381	3.857

Dose Response and NPA assays

The effect of the compounds has so far only been tested at one concentration (8.3 µM), which can be sub- or supra-optimal for their effect. To determine the optimal concentrations and further confirm the effects of the 10 remaining compounds, dose response experiments were performed using Col-0 wild type and *pif4-2,* grown at 22°C and 27°C (**Fig. 2.3**). As expected, NPA abolished hypocotyl elongation in particular in Col-0 under high temperature, whereas Picloram induced elongation in both genotypes and under both temperatures. (**Fig. 2.3A, B**). For Picloram, the optimum was ~5µM. In addition to compound D, also compound F appears to induce hypocotyl elongation in a temperature-independent manner, although with a very distinct dosage-responsiveness (**Fig. 2.3F, G**). Compound G showed no effect on hypocotyl elongation in this experiment (**Fig. 2.3H**). This compound was therefore excluded from further experiments. Compound

A and B induce hypocotyl elongation only in Col-0, over the whole range of concentrations tested, suggesting they may act upstream of PIF4 (**Fig. 2.3C, D**). Compound C, H, I and J induce a stronger elongation effect in Col-0, but elongation is also present in *pif4-2*. The effect of compound C increase up to ~20% increase at 100µM. The effect of compounds H, I and J decrease after 25µM. The strongest effect is induced by compound I, increasing hypocotyl elongation by almost 30% in Col-0 wild type (**Fig. 3.3**). Only limited amounts of compound E were commercially available. We therefore omitted this compound from further analysis, because this compound was not the most interesting *a priori* (**Fig S2.2**).

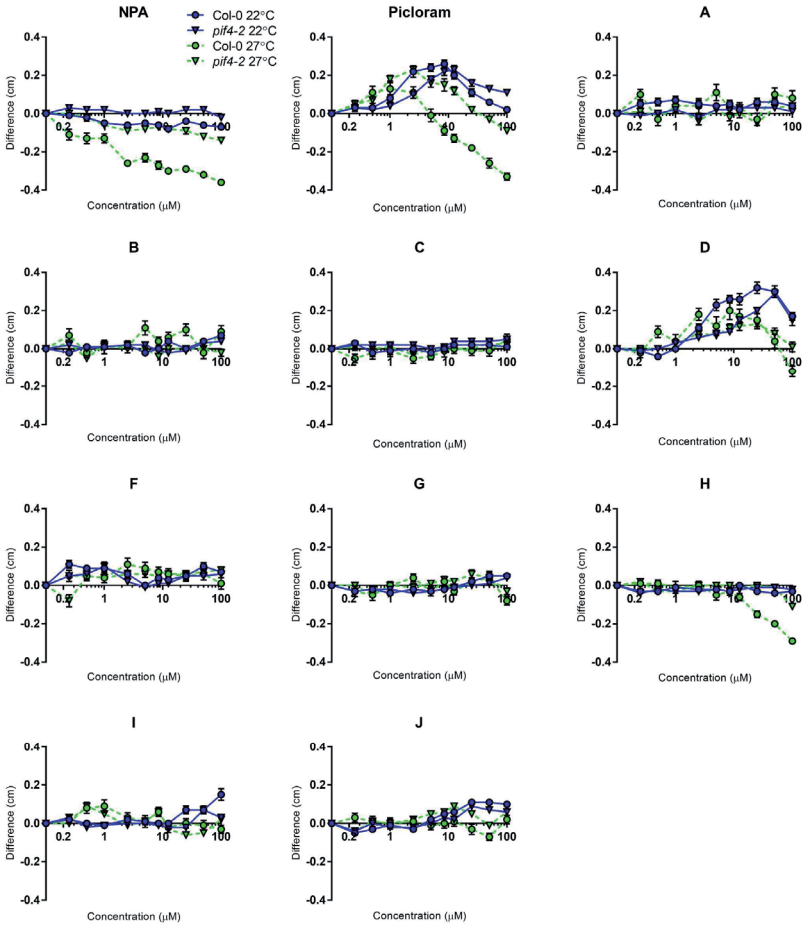

Figure 2.3:

Dose response assays of hypocotyl length in the presence of NPA, Picloram and compounds A - J. Data is absolute effects of each compound on hypocotyl length compared to DMSO solvent control. Compound E was excluded based on lack of commercial availability. Shown are data for Col-0 (blue and grey lines) and *pif4-2* (orange and yellow lines). Seedlings are grown at 22°C (blue and orange lines) and 27°C (grey and yellow lines).

We finally tested the effect of the 8 remaining compounds in the presence of NPA (**Fig. 2.4**). NPA disturbs auxin transport, but has been shown to also abolish the effects of application of other phytohormones on thermomorphogenesis[128]. Picloram was still able to confer a stimulating effect on hypocotyl elongation in the presence of NPA (**Fig. 2.4**). This is likely due to saturation of the tissues by auxin, or passive distribution of Picloram, making the transport obsolete. NPA was able to suppress the high temperature-induced elongation response of compounds A, B, H, I and J (**Fig. 2.4**). These compounds thus might interfere with phytohormones other than auxin or alternatively act in pathways that require, but do not interfere with, auxin activity. Compounds C, D, and F on the contrary apparently maintained the increase in hypocotyl elongation in the presence of NPA (**Fig. 2.4**). The strongest remaining effects are observed for Compound D. This compound was dubbed Heatin, after its thermomorphogenesis inducing and enhancing effects. In the next chapters (**Chapter 3-6**) we describe how Heatin was employed to further gain our understanding of adaptive thermomorphogenesis.

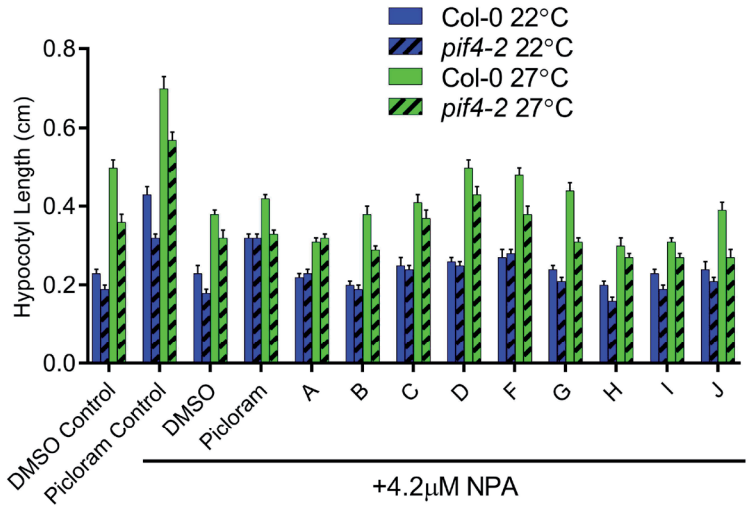

Figure 2.4:

Effects of the compounds A - J and picloram on hypocotyl lengths in the presence of 4.2 µM NPA in Col-0 (blue and gray bars) and *pif4-2* mutants (orange and yellow bars) at 22°C (blue and orange bars) and 27°C (gray and yellow bars). DMSO Control and Picloram Control lacked NPA in the medium. Error bars indicate standard error of the mean.

Discussion

A large chemical compound library was screened for compounds that enhance plant thermomorphogenesis, using hypocotyl elongation as a readout (Fig. 2.1). We developed an efficient screening platform and used this to screen two compound libraries for chemicals that possess the ability to induce hypocotyl elongation under high temperature conditions in the *pif4-2* mutant.

After initial screening, 38 compounds were identified, 36 from the Chembridge library and 2 from the second, smaller, bio-active compounds library. Surprisingly, our quantitative validation experiments indicated that several compounds seemed to specifically induce hypocotyl elongation in Col-0 WT seedlings, and not in *pif4-2* seedlings, used in the initial screen (Fig. 2.3). This prompts the obvious question how they could have been identified in the initial screen that was based on *pif4-2* mutant plants in the first place. It is possible though, that these compounds have effects on *pif4-2* as well, but we did not observe it here, due to the difference in growth conditions between the 24-well screening plates and the petri dishes used in the confirmation experiment.

36 available compounds were tested again from purified powder to exclude possible effects caused by contamination of the compound library or degradation due to long term storage. Of these 36 compounds, the 10 most interesting ones were selected for further experiments. Dose-response assays were performed and the requirement of polar auxin transport for their function was tested by growing plants on medium containing the compound in the presence of NPA. These compounds can be used as a tool to study the molecular mechanistic basis of thermomorphogenesis in plants.

In the next chapters (**Chapter 3-6**), we describe how one of the identified compounds, Heatin (Compound D in **Fig. 2.3 and 2.4**), being the most potent and consistent inducer of thermomorphogenesis in *pif4-2* and enhancer in Col-0, was employed to increase our understanding of adaptive thermomorphogenesis on the molecular level. Heatin increases hypocotyl length consistently under various conditions and in different genotypes, without inducing obvious additional phenotypes and these effects are not fully suppressed by adding NPA.

The effects of the other compounds A, B, H, I and J, appear temperature-specific and were suppressed by NPA. This suggests that they require polar transport of auxin, either through direct effects on auxin, or by affecting upstream phytohormone signaling that feed into the auxin signaling pathway[128]. Compound C also induced thermo-specific hypocotyl elongation, insensitive to NPA addition, making this compound also a very interesting candidate compound for follow-up studies. Compound G did not induce any elongation response in the dose response assays and is probably a false positive from the initial screen, or a contaminated compound in the library.

An assessment of the 10 selected compounds and their homologues was performed to reveal if these compounds were identified earlier in other chemical genetic screenings, using the Chemspider database (www.chemspider.com). No additional data is available for these compounds, underlining their novel character and potential for further characterization. These compounds thus have the potential to contribute to maintaining crop production in a changing climate. This can be achieved either through direct application on crops when warm temperature episodes are expected, or by using them as a tool to unravel molecular thermomorphogenesis signaling and use identified signaling components as breeding targets or markers.

Materials and Methods

Compound library screening

The small aromatic compound library 'Laboratories of Chemical Biology Umeå (LCBU) Screening Set'; http://www.chemistry.umu.se/english/research/infrastructure/lcbu/compound-collection/, purchased from Chembridge, was used for the initial screening. The first 8000 compounds out of the total 17500 were screened. In parallel, a library of 360 compounds previously found to be active in plants[122] was included. 1 µl of each compound was automatically pipetted (Biomek NX, BeckmanCoulter pipetting robot) from the 5mM stock solution to a well in a 24-well plate. 600 µl 1x Murashige-Skoog (MS) plant agar medium was added to each well manually. The final concentration of each compound in the wells was 8.3 µM. As controls, the auxin efflux inhibitor N-1-Naphthylphthalamic Acid (NPA; Duchefa) and the synthetic auxin Picloram (Sigma-Aldrich), both dissolved in di-Methyl Sulfoxide (DMSO) were used. These controls were added manually to a concentration of 4.18 µM to each 24-well plate for internal standardization. 0.1% DMSO lacking an active compound was used as mock solvent control.

pif4-2 (SAIL_1288_E07) knock-out mutants[129] seedlings were used for the screening and Col-0 WT as a controls. Seeds were surface-sterilized using a 0.1% tween-20, 70% ethanol solution for 2 minutes and subsequently washed with 95% ethanol. Six seeds were manually added to each well in a horizontal line and dispersed using a toothpick.

The plates with seeds were stratified in the dark at 4°C for 3 days to synchronize germination. Subsequently, plates were pre-germinated at 22°C, 100 µmol m^{-2} s^{-1} long day (16h photoperiod) conditions for 24h. The plates were then moved to a growth cabinet (Percival Scientific INC., USA) for 8 days, set at 28°C, 75 µmol m^{-2} s^{-1} in short day conditions (8h photoperiod), after which the plates were scanned using a desktop scanner. Hypocotyl lengths were scored visually.

Hit confirmation, dose response and NPA assays

For the confirmation of initial hits detected by the visual screening, the dose response assays, and NPA/Picloram dose-response experiments, seeds were sterilized in a 5% bleach, 95% ethanol solution for 10 minutes and subsequently washed once with ethanol (95%) and twice with water. Seeds were sown in Petri dishes on 1x MS growth medium, with the same composition as described above. Seeds were stratified in the dark at 4°C for 3 days, and subsequently grown for 8 days in growth cabinets (Snijders BV) set at 27°C or 22°C, 200 µmol m^{-2} s^{-1}, in short day conditions (8h photoperiod). Concentrations used for the dose response assay were 100 µM, 50 µM, 25 µM, 12,5 µM, 8,5 µM, 5 µM, 2,5 µM, 1 µM, 0,5 µM and 0,1 µM. For mock treatments, DMSO solvent was added to the same concentration as in the compound treatments.

Plates were scanned using a desktop scanner and hypocotyl lengths were measured using ImageJ (htpps://imagej.nih.gov/ij/). Seedling agravitropy was scored by qualification of the growth direction of hypocotyls relative to the direction of gravity. Hypocotyls that deviated more than 45° from the opposite of the direction of gravity, were considered agravitropic. Of note, under complete random directional growth (total absence of gravitropic response) ~ 75% of the seedlings thus would be marked as agravitropic using this strategy. Subsequent analyses were done using Microsoft Excel software.

Acknowledgements

We thank our research groups for their helpful comments and practical expertise, Dr. Per Anders Enquist (LCBU) for advice on the compound chemistry, and Dr. Martijn Fiers (Wageningen University) for his feedback and advice on the chemical genetic screening approach. This work was supported by a Facility access and support grant for chemical genomics projects to LvdW and MvZ from the Laboratories for chemical biology (LCBU), Umeå, Sweden, Erasmus Placement grant to LvdW and NWO VENI grant 863.11.008 to MvZ.

Supplemental Figures

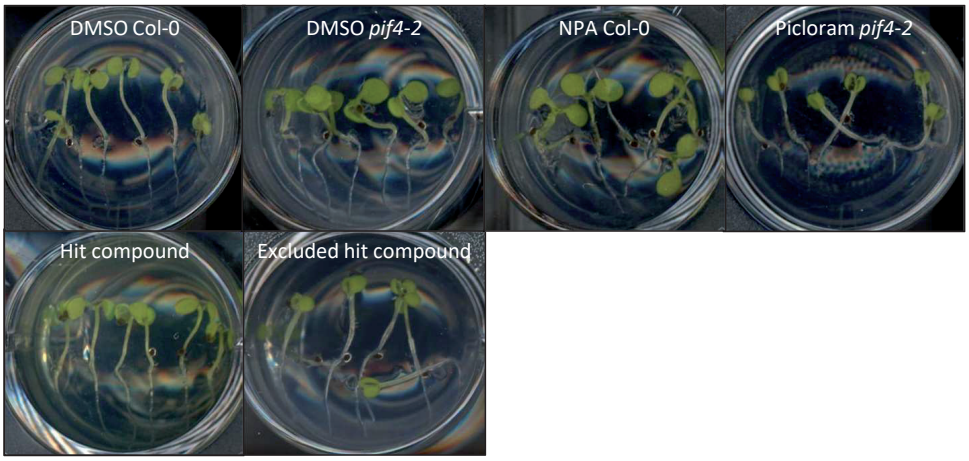

Supplemental figure 2.1:

Controls used during the chemical genetic screen, as well as an example of a candidate hit compound and a hit compound excluded based on phenotypes similar to picloram. Each panel is a single well from a 24-well compound used in the screening.

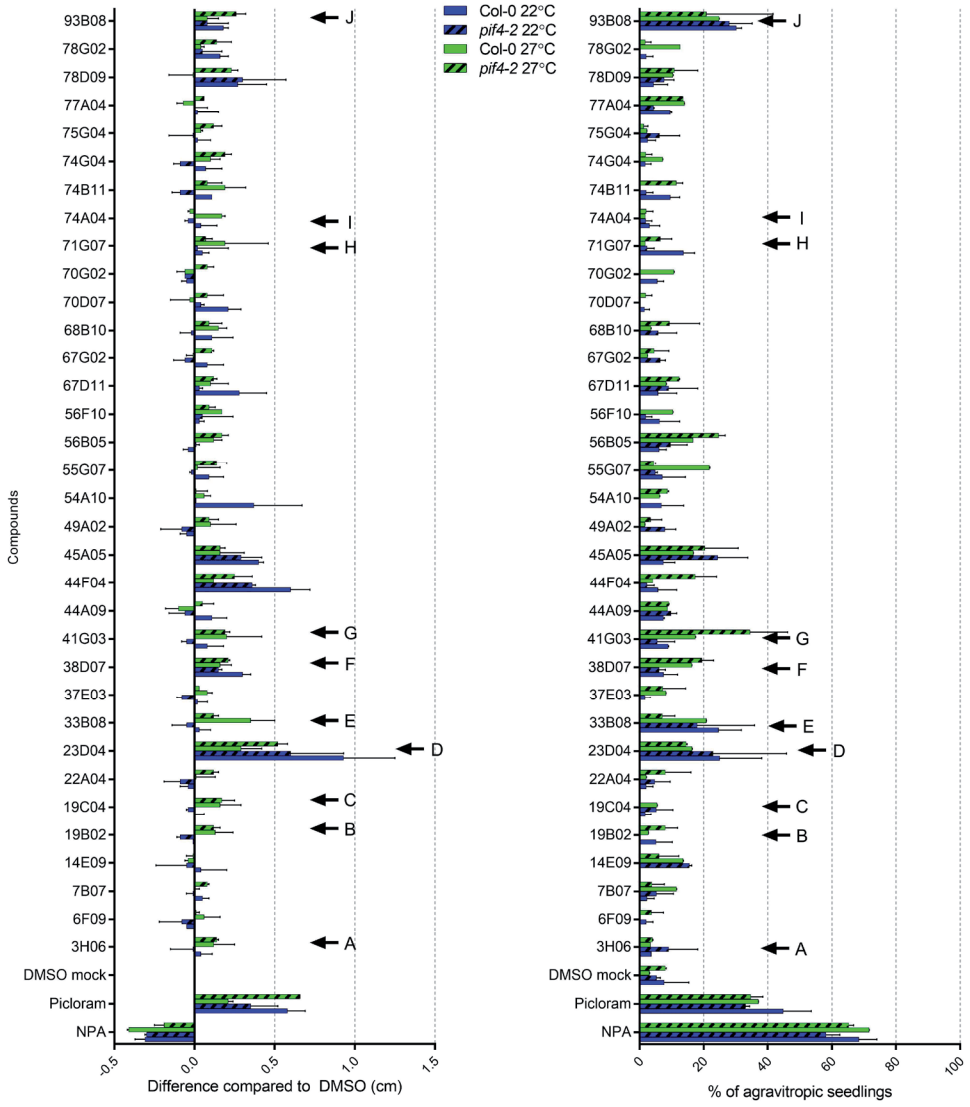

Supplemental figure 2.2:

Hypocotyl lengths (**A**) and agravitropism induction (**B**) of confirmed hit compounds. Hypocotyl length changes are absolute differences compared to the DMSO solvent mock. Agravitropism is displayed as the percentage of seedlings showing agravitropic hypocotyl growth. Seedlings used were Col-0 (blue and gray bars) and *pif4-2* mutants (orange and yellow bars) at 22°C (blue and orange bars) and 27°C (gray and yellow bars. Error bars indicate standard deviation. Arrows show compounds chosen for further analyses. Letters are used in subsequent experiments. Compounds were added at 8.3uM final concentration. Error bars indicate standard error of the mean.

CHAPTER 3

3

Heatin is a novel growth regulator that phenocopies thermomorphogenesis dependent on auxin signalling, but distinct from canonical auxin application

Lennard van der Woude[1] | Gruson Klaasse[3] | Wouter Kohlen[2] | Sjef Smeekens[1] | Nathaniel Martin[3] | Martijn van Zanten[1]

[1] Molecular Plant Physiology, Institute of Environmental Biology, Utrecht University, Padualaan 8, 3584 CH Utrecht, The Netherlands
[2] Laboratory for Molecular Biology, Wageningen University, Droevendaalsesteeg 1, 6708 PB Wageningen, The Netherlands
[3] Department of Chemical Biology & Drug Discovery, Utrecht Institute for Pharmaceutical Sciences, University Utrecht, Universiteitsweg 99, 3584 CG Utrecht, The Netherlands

Abstract

Global temperatures are predicted to rise in the coming century, which will affect plant development and growth. High ambient temperature typically leads to elongation growth of organs, induced to mitigate detrimental effects of warmth. Collectively, the changes induced by mild temperature increases are called thermomorphogenesis.

Using a chemical genetic approach, we identified a compound termed Heatin, that induces thermomorphogenesis already under control temperature. Here we investigate the mechanism by which the Heatin molecule affects thermomorphogenesis. We connect Heatin signalling to known thermomorphogenesis signalling networks by comparing it to the synthetic auxin Picloram and testing the effects on rosette-stage plants. We probe the structure-activity relationship of the Heatin molecule and investigate how Heatin is related to auxin signalling. Results indicate that Heatin induces thermomorphogenesis in a manner distinct from canonical auxin application downstream of *PIF4* and that Heatin also induces thermomorphogenesis-like phenotypes in rosette-stage plants. Additionally, we identify 1-aminomethyl-2-napthol as the minimal active moiety of Heatin and show a relationship to Sirtinol, a previously identified compound affecting plant growth. Finally, we show that auxin signalling is required for Heatin's effects by demonstrating strong resistance in auxin receptor mutants. However, no *DR5*-signalling is activated by Heatin, suggesting that Heatin does not act as a canonical auxin. Moreover, levels of bioactive IAA are unaffected upon Heatin treatment.

Introduction

In order to survive, plants have to continuously adapt to changes in their environment. Many plants adapt their architecture and development in response to achieve optimal fitness in suboptimal conditions[130]. One such an environmental cue that has a strong impact on architecture is ambient temperature. Even changes as small as 1-2°C can affect plant development and architecture[28] in a process called thermomorphogenesis[28,41,131].

During thermomorphogenesis plants elongate specific organs to change from a compact to an open structure. Specifically, the hypocotyl and petioles elongate and hyponasty (upward leaf movement) occurs[36,37,132]. The open rosette architecture caused by these elongation responses has been proposed to enhance cooling capacity[44,45]. Additionally, elongation of the hypocotyl and petioles functions to move the photosynthetic organs (green leaves) away from the heated soil.

In combination with information about light levels and spectral quality, the temperature signal is used to fine-tune the plant's architecture and development to its specific environment (ambient temperature, light intensity), the season and the absence or presence of neighbouring plants. For example, in summer's warmth, plants respond to shading by elongation growth to outgrow its neighbours and reach the top of the canopy to absorb more light. In winter's cold environment however, this elongation response is suppressed, as photosynthesis functions poorly at low temperatures[47].

Understanding of plant responses to small increases in ambient temperature is particularly relevant in the context of maintaining crop performance under conditions of global climate change[133]. Average temperatures on earth have been projected to rise by several degrees in the coming centuries, causing significant reductions in crop productivity[1,133]. Knowledge on how plants respond to imminent changes in the environment could be key to mitigate the projected negative effects of climate change. By understanding the molecular mechanisms controlling the acclimation response, efficient knowledge-based breeding of crops that are adapted to a warmer climate could become possible. Such adapted crops could contribute to improving food security.

The molecular mechanisms controlling thermomorphogenesis overlap partly with light signalling mechanisms that control the shade avoidance response in the model plant *Arabidopsis thaliana*. Phytochrome B (PhyB), a light receptor protein that is activated by red light to supress elongation growth, is passively inactivated in a temperature dependent manner in darkness[48]. This relieves suppression of elongation growth under higher temperatures[42,43]. When activated by red light, PhyB is translocated to the nucleus where it inhibits positive regulators of elongation growth: PHYTOCHROME INTERACTING FACTOR (PIF) transcription factors, by stimulating their degradation[50]. One of these, *PIF4,* is also required for thermomorphogenesis as loss of function of this gene results in a lack of temperature responsiveness[37,134]. In the absence of active

PhyB, PIF4 directly promotes the transcription of the auxin biosynthesis genes: *YUCCA8* (*YUC8*)[39], *TRYPTOPHAN AMINOTRANSFERASE OF ARABIDOPSIS 1* (*TAA1*) and *CYTOCHROME P450, FAMILY 79, SUBFAMILY B, POLYPEPTIDE 2* (*CYP79B2*)[56]. These enzymes catalyse the conversion of L-tryptophan to indole-3-acetic-acid (IAA)[36,39,56]. This bioactive endogenous auxin subsequently triggers thermomorphogenesis[72]. Accordingly, overexpression of *PIF4* leads to a long hypocotyl, which can be suppressed by a *yuc8* knockout mutation[39]. Additionally, the abolished hypocotyl elongation response of the *pif4-2* mutant under high temperature conditions can be rescued by applying the synthetic auxin Picloram[56].

Auxin acts as a 'molecular glue' between its receptor protein complex, the ubiquitin ligase SKP1/CULLIN/F-BOX (SCF)$^{TIR1/AFB}$, and AUXIN/INDOLE-3-ACETIC ACID (AUX/IAA) proteins[65,66]. This interaction leads to polyubiquitination of the AUX/IAA proteins, causing their proteasomal degradation[67]. AUX/IAA degradation releases their inhibition on AUXIN RESPONSE FACTOR (ARF) transcription factors[69]. Transcription of *AUX/IAA 19* and *29* is enhanced at warm temperatures in a PIF dependent manner[52,73]. However, specific degradation of AUX/IAAs under high temperature conditions has not been shown so far. Of the ARFs, *ARF6* has been implicated in general *PIF4*-dependent hypocotyl elongation[72].

In addition to increasing auxin levels, high temperature simultaneously stimulates auxin sensitivity by stabilizing TIR1, the F-BOX protein of the auxin receptor complex in a HEAT SHOCK PROTEIN 90-dependent manner[40]. Additional control in the thermomorphogenesis signalling network comes via a positive feedback loop between brassinosteroid signalling downstream of auxin, and *PIF4*. This has been proposed to allow for tight control on the elongation response to warm temperatures[74].

A subset of the large *SMALL AUXIN UP RNA* (*SAUR*) auxin responsive gene family (*SAUR19-24*) is induced upon high temperature treatment downstream of ARFs activity during thermomorphogenesis signalling. In addition, stabilization of SAUR19 by an N-terminal tag resulted in elongated hypocotyls[56]. SAUR19 has been shown to inhibit a PP2C-D phosphatase. This PP2C-D inhibits the activating interaction between 14-3-3 protein and H^+-ATP-ases[76]. Activated H^+-ATPases pump protons out of the cell into the extracellular matrix, which results in a lower pH, causing elongation according to the 'acid growth model'. This model states that through lowering of the pH, EXPANSINS are activated, causing a weakening of the cell wall, which enables cell expansion as a result of turgor pressure[135,136].

Although our knowledge on thermomorphogenesis signalling is progressing, further unravelling of the thermomorphogenesis signalling networks is required to fully understand how plants respond to high ambient temperature. However, functional redundancy between many factors involved in thermomorphogenesis signalling may hinder their identification by classical genetics approaches such as EMS forward genetic screens. An alternative approach to identify novel players in complex biological systems is chemical genetics or chemical genomics[80,137]. In chemical genetics approaches, small molecules are identified that interfere with a given biological system. These molecules

can be used as tools to study the biological system in detail. Potential advantages of chemical genetics/genomics over classical genetics approaches is that chemicals can hit a broad range of related targets. For example, whereas the effects of a knockout mutation on a single gene could be masked by related genes with a redundant function, a chemical compound could target a full family of genes at once, circumventing the redundancy. Conversely, a chemical compound can also be more specific than an EMS mutation in terms of targeted function, tissue localisation or developmental timing of its effects[85,87,91,137].

We employed a chemical genetics approach to identify novel compounds that affect thermomorphogenesis, using high temperature-induced hypocotyl elongation in *Arabidopsis thaliana* as a fast and reliable assay (**Chapter 2**). As temperature affects nearly all physiological, developmental and phenological processes in the plant, we aimed to identify compounds that specifically affected the architectural response. Among several hits, we identified a compound (named 'Heatin') that rescued the thermomorphogenesis-defective *pif4-2* mutant in a manner that is distinct from canonical auxin application (**Chapter 2**). Aim of this chapter is to investigate connections between Heatin and the known thermomorphogenesis signalling network, and to probe the molecular basis of its activity by performing a structure-activity relationship study. We further explore the effects of Heatin on other thermomorphogenesis phenotypes.

Results

Heatin application resembles high temperature-induced hypocotyl elongation distinct from canonical auxin application.

Plants treated with Heatin exhibit a longer hypocotyl than non-treated mock plants (**Fig. 3.1A, H**). Both Col-0 wildtype (WT) and *pif4-2* mutant plants were Heatin-sensitive and enhanced hypocotyl elongation was observed under control (22°C) and high (27°C) temperature conditions (**Fig. 3.1A**) in a dose dependent manner, in both genetic backgrounds. As indicated by the increasing hypocotyl lengths over increasing concentrations, the sensitivity to Heatin was similar between Col-0 and *pif4-2*, suggesting that the *pif4-2* mutation does not interfere with Heatin effects. Similarly, growth temperature does not apparently affect Heatin-sensitivity (**Fig. 3.1A**).

Because high temperature-induced hypocotyl elongation depends on auxin[36,39,40,56], we compared Heatin dose-responsive growth (**Fig. 3.1A**) with that of the synthetic auxin Picloram and the polar auxin transport inhibitor N-1-naphthylphthalamic acid (NPA) (**Fig. 3.1C, E**). In contrast to Heatin, Picloram was particularly effective in *pif4-2* mutant seedlings grown under high temperatures, where already at low concentrations of Picloram, hypocotyl length was stimulated. These seedlings show the strongest elongation growth stimulation between 1 and 2,5 µM, whereas higher concentrations reduced the effect. This contrasts with control temperature-grown Col-0 WT and *pif4-2*

seedlings, which elongated most between 2,5 and 8,5 µM, and with high temperature-grown Col-0 WT seedlings, which showed only very mild elongation growth effects at concentrations lower than 1 µM and reduced elongation at higher concentrations (**Fig. 3.1C, H**). NPA mainly affected high temperature grown seedlings, reducing hypocotyl elongation in a dose-dependent manner, levelling off at concentrations higher than 1 µM (**Fig. 3.1E**).

Gravitropism, *i.e.* growth coordinated in response to the orientation of the gravity vector, is a typical auxin effect in seedlings and depends on polar auxin transport creating an increased auxin response on the bottom side of the hypocotyl[138]. Likewise, normal root growth and development depends on proper auxin distribution in the root[139]. Both processes are influenced by disturbing auxin distribution in the plant, either by blocking polar transport with NPA or saturating Picloram concentrations (**Fig. 3.1D, F, H**). Notably, Heatin did not interfere with gravitropism (**Fig. 3.1B, H**). In addition, unlike NPA and Picloram (**Fig. 3.1D, F, H**), Heatin did not alter root length (**Fig. 3.1G, H**). Consistent with previously published results, we observed that high temperature results in longer roots, whereas roots of *pif4-2* were shorter than Col-0 WT (**Fig. 3.1G, Supplemental file 3.2**)[140]. Altogether, our results suggest that Heatin induces hypocotyl elongation in a manner distinct from canonical auxin application and auxin transport control.

Heatin treatment phenocopies thermomorphogenesis in vegetative rosettes

We next tested if Heatin-treatment phenocopies other thermomorphogenesis phenotypes, apart from hypocotyl elongation. Col-0 WT and *pif4-2* mutant plants were grown until the ~9-15 rosette leaf stage in tissue culture pots on sterile MS-agar medium containing Heatin or a solvent mock and grown at control and high temperature conditions. Visually, Heatin-grown plants exhibited a more open rosette structure than the mock plants. This effect was enhanced by increased Heatin concentration (**Fig. 3.2A**). We next quantified various thermomorphogenesis parameters, *i.e* fresh weight, leaf number, rosette area, petiole and leaf blade length and hyponasty (**Fig. 3.2 B-G**). High temperature strongly reduced fresh weight, leaf number, rosette area and leaf blade length (**Fig. 3.2 B-D,F**) and induced petiole elongation and hyponastic growth (**Fig. 3.2 E,G**), consistent with literature[115]. As expected, high temperature-induced changes in fresh weight, number of leaves, rosette area, petiole length and hyponasty depended on functional PIF4, as the genotype had a significant effect in the ANOVA analyses of these phenotypes. ANOVA analysis also indicated a significant interaction between the temperature and the genotype for number of leaves, petiole length and hyponasty (**Fig. 3.2 B, C, E, G, Supplemental file 3.2**). Heatin had a significant effect on all measured traits except petiole length (Fig. 3.2 E), but no significant interactions were found between the applied compound (Heatin or mock), the genotype (Col-0 WT or *pif4-2*) or the growth temperature (22°C or 27°C) (**Fig. 3.2, Supplemental file 3.2**). Individual comparisons between different samples using *post-hoc* analyses did not reveal strong significant effects of Heatin but relative effects compared to DMSO within one G*E condition show that the strongest effects are observed on fresh

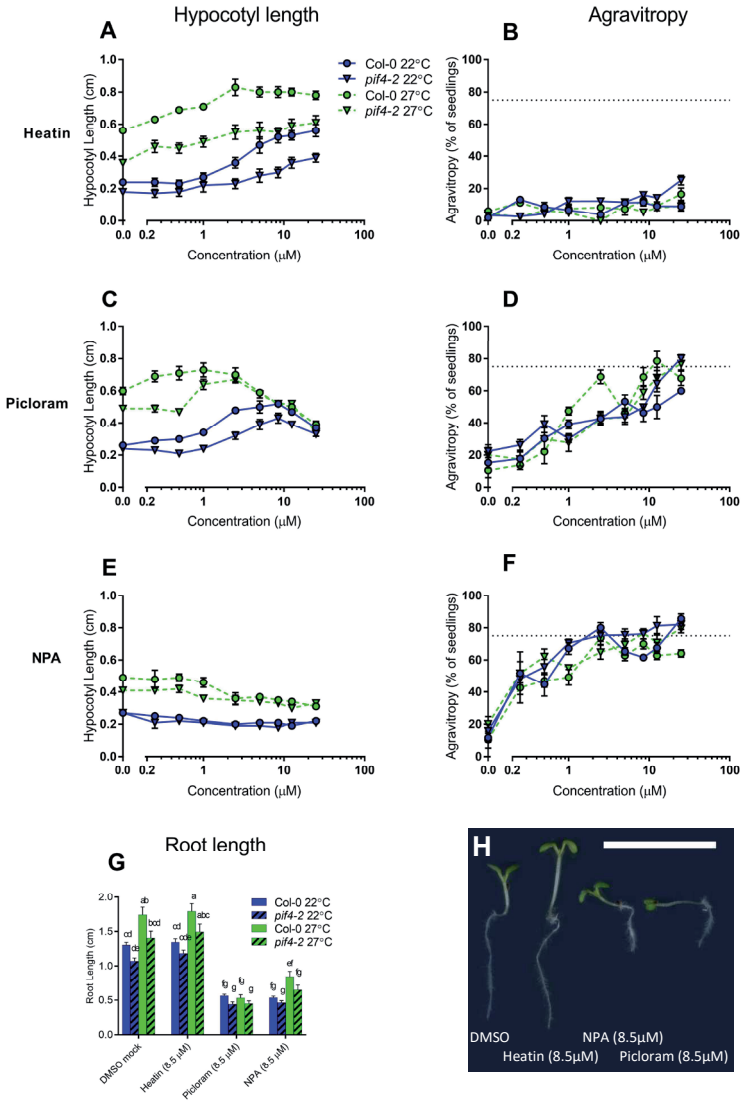

Figure 3.1: Effects of Heatin, Picloram and NPA on hypocotyl length, agravitropy and root length.

(A, C, E) Hypocotyl length of 8-day-old WT (circles) and *pif4-2* (triangles) seedlings over a range of concentrations of Heatin (A), Picloram (C) or NPA (E), grown at 22°C (blue-filled markers) or 27°C (green-filled markers). **(B, D, F)** Agravitropy scores of 8-day-old WT (circles) and *pif4-2* (triangles) seedlings over a range of concentrations of Heatin (B), Picloram (D) or NPA (F), grown at 22°C (blue-filled markers) or 27°C (green-filled markers). Dashed horizontal lines indicates 75% which equals complete agravitropy. **(G)** Root length of 8-day-old WT (clear bars) and *pif4-2* (dashed bars) seedlings growing on 8.5µM Heatin, Picloram or NPA, at 22°C (blue bars) or 27°C (green bars). Letters indicate significance groups following Tukey HSD post-hoc tests, where averages that do not share letters are significantly different at $p<0.05$. Values are averages of 3 times 15-25 seedlings. Error bars denote standard error of mean. (**H**) representative seedlings grown on the indicated compound. Scale bar equals 1cm.

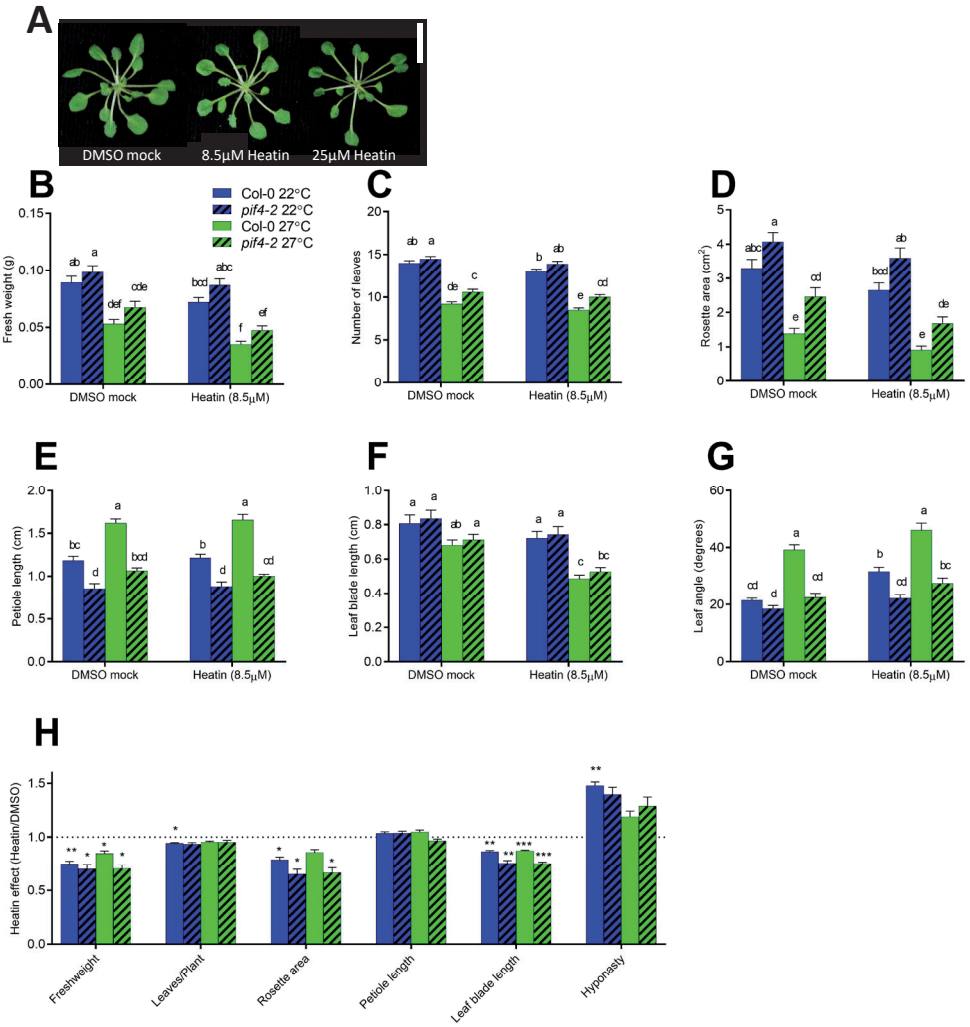

Figure 3.2: Phenotypic traits of Heatin-grown Arabidopsis at the rosette stage.

(**A**) Representative top photos of 5-week-old rosettes of Col-0 plants grown at 22°C on medium containing DMSO solvent mock or Heatin (8.5µM or 25µM). Scale bar equals 1cm. (**B**-**G**) Col-0 WT (clear bars) and *pif4-2* mutant (dashed bars) plants were grown in sterile conditions on control or Heatin-containing medium until the rosette stage and fresh weight (**B**), leaf number (**C**), rosette area (**D**), petiole length (**E**), leaf blade length (**F**) and leaf angle to the horizontal (hyponasty, **G**) were quantified of these plants. Letters indicate significance groups following Tukey HSD post-hoc tests, where averages that do not share letters are significantly different at $p<0.05$. Panel **H** shows the relative Heatin effect (compared to the DMSO mock treatment) on traits described in panel **B**-**G**. The dotted horizontal line denotes no effect of Heatin. Values are averages of 7 replicates of each 8-12 plants. Errors bars denote standard error of mean. Asterisks indicate significant differences from 1 as determined by one-sample t-test. * = $p<0.05$, ** = $p<0.01$, *** = $p<0.001$.

weight, plant surface and leaf blade length but less so on leaf number petiole length and hyponasty (**Fig. 3.2B-H, Supplemental file 3.2**). Taken together, we conclude that Heatin treatment visually phenocopies thermomorphogenesis, although not all temperature-responsive traits are affected by Heatin.

1-aminomethyl-2-naphthol is Heatin's active moiety

A structure-activity relationship study was performed to identify the active moiety of the Heatin molecule. To this aim, several commercially available analogues and derivatives of Heatin (**Table 3.1**) were tested for their effect on hypocotyl elongation. In three successive experiments, comparisons were made between the structures of active and inactive compounds to determine which moieties of the molecule are essential for activity and which parts can be changed or omitted without compromising biological activity.

In the first experiment we tested 12 analogues, assigned **#101** to **#112**, which differed mainly in side chains, but had a largely unchanged 3-Aminopropanehydrazide-based core structure (**Table 3.1**). Analogues **#101**-**#104** were bioactive (**Fig. 3.3A**). Compounds **#101** and **#102** stimulated hypocotyl elongation in WT and *pif4-2* under both temperature conditions. **#103** was active to a lesser degree than Heatin and did not have a significant effect on *pif4-2* seedlings grown under control temperature (**Fig. 3.3A**). **#104** induced elongation growth in both conditions and genotypes, except for high temperature grown WT seedlings. Concerning **#104**, we observed a large variation between replicates in hypocotyl length, possibly due to degradation of the **#104** stock solutions. Analogues **#105** to **#112** did not induce hypocotyl elongation responses different from mock treatment (**Fig. 3.3A**). Interestingly, all active compounds (**#101**-**#104, Heatin**), but not the inactive ones, contained a 2-naphthol moiety.

With this information at hand, a second set of commercially available compounds was tested (**#201**-**#205**), which had different degrees of similarity to the 3-Aminopropanehydrazide Heatin-backbone structure, but all contained the 2-naphthol moiety (**Table 3.1**). Neither 2-naphthol (**#205**) nor 1-methyl 2-napthol (**#204**) were however sufficient for elongation, even at high concentrations (**Fig. 3.3B; Fig. S3.2**). In contrast, compounds **#201**, **#202** and **#203** were bioactive (**Fig. 3.3B**), although compound #**201** and #**202** exhibited a stimulatory effect whereas **#203** notably inhibited hypocotyl elongation under high temperature conditions. Bioactive compounds **#201**, **#202** and **#203** all contained 1-aminomethyl-2-naphthol, which was absent in the inactive **#204** and **#205**, suggesting that 1-aminomethyl-2-naphthol could be the minimal active moiety for hypocotyl elongation effects.

In the third experiment, we therefore tested 1-aminomethyl-2-naphthol as minimal active compound (**M.A.C.**, **#301**) and found that this compound was indeed able to induce hypocotyl elongation without negatively affecting root growth (**Fig. 3.3C, E**), but at concentration of 50 µM or higher and not at 8,5 µM (the concentration used to identify Heatin; **Chapter 2**) (**Fig. 3.1A**). To assess the requirement of the hydroxyl-group

of the M.A.C. for its activity or specificity, 1-Naphthylmethylamine (**#302**), was tested alongside. Although this compound caused hypocotyl elongation at high concentrations similar to **#301/M.A.C.**, a strong inhibitory effect on root growth was observed at these high concentrations (**Fig. 3.3C**), suggesting that the hydroxyl group of **#301/M.A.C.**, and likely that of Heatin as well, is necessary for hypocotyl-specificity of elongation growth in seedlings.

To further probe the structure-activity relationship of the M.A.C. and to identify potential modification sites of the molecule for biomolecule target identification experiments (**Chapter 5**), compounds with additional moieties (**#401-405**) were tested for their bioactivity (**Fig. 3.3D**). In this experiment the endogenous auxin precursor indole acetonitrile (**#402/IAN**) was also included as the molecule resembles that of **#301/M.A.C.** in containing a terminal nitrogen. We observed that the addition of a moiety in-between the 2-napthol and the amide group and similarly, addition of an oxygen group to the amine, abolishes bioactivity. Changing the amino-group into a piperidine (**#401)** did not abolish bioactivity, although high concentrations were needed to observe the activity. Treatment with IAN (**#402**) caused severe growth defects, especially at high concentrations, consistent with previous observations[141]. Interestingly, IAN induced minor elongation at lower concentrations (**Fig. 3.3D**), likely due to its metabolism to bioactive IAA. IAN did not induce hypocotyl elongation to the same extent as Heatin and is not specific for hypocotyl elongation[61], suggesting that Heatin- and IAN induce hypocotyl elongation via different mechanisms.

Taken together, our structure-activity relationship study suggests that the 1-aminomethyl-2-naphthol moiety of the Heatin molecule is responsible for its hypocotyl elongation effect, where the remainder of the structure, including the hydroxyl-group, potentially aids in bioavailability and specificity of its effect.

Notably, analogue **#104** was previously identified in a chemical genetic screen performed on rat cell culture where it was found to affect G-protein dependent signalling[142]. Although being a large family of receptor proteins in mammals, only one copy of each protein in the G-protein complex is present *in planta,* yet the G-protein complex is known to affect hypocotyl elongation[143]. We therefore tested mutants in various G-protein for sensitivity to Heatin but did not find any significant effect that would suggest the involvement of the G-protein complex in Heatin signalling. Thus, Heatin and G-proteins mediate hypocotyl elongation via distinct mechanisms (**Fig. S3.1**).

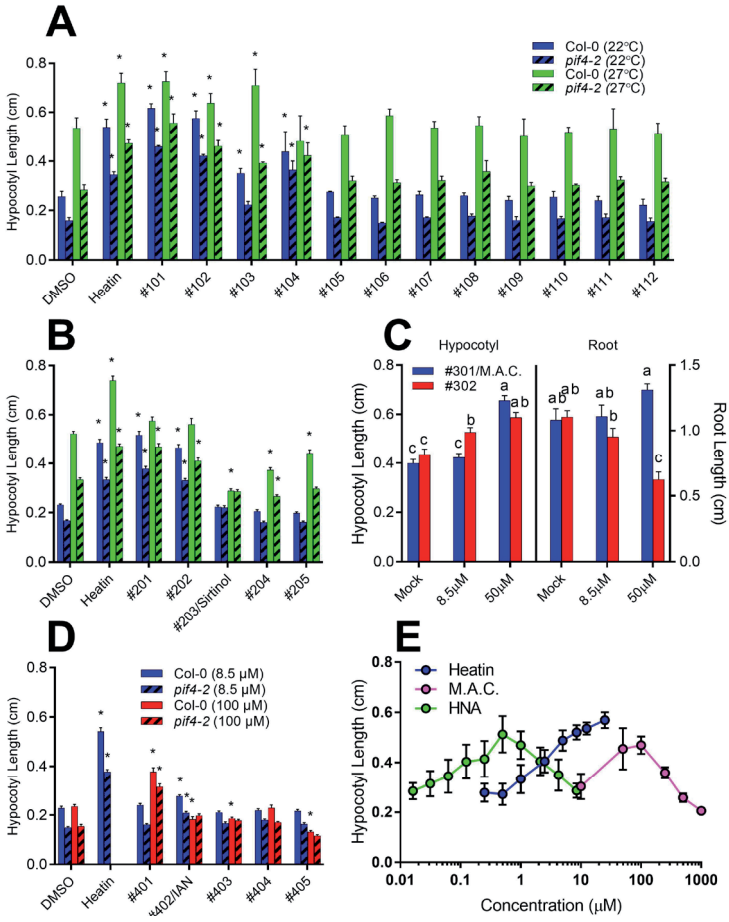

Figure 3.3: Structure-activity relationship study of the Heatin on hypocotyl elongation.

Hypocotyl length (**A**, **B**, **C**, **D**) or root length (**C**) of 8-day-old Col-0 WT (plain bars) or *pif4-2* mutant (dashed bars) seedlings, grown on medium containing different compounds (8.5µM) at 22°C (blue bars) or 27°C (green bars)(**A**, **B**) or on different analogues (**C**: #301; blue bars, #302; red bars) at different concentrations (**D**: 8.5µM; blue bars, 100µM; red bars). (**E**) Hypocotyl length of 8-day-old Col-0 WT seedlings grown on medium containing different concentrations of Heatin (blue line and marker), the minimal active compound (M.A.C., fuchsia line and marker) or 2-Hydroxy-1-naphthaldehyde (HNA, green line and marker). Values are averages of 3 (**A, B, D**) or 4 (**E**) replicates, each containing 15-25 seedlings, or a representative repeat of 20 seedlings (**C**). Asterisks indicate significant difference from the corresponding Col-0 WT averages (**A**, **B**, **D**). Letters indicate significance groups following Tukey HSD post-hoc tests, where averages that do not share letters are significantly different at $p<0.05$ (**C**). Error bars denote standard error of mean.

Table 3.1: Compounds used in this chapter and their sources, Vendor ID and structures.

Analogue ID	Vendor	Vendor ID	Name
Heatin	Chembridge	5713980	N′-[(2-hydroxy-1-naphthyl)methylene]-2-(1-naphthylamino)propanohydrazide
NPA	Sigma-Aldrich	N12507	N-(1-Naphthyl)phthalamidic acid
Picloram	Sigma-Aldrich	P5575	4-Amino-3,5,6-trichloropicolinic acid
101	Chembridge	5539488	N′-[(2-hydroxy-1-naphthyl)methylene]-2-[(2-methylphenyl)amino]acetohydrazide
102	Chembridge	5248195	N′-[(2-hydroxy-1-naphthyl)methylene]-2-[(4-iodophenyl)amino]acetohydrazide
103	Chembridge	5713195	2-[(4-bromophenyl)amino]-N′-[(2-hydroxy-1-naphthyl)methylene]butanohydrazide
104	Chembridge	5723320	2-[(4-ethoxyphenyl)amino]-N′-[(2-hydroxy-1-naphthyl)methylene]acetohydrazide
105	Chembridge	5712115	2-[(4-bromophenyl)amino]-N′-(2,4-dihydroxybenzylidene)propanohydrazide
106	Chembridge	5559595	2-[2-(2-hydroxybenzylidene)hydrazino]-N-(4-methylphenyl)-2-oxoacetamide
107	Chembridge	5725603	N′-(2-hydroxy-3-methoxybenzylidene)-2-(1-naphthylamino)propanohydrazide
108	Chembridge	6143663	2-[2-(2-hydroxybenzylidene)hydrazino]-N-(2-methylphenyl)-2-oxoacetamide
109	Chembridge	5530357	N′-(2-hydroxybenzylidene)-2-[(2-methylphenyl)amino]acetohydrazide
110	Chembridge	5861253	N′-[4-(diethylamino)-2-hydroxybenzylidene]-2-(2-naphthylamino)acetohydrazide
111	Chembridge	5717758	N′-(2,4-dihydroxybenzylidene)-2-(1-naphthylamino)propanohydrazide
112	Chembridge	5864129	N′-(2-hydroxy-4-methoxybenzylidene)-2-(1-naphthylamino)acetohydrazide
201	Sigma-Aldrich	S779644	acetic (2-hydroxy-1-naphthylmethylene)hydrazide
202	Sigma-Aldrich	OTV000008	1-[(Dibenzylamino)methyl]-2-naphthol
203	Sigma-Aldrich	Sirtinol/S7942	Sirtinol
204	Chembridge	4021629	1-methyl-2-naphthol
205	Sigma-Aldrich	185507	2-Naphthol
301	Sigma-Aldrich	CDS019203	1-Aminomethyl-naphthalen-2-ol
302	Sigma-Aldrich	127035	1-Naphthylmethylamine
401	Chembridge	5429881	ethyl 1-[(2-hydroxy-1-naphthyl)methyl]-4-piperidinecarboxylate
402	Sigma-Aldrich	129453	3-Indoleacetonitrile
403	Sigma-Aldrich	732400	1-(α-Aminobenzyl)-2-naphthol hydrochloride
404	Chembridge	5114438	N-[(2-hydroxy-1-naphthyl)methyl]benzamide
405	Chembridge	5929093	N-[(2-hydroxy-1-naphthyl)(4-methylphenyl)methyl]acetamide
HNA	Sigma-Aldrich	H45353	2-Hydroxy-1-naphthaldehyde
HNC	Sigma-Aldrich	H45809	2-Hydroxy-1-naphthoic acid

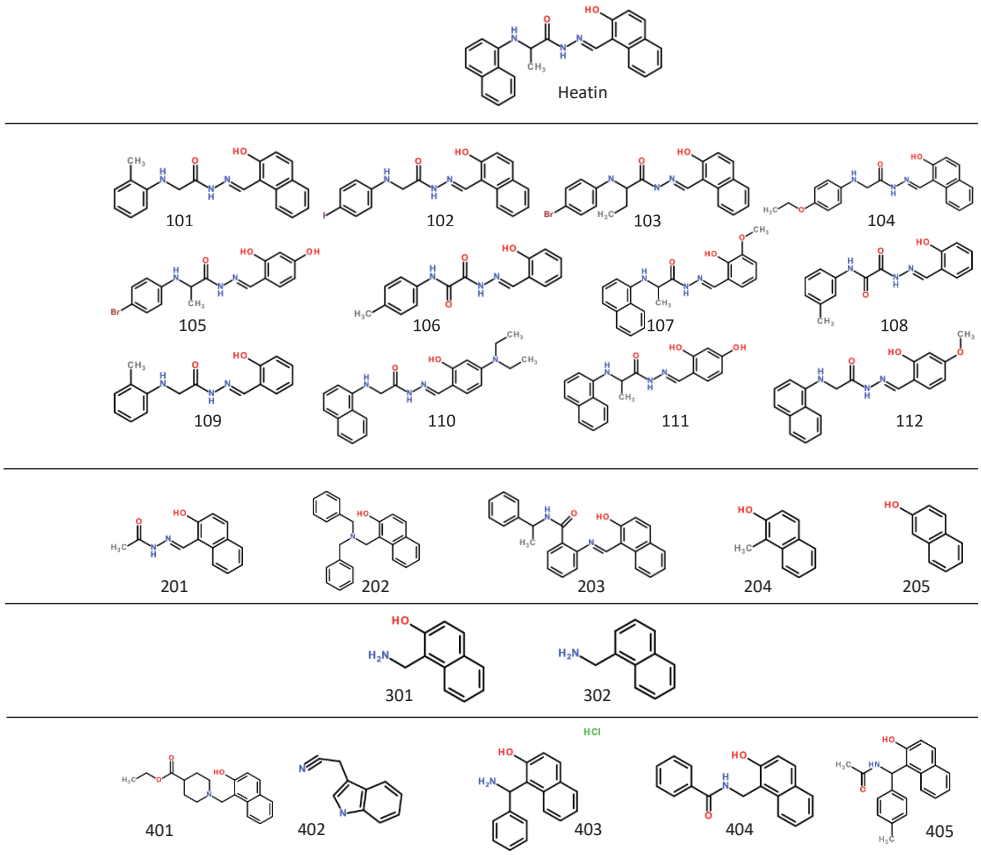

Heatin and Sirtinol act through overlapping signalling cascades

Analogue **#203** has been previously identified as Sirtinol in a chemical genetic screen in Yeast as an inhibitor of the Sirtuin family of NAD-dependent deacetylases[144]. Interestingly, Heatin and Sirtinol share the 1-aminomethyl-2-naphthol minimal active moiety required for hypocotyl elongation. In Arabidopsis, Sirtinol was found to activate the *DR5:GUS* auxin signalling reporter and supress hypocotyl elongation in the dark[145]. We found that **#203/Sirtinol** supressed hypocotyl elongation in our analyses as well, even though the experiments were performed in the light (**Fig. 3.3B**).

Structure-activity relationship studies performed on Sirtinol in Arabidopsis identified the minimal active moiety of Sirtinol to be 2-Hydroxy-1-naphthaldehyde (HNA)[146], which is the same as Heatin's M.A.C. but hydrolysed on the amide. Considering the atypical suppression of hypocotyl elongation by **#203/Sirtinol** and the concentration-dependency of **#301/M.A.C.**-mediated elongation, we assayed HNA effects on hypocotyl elongation over a concentration range. This experiment demonstrated that at concentrations lower than the ones used by Zhao *et al.,* 2003 and Dai *et al.,* 2005[145,146],

HNA is able to induce significant hypocotyl elongation (**Fig. 3.3E**), without significantly affecting other phenotypes such as root growth or gravitropy (data not shown).

Several *sirtinol resistant* (*sir*) mutants were identified in a mutant screen and most *sir* mutants have defects in Molybdenum cofactor (MoCo) biosynthesis[145,146]. Based on structure-activity relationship studies and additional genetic data, the current hypothesis is that Sirtinol is metabolised from its minimal active moiety HNA to active 2-Hydroxy-1naphthoic acid (HNC) by MoCo-dependent aldehyde oxidase activity. HNC subsequently binds the $SCF^{TIR1/AFB}$ auxin receptor complex, resulting in the activation of auxin signalling and (inhibition of) elongation growth effects[147]. Accordingly, several auxin signalling components were identified in a screen for Sirtinol resistant mutants, such as *AtCAND1*, which is involved in functioning of the SCF-complex[148]. Moreover, the *arf7-1 arf19-1* auxin signalling mutant is resistant to Sirtinol[149].

To test for a possible interaction between Sirtinol and Heatin, we assayed hypocotyl elongation in Sirtinol resistant mutants *sir1*, *sir3-1*, *sirN22A* in the presence of Heatin. We found that these mutants were resistant to Heatin as well (**Fig. 3.4A**). The auxin signalling mutant *Atcand1-2* was resistant to Heatin (**Fig. 3.4A**) but remarkably, *arf7-1* and *arf7-1 arf19-1* HNA-resistant auxin mutants[149] retained their sensitivity to Heatin application, showing these *ARF*s do not play a role in Heatin signalling (**Fig. 3.4B**). In addition, *arf7-1 arf19-1* mutants are constitutively agravitropic and when tested in the presence of Picloram show elongated hypocotyls (**Fig. 3.4B**), but not epinasty of cotyledons nor effects on root length (**Fig S3.4A**). This suggests that *ARF7* and *ARF19* are involved in specific auxin responses or are involved in auxin responses in specific tissues. As *ARF7* and *ARF19* are expressed throughout the seedling, including the hypocotyl (TRAVA public database[150], **Fig S3.4B**) the former is the most likely explanation. These findings suggest that auxin signalling is essential for Heatin signalling but in a manner distinct from HNA and Picloram.

To test whether MoCo-dependent aldehyde oxidation is required for Heatin bioactivity, similar to Sirtinol, hypocotyl lengths of various mutants of each of the four aldehyde oxidases in Arabidopsis were quantified in response to Heatin application. Of all tested lines, only *aao2* mutants exhibited mild, yet consistent, reduced sensitivity to Heatin (**Fig. 3.4C**). Expression data from the TRAVA public database indicated that *AAO1* and *AAO2* transcripts are the most abundant in young seedlings tissues[150] (**Fig. S3.3A**). We therefore reasoned that AAO1 and AAO2 could have redundant functions in young seedlings, potentially masking effects on sensitivity in single *aao1* and *aao2* mutants. RT-PCR was performed to check expression levels of *AAO1* and *AAO2* in the *aao1* and *aao2* mutants. We found that no full length *AAO1* and *AAO2* transcripts were produced in *aao1-1* and *aao2-1*, respectively, but that the C-terminal part of the transcripts were still detected, albeit at lower levels (**Fig. S3.3C**). We combined the two mutant alleles by crossing and found that the resulting *aao1aao2* double mutant was almost completely insensitive to Heatin (**Fig. 3.4D**), whereas high temperature-induced hypocotyl elongation was

retained. This suggests that *AAO1* and *AAO2* are the main *AAO*s contributing to the Heatin effect, and that Sirtinol and Heatin likely act through similar molecular mechanisms.

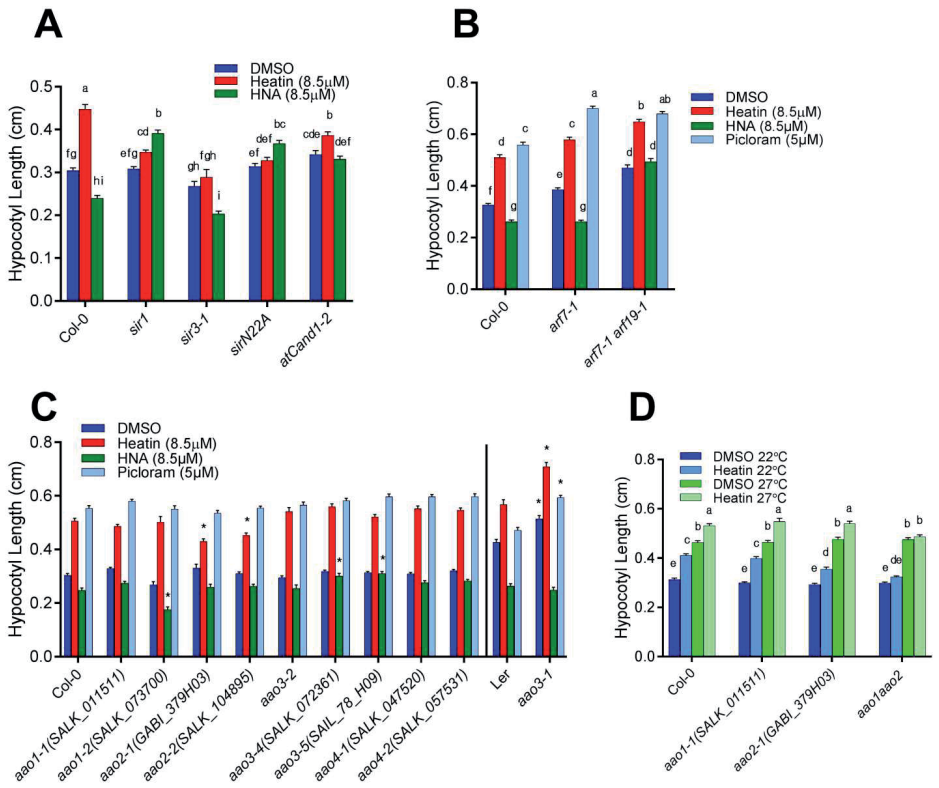

Figure 3.4: The molybdenum cofactor-dependent enzymes *AAO1* and *AAO2* function redundantly in Heatin-induced elongation.

(**A, B, C**) Hypocotyl lengths of 8-day old seedlings of indicated genotypes grown on medium containing either DMSO (blue bars), 8.5µM Heatin (red bars), 8.5µM HNA (green bars) or 5µM Picloram (light blue bars, **B** and **C** only). All mutants are in the Col-0 WT background except *aao3-1*, which is in the L*er* genetic background. (**D**) Hypocotyl lengths of 8-day-old seedlings of indicated genotypes grown on medium containing either DMSO (dark blue and bright green bars) or 8.5µM Heatin (light blue or light green bars) at either 22°C (blue bars) or 27°C (green bars). Error bars indicate standard error of the mean. Values are averages of 3 repeats, each containing 15-25 seedlings (**A**, **B**). Letters indicate significance groups following Tukey HSD post-hoc tests, where averages that do not share letters are significantly different at $p<0.05$ (**A**, **B**, **D**). Asterisks indicate significant difference from the corresponding WT averages at $p<0.05$ (**C**).

Heatin-directed elongation depends on auxin signalling but does not activate the *DR5* reporter nor modulate bioactive auxin levels

Because Sirtinol/HNA effects on hypocotyl elongation depend on auxin signalling[145,146], we tested whether Heatin-mediated hypocotyl elongation has a similar auxin signalling requirement. Sirtinol was identified based on its ability to activate the auxin-sensitive *DR5* promoter. We therefore tested Heatin's ability to stimulate *eDR5:Luciferase* activity[151] but no effect of Heatin on *DR5* promoter activity was observed after 2 days of growth on Heatin containing medium, compared to DMSO. After 6 days, a small reduction in *DR5* signalling at 22°C was observed. In contrast and as expected Picloram induced Luciferase activity 10-100-fold in 2-day-old seedlings grown at 27°C as well as 6-day-old seedlings grown at 22°C or 27°C. NPA treatment caused a slight increase in signal in 6-day-old samples (**Fig. 3.5A**).

Next, mutants disturbed in the $SCF^{TIR1/AFB}$ auxin receptor complex were tested for Heatin sensitivity. Single *tir1-1* and *afb5-5* mutants showed mildly reduced sensitivity to Heatin (**Fig. 3.5B**), whereas the double *tir1-1 afb2-3* mutant was more resistant, suggesting genetic redundancy between different auxin receptors for Heatin activity. Surprisingly, *afb3-4* was hypersensitive to Heatin. *axr1-3* mutants, which are disturbed in a protein that catalyses an essential RUB1 conjugation step in $SCF^{TIR1/AFB}$ complex formation[152,153], was unresponsive to Heatin (**Fig. 3.5B**).

We next compared Heatin-sensitivity to Picloram-sensitivity in these mutants. The *afb5-5* was completely insensitive to Picloram, as previously described[154]. Strikingly, it still retained a reduced but significant responsiveness to Heatin (**Fig. 3.5B**). To further characterise the suspected redundancy, we tested the single mutants as well as the *tir1-1 afb2-3* and *tir1-1afb5* double mutants at two Heatin concentrations. The *tir1-1*, *tir1-1 afb2-3* and *afb5-5* mutants showed significant resistance to both 8.5 µM and 25 µM Heatin but were not fully insensitive. Moreover, at 25 µM Heatin the hypocotyls were longer than at 8.5 µM in all these mutants, whereas the *axr1-3* and *tir1-1 afb5* mutants were insensitive to 8.5 µM Heatin and also strongly resistant to 25 µM Heatin (**Fig. 3.5C**). These data suggest that although *DR5* promoter activity was not activated by Heatin, auxin signalling pathways are essential to Heatin signalling. In particular, TIR1 and AFB5 are two of the main auxin receptors involved, with an apparent lesser role for AFB2.

To test if Heatin application results in increased auxin levels, free IAA levels were measured using liquid chromatography-tandem mass spectrometry. Whereas ANOVA-analysis shows that high temperatures as expected resulted in higher free IAA levels in 7-day old seedlings (**Supplemental file 3.2**,[56,155]), no effects of Heatin on auxin levels were found (**Supplemental file 3.2, Fig. 3.5D**).

Finally, to establish whether Heatin and Picloram work through the same signalling pathways, a Heatin dose-response assay was done in the presence of different concentrations of Picloram. Heatin had an additive effect on hypocotyl elongation at 0.5 µM and 1 µM Picloram, whereas at higher Picloram concentrations Heatin did not further contribute to hypocotyl length at the tested concentrations and in fact caused a reduction

in hypocotyl length at the highest tested concentrations of Picloram (**Fig. 3.5E**). These pharmacological data suggest that Heatin and Picloram satiate the same auxin signalling mechanism, in line with the genetic data (**Fig. 3.5B**).

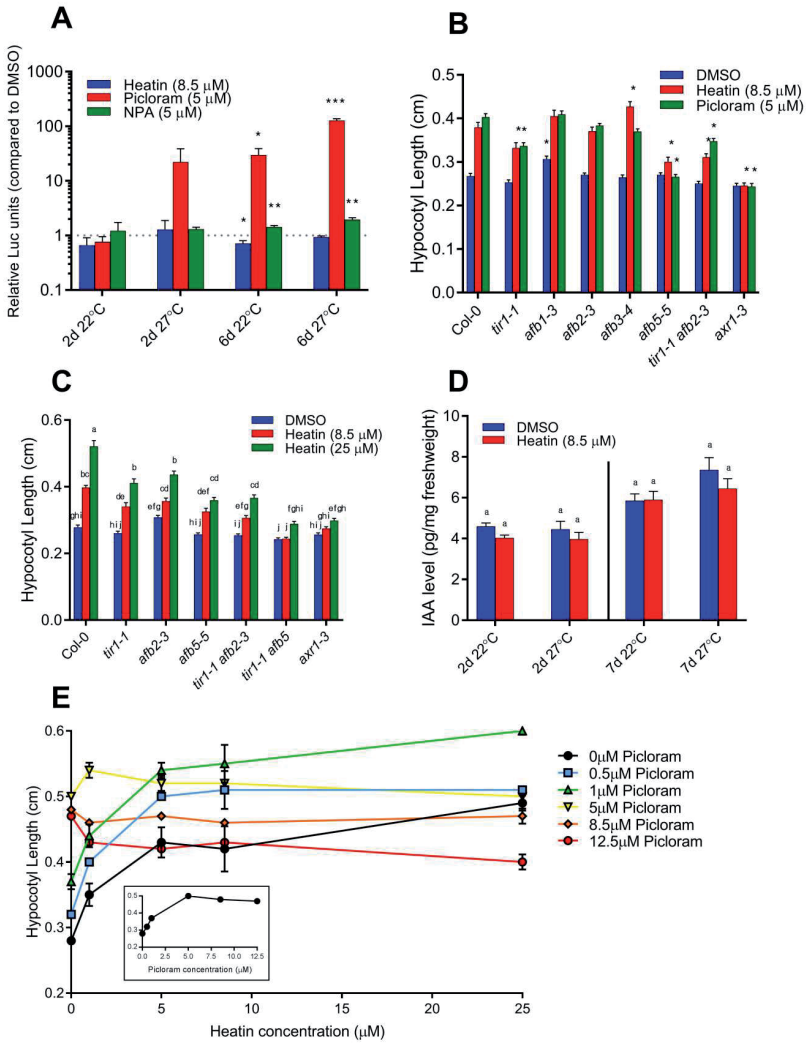

Figure 3.5: Heatin action requires auxin signalling.

(A) Luciferase activity of *eDR5:LUC* seedlings grown on medium containing 8.5μM Heatin (blue bars), 5μM Picloram (red bars) or 5μM NPA (green bars), compared to the DMSO mock treated *eDR5:LUC* activity in 2- or 6-day-old seedlings, grown at the indicated temperature. The dotted horizontal line indicates no change compared to mock. Asteriks indicates significant difference from 1, as tested by one-sample t-test. (B, C) Hypocotyl lengths of 8-day-old seedlings of indicated genotypes grown on medium containing either DMSO (blue bars), 8.5μM Heatin (red bars), 5μM Picloram (green bars) in panel B or containing either DMSO (blue bars), 8.5μM Heatin (red bars), 25μM Heatin (green bars) in panel C. (D) endogenous IAA levels of whole seedlings grown for 2 or 7 days at the indicated

temperatures in medium containing DMSO (blue bars) or 8.5μM Heatin (red bars). (E) Hypocotyl lengths of 8-day old Col-0 WT seedlings grown on medium containing different concentrations of Picloram (0μM: black circles, 0.5μM: blue squares, 1μM: green upward triangles, 5μM: yellow downward triangles, 8.5μM: orange diamonds, 12.5μM: red circles) and at different concentrations of Heatin (indicated on X-axis). Inset shows picloram dose responsive hypocotyl elongation in the absence of Heatin. Error bars indicate standard error of the mean, values are averages of 3-5 repeats of each 15-25 seedlings (A-C, E) or 5-10 repeats containing 25mg of freshweight (D). Asterisks indicate significant differences from 1 as determined by one-sample t-test (A), with * = $p<0.05$, ** = $p<0.01$, or significant difference from the corresponding Col-0 WT averages (B). Letters indicate significance groups following Tukey HSD post-hoc tests, where averages that do not share letters are significantly different at $p<0.05$ (C, D).

Discussion

Heatin is a small molecule that causes hypocotyl elongation in a dose responsive manner in young Arabidopsis seedlings (**Chapter 2**). In this chapter, we demonstrated that Heatin application resembles thermomorphogenesis phenotypes also at the adult vegetative plant stage; *i.e.* Heatin stimulates a more open rosette structure mainly through increased hyponastic growth and a decrease in the leaf/petiole ratio. It is known that the phytohormone auxin is required for thermomorphogenesis[36] and that the synthetic auxin picloram can rescue hypocotyl elongation of plants carrying a mutation in the high ambient temperature signalling hub PIF4[37,56,155]. Our data however indicate that Heatin effects are distinct from those observed after application of the synthetic auxin picloram. Considering young seedlings, Heatin effects were only observed in the hypocotyl, whereas picloram effects are more pleiotropic as effects are also observed on root length and agravitropy (**Fig. 3.1**). Moreover, mutants disturbed in the auxin receptor AFB5 are completely insensitive to picloram, whereas they remain partially sensitive to Heatin (**Fig. 3.5B,C**). Additionally, Picloram strongly induced the artificial *DR5* auxin signalling reporter, whereas no effects on *DR5* were observed upon Heatin application (**Fig. 3.5A**). Together, these data show that Heatin induces thermomorphogenesis in a manner distinct from canonical auxin application.

Detailed structure-activity relationship studies revealed that 1-aminomethyl-2-naphthol is Heatin's active moiety and minimal active compound. The identification of the bioactive part of the Heatin molecule and the capacity of this moiety to tolerate modification without losing its biological activity is key in the design of Heatin probes with additional chemical groups attched that can be utilized for *e.g.* pulldown experiments, or fluorescent probes that would allow identification of interacting proteins and tracking the compound inside living plants. In **Chapter 5** we build on the structure-activity relationship of Heatin to design a probe and pull-down strategy to directly detect proteins that interact with Heatin.

In a previously chemical genetic screen, focussing on hypocotyl elongation, 100 compounds were identified that induced hypocotyl elongation[92]. One of the identified compounds contains the 1-aminomethyl-2-naphthol moiety, suggesting that this compound causes elongation growth through the same mechanism as Heatin. This compound was also tested in our experimental system (**#401**) to compare its effects to Heatin (**Fig. 3.3D**). The main difference between Heatin and analogue **#401** was that the latter needed a higher concentration than Heatin to be active in the hypocotyl. Nevertheless, this independent finding indicates that the effects described in this chapter do not solely depend on our specific experimental conditions but are general and more widely applicable.

Heatin activates auxin signalling

Based on our results, Heatin can be positioned in current models of thermomorphogenesis signalling. Since *pif4-2* retained sensitivity for Heatin (**Fig. 3.1, 3.2**), we conclude that Heatin acts downstream of -or parallel to- PIF4 activity during elongation growhth. Because auxin signalling is essential for Heatin activity, and given its structural homology to the previous described auxigenic compound Sirtinol[145,146,148], Heatin likely acts upstream of the $SCF^{TIR1/AFB}$ auxin receptor complex. Further studies into the requirement of thermo-signalling components for Heatin sensitivity are needed to fully understand the relation between thermomorphogenesis and Heatin-mediated elongation growth.

Although Sirtinol was published as a repressor of hypocotyl elongation[93,105], we found that this compound can stimulate hypocotyl elongation at low concentrations. We show that Heatin and Piclopram act additive and that auxin signalling pathways are essential for Heatin-mediated hypocotyl elongation, but that Heatin does not activate the *DR5* promoter, nor results in elevated levels of bioactive auxin (IAA). Assuming that Heatin and Sirtinol affect the same hypocotyl elongation mechanism[105], would suggest that Heatin is metabolised *in planta* and should be considered an auxigenic compound as well, similar to Sirtinol, despite its inability to induce *DR5*. This is supported by the requirement of intact auxin signalling for Heatin effectiveness and indirectly by the observation that levels of bioactive IAA are not altered by Heatin (**Fig. 3.5B-D**). Moreover, combining low levels of Heatin and IAA that each would stimulate elongation in isolation, leads to repression of hypocotyl elongation (**Fig. 3.5E**). We therefore conclude that Heatin and Picloram likely share signalling pathway(s). Nevertheless, as mentioned above, aspects of the Heatin response differ from the response to auxin application (**Fig. 3.1, 3.5**), suggesting that Picloram and Heatin also act in part through independent mechanisms. This could possibly involve AFB3, since mutants in this auxin receptor component are hypersensitive to Heatin, whereas Picloram sensitivity is retained (**Fig. 3.5B**), or *ARF7* and *ARF19*. *ARF7* and *ARF19* are involved in Sirtinol signalling[149] and function downstream of the $SCF^{TIR1/AFB}$ receptor complex in auxin signalling, but do not play an apparent role in Heatin signalling (**Fig. 3.4B**), arguing that Heatin either uses different *ARF* gene family members, or works

via a different signalling pathway. Published results also indicate that Sirtinol is not able to enhance interactions between TIR1 and Domain II of AUX/IAA proteins *in planta*. This is in contrast to the frequently used synthetic auxin, 1-Naphthaleneacetic acid (NAA)[156]. Thus, Sirtinol and Heatin depend on functional auxin signalling for their effects but likely involve partly different downstream signalling mechanisms compared to classic auxins.

If Heatin would act as a genuine auxin it would be expected to activate the *DR5* promoter, as does Sirtinol[93]. An explanation for the absence of *DR5* reporter activation and IAA accumulation by Heatin application is that Heatin could be cell or tissue specific, unlike Sirtinol, which could mask detection of its activity in the whole seedling. Auxin signalling is also regulated by the circadian clock[151,157], which could mean that any differences in auxin levels or signalling may have been missed due to the time of sampling. Indeed, Covington *et al.* (2007) showed that whereas treatment with IAA resulted in continuously elevated *DR5::LUC* output, 2,4-D, a frequently used synthetic auxin, only resulted in transient elevation[151]. Similarly, Heatin might elevate *DR5* promoter activity transiently, but shows no changes at the dawn of day 3 or 7, the moments when we sampled.

An intruiging question is how Heatin specifically triggers elongation of hypocotyls without affecting root growth, epinasty or agravitropy in seedlings. Although receptor specificity is a possible explanation, it probably does not apply to the TIR1/AFB proteins of the receptor complex, as picloram is highly specific for AFB5[158], but does cause many other auxinic phenotypes (**Fig. 3.1H**). The binding and degradation of specific AUX/IAA proteins could be explanatory, as these form a large family with different substrate specificities and binding dynamics[66].

Another possible explanation for Heatin's hypocotyl specificity in seedlings comes from a previous chemical genetic screen on hypocotyl elongation, which identified several auxin analogues that are effectively transported throughout plants and are metabolised *in situ* to release active auxins that stimulated elongation growth[159]. A similar explanation could fit our observations on Heatin-induced hypocotyl elongation. Our structure-activity relationship data showed that removal of the hydroxyl group on 1-aminomethyl-2-naphthol causes the compound to lose its hypocotyl specificity. Moreover, the removal of the non-essential parts of the Heatin structure strongly affect the concentrations at which activity is observed (**Fig. 3.3**). This supports the idea that Heatin is transported effectivly inside the plant through active or passive mechanisms, and is metabolised *in situ* to release an auxinic compound.

The discovery that, of the four *AAO* family members, *AAO1* and *AAO2* are the main contributors to the Heatin effect, is consistent with previous data showing that AAO2 has a strong and specific affinity for 1-Napthaldehyde, whereas AAO1 has a broad substrate specificity[160]. *AAO1* and *AAO2* expression in seedling tissues is much higher than that of the other two *AAO* genes (**Fig. S3.3**). Our data also provides support for the hypothesis that the resistance of *sir1*, a mutant critically disturbed in MoCo biosynthesis, to Sirtinol

and Heatin is due to a lack of aldehyde oxidation capacity[146] and not due to other MoCo dependent enzymes, and that aldehyde oxidation plays a key role in the conversion of HNA to HNC. Whereas AAO1 has been connected to IAA biosynthesis as well as the biosynthesis of defence-related compounds[161,162], AAO3 and AAO4 have been found to play a role in abscisic acid biosynthesis in developing siliques and dry seeds as well as leaf tissue[163,164]. This is consistent with the discovery of *AAO1* and *AAO2* to be the main contributors to Heatin effects in seedlings. No specific natural function for *AAO2* has been found so far. We show that the *aao1-1 aao2-1* double mutant is still responsive to temperature, showing these genes do not play a role in thermomorphogenesis.

Materials and Methods

Plant materials and growth conditions

Arabidopsis seeds were obtained from the Nothingham Arabidopsis stock center (www.Arabidopsis.info) or were kind gifts of colleagues. The following published lines were used: L*er* and Col-0 wild type, *pif4-2*[165], *sir1*[93], *sir3-1*[146], *sir/N22A*[166], *atCand1-2* (homozygous genotyped SALK_099479)[148], *tir1-1*[167], *afb1-3*[159], *afb2-3*[159], *afb3-4*[168], *afb5-5*[154], *tir1-1 afb2-3*[159], *tir1-1 afb5-5*[169], *axr1-3*[170], *eDR5::LUC*[151], *aao3-1*[163], *aao3-2*[171], *aao3-4* (homozygous genotyped SALK_072361)[163], *aao4-1* (homozygous genotyped SALK_047520)[172], *aao4-2* (homozygous genotyped SALK_057531)[172], *gpa1-4*[173], *agb1-2*[174], *gpa1-4 agb1-2*[174], *gcr1-2*[175], *gcr2-4*[176], *agg1c*[177], *agg1-1cagg2-1*[177], *rgs1-1*[178], *gcr triple*[179], *arf7-1*[180], *arf7-1arf19-1*[180]. The following genotyped homozygous T-DNA insertional lines were generated[181]: SALK_073700 (*aao1-2*), SALK_011511 (*aao1-1*), SALK_104895 (*aao2-2*), GABI_379H03 (*aao2-1*), SAIL_78_H09 (*aao3-5*). The *aao1 aao2* double mutant was made by crossing of the SALK_011511 and GABI_379H03 lines. Selection of homozygous plants was done by checking for the insertion by PCR. Primers for genotyping are shown in **table S3.1**. Expression of *AAO1* and *AAO2* in the double mutant and single mutant parents was checked by RT-PCR and no full-length transcripts was found (**Fig. S3.3**)

Plants for hypocotyl length, root length, Luciferase and IAA level quantification assays were grown on sterile 0.8% plant agar (Duchefa P1001), 1x Murashige-Skoog medium (MS, including MES Buffer and vitamines, Duchefa M0255) without sucrose in petri-dishes. Seeds were surface sterilized by either a solution of 0.8% commercial bleach (Glorix) in ethanol for 10 minutes, followed by twice washing with ethanol for 10 minutes, or by chlorine gas for 3 hours. After sowing, seeds were stratified for 2-3 days at 4°C in the dark. The petri-dishes containing the plants were subsequently grown under 100 µmol m^{-2} s^{-1} white light short day conditions (8 hours light/16 hours darkness) at 70% relative humidity in climate-controlled Microclima 1000 growth cabinets (Snijders) at either 22°C (control) or 27°C (high temperature).

Phenotyping

To enable hypocotyl length measurements, petri-dishes with seedlings were pictured after 8 days using a flatbed scanner. Hypocotyl or root lengths were measured using ImageJ software (https://imagej.nih.gov/ij/).

For rosette trait measurements plants were grown in conditions as indicated above, in 'Sterivent High Containers' (Duchefa, S1686) on sterile 0.8% plant agar (Duchefa P1001), 1x Murashige-Skoog medium (MS, including MES Buffer and vitamines, Duchefa M0255). 6 plants per container were grown in batches until the first plants started bolting. First, photos were taken from the side for leaf angle measurement. The plants were subsequently flattened and photographed from the top. Petiole and leaf blade lengths of all leaves of the plant were measured using ImageJ image-analysis software, starting from the youngest leaf where a petiole was visible. The petiole and leaf blade length per plant was defined as the average of the lengths of the 3th-6th youngest leaves. Plants were weighed and rosette surface was determined using a LI-3100 Surface Area Meter (LI-COR). Hyponastic growth was measured as the average of the angle of two opposing petioles per plant, relative to the horizontal.

Seedling agravitropy was scored by qualification of the growth direction of hypocotyls relative to the direction of gravity. Hypocotyls that deviated more than 45° from the opposite of the direction of gravity, were considered agravitropic. Of note, under complete random directional growth (total absence of gravitropic response) ~ 75% of the seedlings would be marked as agravitropic using this strategy.

Luciferase assays

Protein extracts were made of approximately 25 mg freshly harvested seedlings by grinding with a micro pestle in 100µl 1x passive lysis buffer (PLB, Promega E1941) followed by 10 minutes incubation at RT. Debris was pelleted by 5 minutes maximum speed (rcf 16000) centrifugation. 20µl of supernatant was transferred to a 96-well Lumitrac-200 plate (VWR 82050-726). Luciferase activity was assayed using a Glomax 96 microplate luminometer (Promega, E6521). The 'Luciferase Assay System' (Promega, E1500) was used with the "LUC Assay System with Injector" protocol (2 second delay between injection and measurement, 10 second integration time). Subsequently, protein concentrations were determined of each sample using the Bradford method[182] (Bradford reagent: Sigma-Aldrich, B6916). Absorbance was measured using a Biotech synergy HT plate reader. A Bovine Serum Albumin (Sigma-Aldrich, A7906) standard curve in PLB was used to calculate protein concentrations of each sample. Luciferase signals were corrected for background signal determined by assaying Col-0 wild type, lacking Luciferase, and normalized to the protein concentration of each sample.

Chemical compounds / Structure activity relation assays

Heatin compound used in dose response, structure-activity relationship and mutant analyses experiments was purchased from Chembridge (5713980). Other experiments were performed with *in-house* synthesized Heatin. Synthesis protocol and NMR spectra are in **supplemental information 1**. Names, sources and vendor ID's of all chemicals used for the phenotyping and structure-activity relationship experiments can be found in the **table 3.2**. All compounds were dissolved in DMSO (Sigma-Aldrich, D4540) to a 100mM stock solution. When applicable, stocks were further diluted using DMSO. Solutions were dissolved in the MS-agar medium to a final DMSO concentration of 0.1%. DMSO lacking added compounds was used as solvent (mock) control at the same concentration. Chemical properties of compounds were retrieved from the vendor's information or public chemical databases.

Measurements of free IAA

Indole-3-acetic acid (IAA) was extracted, purified, and analysed as previously described[183] with minor revisions. IAA was extracted from samples of approximately 100 mg at 4°C o/n in 1 ml methanol containing [phenyl $^{13}C_6$]-IAA (0.02 nmol/mL) as internal standard. The methanol fraction was purified by anion-exchange column (Grace Extra Clean Amino 100 mg/1.5 mL Solid Phase Extraction; Grace Davison Discovery Sciences). The volume of the wash and elution solvent was scaled down to 1 ml each to compensate for the reduced column size.

Reverse Transcriptase PCR

For Reverse Transcriptase (RT)-PCR, RNA was isolated from 25mg one week-old whole seedlings using a protocol adjusted from Sánchez & Carbajosa[184]. In short, fresh plant material was ground in 400µl lysis solution (2% SDS, 68mM sodium citrate, 132mM citric acid, 1mM EDTA, pH between 4 and 4.5) and incubated for 5 minutes in movement at room temperature. 133µl protein-DNA precipitation solution (4M NaCl, 16mM sodium citrate, 32mM citric acid) was added to each sample and incubated for 10 minutes on ice. Samples were centrifuged at 16000g for 15 minutes at 4°C. Supernatants were transferred to a new tube and 200µl 2-propanol was added to each sample. After homogenizing, samples were centrifuged at 16000g for 15 minutes at 4°C. supernatants were discarded, and pellets washed twice with 70% ethanol. After drying, pellets were resuspended in 25µl MQ. Nucleotide concentrations were measured using a Nanodrop spectrometer. Subsequently, 2.2µg of total RNA was used for DNAse treatment in a total volume of 20µl, of which 2µl 10x DNAse buffer and 1µl DNAse I enzyme (ThermoScientific). After incubation at 37°C for 30 minutes 2µl 25mM EDTA was added and DNAse I was inactivated by incubating at 65°C for 10 minutes. For cDNA synthesis, 10µl of DNAse treated samples (1µg of RNA) was incubated at 70°C for 5 minutes with 1µl random primers (1pmol/µl) and 1µl anchored oligo dT primers (100pmol/µl). Subsequently 4µl 5x RevertAid

reaction buffer (ThermoScientific EP0452), 2µl 10mM dNTP mix, 0.5µl RevertAid Reverse Transcriptase, 0.3µl Ribolock and 1.2µl MQ was added to each sample and incubated first 60 minutes at 42°C and then 10 minutes at 70°C. cDNA was diluted tenfold before being tested in an RT-PCR with the following program settings: 4 minutes 94°C, 35 cycles of 30 seconds 94°C, 30 seconds 57°C and 1 minute 72°C, followed by 5 minutes at 72°C. For primers see **table S3.1.**

Statistical analyses

All Data was analyzed using ANOVA followed by post-hoc Tukey HSD tests using a script in R (**Supplemental file 3.1**), or when values relative to control are shown, by a one-sample t-test comparing to the number 1.

Acknowledgements

The authors would like to thank Gruson Klaasse and Colin Snoeker for practical assistance and Florian Bittner, Stacey Harmer, Rhonda Foley and Marcel Quint for providing seeds. This work was supported by *NWO Graduateschool Uitgangsmaterialen* grant NWO#831.13.002 to LvdW and MvZ.

Supplemental Figures and Tables

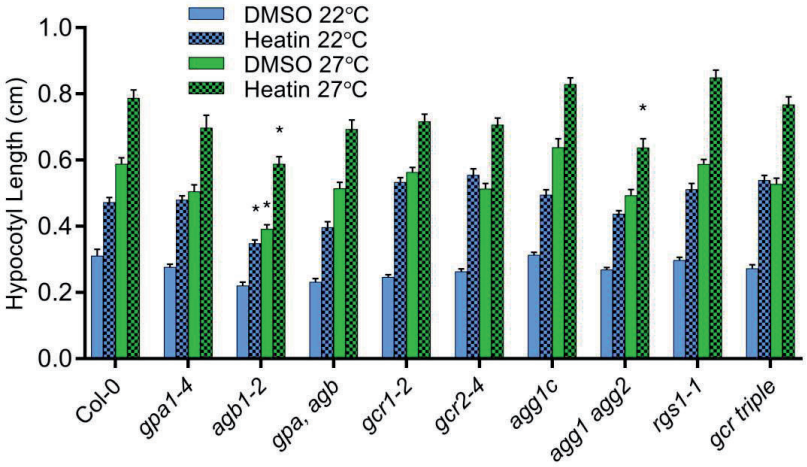

Supplemental figure 3.1: G-protein signalling complex mutants do not show altered Heatin sensitivity.

Hypocotyl length of 8-day-old seedlings of the indicated genotype grown on medium containing either DMSO (clear bars) or 8,5µM Heatin (blocked bars) at 22°C (blue bars) or 27°C (green bars). Values are averages of 2 replicates of each 15-25 seedlings. Error bars denote standard error of mean. Asterisks indicate significant difference compared to the WT value at $p<0.05$ as determined by Student's t-test.

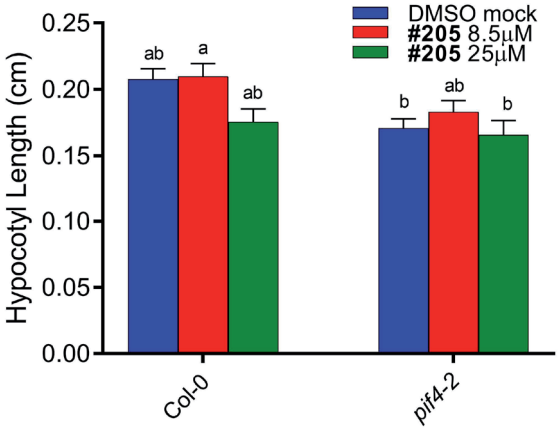

Supplemental figure 3.2: Heatin analogue #205 does not induce hypocotyl elongation.

Hypocotyl length of 8-day-old seedlings of the indicated genotype grown on medium containing either DMSO (blue bars), 8,5µM analogue #205 (red bars) or 25µM analogue #205 (green bars) at 22°C. Higher concentrations were lethal (not shown). Values are averages of ~15 seedlings. Error bars denote standard error of mean. Letters indicate significant groups following Tukey HSD post-hoc tests, where averages that do not share letters are significantly different at $p<0.05$.

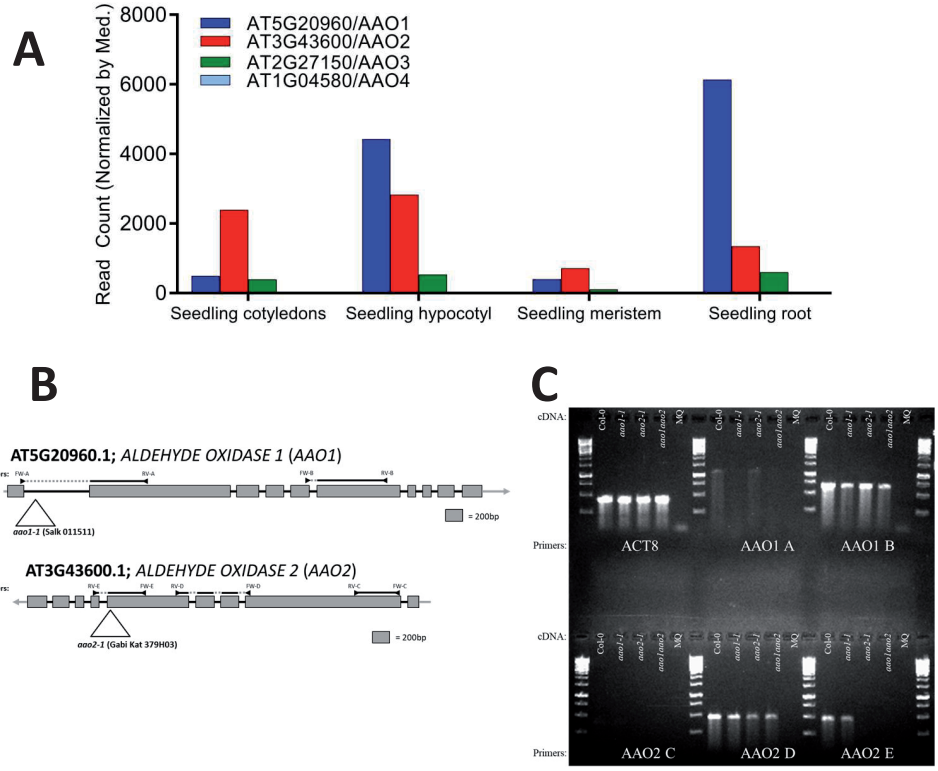

Supplemental figure 3.3: Characterization of *aoo* mutants.

(**A**) Normalized RNA-seq read counts of *AAO1, AAO2, AAO3* and *AOO4* in young Arabidopsis seedlings. Data is derived from the TraVA database (http://travadb.org/). (**B**) gene models for *AAO1* and *AAO2*, showing positions of T-DNA inserts and RT-primer locations. (**C**) Agarose gel showing reverse transcriptase PCR results after 35 cycles. Primers indicated correspond to those indicated in panel **B**. ACT8 is used as a control and the 1-kb gene-ruler (Thermo Fisher) is included as size marker

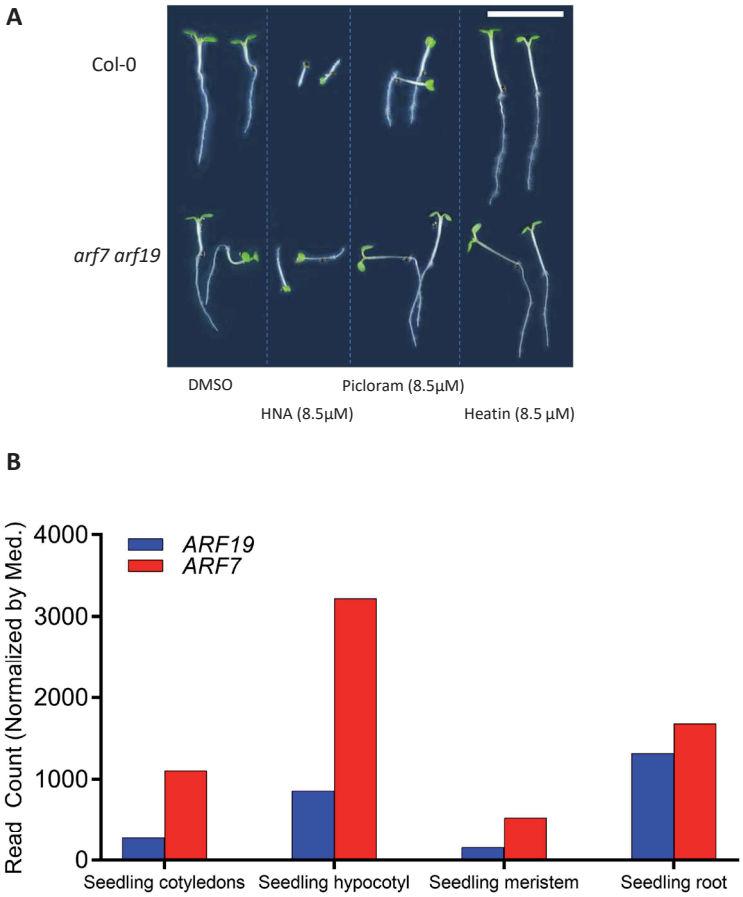

Supplemental figure 3.4:

(**A**) Phenotypes of representative WT and *arf7 arf19* mutant seedlings grown on the indicated compound. Scale bar indicates 1 cm. (**B**) Normalized RNA-seq read count of *ARF7* and *ARF19* in young Arabidopsis seedlings. Data retrieved and selected from the TraVA database (http://travadb.org/).

Supplemental table 3.1: Primers used in this study.

Left, right and insertion primers are given for genotyping primers. Forward and reverse are given for RT-PCR primers. Notes denote the used annealing temperature.

Primers set	Left Primer	Right Primer	Insertion primer	notes
SALK_011511	TGAGGTAGTGATGGAACAGCC	GTGAGAAAGCGATTGACGAAG	ATTTTGCCGATTTCGGAAC (LBb1.3)	57°C
SALK_152424	AACAGGTGATGATGGTGAAGC	CTCTGCTTCCACAACCGTAAG	ATTTTGCCGATTTCGGAAC (LBb1.3)	60°C-56°C
SALK_104895	ACTGCATGGGAGTGTCTTTTG	GAGGTTTTGGAGGGAAATCTG	ATTTTGCCGATTTCGGAAC (LBb1.3)	60°C-58°C, 53°C-50°C
GABI_379H03	TTAACAGCCTGTCTGGTAGCG	TTGGCGTATCTTCCAAGTTTG	GTGGATTGATGTGATATCTCC (o3144/35St)	54°C
SALK_072361	TTCTATTGGAAATGCATTGCC	TAAAACATCGGATGAACCTCG	ATTTTGCCGATTTCGGAAC (LBb1.3)	59°C-50°C
SAIL_78_H09	TTTCTTGAATTGTCTCCGGTG	TAAAACATCGGATGAACCTCG	TAGCATCTGAATTTCATAACCAATCTCGATACAC (LB3)	54°C
SALK_047520	AATTAGTTGTTGGCAACACGG	ATGCTCCATGTAGACAATGGG	ATTTTGCCGATTTCGGAAC (LBb1.3)	60°C-50°C
SALK_057531	ATGCTCCATGTAGACAATGGG	AATTAGTTGTTGGCAACACGG	ATTTTGCCGATTTCGGAAC (LBb1.3)	51°C, 60°C
SALK_099479	ATTTCGGATCCCATCAAAATC	AAGCTATACTCGCGAAGCTCC	ATTTTGCCGATTTCGGAAC (LBb1.3)	58°C
Primers set	**Forward Primer**	**Reverse Primer**		notes
AAO1-1	AAGCTTGGTTGTGGCGAAGGTG	TTCTTCGCGGAGTGCCAAGATG		57°C
AAO1-2	GCCGTGAAATCAATGCCTGTTGC	TCCCGGTGTTGATCGCATGTTC		57°C
AAO2-1	AGTCGAAGATTTCACTGTGAGC	ATCAAACCGAGTTAAACTACTAGAATC		57°C
AAO2-2	GAATGCATCGCCTTCGTGGTTG	ACAGGACGCTGCAGTTTCTTAGC		57°C
AAO2-3	TGTGGAGAAAACGAGGGATA	TCAGGTACTGCATGGGAGTG		57°C

Supplementary information and files

Supplemental files are available on request (lennardcasper@yahoo.com):

Supplemental file 3.1. R script for ANOVA/Tukey HSD analysis

Supplemental file 3.2. Results of ANOVAs performed in this chapter

Supplemental information 3.1 – Heatin synthesis

Ethyl naphthalen-1-ylalaninate

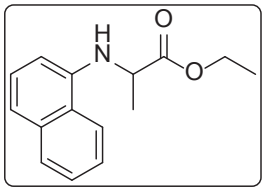

2-napthylamine (2.86 g, 20.00 mmol) and triethylamine (7.00 ml, 2.5 eq.) were dissolved in 30 ml dry DMF. Ethyl-2-bromopropionate (2.85 ml, 1.1 eq.) was added and the mixture was heated to 60°C and stirred for 14H. The mixture was concentrated in vacuo, the residue redissolved in DCM, extracted with H_2O. The organic layer was dried with Na_2SO_4, concentrated in vacuo and purified by column chromatography (4:1 hexanes/EtOAc) yielding ethyl naphthalen-1-ylalaninate (3.94 g, 80%).

Analytical data: ^{1}H NMR (400 MHz, CDCl3) δ 7.89 (m, 1H), 7.83 – 7.71 (m, 1H), 7.52 – 7.37 (m, 2H), 7.35 – 7.21 (m, 2H), 6.53 (d, 1H), 4.94 (d, 1H), 4.40 – 4.26 (m, 1H), 4.26 – 4.11 (m, 2H), 1.59 (m, 3H), 1.26 (m, 3H).

2-(naphthalen-1-ylamino)propanehydrazide

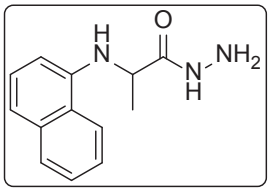

Ethyl naphthalen-1-ylalaninate (4,00 g, 16,44 mmol) was dissolved in 30 ml of ethanol. Hydrazine hydrate (8.4 ml, 10 eq.) was added and the mixture was heated to reflux for and stirred for 3H. The mixture was concentrated in vacuo, redissolved in DCM, extracted with H_2O, the organic layer dried with Na_2SO_4, concentrated in vacuo and purified by column chromatography (97:3 DCM/MeOH) yielding 2-(naphthalen-1-ylamino) propanehydrazide (3.24 g, 86%).

Analytical data: ^{1}H NMR (400 MHz, CD_3OD) δ 8.06 (dd, 1H), 7.69 (dd, 1H), 7.57 – 7.33 (m, 2H), 7.33 – 7.03 (m, 2H), 6.48 (t, 1H), 4.19 – 3.94 (m, 1H), 1.54 (m, 3H).

N′-((2-hydroxynaphthalen-1-yl)methylene)-2-(naphthalen-1-ylamino)propanehydrazide

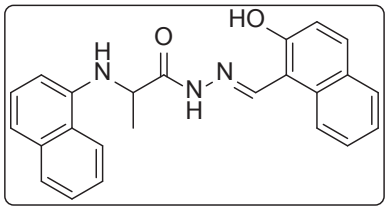

2-(naphthalen-1-ylamino)propanehydrazide (2.8 g, 12.21 mmol) was dissolved in ethanol and 1-hydroxy-2-naphthaldehyde (2.09 g, 1 eq.) was added. The reaction mixture was refluxed for 2H and the yellowish precipitate was collected by vacuum filtration, yielding N′-((2-hydroxynaphthalen-1-yl)methylene)-2-(naphthalen-1-ylamino)propanehydrazide (4.12 g, 88%). ^{1}H NMR spectrum matches the commercially available compound.

Analytical data: ^{1}H NMR (400 MHz, DMSO-*d6*) δ 9.28 (s, 1H), 8.93 (s, 1H), 8.80 (d, , 1H), 8.42 – 8.25 (m, 1H), 8.17 (d, 1H), 7.85 (dd, 2H), 7.78 – 7.67 (m, 1H), 7.63 – 6.99 (m, 7H), 6.46 (d, 1H), 6.39 – 6.14 (m, 1H), 4.99 (dd, 1H), 4.19 (m, 1H), 1.60 (m, 3H).

ethyl naphthalen-1-ylalaninate ^{1}H NMR (400 MHz, $CDCl_3$)

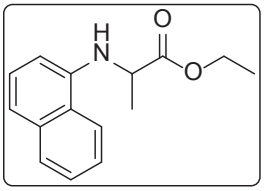

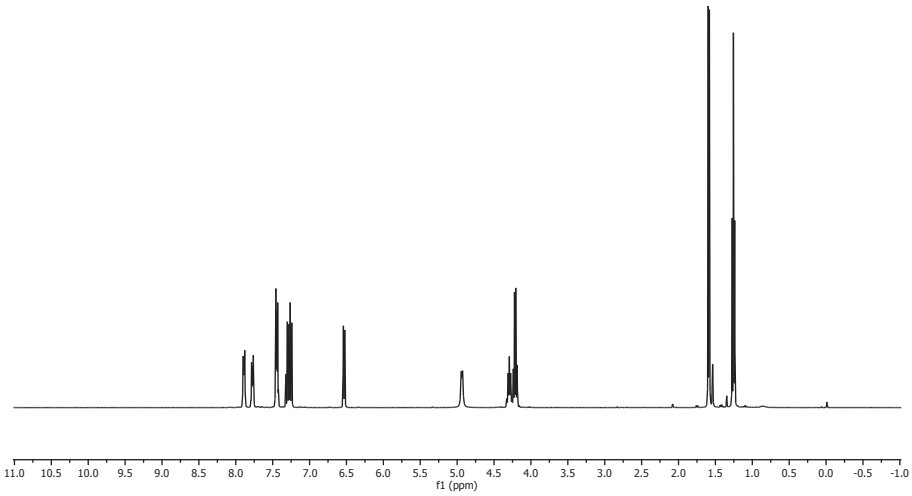

2-(naphthalen-1-ylamino)propanehydrazide 1H NMR (400 MHz, CD3OD)

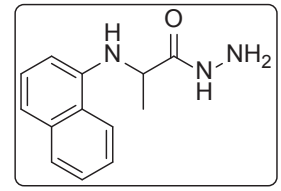

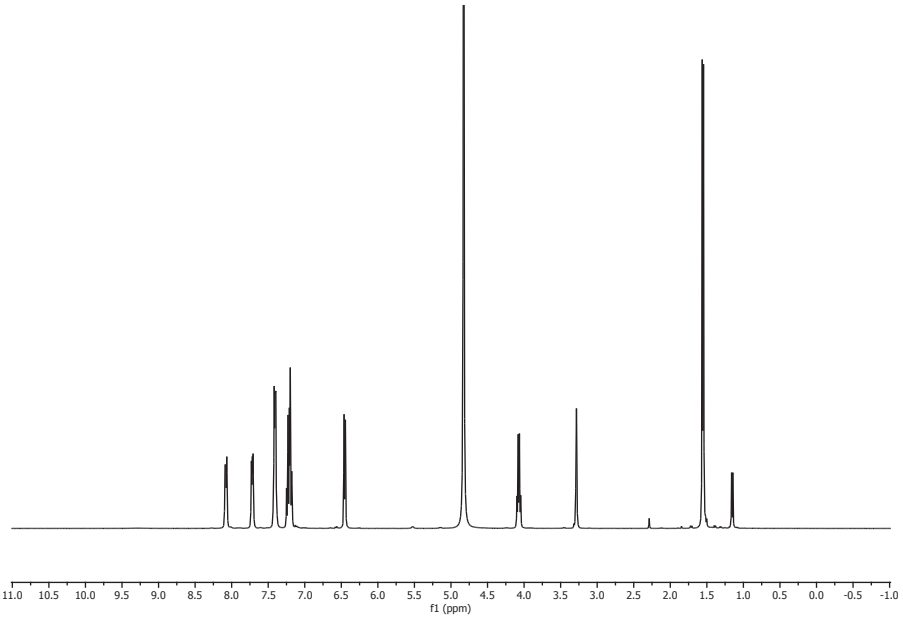

N′-((2-hydroxynaphthalen-1-yl)methylene)-2-(naphthalen-1-ylamino)propanehydrazide
^{1}H NMR (400 MHz, DMSO-*d6*)

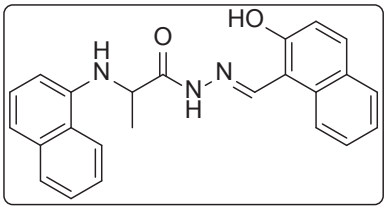

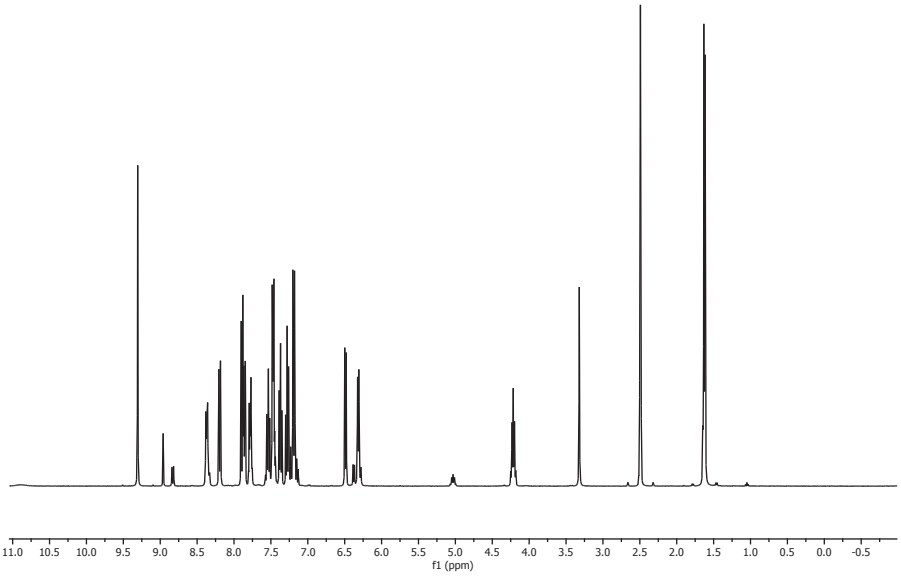

CHAPTER 4

Comparative transcriptomics, proteomics and metabolomics of high ambient temperature and Heatin effects in Arabidopsis seedlings

Lennard van der Woude[1] | Twan America[2] | Henriëtte van Eekelen[2] | Roland Mumm[2] | Marcel van Verk[3,4*] | Sjef Smeekens[1] | Martijn van Zanten[1]

[1] Molecular Plant Physiology, Institute of Environmental Biology, Utrecht University, Padualaan 8, 3584 CH Utrecht, The Netherlands
[2] Wagening Plant Research, Wageningen University and Research, Droevendaalsesteeg 1, 6708 PB Wageningen, The Netherlands
[3] Plant-Microbe Interactions, Institute of Environmental Biology, Utrecht University, Padualaan 8, 3584 CH Utrecht, The Netherlands
[4] Theoretical Biology and Bioinformatics, Institute of Biodynamics and Biocomplexity Utrecht University, Padualaan 8, 3584 CH Utrecht, The Netherlands
* Current address: Keygene, Agro Business Park 90, 6708 PW Wageningen, The Netherlands

Abstract

In response to high ambient temperatures, plants display a set of acclimation responses collectively called thermomorphogenesis. We have identified a small molecule termed Heatin that mimics thermomorphogenesis in the model plant Arabidopsis. As high ambient temperature affects many processes in the plant, identifying factors that contribute specifically to thermomorphogenesis has proven difficult. Here we apply high ambient temperature and Heatin to detect thermomorphogenesis-specific factors using large scale comparative -omics approaches.

First, dynamics of high temperature- and Heatin-induced elongation growth over time were quantified. With this data, two relevant time points for sampling were identified, constituting an early and late timepoint. RNA-seq analysis revealed Heatin-induced changes to the transcriptome under control temperature conditions overlapped strongly with the high temperature-induced differential transcriptome, allowing us to identify several candidate genes that potentially regulate thermomorphogenesis. Proteomic and metabolomic analyses do not show changes of the same magnitude and are a poor translation of the results found by RNA-seq.

Introduction

Plants need to continuously adapt to ensure optimal growth under suboptimal environmental conditions. One of the prevalent environmental factors plants have to deal with is high ambient temperature, to which plants acclimate in a process called thermomorphogenesis[131,185]. Thermomorphogenesis is defined as a set of architectural adaptations that enhance plant cooling capacity and stimulate avoidance of heat flux[44,45]. These morphological changes to accommodate optimal growth[115] ultimately result from changes within the plant on the level of physiology and metabolism, which in turn are the result of functional changes on *e.g.* the gene expression and protein abundance level.

Recently, it has been shown that temperature is perceived by the red and far-red light responsive protein Phytochrome B[42,43] at night time. High temperature enhances Phytochrome B deactivation in the dark, which relieves the inhibition of the PHYTOCHROME INTERACTING FACTOR (PIF) family of transcription factors. In particular, PIF4 has been shown to play a critical role in thermomorphogenesis. PIF4 directly stimulates expression of genes involved in the biosynthesis of the phytohormone auxin, more specifically *YUCCA8* (*YUC8*), *TRYPTOPHAN AMINOTRANSFERASE OF ARABIDOPSIS1 (TAA1*) and the cytochrome P450 family member *CYP79B2*[56,155]. Additionally, high temperature increases auxin sensitivity by HEAT SHOCK PROTEIN90-dependent stabilisation of the auxin receptor TRANSPORT INHIBITOR RESISTANT1[40]. This stimulation in auxin level and sensitivity leads to an accumulation of auxin, which in turn stimulates brassinosteroid signalling. Together these form a positive feed-forward loop that stimulates *PIF4* expression and the subsequent activation of downstream auxin-signalling mechanisms[74]. In particular, the transcription of a subset of the *SMALL AUXIN UP RNA* (*SAUR*) gene family is up regulated[56]. The resulting proteins activate H^+-ATPases that pump H^+ out of the cell, lowering the pH in the apoplast. EXPANSIN proteins are activated by the lower pH and enzymatically weaken the cell wall. This allows turgor-driven cell expansion and subsequent hypocotyl elongation[76]. This mechanism of cell expansion and stem growth is called the acid growth theory[77,186].

The extend of the response to temperature is made evident by transcriptomics experiments, which generally reveal large numbers of regulated genes in response to a relatively mild increase in temperature[34,49,187–189]. Even in mutants disturbed in thermomorphogenesis, temperature still regulates the expression of many genes. This is illustrated by the high temperature transcriptome of the *phyB* mutant or the complex transcriptional regulation controlled by the *PIF* gene family[49,190]. Gene ontology (GO) term enrichment analyses of high temperature transcriptomes in these thermomorphogenesis-defective mutants revealed enrichment of many GO terms in addition to response to temperature[191]. Together, this suggests that at least part of the temperature regulation of gene expression is not directly

related to thermomorphogenesis, and that mutant analyses are complicated by their lack of specificity for a single response.

These extensive genome-wide responses to high temperature complicate dedicated investigations of the poorly understood molecular mechanisms of thermomorphogenesis regulation, as it hampers stringent candidate gene selection for functional studies. In addition, stand-alone -omics approaches are often not sufficient to generate system-level understanding of plant growth, because gene expression levels not necessarily reflect complementary protein abundances[192]. This is notoriously true for temperature effects, that can have both passive effects on biological systems, as well as active effects mediated via thermosensory molecules and downstream thermosignaling pathways. For instance, temperature affects both mRNA transcription and degradation rates[188] and influences protein stability and activity directly or indirectly by e.g. affecting enzymatic activity. Moreover, knowledge on (changes in) protein abundances are not necessarily informative, since it cannot be predicted how this translates into *e.g.* changes in primary metabolite composition of the plant that are important for temperature-mediated control of plant acclimation. For instance, Vasseur *et al.*[193] showed that the carbohydrate status changes in response to high ambient temperature and sugars have already been shown to be important regulators of stem elongation[194,195].

Extensive knowledge is available on changes of the proteome[196–200] and metabolome[201–203] in response to severe heat stress. Among the induced proteins are Heat Shock Proteins (HSP), which represent molecular chaperones that protect plants from heat stress-induced damage, and heat shock transcription factors (HSFs)[196,199,204,205]. In contrast, to the best of our knowledge, the proteome and metabolome in response to mild increase in ambient temperature in the physiological range (*e.g.* from 22°C to 27°C) has not been assessed so far.

In the previous chapters we described Heatin, a chemical compound that stimulates thermomorphogenesis in *Arabidopsis thaliana* seedlings already under control conditions. We have shown that Heatin acts downstream of -or parallel to- *PIF4,* and requires functional auxin signalling but does not act as canonical auxin (**Chapter 3**). In this chapter we catalogue transcriptomic, proteomic and metabolomic changes induced by Heatin treatment in young Arabidopsis seedlings and compare these to transcriptomic, proteomic and metabolomic changes induced by increased ambient temperature. With this combination we aim to isolate thermomorphogenesis specific factors from the extensive global effects of high ambient temperature.

We observed massive transcriptional regulation by high ambient temperature (27°C) whereas relatively few genes were affected by Heatin application. By comparing the regulated genes, we identify genes that are likely involved in hypocotyl elongation under high ambient temperature conditions. Our untargeted proteomics approach revealed that only a fraction of the transcriptional regulation is translated into detectable

changes in protein abundances. The analysis of primary metabolites by GC-MS showed divergent effects of temperature and Heatin, with only a minimal number of co-regulated metabolites. Taken together, this work shows that the effects of Heatin treatment on the transcriptome overlaps with that of high ambient temperature, but that this effect is less apparent in the proteome nor the primary metabolome.

Results

Dynamics of Heatin responsiveness of seedling hypocotyls

We aimed to catalogue the dynamics of the transcriptome, proteome and primary metabolome of *Arabidopsis thaliana* in response to mild increase in ambient temperature (22°C to 27°C) and upon application of Heatin. To this aim, relevant sampling time points during hypocotyl elongation in response to Heatin and high temperature were identified. A near infrared-light camera system was developed that allowed accurate and continuous quantification of growth with 2-hour resolution throughout the photoperiod and during darkness, from imbibed seed to 8 day-old seedling. The applied near infra-red light did not affect seedling etiolation nor germination, when compared to complete darkness (**Fig. S4.1**). This ensured that the observed growth dynamics in response to Heatin and high ambient temperature can be assigned to the respective treatment and are not side effects of the experimental setup.

Hypocotyl elongation of Col-0 wildtype (WT) seedlings grown on DMSO agar medium under control temperature conditions was similar to seedlings grown on Heatin agar medium during the first 48 hours after transferring seeds to the growth cabinet. The first obvious Heatin-induced differences in hypocotyl length started to occur after ~48 hours. This contrasted with high temperature-induced hypocotyl elongation, which initiated directly after germinating (t=~24 hours). Moreover, over the monitored first 8 days of growth, differential hypocotyl elongation (Heatin – DMSO, 27°C - 22°C) induced by high ambient temperature occurred largely during the first 72 hours, whereas Heatin-induced differential elongation started after 48 hours and continued until at least 192 hours (**Fig. 4.1A, S4.2A, B**).

Remarkably, *pif4-2* seedlings, lacking the thermomorphogenesis response, responded differently to Heatin treatment (**Fig. 4.1B, S4.2**). In these mutants, effects of Heatin first became visible after 48 hours in seedlings grown under high temperatures and after 56 hours in seedlings grown under control temperature. This suggests a potential role for *PIF4* in mediating Heatin sensitivity in a temperature-dependent manner, possibly through its interaction with the circadian clock, which has been shown to control elongation growth[206,207]. Interestingly, the initial high temperature-induced elongation response observed in the first 48 hours in Col-0 WT was also observed in *pif4-2* (**Fig. S4.2B, C**). This suggests that early thermomorphogenesis occurs independently

of PIF4, and that this transcription regulator becomes critical for the response to high ambient temperature only at the later stages of seedling establishment (**Fig. 4.1A, S4.2A, B**) and later throughout vegetative plant development[32,39,56]. Although timing of the initial Heatin effect was affected by the *pif4-2* mutation, the overall sensitivity to Heatin was comparable between *pif4-2* and WT seedlings, as shown by the similar trend in differential growth caused by Heatin (**Fig. S4.2A**). This observation that *PIF4* is not required for Heatin effects confirm our findings of Chapter 2 and 3 indicating that Heatin acts downstream, or parallel, to PIF4 in elongation growth control.

Over all conditions and genotypes, Heatin effects were first visible after 48 hours and continued to induce differences in hypocotyl growth during at least the 8 days that were assayed in this experiment (**Fig. 4.1, S4.2**). Based on these findings, we defined an early and late sampling time point for transcriptomics, proteomics and metabolomics experiments; 2 days (48 hours) and 7 days (168 hours) after placing seeds in the growth cabinet, respectively. Given that Heatin appears active throughout seedling growth, using these timepoints allows us to gain comprehensive insight in both early and late Heatin-responsive processes (expression, protein abundance and metabolite changes).

Transcriptomic changes in response to high ambient temperature and Heatin treatment

RNA-sequencing revealed that high temperature has a significant impact on the transcriptome as 13100 and 12047 genes were differentially expressed in 2-day-old or 7-day-old seedlings, respectively. 49.8% and 49.9% of the differentially expressed genes were up regulated in 2- and 7-day samples, respectively. 50.2% and 50.1% were down (**Table 4.1**). To assess the level of regulation of the affected genes, we determined the number of genes genes with at least two-fold up or down regulation. The number of genes above this cut-off was higher for 2-day old seedlings than for 7-day old seedlings (4140 and 2463, respectively, **Table 4.1, Fig. S4.3**). A ~50/50 (49.8%/50.2%) ratio (of up- and down-regulated genes) was maintained in 2-day old seedlings, but slightly shifted in 7-day old seedlings, where the ratio became closer to 40/60 (41.9% up vs. 58.1% down; **Table 4.1**).

The large number of high temperature-regulated genes was in stark contrast with the transcriptional regulation caused by Heatin (**Table 4.1**). In 2 day-old seedlings the expression of only 2 genes was significantly regulated at 22 °C and 10 genes at 27 °C. When considering the 2-fold threshold, 0 genes were differentially regulated at 22 °C and only 6 at 27 °C. The Heatin-transcriptome was more pronounced in 7 day-old seedlings, where the expression of 406 genes was significantly regulated at 22°C and 606 genes at 27°C. The expression of 49 (22°C) and 193 (27°C) genes was regulated when the 2-fold change cut-off was considered (**Table 4.1**).

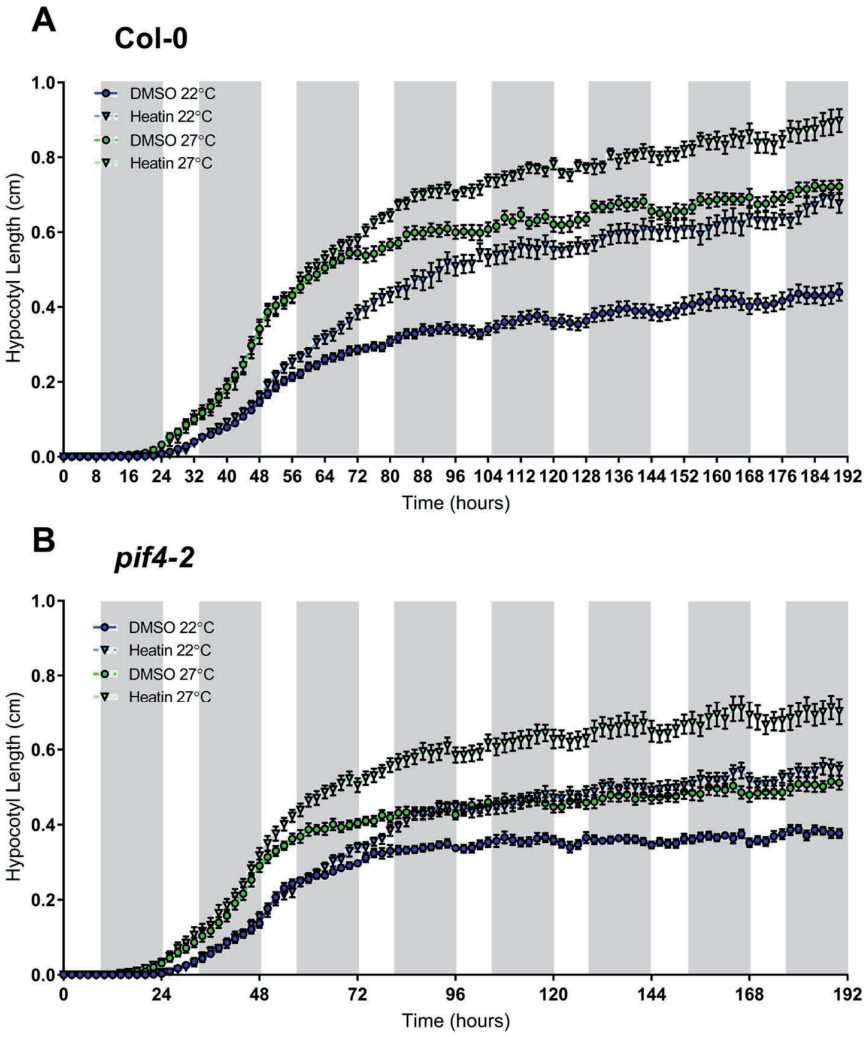

Figure 4.1: High resolution imaging of hypocotyl growth dynamics of WT and *pif4-2* seedlings.

(**A, B**) Hypocotyl length of seedlings of indicated genotype photographed every two hours for 8 days in the presence of a DMSO mock (bright coloured circles) or 8.5μM Heatin (light coloured triangles) at 22°C (blue symbols) or 27°C (green symbols). Grey bars indicate the dark period. Values are averages of 12-18 repeats of each 5-10 seedlings. Error bars indicate standard error of the mean.

We noted that high temperature enhanced the transcriptomic response to Heatin, as at both probed timepoints more genes were differentially regulated by Heatin under high temperature conditions compared to control conditions, including when the 2-fold change cut-off was considered (from 0/2 to 6/10 in 2-day-old seedlings and from 49/406 to 193/606 in 7-day-old seedlings). The latter suggests that not only more genes are

transcriptionally controlled, but the changes in expression are also stronger (**Table 4.1, Fig. S4.3**).

Table 4.1: Numbers of significantly differentially regulated genes from different comparisons.

Numbers represent genes of which the expression is significantly changed at least two-fold, or between brackets without this two-fold cut-off.

Comparison	>2 fold up (no cut-off)	>2 fold down (no cut-off)	Total
2d: 27°C - 22°C	2062 (6521)	2078 (6579)	4140 (13100)
7d: 27°C - 22°C	1032 (6012)	1431 (6033)	2463 (12047)
2d 22°C: Heatin - DMSO	0 (2)	0 (0)	0 (2)
2d 27°C: Heatin – DMSO	5 (8)	1 (2)	6 (10)
7d 22°C: Heatin – DMSO	26 (219)	23 (187)	49 (406)
7d 27°C: Heatin – DMSO	86 (291)	107 (315)	193 (606)

Transcriptomic regulation by Heatin in 2 day-old seedlings

As the number of Heatin-regulated genes is small, enrichment analyses and systematic comparisons are hampered as they would be highly susceptible to false positive and negative results. Therefore, we assessed the regulated genes manually (**Table 4.2**). The two by Heatin-up regulated genes (AT4G33550, a Bifunctional inhibitor/lipid-transfer protein/seed storage 2S albumin and AT5G03350/*SA-induced legume lectin-like protein* 1(*SAI-LLP1*)) in seedlings gown at 22 °C have both been described to have a function in defence responses[208–211].

At 27°C, AT4G33550 was also up regulated in response to Heatin, together with another Bifunctional inhibitor/lipid-transfer protein/seed storage 2S albumin superfamily protein. Four genes with up regulated expression are known auxin responsive genes (*INDOLE-3-ACETIC ACID INDUCIBLE 5* (*IAA5*), *GH3.1*, *GH3.3* and *1-AMINOCYCLOPROPANE-1-CARBOXYLATE SYNTHASE 4* (*ACS4*)). The remaining two genes, *ROTUNDIFOLIA like 13* and *ATPMEPCRD* have been implicated in cell proliferation and cell wall modification/defence, respectively. The two downregulated genes are involved in defence and stress response (**Table 4.2**). Together, these data show auxin responsive genes form half (4/8) of the upregulated genes, and also defence was a recurring theme in the regulated genes.

Table 4.2: Significantly differentially regulated genes in Heatin treated 2 day-old seedlings.

Shown are the condition where genes are regulated, the Arabidopsis gene identifier (AGI code), gene product, description of the gene as well as functional annotation (involved in) according to The Arabidopsis Information Resource (TAIR, www.arabidopsis.org), fold change and corrected significance of the regulation (p adj.). The last column indicates differential expression at 27°C compared to 22°C, where the green and red font indicates up and down regulation respectively, and no number means no significant change in expression. Genes are ordered according to up- or down regulation by Heatin.

Condition	AGI code	Gene product	Fold change	p adj.	Sig. fold-change 27°C
22°C Up	*AT4G33550*	Bifunctional inhibitor/lipid-transfer protein/seed storage 2S albumin superfamily protein; **involved in:** lipid transport	1.803156	2.61E-05	1.434248
	AT5G03350	*SAI-LLP1*; Legume lectin family protein; **involved in:** cellular response to salicylic acid stimulus, phosphorylation, systemic acquired resistance	1.728743	0.02051	0.271099
27°C Up	*AT2G22810*	*ACS4*; key enzyme in the biosynthesis of ethylene. ACS4 is specifically induced by auxin; **involved in:** 1-aminocyclopropane-1-carboxylate biosynthetic process, cellular response to iron ion, ethylene biosynthetic process, fruit ripening, response to auxin	6.230051	0.051023	-
	AT1G15580	*IAA5*; Auxin induced protein; **involved in:** auxin-activated signalling pathway, regulation of transcription, response to auxin	3.487447	0.051023	-
	AT2G37870	Bifunctional inhibitor/lipid-transfer protein/seed storage 2S albumin superfamily protein; **involved in:** lipid transport	2.611666	0.011843	11.02864
	AT2G14960	*GH3.1*; encodes a protein similar to IAA-amido synthases; **involved in:** response to auxin	2.31143	0.071511	0.664841
	AT3G23635	*ROTUNDIFOLIA like 13*	2.221234	0.040451	9.451335
	AT4G33550	Bifunctional inhibitor/lipid-transfer protein/seed storage 2S albumin superfamily protein; **involved in:** lipid transport	1.735164	0.040451	1.434248
	AT2G23170	*GH3.3*; encodes an IAA-amido synthase that conjugates amino acids to auxin; **involved in:** auxin homeostasis, response to auxin	1.671579	0.000557	0.588388
	AT2G43050	*ATPMEPCRD*; Plant invertase/pectin methylesterase inhibitor superfamily; **involved in:** cell wall modification, pectin catabolic process	1.643742	0.007324	10.44842
27°C Down	*AT4G01700*	Chitinase family protein; **involved in:** carbohydrate metabolic process, cell wall macromolecule catabolic process, chitin catabolic process, defense response to fungus	0.486268	0.040451	0.802281
	AT4G21680	*NRT1.8*; Encodes a nitrate transporter (NRT1.8). Functions in nitrate removal from the xylem sap. Mediates cadmium tolerance; **involved in:** nitrate assimilation, oligopeptide transport, response to cadmium ion, response to nitrate, transmembrane transport	0.591377	0.000597	3.18014

Transcriptomic regulation by Heatin in 7 day-old seedlings

Of the 406 Heatin-regulated genes regulated at 22°C in 7 day-old seedlings, 219 were upregulated and 187 were downregulated. At 27°C, 291 genes were upregulated and 315 downregulated (**table 4.1**). To identify signalling pathways that potentially explain Heatin effectiveness in 7 day-old seedlings, we compared the Heatin-regulated gene pools of the 22°C and 27°C grown, Heatin-treated seedlings. ~29% (63/219) of the upregulated genes at 22°C are also among the 291 upregulated genes at 27°C. ~18% (34/187) of

the downregulated genes at 22°C are also among the 315 downregulated genes at 27°C. 2 genes were upregulated at 22°C and downregulated at 27°C and 1 gene was downregulated at 22°C and upregulated at 27°C (**Fig. 4.2A**). Together, the transcriptome analyses showed relative little overlap between the Heatin responses at the two tested temperatures. However, since Heatin treatment results in the same elongated hypocotyl phenotype, regardless of the tested temperature (**Fig. S4.4, Chapter 2 and 3**), we reason that key responsible genes for Heatin-induced hypocotyl elongation are likely to be found among the overlap between the two samples.

GO-term enrichment of Heatin upregulated genes at 22°C revealed overrepresentation of genes annotated as '*response to a chemical stimulus'*, with *'response to auxin stimulus'* as significant sub-category. Also *'microtubule-based processes'* was significantly enriched (**Table S4.1**). At 27°C *'response to auxin stimulus'* was also significantly enriched, in addition to among others; '*iron ion homeostasis*', '*iron ion transport*', '*unidimensional cell growth*', '*cell wall modification*', '*response to heat*', and '*response to bacterium*' (**Table S4.1**).

Overrepresented GO terms among the Heatin downregulated genes at both 22°C and 27°C were more numerous than among the upregulated genes at the same temperatures. Among the overrepresented GO terms at Heatin downregulated genes at 22°C genes are: '*response to cold*', '*response to ABA stimulus*', '*lipid localisation*', '*carbohydrate catabolic process*' and '*root development'* (**Table S4.1**). Enriched amongst genes with down regulated expression at 27°C was also '*lipid localisation*' in addition to '*triterpenoid metabolic processes*' and '*seed development*' (**Table S4.1**).

Overall our GO term analyses are in line with the 2-day transcriptomic induced changes, where 4/8 regulated were auxin regulated genes. Together, this supports the previously proposed link of Heatin with auxin (**Chapter 3**). 7-day GO-term analyses also suggests a link to temperature responsive growth, exemplified by the down regulation of expression of cold responsive genes and up regulation of heat responsive genes.

Strong overlap between Heatin and high temperature transcriptomes

To probe for possible overlap between Heatin and high temperature signalling towards hypocotyl elongation, we compared the transcriptomic responses to Heatin and to high temperature treatment. At 22°C, 56.6% (124/219) of the genes that were up regulated in response to Heatin were also up regulated by high temperature conditions in the absence of Heatin. Genes differentially expressed in response to Heatin treatment at 27°C showed 28.2% (82/291) overlap with the high temperature transcriptome in the absence of Heatin. Among the down regulated genes a similar trend was observed with 71.7% (134/187) overlap at 22°C and 33.7% (106/315) at 27°C (**Fig. 4.2B, C**).

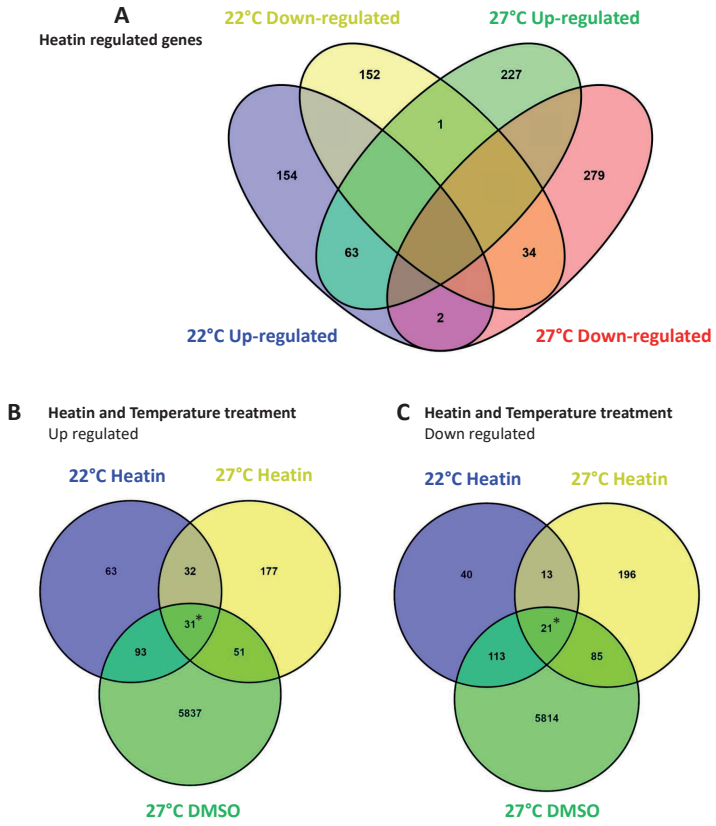

Figure 4.2: Venn-diagrams showing numbers and overlap of differentially regulated genes.

Numbers indicate the number of genes that showed significant differential regulation as compared to the control sample (22°C DMSO for 22°C Heatin and 27°C DMSO; 27°C DMSO for 27°C Heatin). (**A**) Heatin regulated genes under two temperature conditions. Impossible combinations are left blank (*e.g.* up and down simultaneously in the same condition). (**B-C**) Overlap between Heatin regulated genes and high temperature regulated genes, split between up regulated (**B**) and down regulated (**C**). genes in the fields marked with asterisks are shown in table 3.

Among the overlap of 124 genes with up regulated expression at high temperature in the absence of Heatin on one hand and Heatin treatment at 22°C on the other, 31 genes were found to be also regulated significantly by Heatin at 27°C (**Fig. 4.2B**). Among the down regulated genes, 134 were shared by high temperature without Heatin on one hand and Heatin treatment at 22°C on the other. 21 genes were found to be shared by all 3 comparisons of down regulated genes (**Fig. 4.2C**). These 52 (31 up + 21 down) genes were assessed in more detail (**Table 4.3**).

Of the 31 genes with up regulated expression in all 3 comparisons, we consistently found the highest RNA-seq read counts in Heatin 27°C samples (**Table 4.3**). This correlates

with hypocotyl length observations of these three groups (**Fig. S4.4A**), suggesting that these genes could be tightly linked with the observed phenotype. Interestingly, among the genes in this group is *IAA19*, previously shown to contribute to high temperature induced hypocotyl elongation[212], and the transcription factors *BREVIPEDICELLUS 1* (*BP1/KNAT1*), *PACLOBUTRAZOL RESISTANCE 5* (*PRE5*) and *bHLH039*, which potentially control downstream gene expression leading to hypocotyl elongation. No functional annotations (GO terms) were significantly enriched in this group, however.

Down regulated genes showed a similar trend, where 18 of the 21 overlapping genes had the lowest RNA-seq read count in Heatin-treated samples grown at 27°C (**Table 4.3**). We found no significant GO enrichment in this group of genes. Together with the 31 up regulated genes, the remaining 18 genes are considered high interest candidate genes for further functional validation.

Table 4.3: Normalized read counts of genes differentially regulated by Heatin and high temperature in 7 day old seedlings.

Commonly up (top part of table) and down (lower part of table) regulated genes (indicated by AGI codes and gene description) as found in the Venn diagram (**Fig. 3B, C**). Values are colour-coded according to their relative expression compared with the other two samples. Blue, white and red respectively correspond with lowest, middle and highest values respectively. Shown are gene summarized gene descriptions retrieved from TAIR (www.arabidopsis.org).

Up

AGI code	Heatin 22°C	Heatin 27°C	DMSO 27°C	Gene description
AT2G43050	747.2095	2267.798	706.0377	Plant invertase/pectin methylesterase inhibitor superfamily (ATPMEPCRD)
AT1G65310	1109.476	1554.834	873.8306	XYLOGLUCAN ENDOTRANSGLUCOSYLASE/HYDROLASE 17 (ATXTH17)
AT2G23170	849.7201	4468.59	809.5	encodes an IAA-amido synthase that conjugates Asp and other amino acids to auxin in vitro. (GH3.3)
AT1G78970	941.7625	1199.811	545.1526	LUPEOL SYNTHASE 1 (LUP1)
AT1G70830	6353.93	19925.13	10766.23	MLP-LIKE PROTEIN 28 (MLP28)
AT1G27020	366.6233	1031.431	460.4124	plant/protein
AT1G70890	1038.91	1937.954	1090.275	MLP-LIKE PROTEIN 43 (MLP43);MAJOR LATEX PROTEIN LIKE 43 (MLP43)
AT3G15540	735.9883	1097.294	683.396	INDOLE-3-ACETIC ACID INDUCIBLE 19 (IAA19);MASSUGU 2 (MSG2)
AT1G20620	48186.53	178894.6	117815.1	Catalase, catalyses the breakdown of hydrogen peroxide (H2O2) into water and oxygen. CATALASE 3 (CAT3);SENESCENCE 2 (SEN2)
AT5G07010	3603.405	13510.22	9136.697	Encodes a sulfotransferase that acts specifically on 11- and 12-hydroxyjasmonic acid. SULFOTRANSFERASE 2A (ST2A)
AT3G20470	1007.287	2877.741	1706.545	GLYCINE-RICH PROTEIN 5 (GRP5)
AT4G08150	786.2683	1294.725	871.4705	A member of class I knotted1-like homeobox gene family (together with KNAT2). KNOTTED-LIKE FROM ARABIDOPSIS THALIANA (KNAT1);BREVIPEDICELLUS 1 (BP1)
AT5G20710	143.0779	581.7532	233.0679	BETA-GALACTOSIDASE 7 (BGAL7)
AT3G26170	75.21313	841.1999	538.6211	putative cytochrome P450 (CYP71B19)
AT4G19420	876.0811	2720.572	1759.976	Pectinacetylesterase family protein PECTIN ACETYLESTERASE 8 (PAE8)
AT2G18050	1358.086	5678.489	3638.176	encodes a structurally divergent linker histone whose gene expression is induced by dehydration and ABA. HISTONE H1-3 (HIS1-3)
AT2G36220	729.9189	1966.355	1465.972	hypothetical protein;(source:Araport11) protein_coding
AT5G19530	2271.289	4641.809	3445.932	Encodes a spermine synthase. ACAULIS 5 (ACL5)
AT4G18970	1692.008	2506.265	1891.142	GDSL-motif esterase/acyltransferase/lipase. Enzyme group with broad substrate specificity
AT2G43060	518.3309	1192.068	733.6907	IL1 BINDING BHLH 1 (IBH1)
AT3G28857	66.84184	110.8382	54.90018	Encodes a atypical member of the bHLH family transcriptional factors. PACLOBUTRAZOL RESISTANCE 5 (PRE5)
AT5G37950	15.85963	44.55112	6.467209	UDP-Glycosyltransferase superfamily protein
AT2G37130	5525.472	15467.37	7857.298	Peroxidase superfamily protein;(source:Araport11) protein_coding
AT1G67810	360.3545	908.1091	492.7664	Encodes a protein capable of stimulating the cysteine desulfurase activity of CpNifS (AT1G08490) in vitro. SULFUR E2 (SUFE2)
AT3G56980	280.0405	826.2258	256.365	Encodes a member of the basic helix-loop-helix transcription factor protein. OBP3-RESPONSIVE GENE 3 (ORG3); (BHLH039)
AT1G64710	744.3602	1737.071	1055.361	GroES-like zinc-binding alcohol dehydrogenase family protein
AT1G09480	108.8401	231.3696	144.3987	similar to Eucalyptus gunnii alcohol dehydrogenase of unknown physiological function
AT3G25717	937.2998	1623.655	1194.445	ROTUNDIFOLIA LIKE 16 (RTFL16);DEVIL 6 (DVL6)
AT5G04080	440.3337	873.3245	634.8393	cysteine-rich TM module stress tolerance protein
AT5G03545	134.862	258.0086	154.5678	Expressed in response to phosphate starvation, this response is enhanced by the presence of IAA. (AT4) INDUCED BY PI STARVATION 2 (ATIPS2); (AT4)
AT2G01670	1342.098	2225.146	1713.535	NUDIX HYDROLASE HOMOLOG 17 (NUDT17)

Lowest
Middle
Highest

Down

AGI code	Heatin 22°C	Heatin 27°C	DMSO 27°C	Description
AT5G48000	48.95991	78.43973	148.5338	Encodes a member of the CYP708A family of cytochrome P450 enzymes. THAH appears to add a hydroxyl group to the triterpene thalianol. "CYTOCHROME P450, FAMILY 708, SUBFAMILY A, POLYPEPTIDE 2" (CYP708A2);THALIANOL HYDROXYLASE 1 (THAH1)
AT5G20630	1076.235	829.6481	1160.156	Encodes a germin-like protein GERMIN 3 (GER3) GERMIN-LIKE PROTEIN 3 (GLP3)
AT1G79840	261.5464	220.5388	285.2976	Glabra 2, a homeodomain protein affects epidermal cell identity including trichomes, root hairs, and seed coat. GLABRA 2 (GL2)
AT2G33850	313.281	107.9272	191.1522	E6-like protein
AT3G09220	1103.349	959.5911	1483.293	putative laccase LACCASE 7 (LAC7)
AT4G28940	165.1746	68.07668	105.2761	Phosphorylase superfamily protein
AT3G14210	2282.588	1445.559	1820.469	A semidominant QTL which has an epistatic effect on the Epithiospecifier gene. Represses nitrile formation and favors isothiocyanate production during glucosinolate hydrolysis. EPITHIOSPECIFIER MODIFIER 1 (ESM1)
AT3G46700	167.2139	213.896	298.2333	UDP-Glycosyltransferase superfamily protein
AT5G24140	32.98181	24.97136	53.47751	Encodes a protein with similarity to squalene monoxygenases. SQUALENE MONOOXYGENASE 2 (SQP2)
AT1G66280	1892.105	1478.314	2207.717	Glycosyl hydrolase superfamily protein (BGLU22)
AT5G62480	236.1034	226.3598	282.8259	Encodes glutathione transferase belonging to the tau class of GSTs. GLUTATHIONE S-TRANSFERASE TAU 9 (GSTU9) ;GLUTATHIONE S-TRANSFERASE 14 (GST14)
AT5G48010	150.1205	165.9923	256.1203	Encodes an oxidosqualene cyclase involved in the biosynthesis of thalianol, a tricyclic triterpenoid of unknown function. THALIANOL SYNTHASE 1 (THAS1)
AT3G20370	1876.806	885.1374	1104.548	TRAF-like family protein
AT2G29750	390.5076	246.6302	385.7497	UDP-glucosyl transferase 71C1; UDP-GLUCOSYL TRANSFERASE 71C1 (UGT71C1)
AT1G24020	178.7816	25.90262	53.24399	MLP-LIKE PROTEIN 423 (MLP423)
AT4G33610	876.7477	481.3765	609.2147	glycine-rich protein
AT4G15160	1018.81	938.0513	1330.269	Bifunctional inhibitor/lipid-transfer protein/seed storage 2S albumin superfamily protein
AT1G12040	77.1701	7.908191	29.22345	encodes a a chimeric leucine-rich repeat/extensin protein that regulates root hair morphogenesis and elongation. LEUCINE-RICH REPEAT/EXTENSIN 1 (LRX1)
AT5G10230	104.8928	23.26215	43.80854	Encodes a calcium-binding protein annexin ANNEXIN 7 (ANN7)
AT4G00700	356.6288	299.0846	438.2514	C2 calcium/lipid-binding plant phosphoribosyltransferase family protein
AT2G43150	9211.727	8695.316	9916.654	Proline-rich extensin-like family protein

Transcriptome regulation translates poorly into proteome changes

As the expression of only 10 genes was found to be differentially regulated in our 2 day-old seedling samples, we considered the possibility that early regulation takes place at the protein level rather than the transcriptional level. To identify differentially present proteins, we performed untargeted proteomics by LC-MS/MS on 2 day-old seedlings grown in the absence and presence of Heatin at 22°C and 27°C.

Over all treatments, we identified 7330 different proteins, of which only 3.8% (285; 134 up, 151 down) were significantly differentially abundant at 27 °C conditions (**Fig. 4.3A, S4.1**). When comparing proteins that are differentially abundant with differentially expressed genes as found by RNA-seq, we found that ~47% were regulated in the same direction (62 proteins and gene expression upregulated, 72 proteins and gene expression downregulated). 19% were regulated in opposite direction (53/285) and ~34% of the regulated proteins were not affected on transcription level (98/285) (**Fig. 4.3B**). This low correlation between transcriptome and proteome is in line with the generally low correlation found in other eukaryotic systems[213,214], despite that on the phenotype level (hypocotyl length) the samples were very similar (**Fig. S4.4**).

Functional annotation enrichment of the differentially abundant proteins under high temperature however, revealed a striking enrichment in proteins annotated with functions in '*ATPase activity, coupled to transmembrane movement of substances*' and '*water channel activity*' (**Table S4.2**), which is in line with the observations that high temperature-induced hypocotyl elongation growth occurs via the acid growth mechanism[76,215].

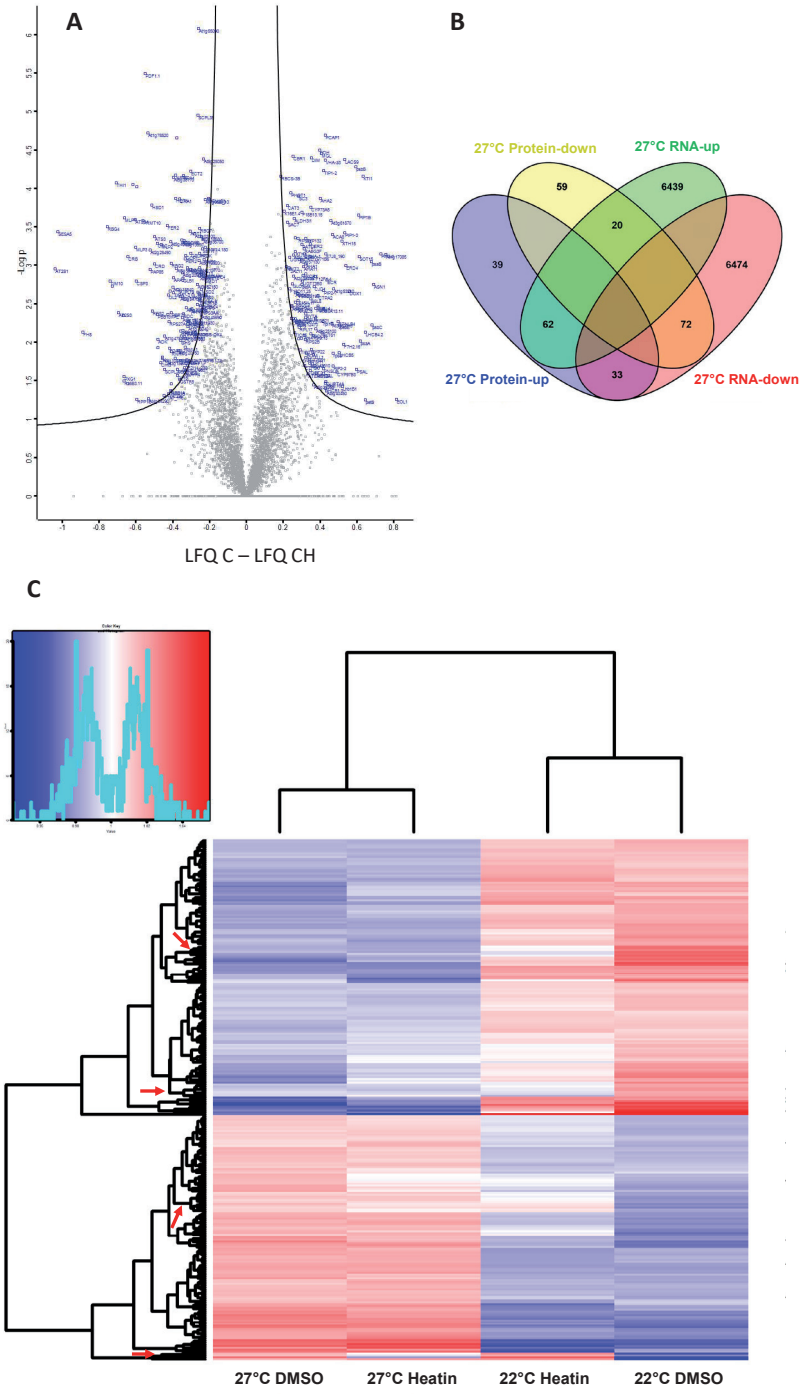

Figure 4.3: Overview of high temperature and Heatin regulated proteins in 2 day-old seedlings.

(**A**) Volcano plot showing proteins differentially present, as found by t-test with permutation-based FDR correction. X-axis shows differences in median LFQ intensities between 22°C and 27°C samples and the Y-axis indicates the –log p-values of the t-test comparisons. Black curved lines show FDR-cut-off line. Significantly regulated proteins are shown in blue with their corresponding gene name. Not significantly regulated proteins are shown in grey. (**B**) Venn-diagram showing number of overlapping proteins and genes regulated at 27°C, compared to 22°C, as found by RNA-seq (**Table 1**) and proteomics (Panel A). Impossible combinations are left blank (*e.g.* up and down simultaneously in the same analysis). (**C**) Heatmap showing relative abundance of the 285 differentially affected proteins under 27°C from panel **A** for 22°C and 27°C DMSO and 22°C and 27°C of Heatin samples. Column and row order is determined by Euclidean clustering and resulting dendograms are shown to the left (proteins) and above (treatments) of the heatmap. The cyan-coloured line in the colour-key legend (top left inset) shows histogram of represented values. Values are internally standardized by dividing by average LFQ intensity of each protein. Red arrows in left dendrogram indicate classes of proteins that similarly affected by Heatin and high temperature. These later proteins are listed in table S3.

Heatin treatment did not result in any differential abundance of proteins compared to the DMSO control samples at the same temperature, despite the clear stimulation of hypocotyl length by the compound (**Fig. S4.4**). To probe general trends in proteomic changes induced by Heatin and high temperature, a heatmap was generated comparing the 285 differentially abundant proteins at 27 °C conditions, with the same proteins (despite not being significantly differentially regulated) in the Heatin-treated samples. Sample clustering confirmed temperature to be the major factor influencing the proteome (**Fig. 4.3C, upper dendrogram**). Strikingly, despite of the lack of significance, we found several protein clusters where Heatin treatment under control temperature better resembled high temperature treatment conditions than the DMSO mock control (**Fig. 4.3C, red arrows**). These proteins are shown in **Table S4.3**.

Profiling of primary metabolites at different temperatures and Heatin treatment

We analysed the composition of polar metabolites, mostly of the central (primary) metabolism, in Arabidopsis seedlings grown at different temperatures and after treatment with Heatin. In total, we detected 84 metabolites in samples of 2 day-old and 7 day-old WT seedlings grown at 22 °C and 27 °C (**Fig. 4.4A, Suppl. File 4.2**). Based hierarchical clustering of the metabolite profiles, we found samples were separated mostly by age (7 day-old vs. 2 day-old seedling), followed by growth temperature (22°C vs. 27°C) and lastly the compound (Heatin vs DMSO mock) (**Fig. 4.4A, upper dendrogram**). However, inter-replicate variation for all 7-day samples was larger than variation between treatments based on PCA analysis (data not shown). We therefore focused on 2-day samples for the further analyses.

Although the metabolite profile of Heatin-treated seedlings consistently resembled those of the corresponding control profile (at the same temperature treatment), some

A

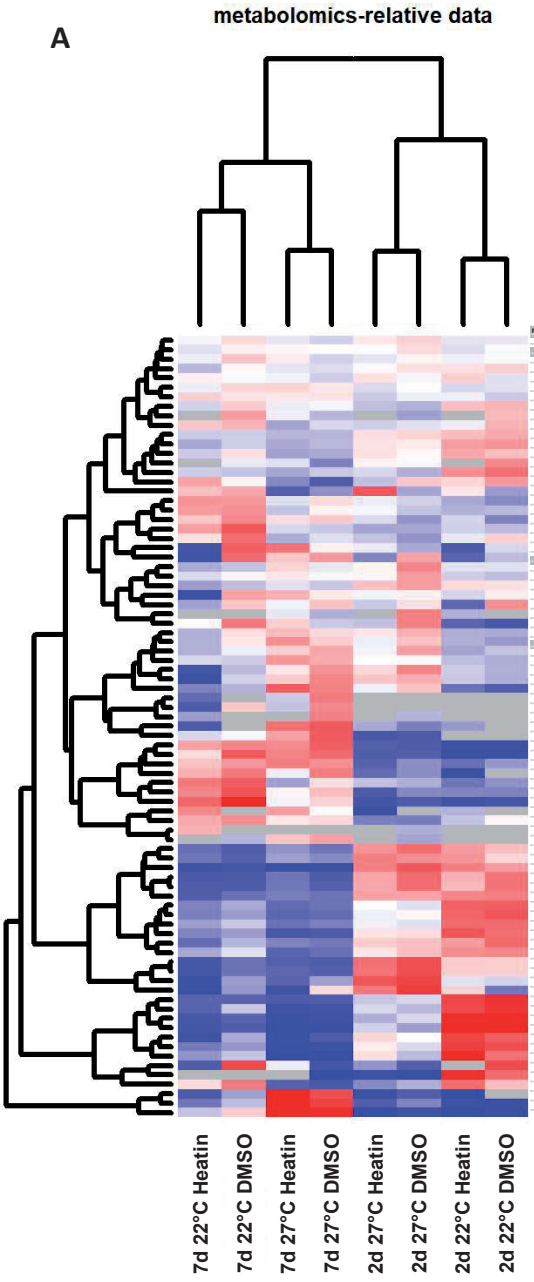

Metab. ID	Manual Annot.	Autoantic Annot.	Avg. Score
1385	Phosphoric acid (3TMS)	Phosphoenolpyruvate	860
2786	***Glutamine***	***L-Proline, 5-oxo-1-(trimethylsilyl)-, trimethylsilyl ester***	***916.5***
699		1,3-Dimethyl-5-(perfluoroethyl)cyclohexane	880
1247	Ethanolamine (3TMS)	Silanamine, 1,1,1-trimethyl-N-(trimethylsilyl)-N-[2-[(trimethylsilyl)oxy]ethyl]-	848
2342		Betaprodine	569
113		N-Methyl-N-n-butyltrifluoroacetamide	628.5
415	Propanoic acid, 2-[(trimethylsilyl)oxy]	Propanoic acid, 2-[(trimethylsilyl)oxy]-, trimethylsilyl ester	868
4967		2-Propenoic acid, 2-[(trimethylsilyl)oxy]-, trimethylsilyl ester	596
7787		NA	739.5
2633	Pyroglutamic acid (1TMS)	2-Hexene	859.5
8205	Sucrose	Sucrose	911
4563		?-D-Galactofuranoside, ethyl 2,3,5,6-tetrakis-O-(trimethylsilyl)-	779
7019	Sugar	Sucrose	722
4403		1(2H)-Quinolinecarboxylic acid, 2-cyano-, ethyl ester	506
2940	Glutamic acid (2TMS)	Glutamic acid (2TMS)	879.5
6650		?-L-Galactopyranoside, methyl 6-deoxy-2,3,4-tris-O-(trimethylsilyl)-	787.5
6281	Sugar	ß-D-Mannopyranoside, methyl 2,3,4,6-tetrakis-O-(trimethylsilyl)-	750.5
4103	NA	NA	868.5
2995		Glutamine [-H2O] (2TMS) BP	883
7551		1,1-Dichloro-1-fluoroethane	630.5
2195		N-Nitroso-O,O'-bis[trimethylsilyl]diethanolamine	652
3657		2,5-Diamino-6-methyl-4-pyrimidinol	845.5
4398		Malonamide, 2-(propylamino)-N,N'-dihepthyl-N,N'-dimethyl-	577.5
4388	***Glutamine***	***N-Acetylglutamine,N,N',O,O'- tetrakis(trimethylsilyl)-***	***920.5***
6395		D-Xylose, tetrakis(trimethylsilyl)-	852
5229	Ascorbic acid	Ascorbic acid	693
3497	Glutamic acid	Glutamic acid	876
5192		ß-DL-Lyxofuranoside, methyl 2,3,5-tris-O-(trimethylsilyl)-	606
8756		Tricarbomethoxyethylene	455.5
5208		Butane, 1,1-diethoxy-	742
2517		1,2-Ethanediol, 1,2-di-1-cyclopenten-1-yl-	621.5
1188	Serine (2TMS)	Serine (2TMS)	846
4695	***Glutamine***	***Glutamine***	***920***
2677	Asparagine	Asparagine	877
1596	Glycine (3TMS)	Glycine (3TMS)	842.5
1954	Serine	Serine	770
2063		Threonine	743
6198		L-Lysine, N2,N6,N6-tris[trimethylsilyl)-, trimethylsilyl ester	627.5
3204		Glutamine [-H2O] (3TMS)	446.5
7435		Mannose, 6-deoxy-2,3,4,5-tetrakis-O-(trimethylsilyl)-, L-	760.5
5564		Urea, triethylnitroso-	707
4949		Hexane, 1,1-diethoxy-	616
8987		2-O-Glycerol-ß-d-galactopyranoside, hexa-TMS	715
3325	Asparagine (2TMS)	Asparagine (2TMS)	852.5
2538	Threitol	Ribitol, 1,2,3,4,5-pentakis-O-(trimethylsilyl)-	568
8382	Lactose	1,2-Benzisothiazole, 3-methoxy-, 1,1-dioxide	566
1126		Urea, N,N'-bis(trimethylsilyl)-	594
3648		Levoglutamide	776
1875	Fumaric acid	Fumaric acid	956
3099		2,3,4-Trihydroxybutyric acid tetrakis(trimethylsilyl) deriv.	653
6189	NA	NA	562
7586		Sinapic acid, cis- (2TMS)	717.5
6407		Benzeneacetic acid, 4-ethenyl-, ethyl ester	801
3578		1,2-Bis(1,4,7-trioxa-10-azacyclododec-10-yl)-ethane	643
5874		NA	619.5
5910		4-Propyl-3-thiosemicarbazide	589.5
3701		NA	634
6065	Glucose	Mannose	886
5743	Glucose	Mannose	940
7198	Myo-inositol	Myo-Inositol, 1,2,3,4,5,6-hexakis-O-(trimethylsilyl)-	877
4678		(+)-Dibenzoyl-L-tartaric acid anhydride	808.5
2454	Malic acid	Malic acid	922
3974		Benzoylformic acid	917
3724	NA	NA	733
8811		Mannose, 6-deoxy-2,3,4,5-tetrakis-O-(trimethylsilyl)-, L-	741
826		N-Ethyl-3-methyl-3-nonanamine	787.5
5344	Sorbose	Sorbose	907
5473	Fructose	Fructose	891
2220		Glycine	599
1030		L-Valine, N-(trimethylsilyl)-, trimethylsilyl ester	831
5095	Citric acid	Citric acid	782
8895		NA	772.5
1687	Succinic acid	Succinic acid	876
6493	NA	NA	886
7471		NA	649
1058		Pentanenitrile, 5-(methylthio)-	850
8490		NA	648.5
8033		2-Naphthonitrile, 5,6,7,8-tetrahydro-	470.5
2026		1,3,2,4,6-Dithia[3-Si]triazine, 5-[(trimethylsilyl)oxy]-, 1,1-dioxide	648
8332		NA	866
3913		5-(1-Hydroxyethyl)-4-methylthiazole	540.5
3804	Asparagine (3TMS)	L-Asparagine, N,N2-bis(trimethylsilyl)-, trimethylsilyl ester	885.5
3225		Thiazolo[5,4-d]thiazole-2(3H)-thione, 3-ethyl-5-methyl	533.5

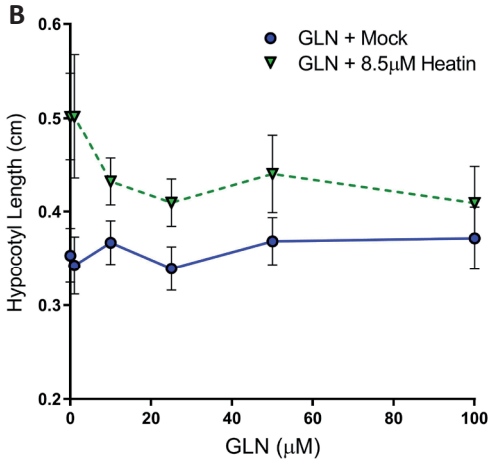

Figure 4.4: Overview of high temperature and Heatin regulated metabolomic responses.

(**A**) Heatmap showing relative abundance of the 84 identified metabolites at 22°C and 27°C, DMSO and Heatin, and 2 day-old and 7 day-old (noted as 2d, 7d respctively) seedling samples and all combinations of these conditions. Column and row order were determined by Euclidean clustering and resulting dendrograms are shown left (metabolites) and above (treatments) of the heatmap. The cyan-coloured line in the colour-key legend (top left inset) shows histogram of represented values. Values are internally standardized by dividing by average abundance of each metabolite. Grey fields represent metabolites that were not detected under that conditions. The table on the right shows metabolite IDs, manual annotated compound name/class and automated matched compound name, as well as average score corresponding to Supplemental file 2. (**B**) Hypocotyl lengths of 8 day-old seedlings grown on DMSO (blue circles, closed line) or 8.5μM Heatin (green triangles, dashed line) in the presence of different concentrations of glutamine. Error bars denote standard error of the mean.

compounds were consistently differentially present in Heatin-treated samples compared to the mock control, making them interesting metabolites to study for a potential role in Heatin-directed hypocotyl elongation and thermomorphogenesis. In particular, our results indicated that Glutamine (GLN) levels are reduced in Heatin-treated 2 day-old seedlings, as compared to the DMSO samples grown under the same temperature. This was the case in 5 out of total 6 comparisons of GLN levels between Heatin and DMSO treated samples for 3 different determinations of GLN levels (**Fig. 4.4A**). To test if GLN levels were linked with Heatin-induced hypocotyl elongation, we grew plants at 22 °C on Heatin-containing agar plates in the presence of different concentrations of GLN (**Fig. 4.4B**). We found that GLN inhibits Heatin-induced hypocotyl elongation in a dose-responsive manner. Future experiments will determine if the suppression of hypocotyl elongation by GLN also applies high temperature induced hypocotyl elongation and thermomorphogenesis on a whole. Taken together, whereas high temperature treatment and Heatin treatment share a significant portion of regulation at the transcriptional level in particular, this does not

translate directly to corresponding changes in the proteome nor metabolome. We were however able to identify clusters of regulated proteins and metabolites that are regulated by Heatin in a manner similar to regulation under high temperature conditions. Possibly, these proteins and metabolites functionally contribute to Heatin-mediated hypocotyl elongation. This should be further validated in future studies.

Discussion

High resolution time-lapse imaging revealed the dynamics of hypocotyl elongation in response to high temperature and Heatin treatment, in Col *WT* and *pif4* mutant, from seed to established seedling (**Fig. 4.1**). We observed a strong temperature-dependent hypocotyl elongation response between 24 and 48 hours after the start of the experiment and show that this effect occurs independent of both Heatin and PIF4 (**Fig. S4.2**). This indicates that regulation of early thermomorphogenesis during the first 48 hours of the seedling's life is different from the responses in older plants, which requires functional PIF4[37]. High temperature-induced hypocotyl elongation after 48 hours is *PIF4* dependent and the PIF4 requirement lasts for the rest of the measured experiment duration (**Fig. 4.1, S4.2**). The differences established during the 24 hours between t=48h and 72h largely explains most of the impaired hypocotyl elongation of *pif4* mutants at warm temperature observed in 8-day-old seedlings (**Chapter 3**). Our time series data are consistent with previously published time series on hypocotyl elongation growth under similar conditions[216].

We observed the first effects of Heatin treatment at 48 hours after the start of the experiment. Surprisingly, this effect was observed in Col-0 WT seedlings grown under control temperatures and *pif4-2* seedlings grown at high temperature conditions. Under high temperature conditions in Col-0 WT or control temperature in *pif4-2,* the effects were first observed after 56 hours (**Fig. 4.1, S4.2**). A possible explanation for this discrepancy is that a disturbed circadian growth in the *pif4-2* mutant[207] could limit the response to Heatin at control temperature during the photoperiod. This notion is supported by a striking increase in growth rate of *pif4-2* at control temperature between 48 and 56 hours after the start of the experiment, which follows a similar trend as Heatin-induced growth in WT seedlings (**Fig. 4.1**).

Heatin-induced hypocotyl elongation after these initial discrepancies is however comparable between genotypes and temperature conditions, as shown by similar differential growth trends. Differences between seedlings on DMSO mock and Heatin continue to increase during the experimental period where growth was followed (**Fig. 4.1, S4.2A**).

We hypothesized that Heatin-induced transcriptomic changes at the early time point (2 day-old seedlings) should yield early responsive genes that are close to the initial Heatin

perception event. Along the same line of reasoning, transcriptomic changes at the late time point (7 day-old seedlings) were expected to reveal factors that maintain the response and act more downstream of Heatin sensing and that feedback signalling mechanisms could be uncovered. The numbers of regulated genes at the different timepoints support these hypotheses, as the total number of differentially regulated genes at the early timepoint (2 day-old seedlings; 12 genes) was much lower that the number of regulated genes at the later timepoint (7 day-old seedlings; 1012 genes) (**Table 4.1**). The lack of a clear transcriptional response in 2 day-old seedlings was surprising, as this contrasts with early transcriptomic responses induced by *e.g.* auxin, where large numbers (100+) of regulated genes were already found after very short treatment periods (minutes – hours)[217,218]. If indeed the genes regulated at the early timepoint are close to the initial response of Heatin, then the observation that half of the genes of which the expression is regulated by Heatin under high temperature conditions are known auxin responsive genes, suggests that Heatin acts like an auxin, even though previous results show Heatin is distinct from canonical auxins (**Table 4.2 and Chapter 3**). The notion that Heatin acts like an auxin is further supported by the significant enrichment of genes involved in auxin signalling at the later timepoint, as shown by GO-term analysis (**Table S4.1**). The published transcriptomic response to a 2 hour treatment with a Heatin analogous compound, Sirtinol (**Chapter 3**), also shows a strong auxin footprint[93], but revealed many more regulated genes than Heatin treatment, in line with the hypocotyl specific effect of Heatin (**Chapter 3**).

Our transcriptome analysis showed an interaction between Heatin and high temperature at several levels. First, at our early timepoint we found five times the number of genes regulated by Heatin under high temperature (2 compared to 10, **Table 4.1, 4.2**). Second, also at the later timepoint we find regulation of more genes with larger differences in expression (406 compared to 606, **Table 4.1, Fig. S4.3**). A possible explanation for this effect is that temperature could alter the sensitivity to Heatin. This would not be without precedent, as high temperature is known to increase sensitivity to auxin through HSP90-dependent stabilisation of the auxin receptor TIR1[40]. Indeed, we have shown that the *tir1-1 afb5-5* double mutant is almost completely insensitive to Heatin, which is in accordance with the notion that increased TIR1 stability at warm temperature would lead to increased Heatin sensitivity (**Chapter 3**). It should be noted however that the number of genes that are jointly regulated by Heatin at both tested temperatures is small (**Fig. 4.2A**). Therefore, an increase in sensitivity to Heatin does not explain the entire Heatin x temperature interaction. Nevertheless, as Heatin stimulates hypocotyl elongation regardless of the tested temperature (**Fig. 4.1, S4.4**), we hypothesize that the genes involved in hypocotyl elongation are among the overlapping genes. This hypothesis is supported by another observed interaction between Heatin and temperature: Heatin-induced changes at control temperature conditions have more in common with high temperature treatment (without Heatin), than Heatin-induced changes at high temperature conditions (**Fig. 4.2B,**

C). Genes involved in hypocotyl elongation are expected to be already regulated under high temperature conditions, and therefore are less likely to be found additively regulated by Heatin under high temperature as well. Indeed, amongst the overlap between the expression of the genes that are significantly regulated, the normalized read-count of the samples correlates with hypocotyl length of these samples (**Table 4.3, Fig. S4.4**). An example of an explanatory gene amongst the overlap is *IAA19*. Mutants disturbed *IAA19* are defective in high temperature-induced hypocotyl elongation[212].

As transcriptomic responses were small at the early (2-day-old seedling) timepoint, we hypothesized that proteomic changes might be responsible for the observed initial effects. Although the sampled seedlings showed the expected phenotypes (**Fig. S4.4**) and we were able to detect over 7000 unique proteins, we did not find significant regulation by Heatin. High temperature on the contrary did significantly affect the abundance of 285 proteins (**Fig. 4.3A**) in a manner that is significantly correlated to our transcriptomic analysis (**Fig. 4.3B**). Previous proteomic studies into high temperature responses mainly studied heat stress conditions at temperatures beyond the ambient temperature, where Arabidopsis is prone to induce tolerance to cope with the stress, such as induction of protective mechanisms against oxidative stress and maintenance of membrane integrity, rather than acclimative growth responses such as thermomorphogenesis, that are induced to relieve the impact of (mild) stress[196–198]. We were indeed able to identify proteins related to the mechanistic underpinnings of cell expansion (*e.g.* water channels and H^+ pumps), which is the direct cause for elongation responses associated with thermomorphogenesis[41,76,215].

Data analysis by hierarchical clustering and visualisation using a heatmap were used to assess whether Heatin treatment overlapped with high temperature treatment under less stringent conditions (**Fig. 4.3C**). Such analysis should be interpreted with care but 4 clusters were identified of potential Heatin-regulated proteins under control temperature that were also found regulated in our high temperature-treated samples (**Table S4.3**).

A possible explanation for the discrepancy between high temperature-induced transcriptomic regulation and the relatively weak corresponding proteomic regulation, is that the plant possibly negates temperature effects by regulating mRNA stability or the effectiveness of the translational machinery[188]. Additionally, signalling components such as transcription factors are usually lowly abundant and therefore difficult to measure using untargeted proteomic approaches, especially when whole seedlings are considered as in our study, rather than isolated tissues such as the hypocotyl only.

The metabolic analyses reveal a potential role for Glutamine in supressing Heatin-directed elongation. The observation that addition of Gln is able to supress elongation suggests that this happens through active mechanisms. How Gln possibly modulates hypocotyl length remains to investigated.

Materials and methods

Plant materials and growth conditions

Arabidopsis Col-0 wild type and *pif4-2*[165] seeds were obtained from the Nothingham Arabidopsis stock center (www.Arabidopsis.info). Seedlings were grown under 100 µmol m^{-2} s^{-1} white light short day conditions (8 hours light/16 hours darkness) at 70% relative humidity in climate-controlled Microclima 1000 growth cabinets (Snijders Labs) at either 22°C (control) or 27°C (high temperature).

Time lapse growth assays

A custom digital time-lapse camera system was developed to monitor hypocotyl growth continuously throughout the diurnal cycle (photoperiod and dark period). A Canon EOS 350D DSLR camera was used in which the standard internal IR and UV filters were replaced by a 715nm long pass filter[219]. Photos were taken with 2-hour intervals for 8 days, using an Aputure AP-R1C LCD Timer Remote controller. A LED spotlight (940 nm, Spectral Line Half-width 50 nm; Kingbright, #BL0106-15-28) was used to illuminate seedlings continuously, in addition to the growth cabinet lights. The emitted light did not interfere with plant development as no de-etiolation of dark-grown etiolated plants, nor germination of imbibed seeds was observed (**Fig. S4.1**) in otherwise continuous darkness. Hypocotyl lengths were measured using ImageJ Image analysis software as described in **Chapter 2 and 3**.

Generation of plant material for ~omics analyses

To generate samples for RNA sequencing, proteomics and metabolomics, seedlings were grown on sterile 0.8% (RNA/seq) or 1.2% (proteomics and metabolomics) plant agar (Duchefa P1001) 1x Murashige-Skoog medium (MS, including MES Buffer and vitamins, Duchefa M0255) without sucrose. Seeds were surface sterilized by chlorine gas for 3 hours. After sowing, seeds were stratified for 2-3 days at 4°C in the dark. At the start of the photoperiod of day 3 and day 8, the plates were photographed from the top for hypocotyl length measurements and thereafter seedlings were harvested into 1,5ml reaction tubes and snap-frozen in liquid N_2 (2 day-old and 7 day-old old seedlings). Each sample contained 100 - 200 seedlings. Plant tissues were ground by adding glass beads to the reaction tubes and homogenized in a TissueLyser II (QIAGEN, 60 second runtime, 30 hertz). For the RNA seq samples three samples (50-100 seedlings) harvested and grown independently in time were combined. Effectiveness of the treatments was confirmed by measuring the hypocotyl lengths of the replicates using ImageJ (**Fig. S4.4**).

Dose response assay

Seedlings were grown on sterile 0.8% plant agar (Duchefa P1001) 1x Murashige-Skoog medium (MS, including MES Buffer and vitamins, Duchefa M0255) without sucrose.

Medium was supplemented with DMSO solvent or 8.5µM Heatin (final concentration) predissolved in DMSO. DMSO concentration was kept at 0.1% (v/v) for all plates. Glutamine was pre-dissolved in milli-q water, and added volumes were kept equal for all plates. Seedlings were pictured after 8 days of growth using a flatbed scanner and hypocotyl lengths were measured using ImageJ software (https://imagej.nih.gov/ij/).

RNA sequencing

For transcriptomics, RNA was isolated using the Sigma Spectrum Plant Total RNA isolation kit and gDNA was removed by on-column DNAse treatment (Sigma-Aldrich). RNA integrity and concentration were checked using RNA 6000 Nano Chips on a Bioanalyzer (Agilent-2100). For RNA-seq library preparation in total 3 samples were prepared for each treatment and time-point, by combing isolated RNA of 3 individually harvested batches per sample, each containing multiple seedlings. Illumina TruSeq RNA Library preparation and Illumina HiSeq2500 (high-throughput) single-end 50 bp sequencing was outsourced to Macrogen, Korea. Quality Control (QC) was performed in house on the raw sequencing reads prior to analysis using FastQC (www.bioinformatics.babraham.ac.uk/projects/fastqc). Subsequently the raw reads were aligned to the Arabidopsis genome (TAIR10) using TopHat v2.0.131 with the parameter settings: 'bowtie[220]', 'no-novel-juncs', 'p 6', 'G', 'min-intron-length 40', 'max-intron-length 2000'. On average 91.6% (54.4 – 97.9%) of the RAW reads could be aligned to the genome per biological replicate. This represents an average of 45.1 (23.2 – 71.3) million mapped reads per sample. Aligned reads were summarized over annotated gene models using HTSeq-count[221] v0.6.12 with settings: '-stranded no', '-i gene_id'. From the TAIR10 GTF file all ORFs of which the annotation starts with 'CPuORF' were manually removed prior summarization to avoid not counting all double annotated bZIP TF family members. Sample counts were depth-adjusted and differential expression was determined using the DESeq package[222], with default settings. All statistics associated with testing for differential gene expression were performed with R (www.r-project.org). Gene expression profiles were hierarchically clustered using the Euclidean distance measure with average linkage using the Bioinformatics package of Matlab release 2014a.

Proteomics

For proteomics, proteins were isolated from seedling samples, digested with trypsin and peptides isolated. Peptides were analyzed for their quantitative profiles using 2-dimensional nanoLC-HR MS/MS (nanoAcquity-Qexactive). To obtain optimal proteome depth the peptide samples were separated in 4 fractions using on-line two-dimensional nanoLC. Ultra-high-resolution LC-MS/MS was used for maximal coverage of identification and quantitative detail. Data acquisition time was 9h per injection. After processing, normalization, quantitation and database matching, quantitative data were reported in excel tables. The quantitative abundance values for in total 7330 proteins were reported

(all samples together), based on the underlying data library from circa 56000 (non-redundant) peptides. Hierarchical cluster analysis showed clear separation of samples on temperature and Heatin effect.

Metabolomics analysis of polar metabolites

Profiling of Arabidopsis seedlings for polar (primary) metabolites was done by gas chromatography time of flight mass spectrometry (GC-ToFMS) after automated derivatization. For this, 100mg of frozen and ground material was prepared as described by Villafort Carvalho *et al.* (2015)[223]. The dried samples were derivatised online as described by using a CombiPAL autosampler (CTC Analytics AG; http://www.ctc.ch) and were subsequently analysed on a GC-ToFMS system (Agilent 6890 GC (Agilent Technologies, http://www.agilent.com) coupled to a Pegasus III ToFMS (Leco Instruments, http://www.leco.com)) as described by Villafort Carvalho et al. (2015)[223]. Raw GCMS data were processed using an untargeted metabolomics workflow established at WUR (Villafort Carvalho et al. 2015 and references therein). Metabolites were identified by matching mass spectra to those of authentic reference standards, available mass spectral databases (NIST08; National Institute of Standards and Technology, Gaithersburg, MD, USA, http://www.nist.gov/srd/; Golm DB, http://gmd.mpimp-golm.mpg.de/) and by comparison of RIs with those published in literature. RIs were calculated using a series of alkanes (injected with every sample) that were fitted with a third-order polynomial function. The processed data were evaluated by multivariate statistical analysis including hierarchical clustering analysis (HCA).

Data analyses

GO-term analyses were performed using the AgriGO online tool at: http://bioinfo.cau.edu.cn/agriGO/analysis.php using standard settings. Venn-diagrams were made using Venny 2.1.0 at http://bioinfogp.cnb.csic.es/tools/venny/. Proteomics data analysis was done using Perseus version 1.5.5.3, using ANOVA and volcano plot functions. Heatmaps were generated using the heatmap.2() function in R (www.r-project.org).

Acknowledgements

This work was supported by *NWO Graduateschool Uitgangsmaterialen* grant NWO#831.13.002 to LvdW and MvZ. Metabolomics and proteomics experiments were supported by Enabling Technology Hotel grants #435002019 to MvZ & RM, respectively #435003004 to MvZ & TA, of The Netherlands Organisation for Health Research and Development ZonMW.

Supplemental figures and tables

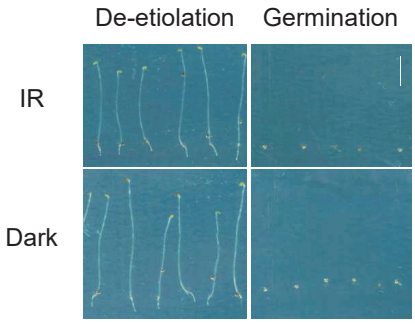

Supplemental Figure 4.1: Validation of time-lapse imaging setup.

Shown are scans of seedlings grown for 7 days while irradiated with the infra-red spotlight used in our time-lapse setup (top panels) in otherwise dark conditions, or grown in complete darkness achieved by aluminum foil (bottom panels). Seedlings (left panels, de-etiolated) were exposed to light for 6 hours to trigger germination, while non-germinated seeds (right panels) were transferred directly to darkness. Scale bar represents 5mm.

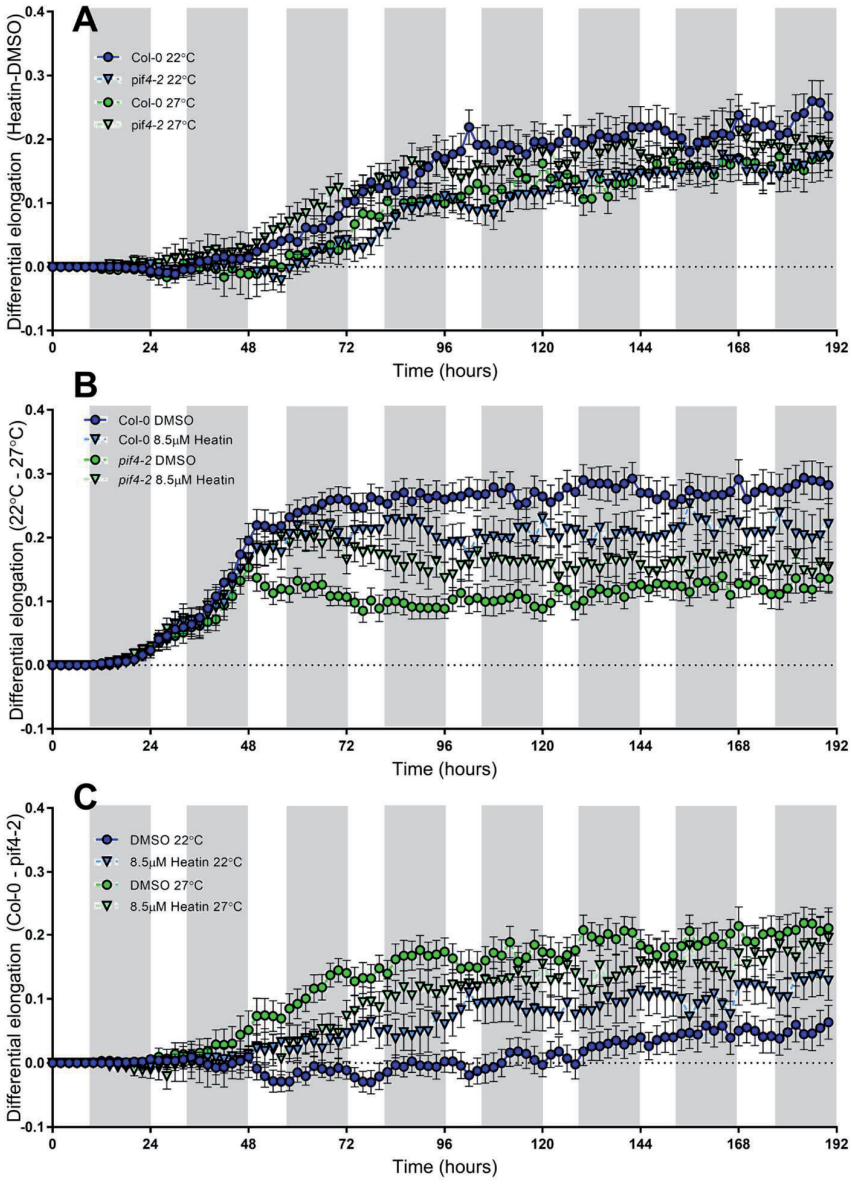

Supplemental Figure 4.2: Differential hypocotyl elongation caused by Heatin (A), temperature (B) and genotype (C).

(**A**) Difference in hypocotyl length between DMSO- and Heatin-grown Col-0 (circles) and *pif4-2* (triangles) seedlings, grown at either 22°C (blue symbols) or 27°C (green symbols). (**B**) Difference in hypocotyl length between 22°C and 27°C grown Col-0 (blue symbols) and *pif4-2* (green symbols) seedlings on DMSO (circles) or Heatin (triangles). (**C**) Difference in hypocotyl length between Col-0 and *pif4-2* seedlings grown at 22°C (blue symbols) or 27°C (green symbols) on DMSO (circles) or Heatin (triangles). These differentials are based on the time series data in Figure 1. Dotted line indicates no difference between the two groups. Values are averages of 12-18 repeats of each 5-10 seedlings. Grey bars indicate night in photoperiod. Error bars denote standard error of mean.

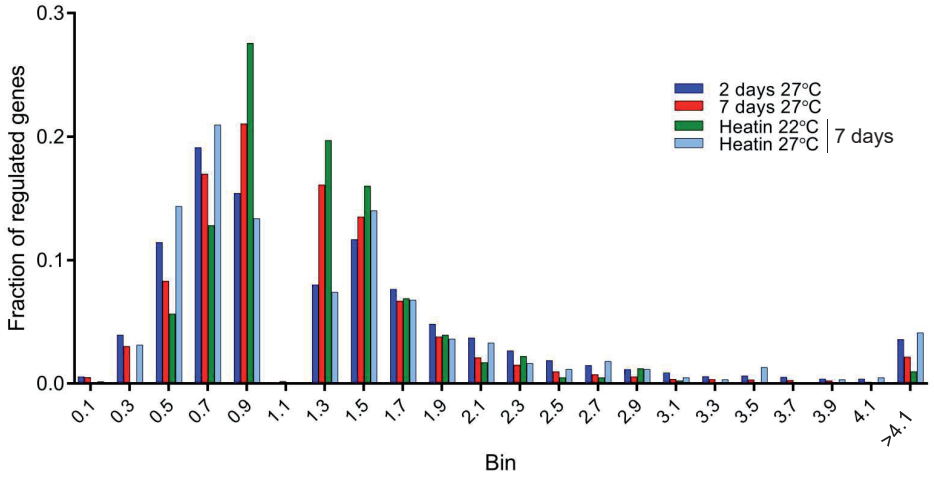

Supplemental Figure 4.3: Fraction of regulated genes in the indicated fold change bin compared to the total amount of regulated genes in a condition compared to control.

Blue and red bars represent genes regulated at 27°C compared to 22°C in 2 day-old and 7 day-old seedlings respectively. Green and light blue bars represent genes regulated by Heatin in 7 day old seedlings under 22°C or 27°C, respectively.

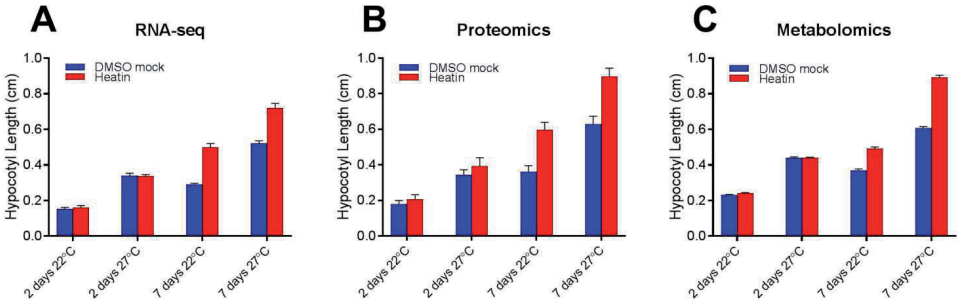

Supplemental Figure 4.4: Hypocotyl length validation of seedlings sampled for RNA-seq, proteomics and metabolomics experiments.

Hypocotyl lengths were measured from photos taken just before harvesting samples for the RNA-seq (**A**), proteomics (**B**) and metabolomics (**C**) analyses and confirm the effectivity and uniformness of our treatments between replicates and type of analysis. Blue bars represent DMSO mock treatment and red bars Heatin treatment. Error bars denote standard error of the mean. Values are averages of 12 (**A**), 8-10 (**B**) and 9-11(**C**) replicates consisting of ~50-100 seedlings each.

Table S4.1: GO-terms of biological processes significantly enriched amongst Heatin regulated genes after 7 days.

Shown are results for the two tested temperatures (22, 27) for up (UP) and down (DN) regulated genes, separately, by GO accession identifier, the term description and the FDR-corrected p-value.

Condition	GO accession	Term	FDR p-value
22-UP	GO:0050896	response to stimulus	5.70E-05
	GO:0042221	response to chemical stimulus	0.00026
	GO:0009733	response to auxin stimulus	0.0014
	GO:0009719	response to endogenous stimulus	0.0017
	GO:0010033	response to organic substance	0.0031
	GO:0009725	response to hormone stimulus	0.014
	GO:0007017	microtubule-based process	0.037
22-DN	GO:0010876	lipid localization	1.30E-09
	GO:0006629	lipid metabolic process	0.00029
	GO:0006869	lipid transport	0.00035
	GO:0009409	response to cold	0.00086
	GO:0050896	response to stimulus	0.0012
	GO:0044255	cellular lipid metabolic process	0.0012
	GO:0019748	secondary metabolic process	0.0027
	GO:0044275	cellular carbohydrate catabolic process	0.0029
	GO:0016052	carbohydrate catabolic process	0.0029
	GO:0009628	response to abiotic stimulus	0.0064
	GO:0006631	fatty acid metabolic process	0.0069
	GO:0009266	response to temperature stimulus	0.0071
	GO:0042221	response to chemical stimulus	0.0094
	GO:0048869	cellular developmental process	0.01
	GO:0009607	response to biotic stimulus	0.012
	GO:0006950	response to stress	0.014
	GO:0051707	response to other organism	0.025
	GO:0032787	monocarboxylic acid metabolic process	0.026
	GO:0009414	response to water deprivation	0.026
	GO:0009555	pollen development	0.026
	GO:0005976	polysaccharide metabolic process	0.026
	GO:0044262	cellular carbohydrate metabolic process	0.027
	GO:0044248	cellular catabolic process	0.028
	GO:0009415	response to water	0.028
	GO:0006720	isoprenoid metabolic process	0.032
	GO:0008610	lipid biosynthetic process	0.032
	GO:0022622	root system development	0.033
	GO:0048364	root development	0.033
	GO:0033036	macromolecule localization	0.039
	GO:0009737	response to abscisic acid stimulus	0.049
	GO:0048513	organ development	0.049
	GO:0048731	system development	0.049

Condition	GO accession	Term	FDR p-value
27-UP	GO:0050896	response to stimulus	2.20E-09
	GO:0042221	response to chemical stimulus	5.60E-07
	GO:0006979	response to oxidative stress	2.20E-05
	GO:0009607	response to biotic stimulus	3.70E-05
	GO:0055072	iron ion homeostasis	4.00E-05
	GO:0051707	response to other organism	4.00E-05
	GO:0065008	regulation of biological quality	4.00E-05
	GO:0006826	iron ion transport	4.60E-05
	GO:0006950	response to stress	5.40E-05
	GO:0009617	response to bacterium	6.40E-05
	GO:0000041	transition metal ion transport	6.50E-05
	GO:0048878	chemical homeostasis	0.00012
	GO:0015674	di-, tri-valent inorganic cation transport	0.00012
	GO:0050801	ion homeostasis	0.00013
	GO:0042545	cell wall modification	0.00042
	GO:0051704	multi-organism process	0.00062
	GO:0010035	response to inorganic substance	0.00073
	GO:0009628	response to abiotic stimulus	0.0014
	GO:0009664	plant-type cell wall organization	0.0021
	GO:0042592	homeostatic process	0.0024
	GO:0009827	plant-type cell wall modification	0.0024
	GO:0000302	response to reactive oxygen species	0.0026
	GO:0055080	cation homeostasis	0.0034
	GO:0006873	cellular ion homeostasis	0.0045
	GO:0055082	cellular chemical homeostasis	0.0046
	GO:0009605	response to external stimulus	0.0049
	GO:0006576	cellular biogenic amine metabolic process	0.0049
	GO:0055066	di-, tri-valent inorganic cation homeostasis	0.0058
	GO:0009719	response to endogenous stimulus	0.0074
	GO:0009266	response to temperature stimulus	0.012
	GO:0042742	defense response to bacterium	0.014
	GO:0009733	response to auxin stimulus	0.015
	GO:0010038	response to metal ion	0.015
	GO:0030003	cellular cation homeostasis	0.015
	GO:0048589	developmental growth	0.016
	GO:0060560	developmental growth involved in morphogenesis	0.016
	GO:0009826	unidimensional cell growth	0.016
	GO:0010033	response to organic substance	0.017
	GO:0048869	cellular developmental process	0.017
	GO:0000902	cell morphogenesis	0.022
	GO:0032502	developmental process	0.034
	GO:0009725	response to hormone stimulus	0.034
	GO:0009408	response to heat	0.034
	GO:0006812	cation transport	0.035
	GO:0006811	ion transport	0.035
	GO:0030001	metal ion transport	0.035
	GO:0032989	cellular component morphogenesis	0.035
	GO:0051179	localization	0.035
	GO:0006810	transport	0.037
	GO:0051234	establishment of localization	0.038
	GO:0042398	cellular amino acid derivative biosynth. process	0.04
	GO:0019725	cellular homeostasis	0.041
27-DN	GO:0010876	lipid localization	7.80E-08
	GO:0048316	seed development	0.00048
	GO:0006722	triterpenoid metabolic process	0.00048
	GO:0010154	fruit development	0.00069
	GO:0009791	post-embryonic development	0.003
	GO:0009790	embryonic development	0.0042
	GO:0009793	embryonic develop. ending in seed dormancy	0.012
	GO:0019748	secondary metabolic process	0.017
	GO:0015833	peptide transport	0.017
	GO:0006857	oligopeptide transport	0.017
	GO:0032502	developmental process	0.032
	GO:0006950	response to stress	0.033
	GO:0009415	response to water	0.04
	GO:0007275	multicellular organismal development	0.044
	GO:0051179	localization	0.044

Table S4.2: GO-terms of biological processes significantly enriched amongst temperature regulated proteins in 2 day-old seedlings.

Shown are the significantly enriched processes (P), functionality (F) and cell compartment (C), by GO accession identifier, the term type, the term description and the FDR-corrected p-value.

GO accession	Term type	Term description	FDR p-value
GO:0009628	P	response to abiotic stimulus	3.80E-14
GO:0050896	P	response to stimulus	1.90E-12
GO:0010876	P	lipid localization	9.80E-12
GO:0006950	P	response to stress	1.80E-10
GO:0015979	P	photosynthesis	8.10E-09
GO:0019684	P	photosynthesis, light reaction	1.40E-06
GO:0009416	P	response to light stimulus	3.70E-06
GO:0009314	P	response to radiation	5.00E-06
GO:0033036	P	macromolecule localization	4.60E-05
GO:0009414	P	response to water deprivation	0.00012
GO:0009409	P	response to cold	0.00012
GO:0008152	P	metabolic process	0.00015
GO:0009415	P	response to water	0.00015
GO:0006091	P	generation of precursor metabolites and energy	0.00062
GO:0042180	P	cellular ketone metabolic process	0.00062
GO:0042221	P	response to chemical stimulus	0.00068
GO:0009266	P	response to temperature stimulus	0.0009
GO:0043436	P	oxoacid metabolic process	0.0011
GO:0006082	P	organic acid metabolic process	0.0011
GO:0019752	P	carboxylic acid metabolic process	0.0011
GO:0006979	P	response to oxidative stress	0.0017
GO:0006519	P	cellular amino acid and derivative metabolic process	0.002
GO:0006631	P	fatty acid metabolic process	0.002
GO:0010118	P	stomatal movement	0.0029
GO:0051179	P	localization	0.0031
GO:0034641	P	cellular nitrogen compound metabolic process	0.0036
GO:0009637	P	response to blue light	0.0056
GO:0009987	P	cellular process	0.0065
GO:0006869	P	lipid transport	0.0066
GO:0006970	P	response to osmotic stress	0.0069
GO:0009791	P	post-embryonic development	0.007
GO:0009605	P	response to external stimulus	0.0094
GO:0044237	P	cellular metabolic process	0.0094
GO:0019438	P	aromatic compound biosynthetic process	0.0099
GO:0009737	P	response to abscisic acid stimulus	0.013
GO:0006810	P	transport	0.013
GO:0051234	P	establishment of localization	0.013
GO:0009642	P	response to light intensity	0.013
GO:0006633	P	fatty acid biosynthetic process	0.014
GO:0009699	P	phenylpropanoid biosynthetic process	0.014
GO:0006725	P	cellular aromatic compound metabolic process	0.016
GO:0032787	P	monocarboxylic acid metabolic process	0.019
GO:0006996	P	organelle organization	0.019
GO:0016053	P	organic acid biosynthetic process	0.02
GO:0046394	P	carboxylic acid biosynthetic process	0.02
GO:0019748	P	secondary metabolic process	0.02
GO:0016043	P	cellular component organization	0.021
GO:0006520	P	cellular amino acid metabolic process	0.024
GO:0044106	P	cellular amine metabolic process	0.027
GO:0032502	P	developmental process	0.028
GO:0042398	P	cellular amino acid derivative biosynthetic process	0.028
GO:0009698	P	phenylpropanoid metabolic process	0.03
GO:0009657	P	plastid organization	0.03
GO:0006508	P	proteolysis	0.042

GO accession	Term type	Term description	FDR p-value
GO:0005737	C	cytoplasm	1.00E-25
GO:0044444	C	cytoplasmic part	3.60E-25
GO:0044424	C	intracellular part	5.20E-25
GO:0044464	C	cell part	4.80E-24
GO:0005623	C	cell	4.80E-24
GO:0005622	C	intracellular	1.90E-23
GO:0043229	C	intracellular organelle	6.00E-22
GO:0043226	C	organelle	6.00E-22
GO:0043227	C	membrane-bounded organelle	5.30E-21
GO:0043231	C	intracellular membrane-bounded organelle	1.50E-20
GO:0044446	C	intracellular organelle part	1.30E-17
GO:0044422	C	organelle part	1.30E-17
GO:0016020	C	membrane	5.20E-14
GO:0044435	C	plastid part	1.60E-13
GO:0009579	C	thylakoid	6.70E-12
GO:0009536	C	plastid	2.00E-10
GO:0032991	C	macromolecular complex	3.30E-10
GO:0044434	C	chloroplast part	5.00E-10
GO:0031090	C	organelle membrane	1.30E-09
GO:0009507	C	chloroplast	6.80E-09
GO:0034357	C	photosynthetic membrane	8.80E-09
GO:0009521	C	photosystem	6.70E-08
GO:0044436	C	thylakoid part	2.90E-07
GO:0010287	C	plastoglobule	3.20E-07
GO:0043234	C	protein complex	6.50E-07
GO:0009523	C	photosystem II	1.40E-06
GO:0005886	C	plasma membrane	2.40E-06
GO:0009532	C	plastid stroma	2.80E-06
GO:0043232	C	intracellular non-membrane-bounded organelle	1.50E-05
GO:0043228	C	non-membrane-bounded organelle	1.50E-05
GO:0005774	C	vacuolar membrane	1.50E-05
GO:0044437	C	vacuolar part	1.90E-05
GO:0009534	C	chloroplast thylakoid	2.80E-05
GO:0005840	C	ribosome	2.90E-05
GO:0031976	C	plastid thylakoid	2.90E-05
GO:0031984	C	organelle subcompartment	3.10E-05
GO:0030076	C	light-harvesting complex	5.90E-05
GO:0042651	C	thylakoid membrane	0.00018
GO:0030529	C	ribonucleoprotein complex	0.00023
GO:0005773	C	vacuole	0.00034
GO:0005783	C	endoplasmic reticulum	0.0005
GO:0009570	C	chloroplast stroma	0.0011
GO:0022626	C	cytosolic ribosome	0.0021
GO:0000325	C	plant-type vacuole	0.0021
GO:0015935	C	small ribosomal subunit	0.0021
GO:0055035	C	plastid thylakoid membrane	0.003
GO:0009535	C	chloroplast thylakoid membrane	0.003
GO:0031967	C	organelle envelope	0.0041
GO:0031975	C	envelope	0.0041
GO:0044425	C	membrane part	0.0041
GO:0031974	C	membrane-enclosed lumen	0.0062
GO:0009526	C	plastid envelope	0.0064
GO:0005730	C	nucleolus	0.0072
GO:0005739	C	mitochondrion	0.0094
GO:0043233	C	organelle lumen	0.016
GO:0070013	C	intracellular organelle lumen	0.016
GO:0033279	C	ribosomal subunit	0.017
GO:0005829	C	cytosol	0.022
GO:0009941	C	chloroplast envelope	0.024
GO:0005634	C	nucleus	0.039
GO:0031981	C	nuclear lumen	0.042
GO:0019866	C	organelle inner membrane	0.045

GO accession	Term type	Term description	FDR p-value
GO:0045735	F	nutrient reservoir activity	1.00E-10
GO:0016168	F	chlorophyll binding	3.00E-10
GO:0046906	F	tetrapyrrole binding	6.90E-10
GO:0003824	F	catalytic activity	2.30E-06
GO:0015250	F	water channel activity	8.10E-05
GO:0005372	F	water transmembrane transporter activity	8.10E-05
GO:0008289	F	lipid binding	0.00035
GO:0015405	F	P-P-bond-hydrolysis-driven transmembrane transporter activity	0.00064
GO:0016887	F	ATPase activity	0.00064
GO:0015399	F	primary active transmembrane transporter activity	0.00064
GO:0016787	F	hydrolase activity	0.0011
GO:0016491	F	oxidoreductase activity	0.0011
GO:0017111	F	nucleoside-triphosphatase activity	0.0082
GO:0042623	F	ATPase activity, coupled	0.0084
GO:0008233	F	peptidase activity	0.0084
GO:0003735	F	structural constituent of ribosome	0.0084
GO:0042626	F	ATPase activity, coupled to transmembrane movement of substances	0.0086
GO:0043492	F	ATPase activity, coupled to movement of substances	0.0086
GO:0016820	F	hydrolase activity, acting on acid anhydrides, catalyzing transmembrane movement of substances	0.0087
GO:0016818	F	hydrolase activity, acting on acid anhydrides, in phosphorus-containing anhydrides	0.0089
GO:0016817	F	hydrolase activity, acting on acid anhydrides	0.0089
GO:0016462	F	pyrophosphatase activity	0.0089
GO:0016209	F	antioxidant activity	0.014
GO:0022803	F	passive transmembrane transporter activity	0.014
GO:0015267	F	channel activity	0.014
GO:0022838	F	substrate-specific channel activity	0.014
GO:0070011	F	peptidase activity, acting on L-amino acid peptides	0.017
GO:0016684	F	oxidoreductase activity, acting on peroxide as acceptor	0.032
GO:0004601	F	peroxidase activity	0.032
GO:0005215	F	transporter activity	0.037
GO:0005198	F	structural molecule activity	0.042
GO:0022857	F	transmembrane transporter activity	0.048

Table S4.3: List of candidate proteins of interest for further studies based on LFQ levels under high temperature and Heatin treatment.

List is based on the heatmap in figure 3 and shows the corresponding Arabidopsis gene Identifier (AGI), synonym and a brief description.

AGI	Other name	brief description
AT4G12800	PSAL	photosystem I subunit l
AT4G21800	QQT2	P-loop containing nucleoside triphosphate hydrolases superfamily protein
AT4G02680	EOL1	ETO1-like 1
AT4G17085	AT4G17085	Putative membrane lipoprotein
AT5G58060	YKT61	SNARE-like superfamily protein
AT2G34660	ABCC2	multidrug resistance-associated protein 2
AT5G17790	VAR3	zinc finger (Ran-binding) family protein
AT4G34131	UGT73B3	UDP-glucosyl transferase 73B3
At5g16280	AT5G16280	Tetratricopeptide repeat (TPR)-like superfamily protein
At5g47700	AT5G47700	60S acidic ribosomal protein family
At1g78520	AT1G78520	Carbohydrate-binding X8 domain superfamily protein
	Expressed protein	#N/A
At1g75830	LCR67	low-molecular-weight cysteine-rich 67
At5g05270	CHIL	Chalcone-flavanone isomerase family protein
At4g34290	AT4G34290	SWIB/MDM2 domain superfamily protein
AT3g02480	AT3G02480	Late embryogenesis abundant protein (LEA) family protein
At3g05560	AT3G05560	Ribosomal L22e protein family
AT3G58680	MBF1B	multiprotein bridging factor 1B
At4g01610	AT4G01610	Cysteine proteinases superfamily protein
At5g38170	AT5G38170	Bifunctional inhibitor/lipid-transfer protein/seed storage 2S albumin superfamily protein
At1g02560	CLPP5	nuclear encoded CLP protease 5
AT5g20160	AT5G20160	Ribosomal protein L7Ae/L30e/S12e/Gadd45 family protein
AT1G67330	AT1G67330	glucuronoxylan 4-O-methyltransferase-like protein (DUF579)

Supplementary files

Supplemental files are available on request (lennardcasper@yahoo.com):
Supplemental file 4.1. List of proteins significantly regulated under high temperature
Supplemental file 4.2. Metabolomics data

CHAPTER 5

5

Heatin inhibits the activity of the NIT1 sub-family of Nitrilases via a direct interaction

Lennard van der Woude[1] | Markus Piotrowski[2] | Gruson Klaasse[3] | Kamaleddin Hajmohammadebrahimtehrani[3] | Judith Paulus[4] | Daniel Krahn[4] | Sabrina Ninck[5] | Farnusch Kaschani[5] | Markus Kaiser[5] | Ondrej Novak[6] | Karin Ljung[7] | Renier A. L. van der Hoorn[4] | Nathaniel Martin[3] | Sjef Smeekens[1] | Martijn van Zanten[1]

[1] Molecular Plant Physiology, Institute of Environmental Biology, Utrecht University, Padualaan 8, 3584 CH Utrecht, The Netherlands
[2] Lehrstuhl für Pflanzenphysiologie, Ruhr-Universität Bochum ND 3/49, Universitätsstraße 150, 44801 Bochum, Germany
[3] Department of Chemical Biology & Drug Discovery, Utrecht Institute for Pharmaceutical Sciences, University Utrecht, Universiteitsweg 99, 3584 CG Utrecht, The Netherlands
[4] Plant Chemetics Laboratory, Department of Plant Sciences, University of Oxford, South Parks Road, OX1 3RB Oxford, United Kingdom
[5] Chemische Biologie, Zentrum für Medizinische Biotechnologie, Fakultät für Biologie, Universität Duisburg-Essen, Universitätsstr. 2, 45117 Essen, Germany.
[6] Laboratory of Growth Regulators, Centre of the Region Haná for Biotechnological and Agricultural Research, Institute of Experimental Botany CAS & Faculty of Science of Palacký University, Šlechtitelů 27, 78371 Olomouc, Czech Republic
[7] Umeå Plant Science Centre, Department of Forest Genetics and Plant Physiology, Swedish University of Agricultural Sciences, SE-901 83, Umea, Sweden

Abstract

Global temperatures are predicted to rise in the coming decades due to climate change. This will likely negatively impact development and growth of crops and thereby threatens food security. Many plants respond to mild increases in ambient temperature by adjusting their architecture in a process called thermomorphogenesis, to mitigate negative effects of high temperatures. Understanding the molecular regulation of thermomorphogenesis can facilitate the development of climate change resilient crops and helps to prevent future crop losses. Using a chemical genetic approach, we identified a compound, named Heatin, that induces thermomorphogenesis phenotypes already under control temperature conditions. Here we present a chemical proteomics experiment using beads covered with a Heatin analogue modified with a linker-moiety, aimed to identify Heatin interacting proteins. We pulled-down NITRILASE 1, 2 and 3 that together constitute the full NIT1 subfamily of Arabidopsis Nitrilases. Subsequent mutant analyses confirmed that Nitrilases are required for Heatin-mediated elongation and we demonstrate that Heatin directly inhibits Nitrilase enzymatic activity. This work provides mechanistic insight into Heatin mediated elongation growth, by binding and affecting Nitrilase activity. Assessing the effects of Heatin on auxin metabolism revealed complex regulation resulting in increases in IAN, IAA ANT and TRP, in a time and genotype dependent manners.

Introduction

Average global temperatures have increased in the past decades[224] and are predicted to continue to rise in the coming decades[4]. Several models predict dramatic losses of staple crop productivity due to these changes, imposing a significant threat for global food security[13]. Breeding for climate change resilient crops could increase crop performance under the changing environment and thereby increase food security[19,20]. Next generation breeding techniques will allow for more efficient and faster breeding cycles[22,23], provided that fundamental knowledge is available to direct such breeding for the looming problems[25]. Next to knowledge-based breeding of climate change resistant crops also the identification and use of specific chemicals that induce desired plant responses can be a promising strategy to negate climate effect.

In response to an increase in temperature of just a few degrees within the ambient range, many plants display thermomorphogenesis. In the model plant *Arabidopsis thaliana*, thermomorphogenesis consists among other traits of elongation of the hypocotyl and leaf stalks and an increased leaf angle relative to the horizontal[115]. This response is induced to enhance leaf cooling capacity and to avoid direct heat flux from the sun[44,45].

In recent years, several key components of the molecular thermomorphogenesis signaling network have been discovered[36,42,43,56,74,216]. A central hub in the network is the transcription factor PHYTOCHROME INTERACTING FACTOR 4 (PIF4), since mutants in *PIF4* lack the ability to induce thermomorphogenesis[37]. A key function of PIF4 in thermomorphogenesis signaling is to stimulate biosynthesis of the endogenous auxin indole-3-acetic acid (IAA)[39,56], which subsequently causes elongation growth through the acid growth mechanism[76] (**Chapter 4**). PIF4 stimulates IAA biosynthesis by direct binding to and stimulating the expression of the auxin biosynthesis genes *YUCCA8* (*YUC8*), *TRYPTOPHAN AMINOTRANSFERASE OF ARABIDOPSIS1 (TAA1*) and the cytochrome P450 family member *CYP79B2*[39,56]. *YUC8* and *TAA1* function in the dominant biosynthesis pathway where L-tryptophan (TRP) is converted into indole-3-pyruvic acid (IPyA) by TAA1, and subsequently into bioactive IAA by YUC8[59]. *CYP79B2* functions in a *Brassicaceae*-specific parallel pathway where it converts TRP into indole-3-acetaldoxime (IAOx)[60]. IAOx is subsequently converted into indole-3-acetonitrile (IAN) by CYP71A1 and then hydrolyzed by Nitrilase proteins into bioactive IAA[61]. This alternative IAA biosynthesis pathway involving IAN and Nitrilases has also been implicated in metabolism of defense-related compounds[62,63].

With the aim of understanding thermomorphogenesis signaling in Arabidopsis, we performed a chemical genetic screen to identify small synthetic compounds that could rescue the suppressed elongation response of *pif4-2* mutant seedlings at high temperatures (**Chapter 2**). The identification of such novel bioactive molecules is typically done by screening large chemical libraries for compounds eliciting a desired phenotype

or biological effect of interest. The application of this strategy to plant-based studies has resulted in the identification of many novel bioactive compounds that have a variety of targets and effects (reviewed in[80]). Subsequently, typical chemical genetic studies involve unravelling the mechanism of action of the identified compound(s). This entails identification of the targeted biomolecules, such as proteins, and subsequent follow-up studies into the validation of the interaction(s)[85] between compound and biomolecule, followed by assessment of the underlying molecular mechanisms and signaling networks. One major advantage of a chemical genetic strategy over classical genetic approaches is that small molecules can potentially target multiple members of the same protein family. This allows assessing phenotypes that are otherwise masked by genetic redundancy in classical mutation-based genetic approaches[85].

In our chemical genetic screen, we identified compounds that triggered elongation under high temperature in *pif4-2* and focused on one compound named Heatin, because this compound did not induce unrelated auxigenic phenotypes like agravitropy or root growth inhibition (**Chapter 2, 3**). Subsequently, we used Heatin as a tool to further unravel elongation growth (**Chapter 3, 4**). In chapter **Chapter 3** we showed that Heatin acts downstream or parallel to *PIF4* during thermomorphogenesis control and acts upstream of auxin signaling or directly as a hypocotyl-specific auxigenic compound. Transcriptomic analysis further supported a link between Heatin and auxin (**Chapter 4**). Additionally, we showed in **Chapter 3** that Heatin activity relies on the activity of the aldehyde oxidation enzymes *ARABIDOPSIS ALDEHYDE OXIDASE 1* (*AAO1*) and *AAO2*, of which the former has been implicated in IAA biosynthesis[225] as well, although this role has been disputed[226,227].

Although these approaches are informative for Heatin's mechanism of action, it does not indicate which biomolecules are directly targeted. Identification of such targeted biomolecules constitutes a major challenge. One approach could be to isolate mutants that are resistant to the compound under study. For instance, an ethyl methanesulfonate (EMS) mutagenized population could be used to screen for mutants that exhibit compound resistance, the mutated proteins could be identified and tested for interaction with the compound in question *in vitro*[91]. This approach can however only be reasonably successful when there is no genetic redundancy in the system; *e.g.* if only a single target biomolecule interacts with the compound[85]. In cases where the compound targets a larger family of redundant proteins, chemical proteomic strategies can be used to directly identify interactors[113,228]. Chemical proteomics typically requires untargeted techniques to identify interacting proteins, following a method of discerning the true targets from non-target proteins, such as a solid phase extraction or increased protease resistance.

Here we performed a pull-down experiment using a tagged Heatin analogue and enrich for specific Heatin interactors. By subsequent comparative proteomics analysis, we found that the full NIT1-subfamily of proteins was significantly enriched in Heatin eluates. Interestingly, mutants disturbed in NIT functioning are less sensitive to

Heatin and subsequent *in vitro* assays for Nitrilase activity showed that Heatin reduces Nitrilase activity. Moreover, we confirm that Heatin affects auxin metabolism in a manner dependent on Nitrilase and Aldehyde Oxidation functioning in 3-day-old seedlings, by profiling of auxin metabolites. Together these findings indicate that Heatin modulates NIT enzyme activity to cause auxin-induced hypocotyl elongation.

Results

Identification of Heatin interacting proteins by chemical proteomics

An important step in understanding Heatin-induced elongation growth is the identification of Heatin's biomolecular targets. The chemical library (LCBU screening library), used to identify Heatin, consisted mainly of aromatic druglike molecules that cover a wide range of chemical space. We therefore followed a chemical proteomics[229] strategy - using an *in house* synthesised azide-functionalized Heatin analogue (**Supplemental information 5.1**) coupled to alkyne-functionalized magnetic beads to identify Heatin interacting proteins (**Fig. 5.1A**).

Structure activity relationship studies on the Heatin compound revealed 1-aminomethyl–naphthalene-2-ol as bioactive moiety (**Chapter 3**). Analogue **#202** (**Table 3.1**) is also bioactive similar to Heatin, and shares the 2-napthol moiety, but instead of a central hydrazide bond, the nitrogen is attached by a 3° amine bond, which is less prone to hydrolysis (**Fig. 5.1B**). Additionally, **#202** is more readily chemically modified into the required probe. Therefore analogue **#202** was used as a starting point for probe synthesis for the chemical proteomics approach. An azide-functionalized version of analogue **#202** was designed and synthesized (**Supplemental information 5.1, Fig. 5.1B**) without disturbing the active moiety. Next, the azide-functionalized **#202** was attached to magnetic beads to form the 'Heatin-covered beads' required for the chemical proteomic approach by a Cu(I)-catalysed Huisgen azide-alkyne 1,3-dipolar cycloaddition reaction (**Fig. 5.1A**).

Heatin-covered beads were incubated with a protein extract of 2-3 day-old seedlings. After incubation the magnetic beads were stringently washed to remove unbound proteins. To enrich for Heatin-specific targets on one hand and to omit unspecific proteins attached to the beads or different parts of the probe on the other, an elution was performed with the original Heatin molecule (**Fig. 5.1A**). The resulting elute-fraction and the 'on-bead' remaining fractions were collected separately and proteins in these fractions were identified by Liquid Chromatography-tandem Mass Spectrometry analysis (LC-MS/MS) (**Fig. 5.2**). A total of 2204 (excluding 'known contaminants' *i.e.* human proteins picked up during sample preparation and handling and proteins identified by less than two unique peptides) different proteins were identified over all samples. We first separated false

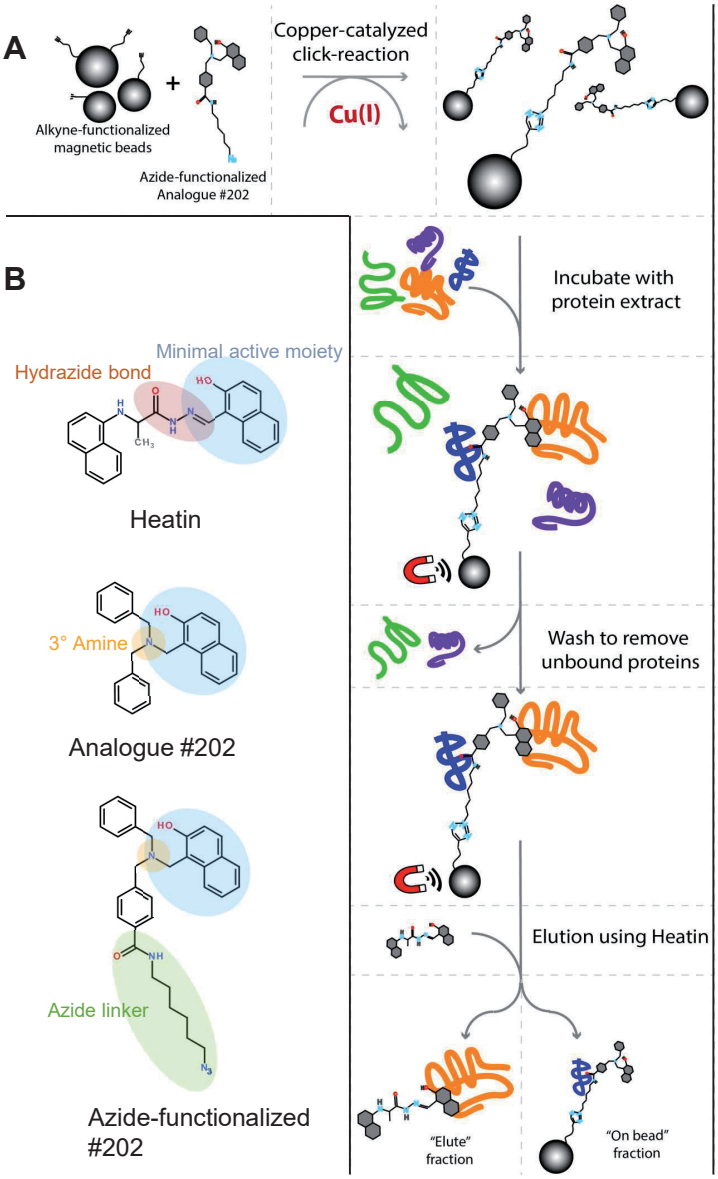

Figure 5.1: Targeted pulldown strategy and probe design.

(**A**) schematic representation of the followed chemical proteomics strategy to pull down Heatin-bound proteins. Alkyne-functionalized magnetic beads are covered by azide-functionalized Heatin analogue #202 through a copper catalyzed click reaction (top). Next, interacting proteins from seedling-derived extracts are isolated by a pull-down using a magnet to retain the beads and washing away unbound proteins. Subsequently, true Heatin targets are separated from background signal by eluting them from the beads using Heatin, generating two fractions that are separately analyzed by mass-spectrometry analysis (right bottom). (**B**) Chemical structures of Heatin, Heatin analogue #202 and Azide-functionalized #202, which functions as Heatin-derived probe. Highlighted are the minimal active moiety of Heatin (blue), Heatin's hydrazide bond (red) and analogye #202's corresponding amine bond (yellow) and the azide linker group (green).

positives; *e.g.* proteins that non-specifically stick to the beads or the probe, or those that are likely stoichiometrically present due to their high abundance in young seedlings, from potential true Heatin targets, by selecting significantly overrepresented proteins in the elute-fraction, with a minimal difference of 1 'Label Free Quantification' (LFQ) unit. This reduced the number of potential interactors by 91.3%, to 162 proteins (**Fig. 5.2, Table S5.1**).

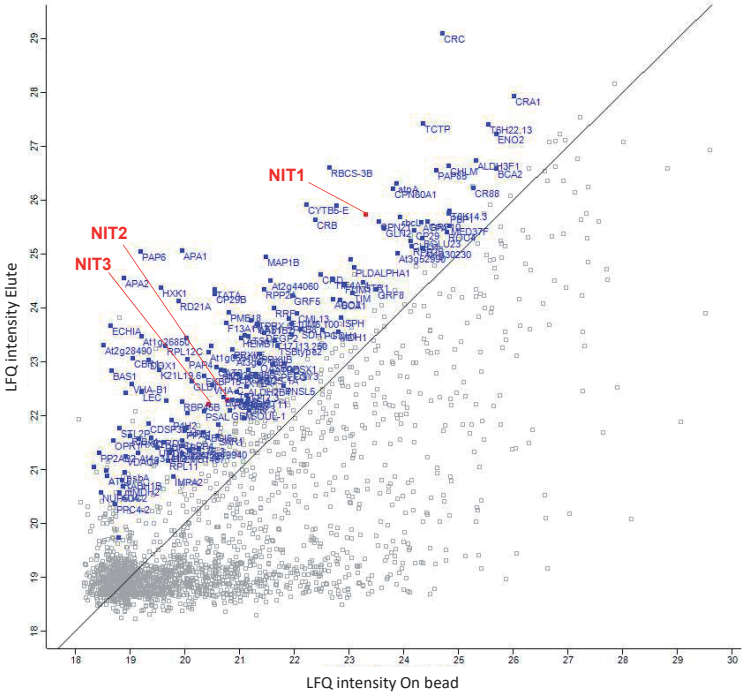

Figure 5.2: Proteins enriched in the Heatin-eluted fraction of the chemical proteomics approach.

LFQ intensity of 'On-Bead' fraction (x-axis) and 'Elute' fraction (y-axis). Each square represents a protein identified in both fractions. Blue squares, annotated with gene name (if available) represent protein that are significantly more abundant in the 'Elute' (Heatin eluted) fraction than in the 'On Bead' fraction, as calculated by t-test comparisson ($p<0.05$, permutation-based FDR) and with a minimum difference of 1 LFQ unit. Red squares represent NIT1, NIT2 and NIT3. vertical grey dotted line is the function y=x.

Small molecules can bind multiple members of multi-protein families, and hence chemical genetic approaches are particularly useful to overcome genetic redundancy[80,96]. We therefore aimed to identify protein families targeted by Heatin. To identify protein families amongst the 162 identified proteins, we analysed the 162 amino acid sequences by 'all vs all' BLASTp and proteins with high homology (E<1E-5) with at least one other protein in the set of 162 proteins were selected (**Table 5.1, Fig. S5.1**).

Table 5.1: Homology clusters identified amongst Heatin interacting proteins.

Shown are the group member's Arabidopsis gene identifier (AGI) codes corresponding to the identified proteins, their synonyms, and a brief description as derived from Araport (www.araport.org). The most specific common molecular annotation of the group is used to determine whether it is often found in eukaryotic proteomic analyses, according to Wang *et al.*[230] indicated by an X and text is grey if it is, black if not. The total number of genes (#genes) with the common annotation, the total number of detected genes in the homology group (*A. thaliana* genes with annotation) and the representation percentage (%) of identified genes compared the total, are shown in the last three columns.

Homology cluster	AGI code of protein	Synonym	Brief description	Molecular annotation	Usual suspect (Wang *et al.*)	# genes	*A. thaliana* genes with annotation	%
1	at3g53460	CP29	chloroplast RNA-binding protein 29	RNA Binding		5	1186	0.42
	at3g52150	PSRP2	RNA-binding (RRM/RBD/RNP motifs) family protein					
	at2g35410		RNA-binding (RRM/RBD/RNP motifs) family protein					
	at2g37220		RNA-binding (RRM/RBD/RNP motifs) family protein					
	at1g49760	PAB8	poly(A) binding protein 8					
2	at3g22640	PAP85	cupin family protein	nutrient reservoir activity		6	67	8.96
	at2g28490		RmlC-like cupins superfamily protein					
	at1g03880	CRU2	cruciferin 2					
	at4g28520	CRU3	cruciferin 3					
	at1g03890		RmlC-like cupins superfamily protein					
	at5g44120	CRA1	RmlC-like cupins superfamily protein					
3	atcg00120	ATPA	ATP synthase subunit alpha	ATPase activity, coupled to transmembrane movement of ions, rotational mechanism	x	4	27	14.81
	at5g08690		ATP synthase alpha/beta family protein					
	at1g76030	VAB1	ATPase, V1 complex, subunit B protein					
	atmg01190	ATP1	ATP synthase subunit 1					
4	at3g44320	NIT3	nitrilase 3	indole-3-acetonitrile nitrile hydratase activity		3	3	100.00
	at3g44300	NIT2	nitrilase 2					
	at3g44310	NIT1	nitrilase 1					
5	at3g01500	CA1	carbonic anhydrase 1	carbonate dehydratase activity		3	18	16.67
	at4g33580	BCA5	beta carbonic anhydrase 5					
	at5g14740	CA2	carbonic anhydrase 2					
6	at1g22300	GRF10	general regulatory factor 10	protein phosphorylated amino acid binding	x	3	17	17.65
	at5g16050	GRF5	general regulatory factor 5					
	at5g65430	GRF8	general regulatory factor 8					
7	at3g23400	FIB4	Plastid-lipid associated protein PAP / fibrillin family protein	chloroplast thylakoid			?	
	at3g26070		Plastid-lipid associated protein PAP / fibrillin family protein					
	at5g19940		Plastid-lipid associated protein PAP / fibrillin family protein					

8	at3g52960		Thioredoxin superfamily protein	peroxiredoxin activity	x	4	10	40.00
	at1g65980	TPX1	thioredoxin-dependent peroxidase 1					
	at3g11630		Thioredoxin superfamily protein					
	at3g26060	PRXQ	Thioredoxin superfamily protein					
9	at3g62030	ROC4	rotamase CYP 4	peptidyl-prolyl cis-trans isomerase activity		2	58	3.45
	at5g13120	Pnsl5	cyclophilin 20-2					
10	at3g48000	ALDH2B4	aldehyde dehydrogenase 2B4	aldehyde dehydrogenase (NAD) activity	x	2	10	20.00
	at4g36250	ALDH3F1	aldehyde dehydrogenase 3F1					
11	at3g13920	EIF4A1	eukaryotic translation initiation factor 4A1	ATP-dependent RNA helicase activity	x		?	
	at5g11200	UAP56b	DEAD/DEAH box RNA helicase family protein					
12	at2g36580		Pyruvate kinase family protein	pyruvate kinase activity		2	14	14.29
	at3g52990		Pyruvate kinase family protein					
13	at2g34420	LHB1B2	photosystem II light harvesting complex protein B1B2	chlorophyll binding		2	38	5.26
	at3g08940	LHCB4.2	light harvesting complex photosystem II					
14	at2g27710		60S acidic ribosomal protein family	structural constituent of ribosome		2	340	0.59
	at2g27720		60S acidic ribosomal protein family					
15	at2g19860	HXK2	hexokinase 2	hexokinase activity		2	3	66.67
	at4g29130	HXK1	hexokinase 1					
16	at1g67090	RBCS1A	ribulose bisphosphate carboxylase small chain 1A	chloroplast ribulose bisphosphate carboxylase complex biogenesis			?	
	at5g38410	RBCS3B	Ribulose bisphosphate carboxylase (small chain) family protein					
17	at1g56070	LOS1	Ribosomal protein S5/Elongation factor G/III/V family protein	translation elongation factor activity	x	2	55	3.64
	at1g62750	SCO1	Translation elongation factor EFG/EF2 protein					
18	at1g11910	APA1	aspartic proteinase A1	aspartic-type endopeptidase activity		2	22	9.09
	at1g62290		Saposin-like aspartyl protease family protein					
19	at1g06690		NAD(P)-linked oxidoreductase superfamily protein	oxidation-reduction process			?	
	at1g60710	ATB2	NAD(P)-linked oxidoreductase superfamily protein					
20	at2g44610	RAB6A	Ras-related small GTP-binding family protein	GTP binding		2	696	0.29
	at3g62290	ARFA1E	ADP-ribosylation factor A1E					

In total, 55 proteins in 20 homology groups were identified, of which seven groups with 26 proteins contained at least three proteins. By comparing molecular function annotations of each homology group to frequently found false positive proteins in comparative proteomic studies performed on animals[230], we excluded groups 3, 6, 8, 10, 11, 17 from further analysis as these are less likely Heatin-interacting proteins than those in the other groups (**Table 5.1**). We next compared the number of proteins in each remaining group with the total amount of proteins annotated with the same term. Group 4 and 15, strikingly had a very high percentage of proteins with the annotations present; *i.e.* 100% for group 4 (NIT1 sub-family of Nitrilases) and 66,67% for group 15 (Hexokinases). This suggests that Heatin might target all, or the majority of the proteins in these protein families. As 100% of NIT1 sub/family members were found we further investigated the possibility that Heatin targets this full protein family.

Nitrilase enzymes hydrolyse nitriles into carboxylic acid and ammonia and are found throughout the plant kingdom, and are mainly involved in cyanide detoxification[62]. In Arabidopsis, Nitrilases can be divided into two sub-families: the NIT4 and the NIT1 sub-family. NIT4 has a high substrate specificity and has a well understood function in cyanide detoxification, whereas the NIT1 subfamily is restricted to the *Brassicaceae* family and their function is less well defined[62]. Previously, reports have shown effects of NIT1 sub-family members in defence and in auxin metabolism, although the latter is not supported by investigations into the NIT1 sub-family member substrate preferences[62].

***nit* mutants showed reduced sensitivity to Heatin**

Nitrilases have been associated with auxin biosynthesis[61] and since thermomorphogenesis depends on auxin biosynthesis, Nitrilases were studied for their potential role in Heatin directed-hypocotyl elongation. Our transcriptomics data (**Chapter 4**) showed that *NIT1* transcript was highly abundant in our seedling materials, but that *NIT2* and *NIT3* were expressed below and on average, respectively, compared to the total of expressed transcripts (**Fig. S5.2A**). Our proteomics data (**Chapter 4**) showed similar results for NIT protein abundance (**Fig. S5.2B**). It is therefore considered unlikely that NIT2 and NIT3 were isolated due to stoichiometry. Additionally, we did not detect regulation of NIT1, NIT2, and NIT3 transcript nor protein abundance by Heatin, in contrast to temperature, which does have significant effects on *NIT1*, *NIT2* and *NIT3* transcription and on NIT3 protein abundance (**Fig. S5.2**). More specifically, at 27°C NIT1 and NIT3 were both transcriptionally downregulated whereas NIT2 was upregulated compared to 22°C (**Fig. S5.2A**), with proteomic data showing similar trends (**Fig. S5.2B**).

To test for Nitrilase requirement of Heatin-induced hypocotyl elongation we assayed several mutants disturbed in Nitrilase functioning **(Fig. 5.3**). We tested single knock-out mutants for each individual *NIT*, *i.e. nit1-3*[141], *nit2* and *nit3* mutant lines, in addition to *NIT2RNAi* lines that lack observable *NIT1* and *NIT2* expression and NIT1, 2 and 3 protein

could not be detected by Western blot analysis[61,231] in the Col-0 WT background. None of the tested mutants displayed deviant hypocotyl lengths compared to Col-0 WT in control temperature conditions in the absence of Heatin. However, in the presence of Heatin in the growth medium, several sensitivity effects were noted, overall confirming a requirement of NIT1 and NIT2 for Heatin-mediated hypocotyl elongation. In the presence of Heatin, hypocotyls of *nit1-3* and two independent *NIT2 RNAi* lines were significantly shorter than wild type in both control and high temperature conditions (**Fig. 5.3A**). The *nit2* knock-out mutant did not respond differently to Heatin under control temperatures but was significantly shorter under high temperatures. No significant deviant effects were observed in the *nit3* knock-out mutant background, suggesting that NIT3 has no prominent role in Heatin-mediated hypocotyl elongation (**Fig. 5.3A**).

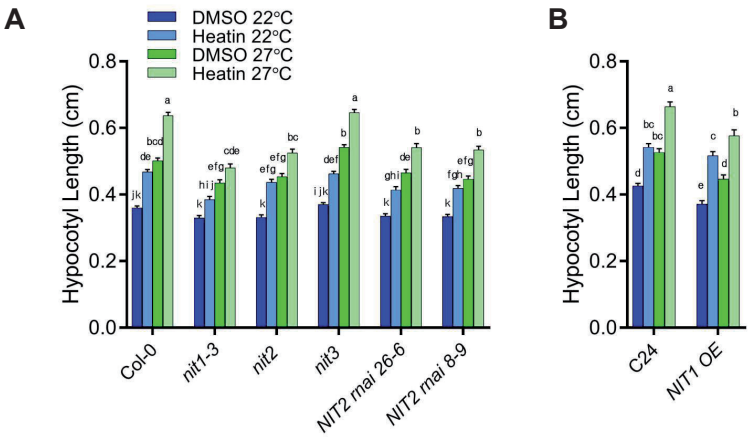

Figure 5.3: Mutants disturbed in NITRILASE functioning have altered Heatin sensitivity.

(**A, B**) Hypocotyl lengths of 8 day-old seedlings of indicated genotypes grown on medium containing either DMSO (dark blue and bright green bars) or 8.5µM Heatin (light blue or light green bars) in the Col-0 (**A**) and C24 (**B**) background with their respective wild types. at either 22°C (blue bars) or 27°C (green bars). Error bars indicate standard error of the mean, values are averages of 6 repeats of 20-30 seedlings. Letters indicate significance groups following Tukey HSD post-hoc tests, where averages that do not share letters are significantly different at $p<0.05$.

In addition to knock-out/down lines in the Col-0 WT background, we also tested a *35S::NIT1* overexpression line in the C24 WT genetic background (*NIT1OE*). This line exhibited shorter hypocotyls under control conditions on control medium, but this difference was not found when grown in the presence of Heatin, suggesting possible hypersensitivity to Heatin (**Fig. 5.3B**). Under high temperature conditions *NIT1OE* however did not display Heatin hypersensitivity, as the hypocotyl was shorter than that of WT when grown with or without Heatin. Together, these results suggest that the Nitrilases contribute to the hypocotyl length effects of Heatin. Based on the phenotypes, *NIT1* seems to be the

main contributor to hypocotyl elongation whereas *NIT2* has a more limited contribution. *NIT3* seemingly does not affect hypocotyl length. The Nitrilases seem to play redundant roles, as the single mutants were all still responsive to Heatin, although to a lesser degree than WT. Alternatively, Nitrilases only partly contribute to Heatin-mediated hypocotyl elongation, and other factors are responsible for the remaining elongation response.

Heatin reduces Nitrilase enzymatic activity

To further characterise the interaction between Heatin and the Nitrilases, we tested the effect of Heatin on Nitrilase enzymatic activity. We employed an *in vitro* assay system[232] using purified recombinant HIS-immunotagged NITs[233] and different substrates and tested NIT activity by colorimetric assays based on the 'Berthelot's' reaction for ammonia produced. Turnover of 3-phenyl-propionitrile (3-PPN) substrate by recombinant NIT1, 2 and 3[232] protein was inhibited in the presence of Heatin as compared to DMSO mock under otherwise identical conditions (**Fig. 5.4A, B, C**). Additionally, turnover of 6-heptenenitrile (6-HN) substrate by NIT2 recombinant protein was reduced by Heatin (**Fig. 5.4D**), showing that Heatin inhibition of NITs is not limited to only one substrate. These data seemingly contradict the hypocotyl elongation phenotypes of *nit* mutants (**Fig. 5.3**). If the reduction in NIT activity by Heatin results in hypocotyl elongation, a complete loss of enzymatic activity in *nit* mutant lines should logically also result in hypocotyl elongation, however the opposite is observed.

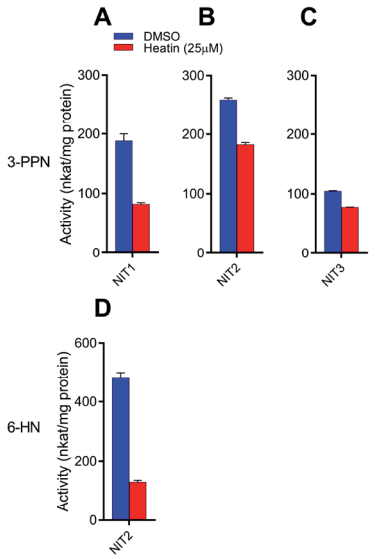

Figure 5.4: Heatin inhibits NITRILASE enzymatic activity *in vitro*.

(**A-D**) *In vitro* enzymatic activity (in nkat/mg protein) of the indicated recombinant NITRILASE protein with 3-propionitrile (3-PPN, **A-C**) or 6-heptanitrile (6-HN, **D**) as a substrate at 37°C. Reactions were performed with DMSO solvent mock (blue bars) or 25µM Heatin (red bars), present in the reaction

mix. Of note, protein amount differed per experiment, altering the protein:Heatin ratio, thus results cannot be directly compared between experiments, but only within. Error bars denote standard error of the mean. Values are averages of 3 technical replicates.

Heatin affects auxin metabolism in a Nitrilase- and aldehyde oxidation-dependent manner

We previously found that free IAA levels are not affected in 2 and 7 day-old seedlings grown in the presence of Heatin (**Chapter 3**). We tested whether the inhibition of Heatin on Nitrilase functioning affected IAA metabolism by quantifying the levels of the auxin metabolites Anthranilate (ANT), TRP, Tryptamine (TRA), IPyA, indole-3-acetamide (IAM), IAN and bioactive auxin IAA. Additionally, the levels of the IAA-conjugates IAA-glutamate (IAA-Glu) and IAA-aspartic acid (IAA-Asp) and the IAA degradation product 2-oxoindole-3-acetic acid (oxIAA) were determined. The *NIT2-RNAi* line and *aao1 aao2* double mutant were included in our analyses since mutants in both *ALDEHYDE OXIDASE1* (*AOO1*) and *AOO2* and in *NIT1* and *NIT2* were found to be (partly) resistant to Heatin (**Fig. 3.4**) and because these factors have been implicated (and questioned) to play roles in IAA metabolism[61–63,225,227]. Two timepoints were assessed, an early timepoint using 2-day old seedlings, where we have previously shown early responsive transcriptomic regulation with a strong auxin footprint (**Chapter 4**), and a moderately later timepoint: 3 day-old seedlings. The plant material used in this analysis was imaged to establish hypocotyl lengths of the seedlings prior to harvesting the materials to ensure consistency with previous results. Quantitative analyses of hypocotyl lengths confirmed the effectiveness of the treatments as well as the expected responses of the mutants (**Fig. S5.5**).

At the early (2d) time-point, Heatin affected ANT and TRP levels significantly in a manner dependent on both NITRILASES and ALDEHYDE OXIDASES (**Fig. 5.5**). These effects disappeared after 3 days of growth, where instead a strong increase in IAN levels was observed in Heatin-treated Col-0 WT seedlings, that was clearly absent in the two mutant backgrounds (**Fig. 5.5**). This finding is consistent with a reduced NIT function mediated by Heatin, as confirmed by our enzymatic assays (**Fig. 5.4**), causing accumulation of IAN. Interestingly, IAA levels were also significantly increased upon Heatin treatment in 3 day-old Col-0 WT seedlings, but not in both mutant backgrounds (**Fig. 5.5**). This indicates that auxin levels are affected by Heatin, but not yet in 2 day-old seedlings that were used in the previous chapters. Similar to our earlier findings reported in **Chapter 3**, IAA levels were not affected by Heatin in 2 day-old seedlings in this broad analysis of auxin metabolism. However, as IAN levels increased in response to Heatin, the source of the precursor of this IAA is likely not IAN. IAM levels increased in a similar manner.

Taken together, the findings presented here point to a complex regulation of auxin metabolism by Heatin, depending on both ALDEHYDE OXIDATION and NITRILASES, progressing from early effects on ANT and TRP to later effects on IAN, IAM and IAA.

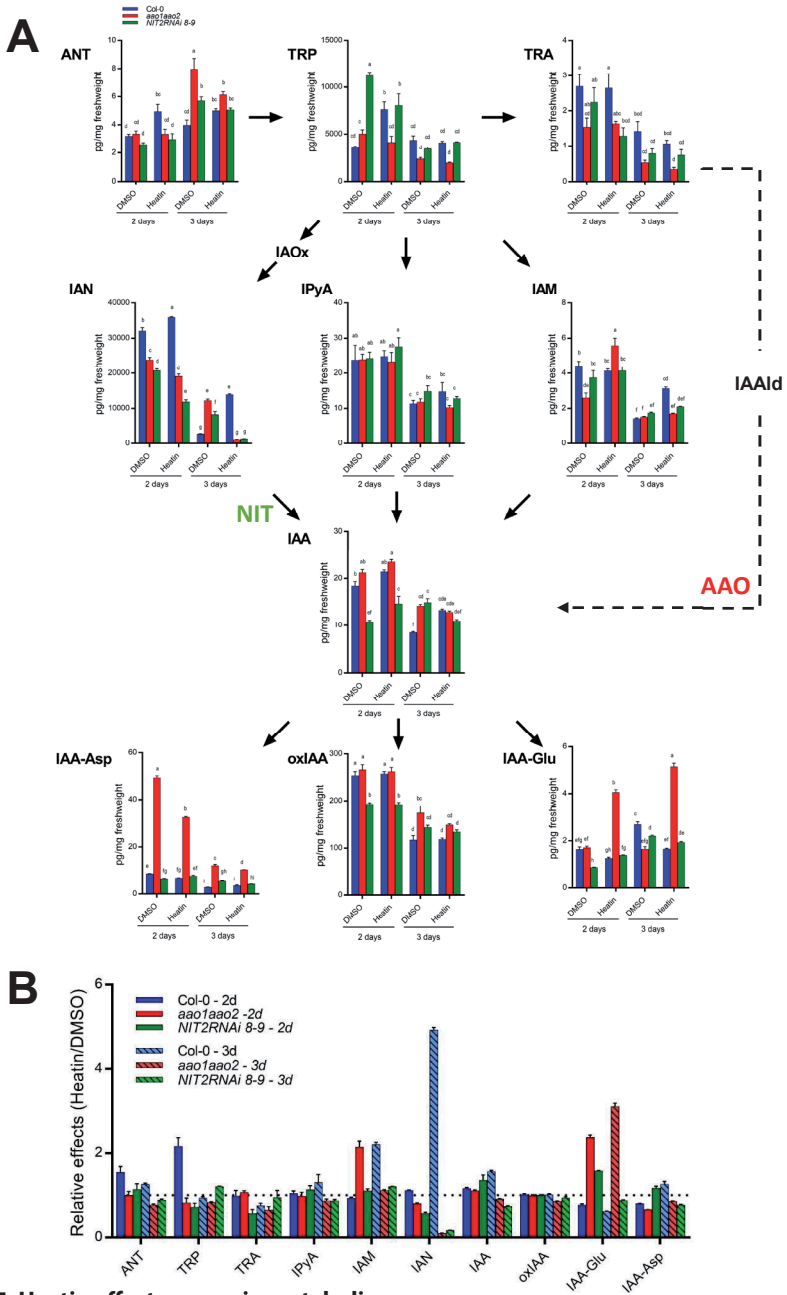

Figure 5.5: Heatin effects on auxin metabolism.

(**A**) Concentrations of indicated auxin metabolites (precursors, conjugates and degradation product) in 2 day-old and 3 day-old seedlings of either Col-0 WT (blue bars), *aao1 aao2* (red bars) or *NIT2-RNAi 8-9* (green bars). Arrows indicate metabolic conversions between compounds. Dashed arrows are not well-defined pathways. Letters indicate significance groups following Tukey HSD post-hoc tests, where averages that do not share letters are significantly different at $p<0.05$. (**B**) Relative Heatin effects based on the data in panel **A.** 2-day-old samples are shown as clear bars and 3-day-old samples are shown as striped bars. Horizontal dotted line indicates no difference between DMSO and Heatin. Error bars denote standard error of the mean. Values are averages of 4 biological replicates

It should be noted that the *NIT2-RNAi* and *aao1 aao2* mutant lines already have altered metabolite levels on control medium. In the case of *aao1 aao2*, an increase in IAA-Asp and decrease in IAN and IAM was observed in 2 day-old samples, whereas in 3 day-old samples increases in ANT, IAN, IAA, IAA-Asp and oxIAA and a decrease in IAA-Glu was observed (Fig. 5.5A). *NIT2-RNAi* samples displayed an increase in TRP and decreases in IAN, IAA, oxIAA and IAA-Glu in 2 day-old samples. In 3 day-old samples increases in ANT, IAN, IAA and IAA-Asp and a decreases in IAA-Glu were observed (Fig. 5.5A). Of note is that results for 3 day-old samples for the *NIT2-RNAi* line are consistent with previously described data concerning IAN and IAA levels in this line[61].

Discussion

Heatin is considered a growth regulating compound that stimulates thermomorphogenesis already under control conditions (**Chapter 2**). We have shown that Heatin acts downstream of or parallel to PIF4 and that auxin signaling is required for Heatin activity. However, Heatin does not act as a canonical auxin (**Chapter 3**), nor stimulates endogenous levels of bioactive IAA, at least not in 2 day-old (**Chapter 3**, and **Fig. 5.5**) and 7 day-old seedlings (**Chapter 3**). Additionally, we have shown that Heatin is related to the bioactive compound Sirtinol (**Chapter 3**) that shares the active moiety of Heatin and that mutants identified in screens for Sirtinol resistance are also resistant to Heatin with respect to hypocotyl elongation (**Chapter 3**). Sirtinol is proposed to be metabolized to 2-hydroxy-1-naphthyl-acetic acid and then acts as an auxin[105]. This metabolic conversion relies on oxidation of the aldehyde precursor by the ARABIDOPSIS ALDEHYDE OXIDASE (AAO) family. We demonstrated that *aao1 aao2* double mutants are also insensitive to Heatin (**Chapter 3**). However, whereas Sirtinol activates the synthetic *DR5* promoter in Arabidopsis[93], a read-out of auxin activity, we did not observe such *DR5* activation for Heatin (**Chapter 3**) in 2 day-old and 7 day old seedlings.

Here, we employed a chemical proteomic strategy that identified Arabidopsis NIT1, 2 and 3 as direct binding targets of Heatin (**Fig. 5.1A**). We showed that this interaction reduces NIT enzymatic activity (**Fig. 5.4**) and that NITs are required for Heatin-mediated hypocotyl elongation (**Fig. 5.3**). Additionally, we observed changes in ANT and TRP levels 2 days after induction of germination, at the moment phenotypic effects of Heatin start to emerge (**Fig. 4.1**). A day later, changes in IAN, IAM and IAA were observed, all of which relied on NITRILASE and ALDEHYDE OXIDASE functioning (**Fig. 5.4**).

For this study we designed and synthesized a novel chemical probe based on the previously identified analogue **#202** (**Chapter 3**) that contained an azide linker moiety (**Fig. 5.1B**). We choose to use analogue **#202** instead of Heatin to circumvent the

possibility that Heatin may be hydrolyzed on Heatin's hydrazide bond *in planta*, which would split the required active moiety and attached azide linker moiety.

The probe used did not contain a crosslinker moiety and the isolation of the Heatin-bound proteins from protein extracts had to be performed with care, not to disrupt potentially weak non-covalent interactions between Heatin and its target proteins. This prohibited stringent washing away of non-specific background binding or denaturing of proteins. Therefore, several false positive interactions were expected and a key challenge was to discern background non-specific protein binding, from biologically relevant Heatin specific binding. We solved this by repeated mild washing steps, as well as enriching for true targets by elution of the proteins with Heatin compound. Moreover, by using a high number of replicates (7x) we were able to statistically determine likely true Heatin targets (**Fig. 5.2**). We identified 162 proteins that were statistically more abundant in the eluted fraction above our minimum difference cut-off of 1 LFQ unit. Although this is already a strong reduction compared to the initial 2204 identified proteins on the beads, the majority of these proteins are probably still non-specific. By focusing on the likelihood of small molecules to target multiple proteins in the same family[85], we further narrowed-down our pool of potential direct targets. We found 20 homology groups of which 6 were excluded based on their common presence in proteomic analyses and, therefore likely to be false positives[230] (**Table 5.1**). Of the remaining 14 groups, the Nitrilase and Hexokinase homology groups stood out as they covered 3/3 and 2/3 of the members of these groups, respectively. This prompted us to further study the notion that Heatin targets a protein family by focusing on the NIT1-subfamily of proteins.

Our *nit* mutant analysis is in line with the detection of the NIT proteins in the pulldown (**Fig. 5.3**). All tested mutants retained sensitivity to Heatin to some extent with mutants in NIT3 retaining full sensitivity. We therefore conclude that NIT1 and NIT2 are required for Heatin-mediated hypocotyl elongation. The remaining Heatin sensitivity could be explained by redundancy in NIT functioning. The fact that even the *NIT2-RNAi* line remains sensitive, is probably due to the fact that this line has no detectable expression of *NIT1* and *NIT2*, but *NIT3* remains expressed[231], and could take over the function of NIT1 and NIT2. However, NIT3 protein was not clearly detectable[61].

Importantly, the reduced high temperature-induced hypocotyl elongation of *nit1-3*, *nit2* and *NIT2-RNAi* line 8-9 (**Fig. 5.3**) in the absence of Heatin, supports a potential novel role for these proteins in thermomorphogenesis control. Nitrilases have been suggested to convert IAN into bioactive auxin (IAA), downstream of *CYP79B2*[61]. *CYP79B2* is stimulated under high temperature conditions in a PIF4 dependent manner[56]. Likely, this proposed IAA biosynthesis pathway contributes to the high temperature-dependent increase in IAA levels. The differential regulation observed at high temperature of the *NIT* genes supports a dynamic temperature-mediated regulation, with a particular role for *NIT2* (**Fig. S5.2**). Previously, NIT2 affinity for IAN was found to be temperature dependent and

decreases with temperatures above 15°C[232]. This seemingly contradicts with an NIT2-mediated increase in IAA biosynthesis. An alternative explanation is that the upregulation of *CYP79B2* and *NIT2* are related to biosynthesis of defense-related compounds such as indole-glucosinolates and camalexin. The Nitrilase proteins have much higher affinities for defense related compound than for IAN[232]. Notably, PIF4 has also been implicated in regulation of defense in response to high temperature[32]. The observed effects on hypocotyl elongation in the *nit* mutants might therefore be a secondary effect of the change in defense signaling as PIF4-mediated induction of defense goes at the expense of expense of thermomorphogenesis[32].

The observed *nit* mutant effects on Heatin sensitivity are remarkable in view of the inhibitory effects on *in vitro* enzymatic activity (**Fig. 5.4**). Heatin induces elongation growth and reduces enzymatic activity of all three NITs. Therefore, we expected that a knockout mutation in *e.g. nit1-3*, would lead to enhanced hypocotyl elongation. Our auxin metabolism quantification underlines the complex Heatin-Nitrilase interactions (**Fig. 5.5**). When assessing relative Heatin effects in the three separate mutants, the strongest effect observed was a five-fold increase of IAN levels in 3 day-old WT seedlings and a strong IAN reduction in the *NIT2-RNAi* and *aao1 aao2* mutants lines (**Fig. 5.5B**). This could be the direct result of inhibition of NITRILASE functioning and therefore accumulation of IAN, a possible substrate of NITs. Surprisingly however, we also observed an increase in IAA levels in the same samples, which is inconsistent with the inhibition of NIT function (**Fig. 5.5B**), assuming that IAN is metabolized into bioactive IAA. Further complicating the interpretations are the absolute levels of *e.g.* IAN in the *nit* mutant lines. Whereas, IAN levels in 3-day old seedlings on DMSO medium are higher in the *nit* mutants than the WT, Heatin causes strong reductions in IAN levels in the mutants, but not the WT (**Fig. 5.5A**).

How these changes in auxin metabolism relate to auxin signaling and thereby elongation growth remains to be investigated. Recent findings suggest that auxin signaling during defense responses can be uncoupled from IAA concentration due to the formation of auxin signaling antagonists following glucosinolate metabolism[63,234]. Additionally, IAN was shown by chemical modelling to be able to bind to the TIR1 auxin receptor and form stable complexes with IAA proteins, although it did not activate auxin signaling in a yeast-2-hybrid assay[63,234].

Taken together our results suggest that Heatin-directed hypocotyl elongation relies on an inhibitory (feedback) interaction between Heatin and the Nitrilases that may affect auxin metabolism – and thus hypocotyl elongation- in a highly complex manner.

Materials and Methods

Plant materials and growth conditions

Arabidopsis thaliana seeds were obtained from the Nothingham Arabidopsis stock center (www.arabidopsis.info) or were generated and characterized in the lab of Dr. Piotrowski. The following lines were used: C24 and Col-0 wild type, *nit1-3*[141], *nit2* (SM_3_24059)[231], *nit3* (GK_04E09)[231], *NIT2-RNAi* lines #8-9 and #26-6[61], *NIT1OE*[61] and *aao1 aao2* (**Chapter 3**). Plants used for hypocotyl length assays, pull-down experiments and auxin metabolism measurements were grown on sterile 0.8% plant agar (Duchefa P1001), 1x Murashige-Skoog medium (MS, including MES Buffer and vitamines, Duchefa M0255), without sucrose in petri-dishes. Seeds were surface-sterilized by chlorine gas for 3 hours. After sowing, seeds were stratified for 2-3 days at 4°C in the dark. The petri-dishes containing the plants were subsequently grown under 100 µmol m^{-2} s^{-1} white light short day conditions (8 hours light/16 hours darkness) at 70% relative humidity in climate-controlled Microclima 1000 growth cabinets (Snijders) at either 22°C (control) or 27°C (high temperature) in the presence of 8.5µM Heatin, pre-dissolved in DMSO or DMSO mock (no Heatin added), with a final concentration of 0.1% (v/v).

Hypocotyl measurements

Petri-dishes with seedlings were pictured after either 8 days of growth (*nit* mutant analysis) using a flatbed scanner or at dawn of day 3 and 4 (auxin metabolite experiments) by photographing them from the top. Hypocotyl lengths were measured using ImageJ software (https://imagej.nih.gov/ij/).

Probe synthesis and click chemistry

Materials and methods used to synthesize the azide-functionalized probe can be found in **supplemental information 5.1.**

Magnetic Heatin-covered beads were generated through a copper catalyzed cycloaddition reaction with the following substituents: 1ml 10mg/ml alkyne-functionalized (24.8nmol alkyne/mg) magnetic beads (total 248nmol alkyne groups; CLK-1035-1, Jena Bioscience), ~1µmol azide-functionalized compound #202 dissolved in 50µl DMSO, 0.05µmol $CuSO_4$ dissolved in water, 0.07µmol Tris[(1-benzyl-1H-1,2,3-triazol-4-yl)methyl]amine (TBTA) dissolved in DMSO and 0.2µmol Tris(2-carboxyethyl)phosphine hydrochloride (TCEP) dissolved in DMSO. The total reaction volume was 3ml, constituting 1ml bead suspension, 900µl water containing the $CuSO_4$, 900µl Tert-butyl alcohol (TBA) and 200µl DMSO containing the other reaction components. TBTA and $CuSO_4$ were mixed first to allow complex formation followed by TCEP and the probe solution and finally the bead suspension. The reaction was incubated overnight while stirring at room temperature (RT). Beads were pelleted with a magnet and washed 3 times with a cycle of DMSO, a 50% TBA solution in water and water. This was followed by 3 final wash steps

with water. Beads were resuspended in water, aliquoted and stored at 4°C until use in the pulldown experiments.

Pulldown experiments

Protein extracts were generated by grinding ~420 seedlings of an equal mix of 2-, 2.5- and 3-day-old seedlings in 200µl extraction buffer, containing 10mM Tris/Cl pH 7.5, 150mM NaCl, 0.3% NP-40, cOmplete™ Mini EDTA-free Protease Inhibitor Cocktail (11836170001 Roche; 1tablet/50ml) and 1mM 1,4-Dithiothreitol (DTT). Debris were pelleted by centrifugation (16000g) at 4°C for 10 minutes and supernatant was transferred to a new tube with 0.2µl DMSO. 100µl of beads was equilibrated using extraction buffer by washing three times and subsequently the bead suspension was added to the protein extracts. The resulting suspension was incubated for one hour at 4°C tumbling end-over-end.

Beads were washed 10x using 1ml extraction buffer. SDS-PAGE protein gel analysis confirmed that proteins could still be detected attached to the beads (**Fig. S5.4**). The beads were transferred to new tubes after the first and the last washing step. Beads were resuspended in 200µl extraction buffer after washing, and 0.2µl 25mM Heatin in DMSO was added to Elute Heatin binding proteins. The elution was incubated for 30 minutes at 4°C. The elutes were separated from the beads. Beads were resuspended in 200µl extraction buffer.

The elutes were *in solute* digested and beads samples *on-bead* digested as follows: Elutes were digested by adding 10µl 1M DTT and incubating one hour at RT, then 10µl 1M iodoacetamide was added. Samples were incubated for 1 hour in darkness at RT. 2.5µl 1M Cysteine was added to capture free iodoacetamide. Proteins were precipitated using a methanol/chloroform extraction and resuspended in 50µl 6M Urea in Tris/Cl pH 8. 1.9µl trypsin/Lys-C mix (Promega) was added and incubated for 3h at 37°C. 250µl Tris buffer was added to bring the urea concentration <1M. samples were incubated overnight. The digestion was stopped by adding 1.5µl trifluorocetic acid (0.5%). Samples were centrifugated at max speed for 10min and supernatant were purified by Sep-Pak C18 (Waters, WAT020515) and analysed by LC-MS/MS.

On-bead samples were digested by washing twice with 1ml 50mM Tris buffer pH 8.0 and subsequently resuspended in 50µl of the same buffer. This was followed by adding 2.5µl 1M DTT and incubating 1 hour at RT, then by adding 2.5µl 1M iodoacetamide and incubating 1 hour in darkness at RT. 2.5µl 1M Cysteine was added to capture free iodoacetamide. 200µl 8M Urea was added and directly after 1.9µl Trypsin/LysC was added and incubated 3h at 37°C. 1ml of Tris buffer was added to reduce the urea concentration <1M. Samples were incubated overnight. Digestion was stopped by adding 6µl triflurocetic acid (0.5%). Beads were separated from supernatant which was saved and purified by Sep-Pak C18 (Waters, WAT020515) and analysed by LC-MS/MS. All steps in the pulldown experiment were done using Protein LoBind tubes (Eppendorf, Catalog No. 0030108116).

LC-MS/MS.

Experiments were performed on an Orbitrap Elite instrument (Thermo[235]) that was coupled to an EASY-nLC 1000 liquid chromatography (LC) system (Thermo). The LC was operated in the one-column mode. The analytical column was a fused silica capillary (75 µm × 30 cm) with an integrated PicoFrit emitter (New Objective) packed in-house with Reprosil-Pur 120 C18-AQ 1.9 µm resin (Dr. Maisch). The analytical column was encased by a column oven (Sonation) and attached to a nanospray flex ion source (Thermo). The column oven temperature was adjusted to 45 °C during data acquisition. The LC was equipped with two mobile phases: solvent A (0.1% formic acid, FA, in water) and solvent B (0.1% FA in acetonitrile, ACN). All solvents were of UPLC grade (Sigma). Peptides were directly loaded onto the analytical column with a maximum flow rate that would not exceed the set pressure limit of 980 bar (usually around 0.5 – 0.8 µL/min). Peptides were subsequently separated on the analytical column by running a 140 min gradient of solvent A and solvent B (start with 7% B; gradient 7% to 35% B for 120 min; gradient 35% to 80% B for 10 min and 80% B for 10 min) at a flow rate of 300 nl/min. The mass spectrometer was operated using Xcalibur software (version 2.2 SP1.48). The mass spectrometer was set in the positive ion mode. Precursor ion scanning was performed in the Orbitrap analyzer (FTMS; Fourier Transform Mass Spectrometry) in the scan range of m/z 300-1800 and at a resolution of 60000 with the internal lock mass option turned on (lock mass was 445.120025 m/z, polysiloxane)[236]. Product ion spectra were recorded in a data dependent fashion in the ion trap (ITMS) in a variable scan range and at a rapid scan rate. The ionization potential (spray voltage) was set to 1.8 kV. Peptides were analyzed using a repeating cycle consisting of a full precursor ion scan (3.0×10^6 ions or 50 ms) followed by 15 product ion scans (1.0×10^4 ions or 50 ms) where peptides are isolated based on their intensity in the full survey scan (threshold of 500 counts) for tandem mass spectrum (MS2) generation that permits peptide sequencing and identification. Collision induced dissociation (CID) energy was set to 35% for the generation of MS2 spectra. During MS2 data acquisition dynamic ion exclusion was set to 120 seconds with a maximum list of excluded ions consisting of 500 members and a repeat count of one. Ion injection time prediction, preview mode for the FTMS, monoisotopic precursor selection and charge state screening were enabled. Only charge states higher than 1 were considered for fragmentation.

Peptide and Protein Identification using MaxQuant

RAW spectra were submitted to an Andromeda[237] search in MaxQuant (version 1.5.3.30) using the default settings[238]. Label-free quantification and match-between-runs was activated[239]. MS/MS spectra data were searched against the Uniprot *Arabidopspis thaliana* (UP000006548_3702.fasta; 33439 entries. All searches included a contaminants database (as implemented in MaxQuant, 245 sequences). The contaminants database contains known MS contaminants and was included to estimate the level of contamination. Andromeda searches allowed oxidation of methionine residues (16 Da) and acetylation

of the protein N-terminus (42 Da) as dynamic modifications and the static modification of cysteine (57 Da, alkylation with iodoacetamide). Digestion mode was set to "specific", Enzyme specificity was set to "Trypsin/P" with 2 missed cleavages allowed, the instrument type in Andromeda searches was set to Orbitrap and the precursor mass tolerance to ±20 ppm (first search) and ±4.5 ppm (main search). The MS/MS match tolerance was set to ±0.5 Da and the peptide spectrum match FDR and the protein FDR to 0.01 (based on target-decoy approach and decoy mode "revert"). Minimum peptide length was 7 amino acids. Minimum score for unmodified peptides was set to 0. For protein quantification modified peptides (minimum score 40) and unique and razor peptides were allowed. Further analysis, filtering and annotation of identified peptides was done in Perseus v1.5.5.3[240]. Processed data can be found in **supplemental file 5.1.** Only protein groups with at least two identified unique peptides over all runs were considered for further analysis. Comparison of protein group quantities (relative quantification) between different MS runs is based solely on the LFQ's as calculated by MaxQuant (MaxLFQ algorithm). Briefly, Label-free protein quantification was switched on, and unique and razor peptides were considered for quantification with a minimum ratio count of 2. Retention times were recalibrated based on the built-in nonlinear time-rescaling algorithm. MS/MS identifications were transferred between LC-MS/MS runs with the "Match between runs" option in which the maximal match time window was set to 0.7 min and the alignment time window set to 20 min. The quantification is based on the "value at maximum" of the extracted ion current. At least two quantitation events were required for a quantifiable protein[239].

Data analysis

Proteomics data was analysed by Perseus v1.5.5.3[240]. Known contaminants were excluded and remaining LFQ values were log2-transformed. Missing values were imputed from a normal distribution and averages of biological replicates were taken and compared for statistically significant differences by t-test, using a permutation-based FDR with a significance threshold of $p<0.05$. The 162 proteins above the 1 LFQ difference threshold were selected for further analysis. For the resulting 162 proteins protein sequenced were retrieved from TAIR (www.arabidopsis.org; Araport11) and were tested by 'all vs. all' BLASTp using NCBI BLAST v.2.7.1+, selecting homology hits with E-values below $1E^{-5}$. The resulting homology groups are listed in **table 5.1**.

Enzymatic activity assays

Recombinant NIT1, NIT2 and NIT3 was purified from 1 liter *Escherichia coli* culture as described before with minor revisions[233]. In brief, the cell culture was induced to produce protein by 0.3mM final concentration IPTG for 6 hours and subsequently centrifuged at 5000g for 10 minutes at 4°C. supernatant was discarded, and pellets resuspended in lysis buffer (50mM sodium phosphate pH 8.0, 300mM NaCl, 10mM Imidazole, 5mM beta-mercaptoethanol, 1mg/ml lysozyme). Suspension was incubated in an ultrasonic ice

bath for 15 minutes and subsequently further sonicated with four bursts of ultrasound (1 min) using an ultrasound tip (Sonifier B-17, Branson). Debris was pelleted by 10min 10000 g centrifugation at 4°C. Nitrilases were enriched by (NH4)2SO4 precipitation (40% saturation). Precipitate was pelleted by 20 minutes centrifugation for 15min at 4°C and resuspended in 12ml lysisbuffer without lysozyme. Suspension was centrifuged again for 5 minutes at 5000g at 4°C and resulting supernatant was saved as 'Enriched Extract' (**Fig. S5.3**). 6xHis-tagged Nitrilases were purified from extract by Ni-NTA affinity purification column. This was done by loading the enriched extracts onto the column (flow-through was saved for downstream purification analysis ('Flow-through' **Fig. S5.3**), subsequent washing with lysisbuffer with increased imidazole concentration (40mM) and elution with lysisbuffer with higher imidazole concentration (250mM). 2.5ml of Nitrilase containing fraction was saved and desalted using a NAP-10 column (Amersham Pharmacia Biotech). This resulted in highly purified Nitrilase solution in 50mM potassium phosphate, pH 8.0, 1mm DTT solution ('Purified protein', **Fig. S5.3**). Concentration of purified protein fractions was measured by Bradford method, yielding 390ng/ml NIT1, 640ng/ml NIT2 and 870ng/ml NIT3. Purified protein was aliquoted and flash-frozen in liquid nitrogen for storage until activity assays.

Activity assays were performed by measuring produced ammonia at different time points by colorimetric Berthelot's reaction[241]. Assays were performed *in triplo* for DMSO mock samples and *in triplo* for Heatin samples with an additional DMSO and Heatin sample with heat-denatured protein as negative control to determine background signal. The reaction solution consisted of: 50mM potassium phosphate buffer, pH 8.0, 1mM DTT, 2.5mM Substrate unless otherwise stated, 5/10/100µl purified Nitrilase solution and 10µl 1% DMSO in methanol with or without Heatin (final Heatin concentration in the reaction was 25µM). Water was added up to 1ml. Reactions were performed at 37°C. Resulting colorimetric product were analyzed by measuring extinction at 640nm. This was done at different time point to assess the activity over time. To be able to accurately determine the produced ammonia, the amount of protein in each reaction was changed so that we could interpolate the ammonia concentration from our calibration curve. As a consequence, the ratio between Heatin and the protein could not be kept entirely consistent between experiments.

Auxin metabolite profiling

Quantification of auxin metabolites were performed according to the method described by Pěnčík *et al.* (2018)[242]. Samples (10 mg FW) were homogenized and extracted in 1.0 ml of ice-cold Na-phosphate buffer (50 mM, pH 7.0, 4°C) containing 0.1% diethyldithiocarbamic acid sodium salt together with a cocktail of stable isotope-labeled internal standards (5 pmol of [$^{13}C_6$]ANT, [$^{13}C_6$]IAA, [$^{13}C_6$]IAAsp, [$^{13}C_6$]IAGlu, [$^{13}C_6$]IAM, [$^{2}H_5$]IAOx, [$^{13}C_6$]oxIAA and [$^{2}H_2$]TRA, 5 pmol of [$^{13}C_6$]IAN and [$^{2}H_4$]IPyA, and 50 pmol of [$^{2}H_5$]Trp per sample added). The extracts were purified using the in-tip microSPE based on the StageTips

technology[243]. Briefly, a volume of 250 µl of each plant extract was acidified to pH 2.7 with 0.1 M hydrochloric acid (~100 µl). Combined multi-StageTips (containing C18/SDB-XC layers) were activated sequentially, with 50 µl each of acetone, methanol, and water (by centrifugation at 434×g, 15 min, 4°C). After application of aliquots of the acidified sample (678×g, 30 min, 4 °C), the microcolumns were washed with 50 µl of of 0.1% acetic acid (525×g, 20 min, 4°C), and elution of samples was performed with 50 µl of 80% (v/v) methanol (525×g, 20 min, 4°C). Another 250 µl of the extract was derivatized by adding 100 µl of 0.75 M cysteamine (pH 8.2) to convert the labile compound IPyA to its respective thiazolidine derivatives[244]. After 15 min incubation, the sample was adjusted to pH 2.7 and purified as described above. Both eluates were then evaporated to dryness in vacuum and stored at -20°C. The levels of IAA, its precursors, conjugates and catabolites were determined using ultra-high performance liquid chromatography-electrospray tandem mass spectrometry (a 1290 Infinity LC system and a 6490 Triple Quadrupole LC/MS system, Agilent Technologies) using stable isotope-labelled internal standards as a reference[245]. Four independent biological replicates were performed.

Acknowledgements

This work was supported by *NWO Graduateschool Uitgangsmaterialen* grant NWO#831.13.002 to LvdW and MvZ and ERC starting grant No. 258413) to M.K. and DFG grant INST 20876/127-1 FUGG to M.K

Supplemental figures and tables

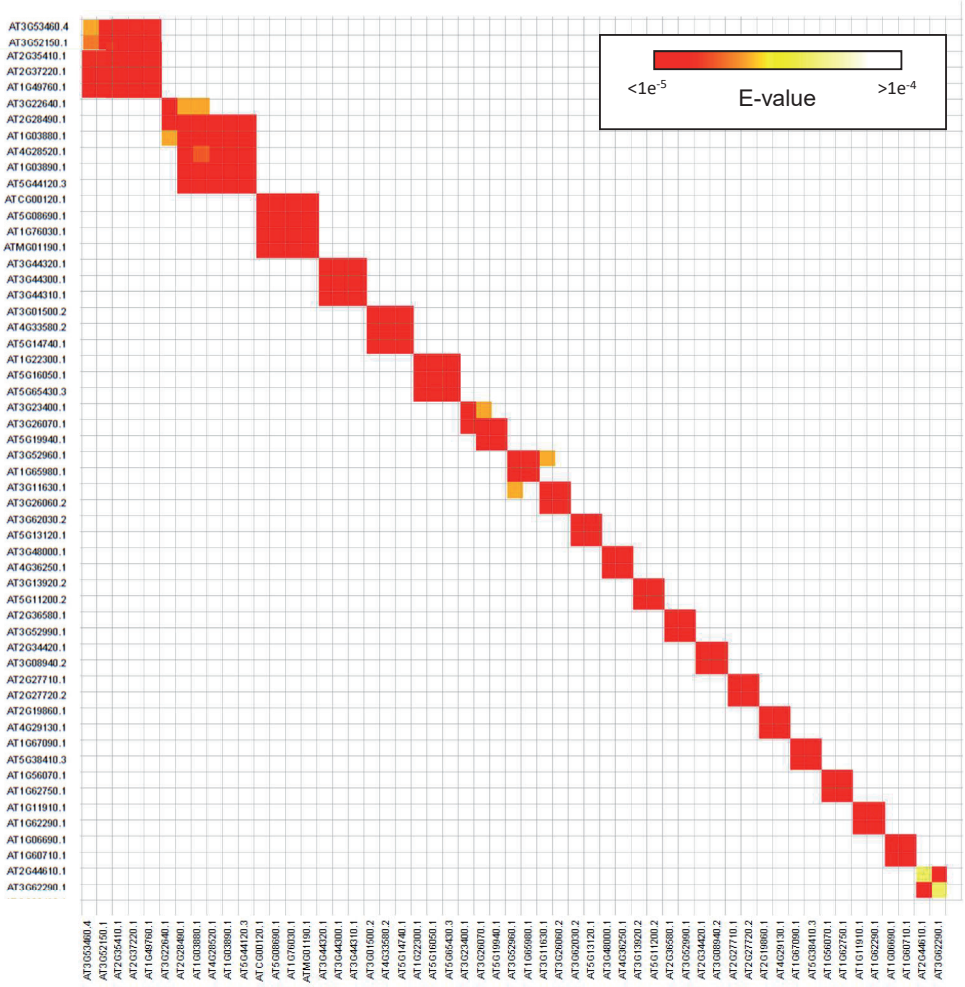

Supplemental Figure 5.1: Gene clusters encoding for proteins identified as significantly enriched in Heatin-eluted fractions from the chemical proteomic experiment.

Genes are clustered based on E-values resulting from 'all vs. all' BLAST analysis. Shown are all proteins with hits other than self, below the E-value threshold of $1e^{-5}$. Values not crossing the threshold were not considered for clustering.

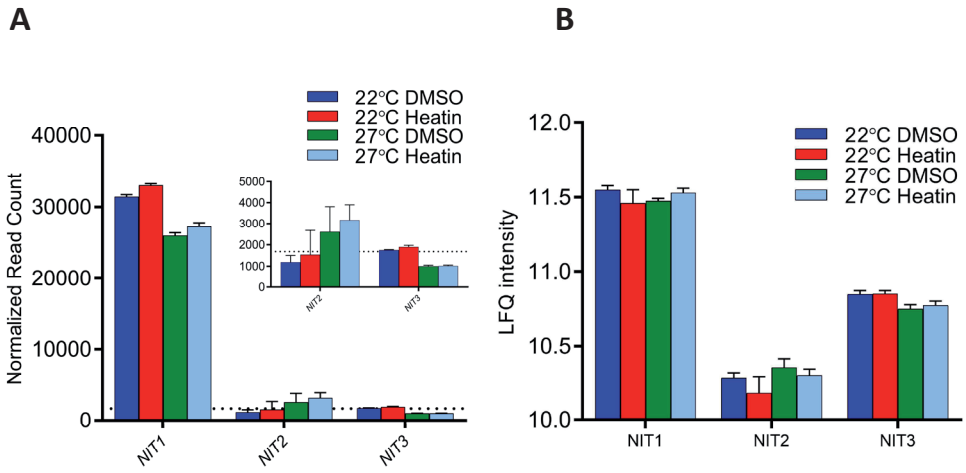

ANOVA	*NIT1*	*NIT2*	*NIT3*
Compound	0.238547	0.365521	0.221442
Temperature	**0.001002**	**0.013668**	**1.03E-06**
Comp*Temp	0.874114	0.818453	0.31033

ANOVA	NIT1	NT2	NIT3
Compound	0.897527	0.428682	0.937594
Temperature	0.550019	0.203497	**0.003606**
Comp*Temp	0.299925	0.980006	0.974379

Supplemental Figure 5.2: NIT1-subfamily transcripts and proteins abundance detected by RNA-seq and proteomics.

(**A**) normalized read counts for *NIT1*, *NIT2* and *NIT3* as detected by RNA sequencing described in chapter 4 of this thesis, under indicated conditions in 2 day-old seedlings. Dotted line represents the average read count of all detected transcripts. (**B**) LFQ intensity values of NIT1, NIT2 and NIT3 as found by LC MS/MS proteomic analysis described in chapter 4, under the indicated conditions in 2 day-old seedlings. Tables below the graphs show ANOVA-calculated p-values with significant values in bold. Error bars indicate standard error of the mean.

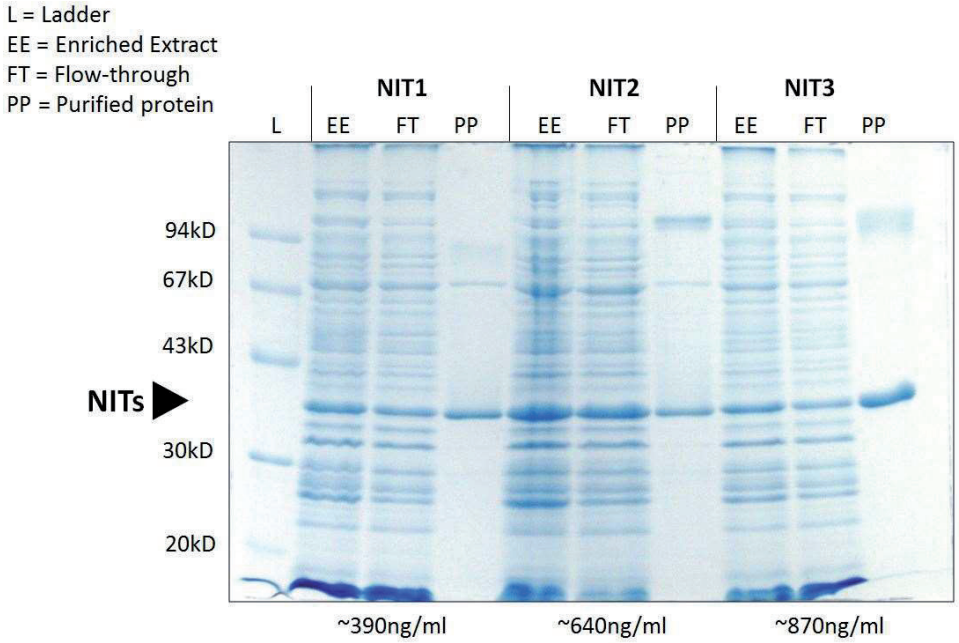

Supplemental Figure 5.3: Purification of recombinant HIS-tagged NIT proteins.

Coomassie-stained gel showing different stages of the NIT purification process from *E. coli* cell culture. EE denotes the post-$(NH_4)_2SO_4$ precipitation NIT protein enriched extracts, FT denotes the Ni-NTA column flow-through depleted of His-tagged NIT proteins and PP denotes the purified His-tagged NIT protein. Slight impurities can be seen in the gel, which correspond to *E. coli* proteins (data not shown). Indicated is a size marker with corresponding band sizes. The arrowhead indicates the predicted sized (~37kD) of recombinant HIS-tagged NIT protein. Number depicted below the gel indicate protein concentrations of the purified protein (PP) as determined by Bradford's assay

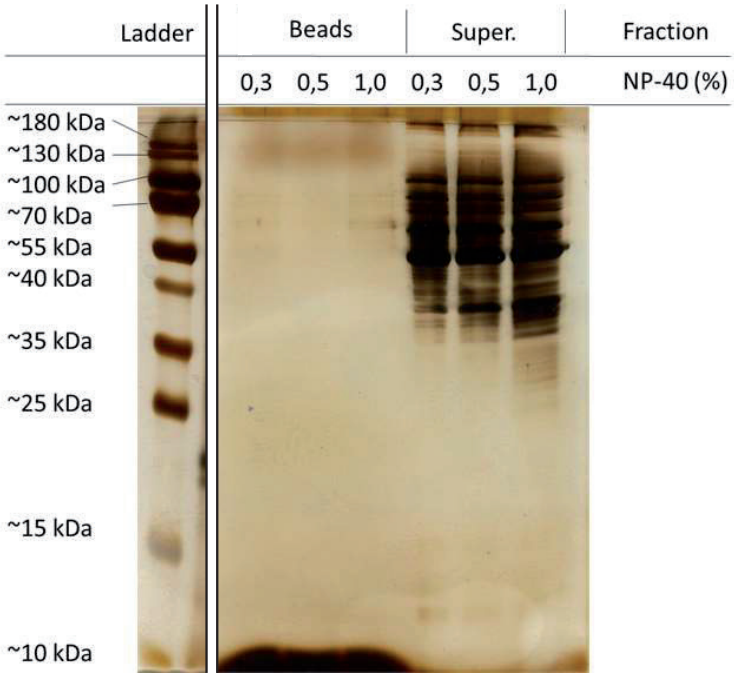

Supplemental Figure 5.4: Silver stain of pre-wash supernatant (Super.) and post-wash on-bead fractions of pulldown procedure.

Different NP-40 percentages (v/v) were tested to optimize washing solution. A size marker was included to visualize protein sizes.

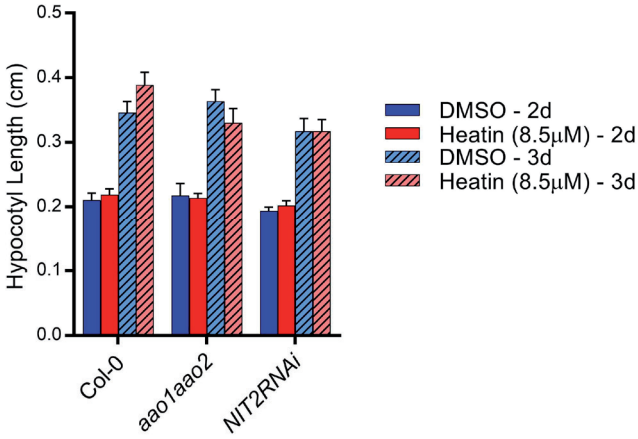

Supplemental Figure 5.5: Hypocotyl length validation of seedlings sampled for auxin metabolism analysis.

Hypocotyl lengths were measured from photos taken just before harvesting samples and confirm both the effectivity of our treatments and expected resistance to Heatin of the mutant lines. Blue bars represent DMSO mock treatment and red bars Heatin treatment, clear bars represent 2-day-old seedlings and striped bars 3-day-old seedlings. Error bars denote standard error of the mean. Values are averages of 6 replicates consisting of ~50-100 seedlings each, of which 4 were used for auxin metabolite measurements.

Supplemental Table 5.1: Proteins significantly enriched in the 'Elute' fraction of the Heatin-covered beads pulldown experiment.

Shown are identified protein ID, corresponding Arabidopsis Gene Identifier, possible other name and a brief description retrieved from Araport (www.araport.org).

Protein ID	Corresponding AGI	symbol	briefDescription
Q9LW57	AT1G03880	CRU2	cruciferin 2
Q8VYL3	AT1G03890	AT1G03890	RmlC-like cupins superfamily protein
Q9SK09	AT1G04410	c-NAD-MDH1	Lactate/malate dehydrogenase family protein
Q6NL24	AT1G05510	AT1G05510	naphthalene 1,2-dioxygenase subunit alpha (DUF1264)
O65390	AT1G06690	AT1G06690	NAD(P)-linked oxidoreductase superfamily protein
Q42525	AT1G09310	AT1G09310	plant/protein (Protein of unknown function, DUF538)
Q96318;F4JLA9	AT1G11580	PMEPCRA	methylesterase PCR A
P10798;P10797;B3H5S2;F4KA76	AT1G11910	APA1	aspartic proteinase A1
Q96291	AT1G12310	AT1G12310	Calcium-binding EF-hand family protein
Q9SGH6	AT1G12840	DET3	vacuolar ATP synthase subunit C (VATC) / V-ATPase C subunit / vacuolar proton pump C subunit (DET3)
B9DFI7;B9DFI7-2;F4HPE1	AT1G13270	MAP1C	methionine aminopeptidase 1B
Q42342	AT1G17720	ATB BETA	Protein phosphatase 2A, regulatory subunit PR55
P11574;Q8W4E2	AT1G22270	AT1G22270	Trm112p-like protein
P43297	AT1G22300	GRF10	general regulatory factor 10
Q9ZNT1	AT1G26850	AT1G26850	S-adenosyl-L-methionine-dependent methyltransferases superfamily protein
Q9FGT8	AT1G30230	eEF-1Bb1	translation elongation factor EF1B/ribosomal protein S6 family protein
P36212;P36210	AT1G30580	AT1G30580	GTP binding protein
P15456	AT1G32200	ATS1	phospholipid/glycerol acyltransferase family protein
Q94A68	AT1G32990	PRPL11	plastid ribosomal protein l11
Q9LKU2	AT1G42960	AT1G42960	inner membrane localized protein
Q9LJR2	AT1G47128	RD21A	Granulin repeat cysteine protease family protein
Q9FV52;F4HQQ8	AT1G49760	PAB8	poly(A) binding protein 8
Q9ZUU4	AT1G52380	AT1G52380	NUP50 (Nucleoporin 50 kDa) protein
O82299	AT1G53240	mMDH1	Lactate/malate dehydrogenase family protein
Q9FVT2	AT1G54870	AT1G54870	NAD(P)-binding Rossmann-fold superfamily protein
P31265	AT1G56070	LOS1	Ribosomal protein S5/Elongation factor G/III/V family protein
P51407;F4IGR5;F4IGR4	AT1G57720	AT1G57720	Translation elongation factor EF1B, gamma chain
Q39221	AT1G60710	ATB2	NAD(P)-linked oxidoreductase superfamily protein
Q9LU85	AT1G61790	AT1G61790	Oligosaccharyltransferase complex/magnesium transporter family protein
Q1JPL7	AT1G62290	AT1G62290	Saposin-like aspartyl protease family protein
Q39247-2;Q39247	AT1G62750	SCO1	Translation elongation factor EFG/EF2 protein
F4I403;Q8LAH7	AT1G65980	TPX1	thioredoxin-dependent peroxidase 1
Q93ZN2	AT1G67090	RBCS1A	ribulose bisphosphate carboxylase small chain 1A
Q9ZWA9	AT1G69740	HEMB1	Aldolase superfamily protein
P47924	AT1G76030	VAB1	ATPase, V1 complex, subunit B protein
O80576	AT1G76080	CDSP32	chloroplastic drought-induced stress protein of 32 kD
Q9C7S3	AT1G76680	OPR1	12-oxophytodienoate reductase 1
Q9SGS4	AT1G77060	AT1G77060	Phosphoenolpyruvate carboxylase family protein
Q9ZVY7	AT1G79230	MST1	mercaptopyruvate sulfurtransferase 1
O65282	AT1G79550	PGK	phosphoglycerate kinase

P93834;A8MRW9	AT2G01470	STL2P	SEC12P-like 2 protein
Q9SJQ0	AT2G04030	CR88	Chaperone protein htpG family protein
Q8GW78	AT2G05710	ACO3	aconitase 3
Q9FZ42;Q9FZ42-2	AT2G14740	VSR3	vaculolar sorting receptor 3
P21238	AT2G19520	FVE	Transducin family protein / WD-40 repeat family protein
Q8LFJ5	AT2G19860	HXK2	hexokinase 2
Q9SUI4	AT2G21170	TIM	triosephosphate isomerase
Q9FKM2	AT2G21270	UFD1	ubiquitin fusion degradation 1
Q9M1X0	AT2G22475	GEM	GRAM domain family protein
Q9SFH9	AT2G25070	AT2G25070	Protein phosphatase 2C family protein
P32961;Q8LFU8	AT2G27710	AT2G27710	60S acidic ribosomal protein family
Q8S4Y1;Q8S4Y1-2	AT2G27720	AT2G27720	60S acidic ribosomal protein family
O49290	AT2G28000	CPN60A	chaperonin-60alpha
P32746	AT2G28490	AT2G28490	RmlC-like cupins superfamily protein
Q38936	AT2G33120	SAR1	synaptobrevin-related protein 1
O80501;Q9SID8;Q9LFT9;Q9SMR4	AT2G34420	LHB1B2	photosystem II light harvesting complex protein B1B2
P83755	AT2G35410	AT2G35410	RNA-binding (RRM/RBD/RNP motifs) family protein
Q949U7	AT2G36530	LOS2	Enolase
Q70E96	AT2G36580	AT2G36580	Pyruvate kinase family protein
Q9SW18-2;Q9SW18	AT2G37220	AT2G37220	RNA-binding (RRM/RBD/RNP motifs) family protein
Q8LGG8	AT2G37970	SOUL-1	SOUL heme-binding family protein
Q39141;Q8VZ87;P0CJ48;P04778	AT2G39080	EMB2799	NAD(P)-binding Rossmann-fold superfamily protein
Q43307	AT2G42790	CSY3	citrate synthase 3
P56757	AT2G43750	OASB	O-acetylserine (thiol) lyase B
F4JBC9;Q9LU86	AT2G43910	HOL1	HARMLESS TO OZONE LAYER 1
P42645	AT2G44060	AT2G44060	Late embryogenesis abundant protein, group 2
Q9ZP06;A8MQK3;Q9LKA3	AT2G44610	RAB6A	Ras-related small GTP-binding family protein
F4JM86;P25819	AT2G47510	FUM1	fumarase 1
Q43127	AT2G47940	DEG2	DEGP protease 2
Q9ASR1	AT3G01420	DOX1	Peroxidase superfamily protein
Q9LUJ7	AT3G01500	CA1	carbonic anhydrase 1
P15455	AT3G01520	AT3G01520	Adenine nucleotide alpha hydrolases-like superfamily protein
Q9C829	AT3G06300	P4H2	P4H isoform 2
Q9ZST4	AT3G08940	LHCB4.2	light harvesting complex photosystem II
Q8VYM4	AT3G09260	PYK10	Glycosyl hydrolase superfamily protein
O03042	AT3G10670	NAP7	non-intrinsic ABC protein 7
P25696	AT3G11630	AT3G11630	Thioredoxin superfamily protein
Q42139	AT3G13920	EIF4A1	eukaryotic translation initiation factor 4A1
O82261;B3H581	AT3G15356	AT3G15356	Legume lectin family protein
P10795	AT3G15730	PLDALPHA1	phospholipase D alpha 1
Q8LBI1;F4J912	AT3G16420	PBP1	PYK10-binding protein 1
Q9SDS7	AT3G16640	TCTP	translationally controlled tumor protein
F4JAU3	AT3G22640	PAP85	cupin family protein
Q94AZ4	AT3G23400	FIB4	Plastid-lipid associated protein PAP / fibrillin family protein
F4I1C1;P48347-2;P48347	AT3G25520	ATL5	ribosomal protein L5
Q9STE8	AT3G25770	AOC2	allene oxide cyclase 2
Q9XEX2;F4ID64	AT3G26060	PRXQ	Thioredoxin superfamily protein
Q9FXA2	AT3G26070	AT3G26070	Plastid-lipid associated protein PAP / fibrillin family protein
Q94CE3;Q94CE3-2	AT3G27850	RPL12-C	ribosomal protein L12-C
P83484;P83483;Q9C5A9	AT3G29360	UGD2	UDP-glucose 6-dehydrogenase family protein

Q9SAB3;Q9SAB3-2	AT3G44300	NIT2	nitrilase 2
P47999	AT3G44310	NIT1	nitrilase 1
P46010	AT3G44320	NIT3	nitrilase 3
Q0WP12-2;Q0WP12;Q0WP12-3;F4IT14	AT3G46740	TOC75-III	translocon at the outer envelope membrane of chloroplasts 75-III
Q9M1P5;Q6ID97;Q9LYJ3;Q9LQC8;P36397;P0DH91	AT3G48000	ALDH2B4	aldehyde dehydrogenase 2B4
Q6NMZ4	AT3G52150	PSRP2	RNA-binding (RRM/RBD/RNP motifs) family protein
Q9LFN6;Q56XG6;F4JWF3;F4JWF7;F4JWF6;Q56XG6-3	AT3G52960	AT3G52960	Thioredoxin superfamily protein
Q2HIR7;F4KBK9	AT3G52990	AT3G52990	Pyruvate kinase family protein
Q9ZPZ4	AT3G53460	CP29	chloroplast RNA-binding protein 29
Q8VZB1	AT3G58610	AT3G58610	ketol-acid reductoisomerase
Q9SJV0;A8MQW3	AT3G62030	ROC4	rotamase CYP 4
Q38882	AT3G62290	ARFA1E	ADP-ribosylation factor A1E
Q9XF88;Q9XF88-2	AT3G63190	RRF	ribosome recycling factor, chloroplast precursor
Q9LF37	AT4G01480	PPa5	pyrophosphorylase 5
P92549	AT4G01900	GLB1	nitrogen regulatory P-II-like protein
Q93Y22	AT4G09650	ATPD	F-type H -transporting ATPase subunit delta
Q9SSS9	AT4G12060	AT4G12060	Double Clp-N motif protein
P32962	AT4G12800	PSAL	photosystem I subunit l
O81716	AT4G16143	IMPA-2	importin alpha isoform 2
Q9FFW8	AT4G16210	ECHIA	enoyl-CoA hydratase/isomerase A
Q9SLF7;F4IGR3	AT4G17600	LIL3:1	Chlorophyll A-B binding family protein
Q94KE3;A8MR07	AT4G18480	CHLI1	P-loop containing nucleoside triphosphate hydrolases superfamily protein
P93033	AT4G25080	CHLM	magnesium-protoporphyrin IX methyltransferase
Q9FKK7;F4KC24	AT4G28520	CRU3	cruciferin 3
O82663	AT4G29130	HXK1	hexokinase 1
P41376;A8MRZ7;F4JEL5;F4JEL4;Q9CAI7	AT4G29510	PRMT11	arginine methyltransferase 11
Q9LKR8	AT4G32260	PDE334	ATPase, F0 complex, subunit B/B', bacterial/ chloroplast
P16127	AT4G33580	BCA5	beta carbonic anhydrase 5
Q05758	AT4G33680	AGD2	Pyridoxal phosphate (PLP)-dependent transferases superfamily protein
Q9SIB9	AT4G34200	EDA9	D-3-phosphoglycerate dehydrogenase
Q9SR37	AT4G34350	HDR	4-hydroxy-3-methylbut-2-enyl diphosphate reductase
Q9LS02;Q9LS03	AT4G34412	AT4G34412	EKC/KEOPS complex subunit tprkb-like protein
Q9SU63	AT4G35090	CAT2	catalase 2
O82597;Q93V56	AT4G36250	ALDH3F1	aldehyde dehydrogenase 3F1
P42737-2;P42737;A8MQY4;F4K875;F4K873	AT4G36910	LEJ2	Cystathionine beta-synthase (CBS) family protein
Q9CAF5	AT5G05010	AT5G05010	clathrin adaptor complexes medium subunit family protein
Q94B60	AT5G08690	AT5G08690	ATP synthase alpha/beta family protein
Q9SIF2;Q9SIF2-2	AT5G11200	UAP56b	DEAD/DEAH box RNA helicase family protein
P27140-3;P27140-2;P27140	AT5G13120	Pnsl5	cyclophilin 20-2
Q9FIJ7	AT5G14660	PDF1B	peptide deformylase 1B
Q9SKP6;A8MRE8	AT5G14740	CA2	carbonic anhydrase 2
Q9FUZ2	AT5G15450	CLPB3	casein lytic proteinase B3
Q9SI75	AT5G16050	GRF5	general regulatory factor 5
Q9SYX1	AT5G17770	CBR	NADH:cytochrome B5 reductase 1
O22607	AT5G19940	AT5G19940	Plastid-lipid associated protein PAP / fibrillin family protein
B9DH97;Q9ZTW3;P47192;Q67YV9	AT5G20720	CPN20	chaperonin 20
Q9SU94	AT5G22340	AT5G22340	NF-kappa-B inhibitor-like protein
Q9SAJ4	AT5G23300	PYRD	pyrimidine d

Q8S8F8;Q8S8F8-2	AT5G28500	AT5G28500	rubisco accumulation factor-like protein
Q93ZN9	AT5G28750	AT5G28750	Bacterial sec-independent translocation protein mttA/Hcf106
F4JAF3;Q43349-2;Q43349	AT5G35630	GS2	glutamine synthetase 2
Q9SK66	AT5G37510	EMB1467	NADH-ubiquinone dehydrogenase
Q9MAP3	AT5G38410	RBCS3B	Ribulose bisphosphate carboxylase (small chain) family protein
Q9LIA8;Q9LF33	AT5G38530	TSBtype2	tryptophan synthase beta type 2
O23193	AT5G38660	APE1	acclimation of photosynthesis to environment
P93819	AT5G42020	BIP2	Heat shock protein 70 (Hsp 70) family protein
O04314;O04314-2	AT5G44120	CRA1	RmlC-like cupins superfamily protein
A8MRC4;P48006	AT5G45390	CLPP4	CLP protease P4
B9DFQ9;Q9FGI6	AT5G47840	AMK2	adenosine monophosphate kinase
Q9SA73	AT5G48230	ACAT2	acetoacetyl-CoA thiolase 2
F4JL11	AT5G48580	FKBP15-2	FK506- and rapamycin-binding protein 15 kD-2
F4IX26;P34791;F4IX28	AT5G53560	CB5-E	cytochrome B5 isoform E
Q9ASS6-2;Q9ASS6	AT5G57490	VDAC4	voltage dependent anion channel 4
Q39043;F4K007	AT5G57655	AT5G57655	xylose isomerase family protein
Q9SYB5	AT5G58070	TIL	temperature-induced lipocalin
F4IRX7	AT5G64300	GCH	GTP cyclohydrolase II
O64530-2;O64530;A8MR47	AT5G65430	GRF8	general regulatory factor 8
O49485	AT5G66760	SDH1-1	succinate dehydrogenase 1-1
Q94B35	ATCG00020	PSBA	photosystem II reaction center protein A
F4K2P2;Q941D3	ATCG00120	ATPA	ATP synthase subunit alpha
F4KHY7;P48348-2;P48348	ATCG00490	RBCL	ribulose-bisphosphate carboxylase
Q9SJH7	ATMG01190	ATP1	ATP synthase subunit 1

Supplementary information files

Supplemental information 5.1 is found at the end of this chapter Supplemental files are available on request (lennardcasper@yahoo.com):

Supplemental file 5.1. Perseus output of chemical proteomics data

Supplemental information 5.1 – Heatin probe Synthesis

All starting materials, reagents and solvents used for probe synthesis were obtained from commercial vendors and used without further purification. The 4-(chloromethylbenzoyl)chloride used in the synthesis of compound **3** was purchased from Sigma-Aldrich. Dry solvents were dried over 4A or 3A molecular sieves. Thin-layer chromatography (TLC) spots were visualized under 254 and 356 nm and by staining with ninhydrine, triphenylphosphine/ninhydrine and phosphomolybdic acid. Nuclear magnetic resonance (NMR) spectroscopy was performed on a 400 MHz Varian NMR machine.

1,6-diazidohexane (1)

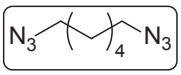

To a solution of 1,6-dibromohexane (8.00 g, 32.8 mmol) in 50 ml of dry N,N-dimethylformamide (DMF) was added sodium azide (6.40 g, 3 eq), and the reaction mixture was stirred for 14 h at 60°C. The mixture was concentrated in vacuum, diluted with Et_2O, extracted with saturated $NaHCO_3$ and water. The water layer was extracted with Et_2O, the organic layers combined, dried with Na_2SO_4, concentrated in vacuum and purified by column chromatography (Petroleum ether (PE), then PE:EtOAc 97:3) yielding 1,6-diazidohexane as a colorless oil (4.30 g, 78%).

Analytical data: R_f 0.6 (PE/EtOAc 97:3); ^{1}H NMR (400 MHz, $CDCl_3$) δ 3.26 (t, 4H), 1.60 (m, 4H), 1.39 (m, 4H).

1-aminohexyl-6-azide (2)

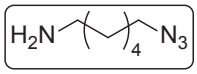

To a solution of 1,6-diazidohexane (4.30 g, 25.6 mmol) in a mixture of Et_2O (25 ml) and EtOAc (25ml) was added 1M HCl (40ml). The mixture was cooled to 0°C and triphenylphosphine (3.36 g, 12.8 mmol) was added in portions over 15 minutes. The mixture was stirred vigorously for 4 h. The layers were separated, and the aqueous layer was extracted with 2x 20 ml Et_2O. The pH of the aqueous layer was adjusted with 4M NaOH until pH 12 and was extracted 3x with 50 mL Et_2O. The combined organic layers were dried with Na_2SO_4, concentrated in vacuum and purified by column chromatography (Dichloromethane (DCM)/MeOH/NH_4OH 9:1:0.1 yielding 1-aminohexyl-6-azide as a colorless oil (2.40 g, 65%).

Analytical data: ^{1}H NMR (400 MHz, $CDCl_3$) δ 3.24 (t, J = 6.9 Hz, 2H), 2.68 (t, J = 7.0 Hz, 2H), 1.59 (m, J = 10.7, 6.9 Hz, 3H), 1.50 – 1.25 (m, 7H).

N-(6-azidohexyl)-4-(chloromethyl)benzamide (3)

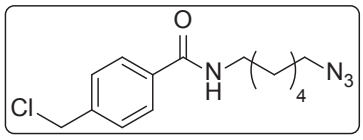

1-aminohexyl-6-azide (1.26 g, 8.86 mmol) was dissolved in dry DCM and cooled to 0°C. DMAP (217 mg, 1.77 mmol, 0.2 eq.), pyridine (1.30 ml, 17.7 mmol, 2 eq.) and 4-(chloromethylbenzoyl)chloride (1.68 g, 8.86 mmol, 1 eq.) were added and the mixture was stirred for 16 h at room temperature (RT). The reaction was quenched with satd. aq. NH_4Cl. The layers were separated, and the aqueous layer was back-extracted with 2x 25 ml DCM. The organic layers were combined, dried with Na_2SO_4 and concentrated in vacuuum. After column chromatography (9:1 DCM/MeOH) N-(6-azidohexyl)-4-(chloromethyl) benzamide was obtained as a yellowish solid (1.38 g, 53 %).

Analytical data: ^{1}H NMR (400 MHz, $CDCl_3$) δ 7.79 – 7.66 (d, 2H), 7.49 – 7.37 (d, 2H), 6.17 (s, 1H), 4.58 (s, 1H), 3.50 – 3.36 (q, 2H), 3.25 (t, 2H), 1.68 – 1.49 (m, 4H), 1.49 – 1.30 (m, 4H).

N-(6-azidohexyl)-4-(iodomethyl)benzamide (4)

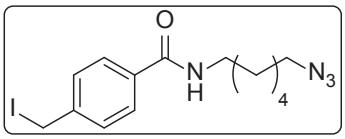

N-(6-azidohexyl)-4-(chloromethyl)benzamide (1.00 g, 3,39 mmol) was dissolved in 50 ml dry acetone. NaI (863 mg, 5.76 mmol, 1.7 eq) was added and the mixture was stirred overnight at 60°C. The reaction mixture was concentrated in vacuum. Et_2O (100 ml) was added and washed twice with H_2O and once with 1M sodium thiosulphate. The aqueous layers were back-extracted with Et_2O (2x20 mL), the organic layers combined, dried with Na_2SO_4 and concentrated in vacuum yielding N-(6-azidohexyl)-4-(iodomethyl) benzamide (1.24 g, 95%) as a yellowish crystalline solid which was used without further purification.

***tert*-butyl benzylcarbamate (5)**

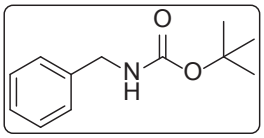

Benzylamine (2,2 ml, 20 mmol) and triethylamine (4.2 ml, 1.5 eq) were dissolved in 50 ml dry DCM. Di-*tert*-butyl dicarbonate (5.24 g, 24 mmol, 1.2 eq) was added in portions at RT. The resulting reaction mixture was stirred at RT for 16H, diluted with Et_2O and washed with 0.1M HCl and brine. The organic layers were dried with Na_2SO_4 and concentrated in vacuum. Column chromatography (9:1 PE/EtOAc) yielded white crystals of tert-butyl benzylcarbamate (1.5 g, 36%).

Analytical data: ^{1}H NMR (400 MHz, $CDCl_3$) δ 7.40 – 7.15 (m, 5H), 4.81 (s, 1H), 4.24 (t, 2H), 1.45 (s, 9H).

tert-butyl (4-((6-azidohexyl)carbamoyl)benzyl)(benzyl)carbamate (6)

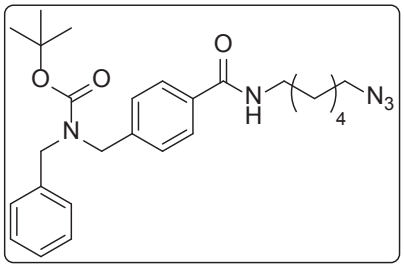

tert-butyl benzylcarbamate (216 mg, 2.41 mmol) was dissolved in dry DMF and cooled to 0°C. NaH (60% in paraffin) (440 mg, 26.5 mmol, 4.5 eq) was added and the reaction mixture was allowed to warm to RT in 30 min. N-(6-azidohexyl)-4-(iodomethyl)benzamide (400 mg, 2.41 mmol, 1 eq) was added and the reaction mixture was stirred at RT for 16 h. Water was added to quench the excess NaH and the mixture was concentrated in vacuum. The residue was dissolved in DCM and washed with H_2O. The aqueous layer was back-extracted with DCM, the organic layers combined, dried with Na_2SO_4 and concentrated in vacuum. The residue was purified by column chromatography (1:1 PE/ EtOAc) yielding tert-butyl (4-((6-azidohexyl)carbamoyl)benzyl)(benzyl)carbamate (336 mg, 30 %) as a waxy solid.

Analytical data: ^{1}H NMR (400 MHz, $CDCl_3$) δ 7.70 (d, 2H), 7.36 – 7.10 (m, 7H), 6.15 (s, 1H), 4.52 – 4.21 (m, 4H), 3.50 – 3.34 (q, 2H), 3.25 (t, 2H), 1.76 – 1.53 (m, 5H), 1.53 – 1.09 (m, 12H), MS (ESI) found 931.30 $(2M+H)^+$

N-(6-azidohexyl)-4-((benzyl((2-hydroxynaphthalen-1-yl)methyl)amino)methyl)benzamide (7)

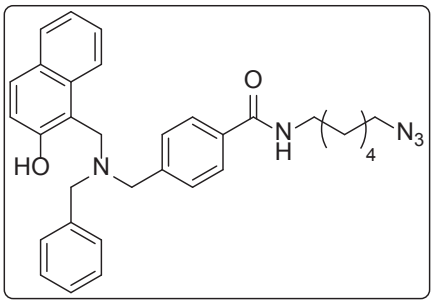

tert-butyl (4-((6-azidohexyl)carbamoyl)benzyl) (benzyl)carbamate (256 mg, 0.55 mmol) was dissolved in 20ml dry DCM and cooled to 0°C. 10 ml Trifluoroacetic acid (TFA) was added and the mixture was stirred for 2H. After TLC indicated completion, the mixture was concentrated in vacuum, co-evaporated with $CHCl_3$ and used without further purification. The amine (200 mg, 0.55 mmol) was dissolved in 1,2-dichloroethane. 3 Å molecular sieves were added, followed by 2-hydroxy-1-naphthaldehyde (190 mg, 1.1 mmol, 2 eq) and sodium triacetoxyborohydride (580 mg, 2.75 mmol, 5 eq). The mixture was stirred at RT for 14 H, filtered and concentrated in vacuum. The residue was partitioned between EtOAc and satd. $NaHCO_3$ and the aqueous layers were back extracted with EtOAc. The organic layers were dried with Na_2SO_4, concentrated in vacuum and purified by column chromatography (2:1 PE/EtOAc) and then preparative HPLC yielding N-(6-azidohexyl)-4-((benzyl((2-hydroxynaphthalen-1-yl)methyl)amino) methyl) benzamide as a colorless oil (33 mg, 3.5 %).

Analytical data: ^{1}H NMR (400 MHz, $CDCl_3$) δ 7.81-7.67 (m, 5H), 7.66 – 7.51 (m, 1H), 7.50 – 7.41 (m, 1H), 7.41 – 7.26 (m, 7H), 7.21 – 7.12 (d, 1H) 6.33 – 6.14 (t, 1H), 4.35 – 4.20 (s, 2H), 4.00 – 3.80 (d, 4H), 3.51 – 3.34 (q, 2H), 3.34 – 3.11 (t, 2H), 1.68 – 1.49 (m, 4H), 1.49 – 1.30 (m, 4H). HRMS (ESI) calcd. for $C_{32}H_{36}N_5O_2$ $[M+H]^+$ 522.28690, found 522.2864

Compound 1: ^{1}H NMR (400 MHz, $CHCl_3$)

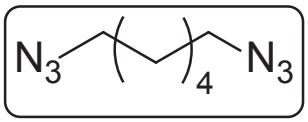

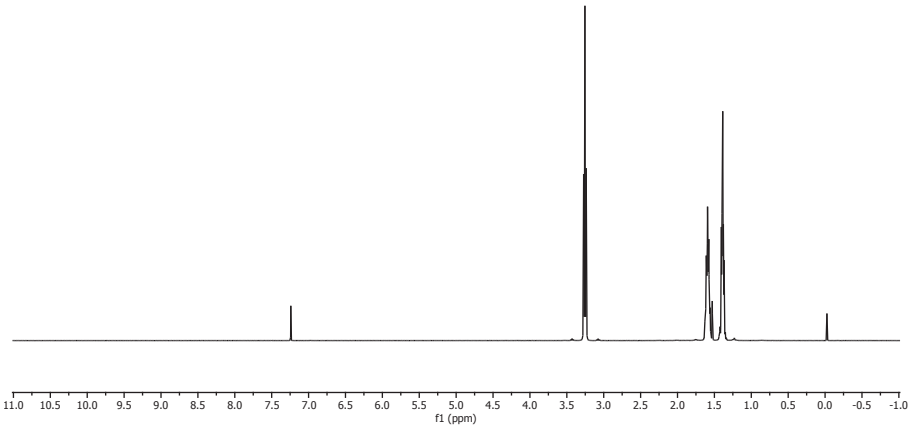

Compound 2: ^{1}H NMR (400 MHz, $CHCl_3$)

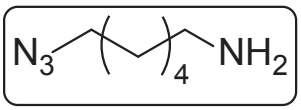

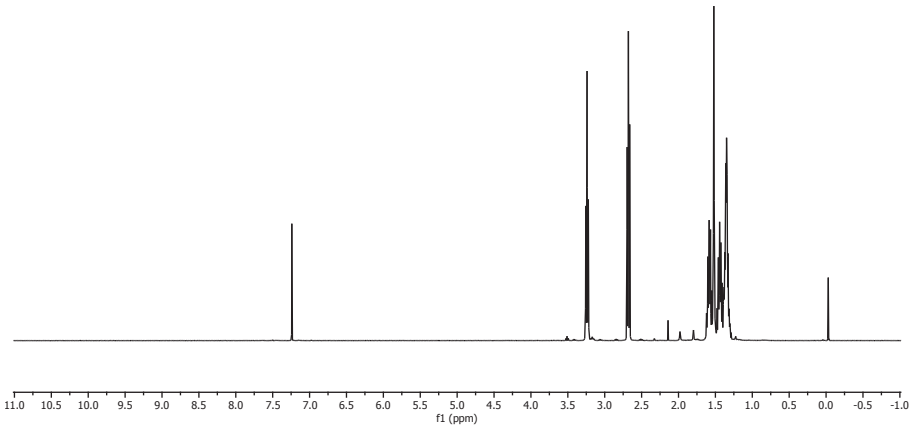

Compound 3: ^{1}H NMR (400 MHz, $CHCl_3$)

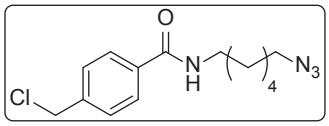

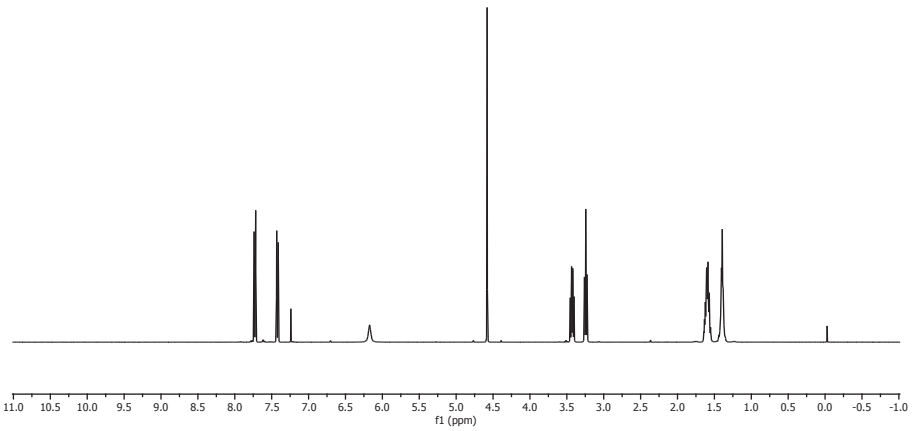

Compound 5: ^{1}H NMR (400 MHz, $CHCl_3$)

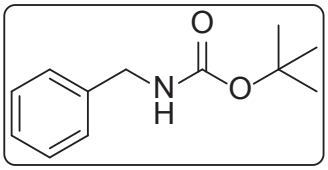

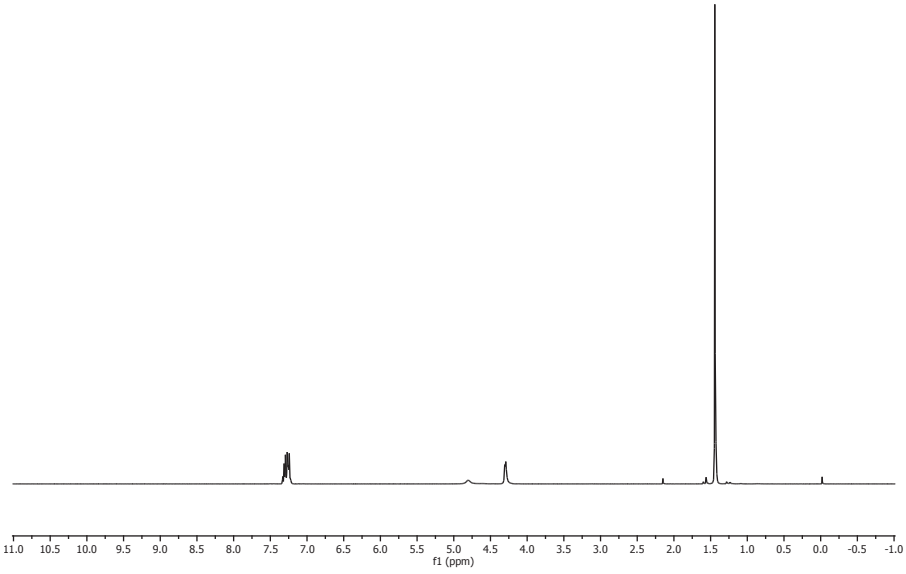

Compound 6: ^{1}H NMR (400 MHz, $CHCl_3$)

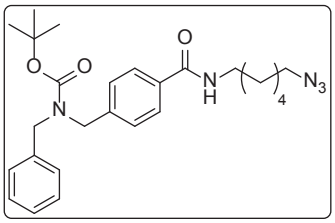

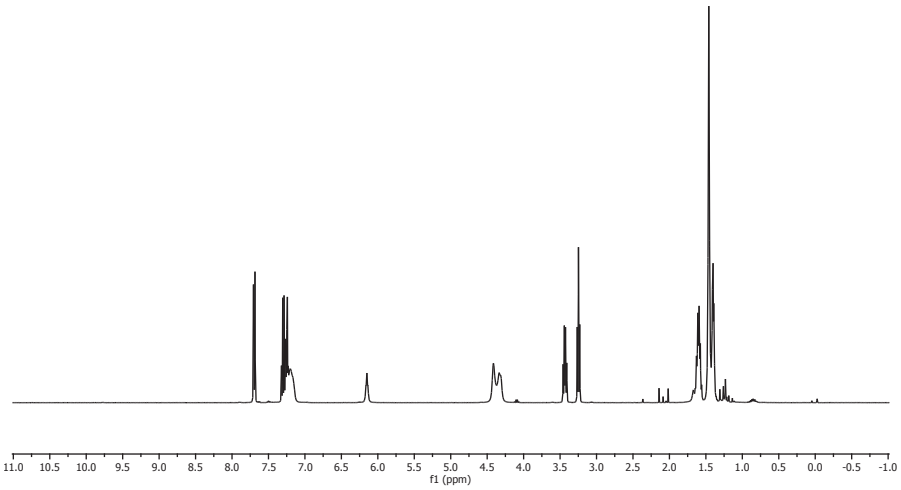

Compound 7: ^{1}H NMR (400 MHz, $CHCl_3$)

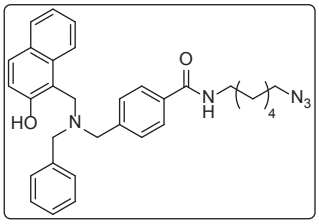

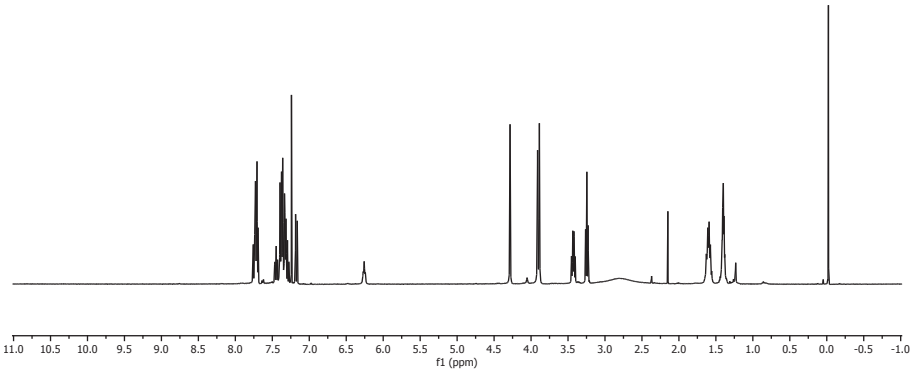

CHAPTER 6

6

Assessment of intra- and interspecific natural variation in Heatin sensitivity by Genome-wide association mapping and crop variety analyses

Lennard van der Woude[1] | Colin Snoeker[1] | Suzanne Bulder[2] | Corine de Groot[2] | Sjef Smeekens[1] | Martijn van Zanten[1]

1 Molecular Plant Physiology, Institute of Environmental Biology, Utrecht University, Padualaan 8, 3584 CH Utrecht, The Netherlands

2 Bejo Zaden B.V., Trambaan 1, 1749 CZ Warmenhuizen, The Netherlands

Abstract

Crop productivity is threatened by current ongoing climate change. Fundamental knowledge of how plants respond to high ambient temperature by adjusting growth and architecture (collectively called 'thermomorphogenesis') can allow for targeted breeding of next-generation thermotolerant crop varieties. Here we studied the applicability of the small molecule compound Heatin that induces thermomorphogenesis phenotypes already under control temperature conditions in Arabidopsis with the aim to understand thermomorphogenesis regulation,

Existing natural variation among Arabidopsis accessions is exploited to identify loci associated with Heatin responsiveness, high temperature responsiveness (thermomorphogenesis) and response to auxin, a phytohormone that is required for thermomorphogenesis. One locus on chromosome 1 significantly associates with sensitivity to Heatin, and with a potential association to high temperature and auxin (Picloram) response as well. Additionally, we tested Heatin applicability in economically relevant crops. Our results show that Heatin is primarily active in members of the Brassicaceae (cabbages) family, which includes Arabidopsis.

Introduction

Ongoing climate change threatens global food security[13]. Projected climate change-imposed crop losses[19] can be prevented, or perhaps revert by development of novel crop cultivars that can better cope with different environments than present-day agricultural varieties. Plants, including many crops, naturally acclimate to small increases in temperature by a process called thermomorphogenesis[47,115]. This response consists of a set of architectural changes that increase the plant´s cooling capacity[44,45]. Notable thermomorphogenesis phenotypes include stem elongation (hypocotyl and/or coleoptile) and leaf stalk elongation[115]. Breeding for different temperature optima of plant developmental processes is difficult due to the limited genetic variation of this trait[24]. However, the thermomorphogenesis strategy to adapt to temperature represents an important breeding target to maintain normal plant development. On the molecular level, thermomorphogenesis relies on Phytochrome B-dependent perception of the high temperature signal[42,43], which is then translated to induce the thermomorphogenesis responses by a signalling cascade that involves *PHYTOCHROME INTERACTING FACTOR 4* (*PIF4*)-dependent biosynthesis of the phytohormones auxin and subsequently brassinosteroids[36,37,39,56,74]. These hormones cause activation of H^+-ATPases leading to a lowering of the apoplastic pH[76]. This results in activation of cell wall modifying enzymes and subsequent cell elongation that drives the typical elongation growth associated with thermomorphogenesis.

The small molecule Heatin was identified in a chemical screen to mimic thermomorphogenesis already under control temperatures in the model plant *Arabidopsis thaliana* (**Chapter 2, 3**). Heatin relies on auxin signalling and acts downstream of *PIF4*. By understanding how Heatin triggers elongation growth, we aim to understand thermomorphogenesis regulation in molecular detail (**Chapter 2-5**). Moreover, in addition to using compounds identified in chemical screens as tools for such mechanistic research[85], a major advantage of chemical genetics is that identified chemical compounds can be directly tested across species-boundaries[246]. This allows for the efficient development of tools in model species like *Arabidopsis thaliana* that can be directly applicable to crop varieties important for agriculture, without the need for time-consuming translational research trajectories to apply fundamental findings in the genetic model system to responsive crops.

Large numbers of natural Arabidopsis accessions have been thoroughly genotyped and sequenced[247] and extensive natural variation has been reported in Arabidopsis for many traits including thermomorphogenesis[123,124,248]. Together, this allows for identification of small differences in the genome sequence (single nucleotide polymorphisms (SNPs), insertions and deletions) contributing to the natural variation in thermomorphogenesis in Genome Wide Association Studies (GWAS)[249].

In this work we followed a comprehensive comparative GWAS approach to identify genomic loci that contribute to Heatin-induced hypocotyl elongation. We included high ambient temperature- and auxin (Picloram)-induced hypocotyl elongation as well to estimate the overlap between Heatin signalling on one hand and thermomorphogenesis/auxin responsiveness on the other. The comparison of these three independent GWAS analyses revealed a single locus on chromosome 1 that significantly associated to the Heatin response. Interestingly, different SNPs at this locus also strongly associated to Picloram-induced and high temperature-induced hypocotyl elongation, suggesting that the causal genetic polymorphism(s) at this locus is a general cause of natural variation in hypocotyl elongation.

Next to testing intraspecific variation in Heatin responsiveness by GWAS in Arabidopsis germplasm, we tested interspecific effect by testing to what extend Heatin is effective in (related) crop species. Strikingly, we found that Heatin activity appears to be restricted to the *Brassicaceae* family, that includes cabbage and broccoli varieties. This corresponds with our previous findings in Arabidopsis (also a member of the *Brassicaceae*), where we identified a *Brassicaceae*-specific sub-family of proteins as direct targets of Heatin (**Chapter 5**). It appears that Heatin has the potential to improve thermotolerance specifically in cabbages and that the Arabidopsis germplasm can be used to identify novel breeding targets for Heatin-mediated thermotolerance improvement.

Results

Assessing natural variation in the responses to Heatin, Picloram and high ambient temperature in *A. thaliana*

To explore the extend of genetic variation in sensitivity to Heatin within the *A. thaliana* germplasm, we quantified hypocotyl elongation in response to Heatin (**Fig. S6.1**) in 321 natural accessions (**Supplemental File 6.1**; subset of a commonly used set of 360 accessions[250–253]). To further confirm the relationship between Heatin on one hand and auxin and high ambient temperature on the other (**Chapters 3 and 4**), we independently assessed hypocotyl elongation in response to Picloram and high temperature treatment (27°C) (**Fig. S6.1**). As a control, Col-0 WT and the *pif4-2* mutant were grown alongside each batch of accessions to test for effectiveness of each treatment. We found consistent effects of each treatment between the batches, especially in Col-0 WT (**Fig. S6.3**). Thermomorphogenesis responsiveness in the *pif4-2* mutant was consistently diminished compared to the Col-0 WT, in line with previous findings[37] (**Fig. S6.3**). As expected, broad variation in hypocotyl length among the accessions was observed in control conditions (22°C, DMSO mock medium). This treatment-independent variation correlated significantly with absolute hypocotyl length in the presence of Heatin, Picloram and high temperature treatments (**Fig. 6.1**). This indicates that initial hypocotyl length is a major predictor of

treatment effect. These treatments are either additive to the initial hypocotyl length, or hypocotyl length under control conditions restricts further elongation in response to treatments. To distinguish between these two options, we generated a matrix of Pearson's correlation coefficients between i) absolute lengths, ii) relative response (treatment divided by control) and iii) absolute response (treatment minus control) (**Fig. 6.1, 6.2, S6.2**). Interestingly, we found a significant positive correlation between relative responses and absolute responses for each of the treatments. Strikingly, absolute hypocotyl length of seedlings grown on control medium (mock DMSO) negatively correlated with the relative response (ii) to each treatment, but not, or to a lesser extent, with the absolute responses (iii) (**Fig. 6.1, DMSO 22°C column**). This indicates that the treatments are additive to the initial (variation in) hypocotyl length.

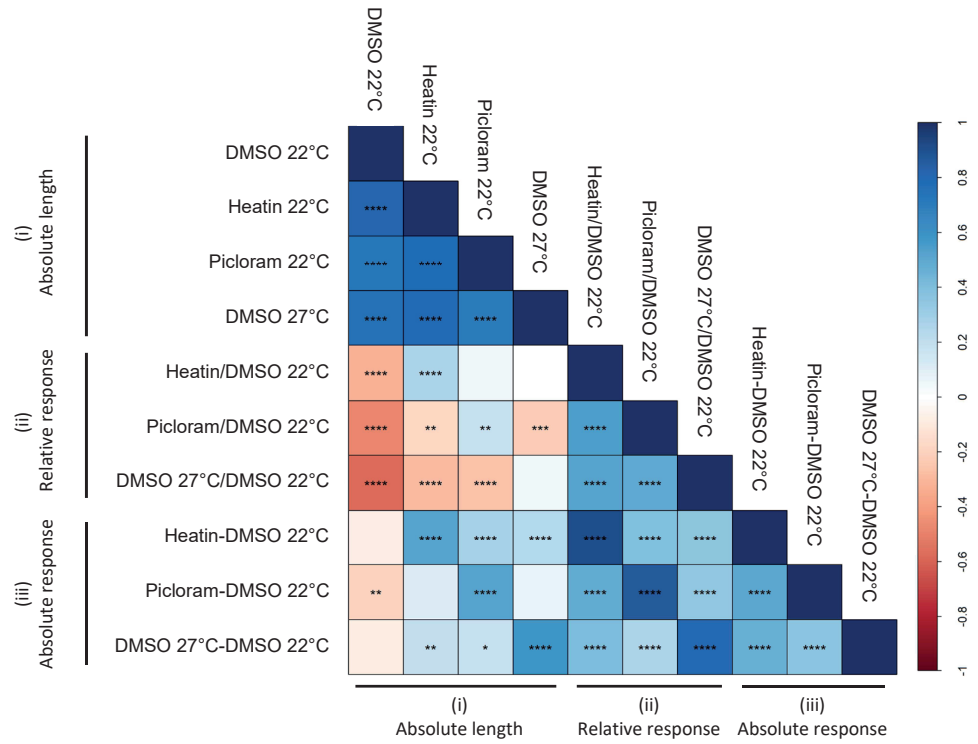

Figure 6.1: Tests for correlation between the natural variation datasets.

(**A**) Pearson correlation coefficient calculated between absolute hypocotyl lengths (i), relative response (ii) and absolute response (iii). Colors represent correlation coefficient from -1 (dark red) over 0 (white) to 1 (dark blue). Asterisks indicate significance as $p<0.01$ (*), $p<0.001$ (**), $p<0.0001$ (***) and $p<0.00001$ (****). Graph was made using the R package "corrplot".

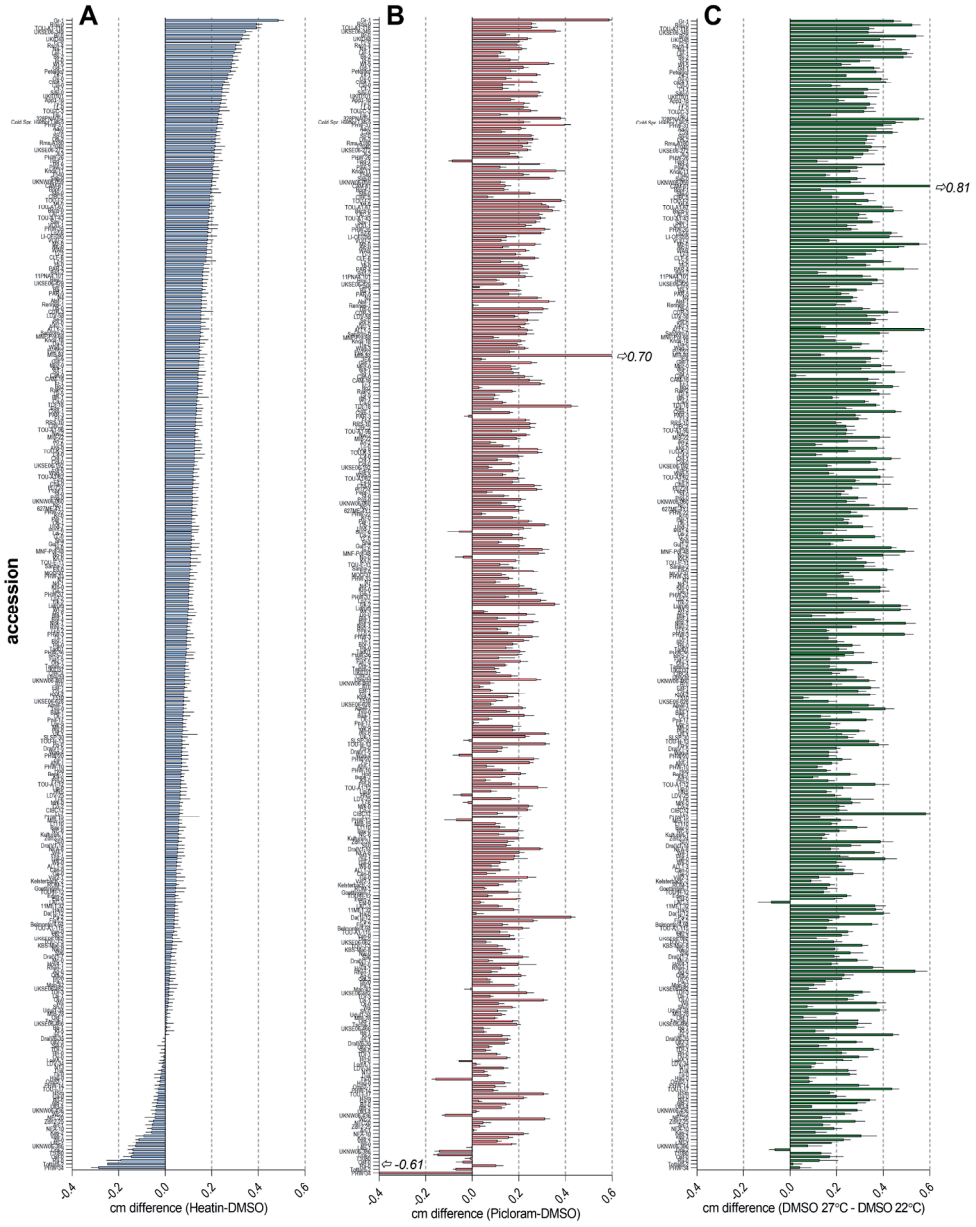

Figure 6.2: Absolute differences in hypocotyl lengths between different treatments and controls for 321 ecotypes.

Differences in cm are shown for all tested ecotypes that grew to give a hypocotyl upon treatment with Heatin (**A**), Picloram (**B**) or 27°C (**C**). Ecotypes are sorted to strength of the response to Heatin treatment. Error bars represent standard error of the mean. Values exceeding the x-axis are indicated with an arrow and the actual value is shown.

Overall, broad natural variation in response to Heatin was observed among the accessions (**Fig. 6.2A**). Most accessions had a positive elongation response to Heatin, (*i.e.* Heatin-treated seedlings were longer than mock-treated seedlings), but 37 accessions showed a negative average response (*i.e.* Heatin-treated seedlings were shorter than mock-treated ones) (**Fig. 6.2A**). Similar variation was observed after Picloram treatment, where most accessions showed a positive elongation response, but 20 accessions were shorter than the DMSO control grown seedlings (**Fig. 6.2B**). Only 2 accessions showed a mild decrease in hypocotyl length when exposed to high temperature compared to control conditions (**Fig. 6.2C**), whereas the others showed a positive response. This suggests that seedling thermomorphogenesis is a more conserved response than the responses to Heatin and Picloram.

Genome-wide association mapping of Heatin, Picloram and high temperature responsiveness

A Genome-Wide Association Study (GWAS) using the observed variation in hypocotyl lengths was performed to identify genetic loci associated with Heatin, Picloram and high temperature sensitivity (**Fig. 6.2**). Specifically, we tested for associations between absolute elongation responses (treatment minus control) (**Fig. 6.2**) and 250k Single Nucleotide Polymorphisms (SNPs) markers scattered over the genome[254]. Using a stringent multiple testing p-value correction we identified a single locus on chromosome 1, containing several SNPs that significantly correlated to Heatin responses (**Fig. 6.3**). For Picloram and high ambient temperature treatments no SNPs were found with a significant association. However, at the same chromosome 1 locus that associated with Heatin response, several SNPs also showed an association with Picloram and high ambient temperature response above background level, but below the significance threshold (**Fig. 6.3B, C**). Remarkably, the highest/peak SNP for the different treatments was found at different locations on the locus (**Fig. 6.3D, arrows**). For the Heatin response, the peak SNP (Chr1:22211794, p=-log10(8.39)) was located in *UB-LIKE PROTEASE 1D /OVERLY TOLERANT TO SALT 1* (*ULP1D/OTS1*, At1G60220). For high ambient temperature and Picloram treatment the peak SNPs were located in *TREHALOSE PHOSPHATE SYNTHASE 10* (*TPS10*, AT1G60140, Chr1:22180556, p=-log10(4.57) and Chr1:22177314, p=-log10(4.03), which are 31.2 kb and 34.5 kb upstream of the Heatin response locus (**Fig. 6.3D**).

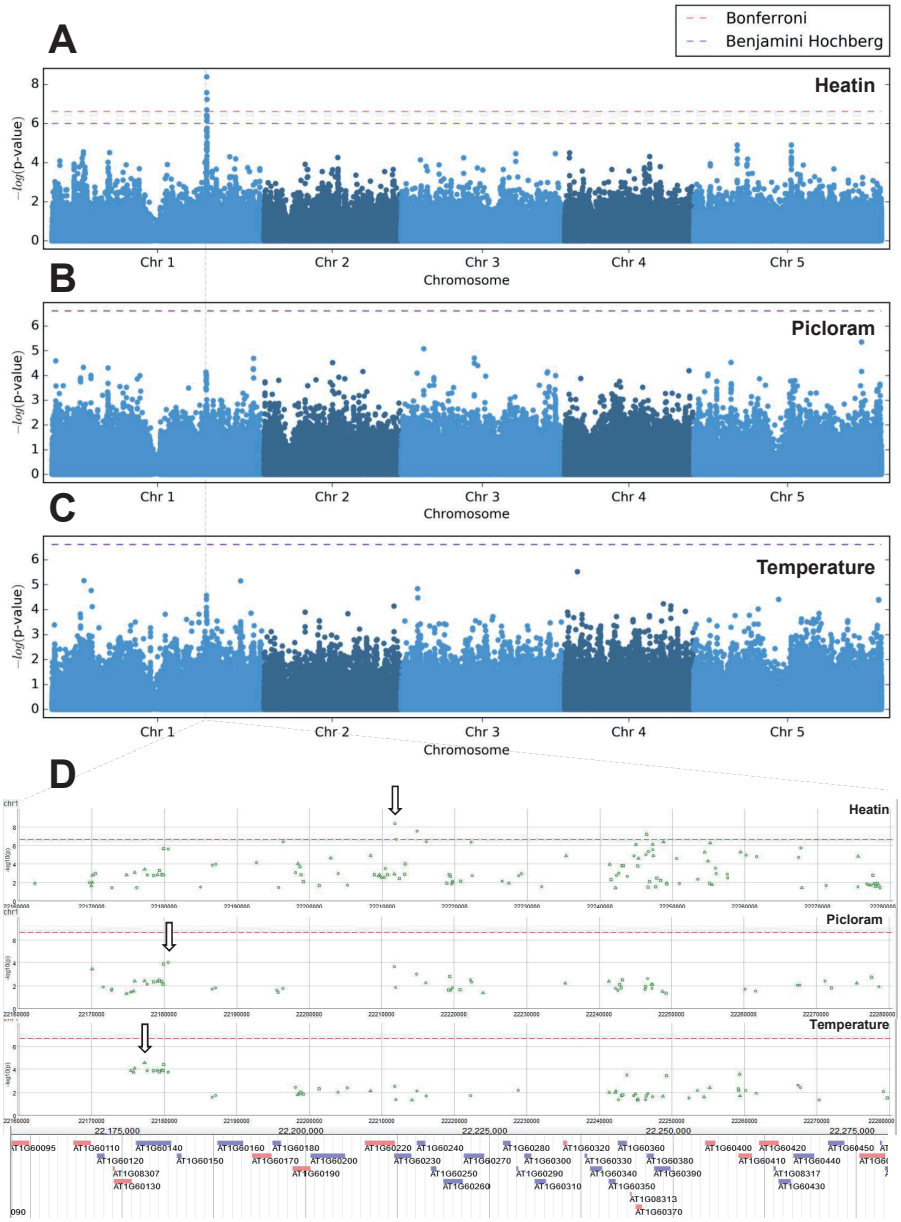

Figure 6.3: Genome Wide Association Study of the response to Heatin, Picloram and High temperature.

(**A, B, C**) Manhattan plots of the GWAS analyses for the indicated treatments. Absolute difference data was used for the analyses. Each dot represents a Single Nucleotide Polymorphism with its location on the X-axis corresponding to its location in the *A. thaliana* genome. Alternating colors represent different chromosomes. Y-axis shows the corresponding p-value of associating to the tested treatment. Dashed horizontal lines represent FDR line. (**D**) magnification of the indicated locus on chromosome 1. Arrows indicate highest SNPs for each treatment on this locus. Lowest bar

shows gene models on this locus.

Despite the intrinsic correction for population structure, GWAS analysis on a limited population of 321 accessions is considered not powerful enough to directly determine the genes responsible for the association, due to genetic linkage[255]. Although previous work demonstrated linkage disequilibrium decay is on average 10Kb around the causal SNP, this distance can be influenced by many factors[254]. As the distance between the peak SNPs of the Heatin treatment GWAS and the Picloram and high temperature treatment GWAS was larger than the average 10Kb (**Fig. 6.3**), we defined the genomic region around the area where all three associations are located as our region of interest (Chr1:22170000 – 22270000). 36 gene models are annotated on this genomic region (**Table 6.1**). We first verified in our RNA-seq experiment which of these genes are expressed in young seedlings, using the average read count of DMSO and Heatin treated samples. Of 12 genes no transcripts could be detected and were therefore considered unlikely causal for the observed natural variation in hypocotyl elongation. Interesting candidate genes include *ULP1D*/*OTS1*, previously found to be involved in salt tolerance and regulation of *PHYB* deSUMOylation[256,257] and *TPS10* is involved in sugar signalling[258], a process linked to hypocotyl elongation in a *PIF*-dependent manner[195,259].

Table 6.1: candidate genes causing the association peak on chromosome 1.

Shown are all genes found in the region Chr1:22160000-22280000. Indicated are the AGI-code, synonym, a brief description, the class of genes, and their expression level as found in the RNA-seq experiment performed in chapter 4. Values are average read counts of DMSO control and Heatin treated seedlings grown at 22°C from our early time point after 48 hours of growth (ET) and our late time point after 7 days of growth (LT). Genes with no detected transcripts are greyed out. Synonyms, brief description and gene class were retrieved from www.araport.org.

AGI	Synonym	Brief description	Class	RNAseq ET	RNAseq LT
AT1G08307			Gene		
AT1G08313			Gene		
AT1G08317		Natural antisense transcript overlaps with AT1G60420	Gene		
AT1G60110	AT1G60110	Mannose-binding lectin superfamily protein	Gene	99.0985	3.81456
AT1G60120	AT1G60120	transposable_element_gene	TransposableElementGene	0.14827	0
AT1G60130	AT1G60130	Mannose-binding lectin superfamily protein	Gene	56.5427	19.71595
AT1G60140	TPS10	trehalose phosphate synthase	Gene	3060.51	3467.533
AT1G60150	AT1G60150	transposable_element_gene	TransposableElementGene	0.15872	0
AT1G60160	AT1G60160	Potassium transporter family protein	Gene	2269.552	981.0713
AT1G60170	emb1220	pre-mRNA processing ribonucleoprotein binding region-containing protein	Gene	2410.933	1509.718
AT1G60180	AT1G60180	pseudogene of RNI-like superfamily protein	Pseudogene	0.780368	0
AT1G60190	PUB19	ARM repeat superfamily protein	Gene	73.85237	74.79807
AT1G60200	AT1G60200	splicing factor PWI domain-containing protein / RNA recognition motif (RRM)-containing protein	Gene	4487.444	3499.993
AT1G60220	ULP1D/OTS1	UB-like protease 1D	Gene	1884.059	763.9919
AT1G60230	AT1G60230	Radical SAM superfamily protein	Gene	1804.427	520.3888
AT1G60240	AT1G60240	NAC (No Apical Meristem) domain transcriptional regulator superfamily protein	Gene	0	0
AT1G60250	BBX26	B-box zinc finger family protein	Gene	0	0
AT1G60260	BGLU5	beta glucosidase 5	Gene	158.723	338.7617
AT1G60270	BGLU6	beta glucosidase 6	Gene	119.1443	128.7403
AT1G60280	NAC023	NAC domain containing protein 23	Gene	0	0
AT1G60290	AT1G60290	pseudogene of Chalcone-flavanone isomerase family protein	Pseudogene	0	0

AT1G60300	AT1G60300	NAC (No Apical Meristem) domain transcriptional regulator superfamily protein	Gene	0	0
AT1G60310	AT1G60310	transposable_element_gene	TransposableElementGene	0	0
AT1G60320	AT1G60320	Toll-Interleukin-Resistance (TIR) domain family protein	Gene	0	0
AT1G60330	AT1G60330	pseudogene of Chalcone-flavanone isomerase family protein	Pseudogene	0	0
AT1G60340	AT1G60340	NAC (No Apical Meristem) domain transcriptional regulator superfamily protein	Gene	0.14827	0
AT1G60350	NAC024	NAC domain containing protein 24	Gene	0.747539	0.47381
AT1G60360	AT1G60360	RING/U-box superfamily protein	Gene	7.683836	26.93346
AT1G60370	AT1G60370	F-box and associated interaction domains-containing protein	Gene	0	0
AT1G60380	AT1G60380	NAC (No Apical Meristem) domain transcriptional regulator superfamily protein	Gene	0	0.296809
AT1G60390	PG1	polygalacturonase 1	Gene	249.0214	134.0229
AT1G60400	AT1G60400	F-box/RNI-like superfamily protein	Gene	0.151365	0
AT1G60410	AT1G60410	F-box family protein	Gene	2.112541	0
AT1G60420	AT1G60420	DC1 domain-containing protein	Gene	1869.625	1304.852
AT1G60430	ARPC3	actin-related protein C3	Gene	698.4198	413.2351
AT1G60440	PANK1	pantothenate kinase 1	Gene	1634.908	544.1211

Heatin stimulates growth of *Brassicaceae* species specifically

In an agricultural setting, Heatin might be applicable for priming crops for thermomorphogenesis, potentially increasing crop survival and production under otherwise high temperature conditions. To assess whether Heatin effects are exclusive to Arabidopsis or are more broadly applicable, we quantified Heatin effects on hypocotyl or coleoptile lengths of several commercial crop varieties (**Fig. 6.4**). For a first test, we included a monocot species: *Allium cepa* (Onion), and eudicot species from the Asterid clade: *Apium graveolens* (celery), *Cichorium intybus* var. *foliosum* (Radicchio Rosso), *Daucus carota* subsp. *Sativus* (carrot) and the Rosid clade: *Brassica oleracea* (white cabbage). We used 8.5µM (**Fig. 6.4A**) and 25µM (**Fig. 6.4B**) Heatin, applied at control and high temperature conditions (22°C and 27°C). When considering the two concentrations, only white cabbage showed a consistent trend towards an increase in hypocotyl length. This was observed only under high temperature conditions. White cabbage was also the only species that exhibited a consistent hypocotyl elongation response to high temperature treatment (**Fig. 6.4**).

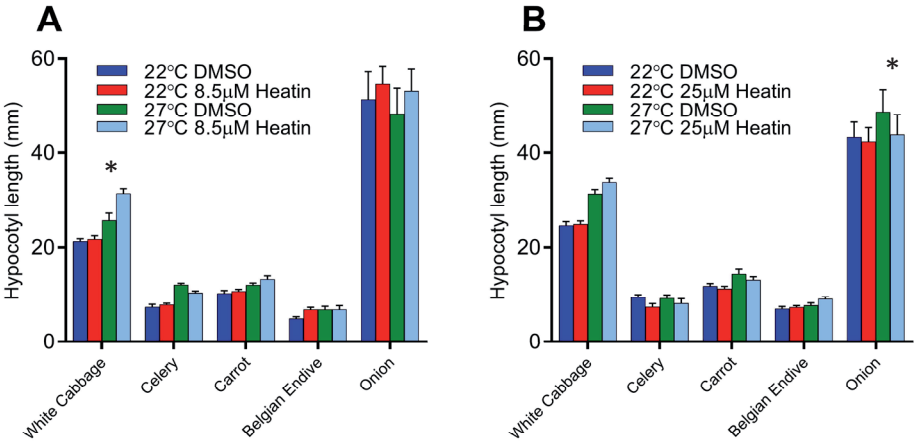

Figure 6.4: Different crops responses Heatin and high ambient temperature.

The indicated crops were grown under 22°C (blue and red bars) and 27°C (green and light blue bars) conditions on medium containing a DMSO solvent mock (blue and green bars) or Heatin (red and light blue bars, **A**: 8.5µM, **B**: 25µM) at the indicated concentration. Error bars indicate standard error of the mean. Values are averages of ~20 seedlings. Heatin effects were tested by t-test vs the corresponding DMSO mock average. Asterisks indicate a significant difference at $p<0.05$.

Alike white cabbage, Arabidopsis is a member of the *Brassicacea* family, suggesting that Heatin may be specific for this family. To further explore this, we tested additional *Brassicaceae* crops: *Brassica oleracea* var. *Italica* (broccoli), *Raphanus raphanistrum* subsp. *Sativus* (radish), *Brassica oleracea* var. *gemmifera* (Brussels sprouts) and *Brassica rapa* subsp.

pekinensis (Chinese cabbage), next to non-*Brassicaceae* crops: *Lactuca sativa* (Butter lettuce and Batavia lettuce), *Solanum lycopersicum* (tomato) and *Capsicum annuum* (chili pepper and bell pepper). For broccoli, radish, Brussels sprouts, Chinese cabbage and tomato 'Low Seed Count' (LSC) and 'High Seed Count' (HSC) seed batches were included, which had a relatively low or relatively high number of seeds per gram respectively and thus is directly related to seed size. Additionally, we tested these crops under high and control temperature conditions on 25µM Heatin and control (mock) medium (**Fig. 6.5**). Significant hypocotyl elongation in response to Heatin was observed in broccoli, Brussels sprouts and Chinese cabbage (**Fig. 6.5**). In broccoli, we observed clear Heatin-induced elongation in the LSC seed batch under both temperatures and in HSC seed batch only in high temperature conditions. In Brussels sprouts, Heatin sensitivity was observed in the HSC seed batch under both temperatures and in Chinese cabbage in the LSC seed batch under high temperature conditions only (**Fig. 6.5**). Strikingly, all the non-*Brassicacea* crops in this experiment (butter lettuce, tomato, chili pepper and bell pepper all), as well as radish, did not respond to Heatin under either temperature condition (**Fig. 6.5**). These results strongly suggest that Heatin activity is restricted to the *Brassicaceae* family. However, not all members of this family are sensitive, as we found no response in radish (**Fig. 6.5**). Additionally, high temperature seems to affect Heatin sensitivity, as broccoli HSC and Chinese cabbage LSC are only sensitive to the compound under high temperature conditions (**Fig. 6.5**).

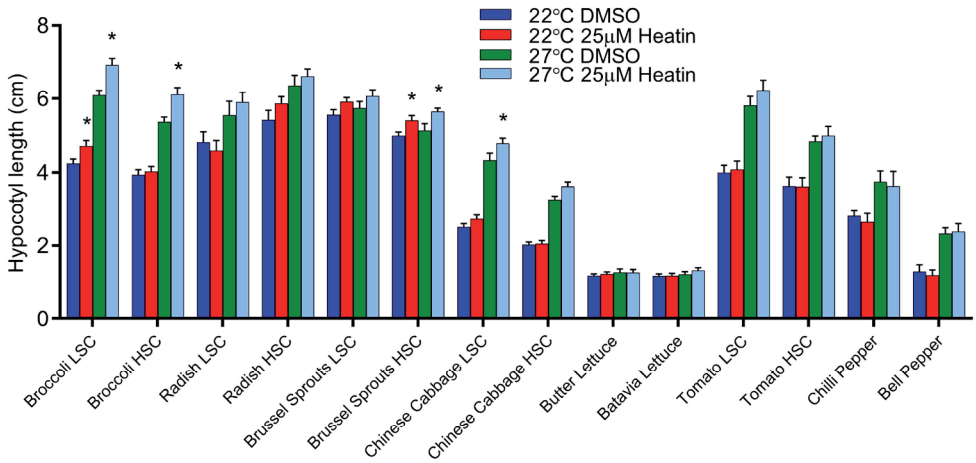

Figure 6.5: Different crops responses Heatin and high ambient temperature.

The indicated crops were grown under 22°C (blue and red bars) and 27°C (green and light blue bars) conditions on medium containing a DMSO solvent mock (blue and green bars) or 25µM Heatin (red and light blue bars). Error bars indicate standard error of the mean. Values are averages of 8 replicates of each ~20 seedlings. Heatin effects were tested by t-test vs the corresponding DMSO mock average. Asterisks indicate a significant difference at $p<0.05$.

High ambient temperature also affected hypocotyl elongation differently across the different tested species and varieties (**Fig. 6.5**). Unlike Heatin sensitivity, the response was not restricted to one family of crops. Broccoli, radish and Chinese cabbage, tomato, chili pepper and bell pepper had longer hypocotyls under high temperature (**Fig. 6.5**). In contrast, Brussels sprouts and both Lettuce variants did not respond to high temperature by hypocotyl elongation (**Fig. 6.5**). Taken together, this suggests that high temperature-induced hypocotyl elongation response capacity originated before diversification of the Rosid and Asterid families and was lost in several species. Alternatively, it was acquired in different species independently.

Hypocotyl elongation in different crop species and varieties is affected differentially by changes in ambient temperature

We next analyzed temperature responsiveness of hypocotyl elongation in 6 *Brassicaceae* species and varieties (broccoli, white cabbage, Chinese cabbage, Brussels sprouts, sprouting broccoli and radish) and *Cucumis sativus* (cucumber) in detail over 4 temperatures (17°C, 22°C, 27°C, 32°C). Large differences were found in hypocotyl length between the species, as well as in temperature responsiveness (**Fig. 6.6**), although all tested species were affected by temperature. Cucumber responded strongest and most linear to the increasing temperature (**Fig. 6.6F**). This contrasted with white cabbage, Brussels sprouts and radish which showed and optimum elongation at temperatures below 32°C (**Fig. 6.6B, D, G**). Broccoli showed a mild increase in hypocotyl elongation with increasing temperature, Chinese cabbage initially had a decrease in hypocotyl elongation between 17°C and 22°C, after which it increased with the increasing temperature and sprouting broccoli was unaffected by temperature, except for 32°C (**Fig. 6.6A, C, E**). Thus, extensive variation exists in thermomorphogenesis capacity among crops.

To test if the thermomorphogenesis responsiveness is indeed optimized for the cultivation environment, we selected a set of white cabbage varieties that have been bred for their performance in different geographic regions/climates, under a range of temperatures (17°C, 22°C, 27°C, 32°C). We tested 2 varieties bred for a continental climate, 2 for a cold climate and 4 varieties bred for a tropical climate, as well as a reference control variety (**Fig. 6.7A**). Strikingly, the varieties bred for a tropical climate had the longest hypocotyls, in particular variety 1 under 27°C and 32°C, variety 3 under 27°C and variety 4 under 22°C conditions (**Fig. 6.7A**). Additionally, both tested varieties bred for cold climates responded very mildly to changes in temperature (**Fig. 6.7A**). Together, this data supports the notion that hypocotyl elongation indeed functions as a marker for climate adaptation.

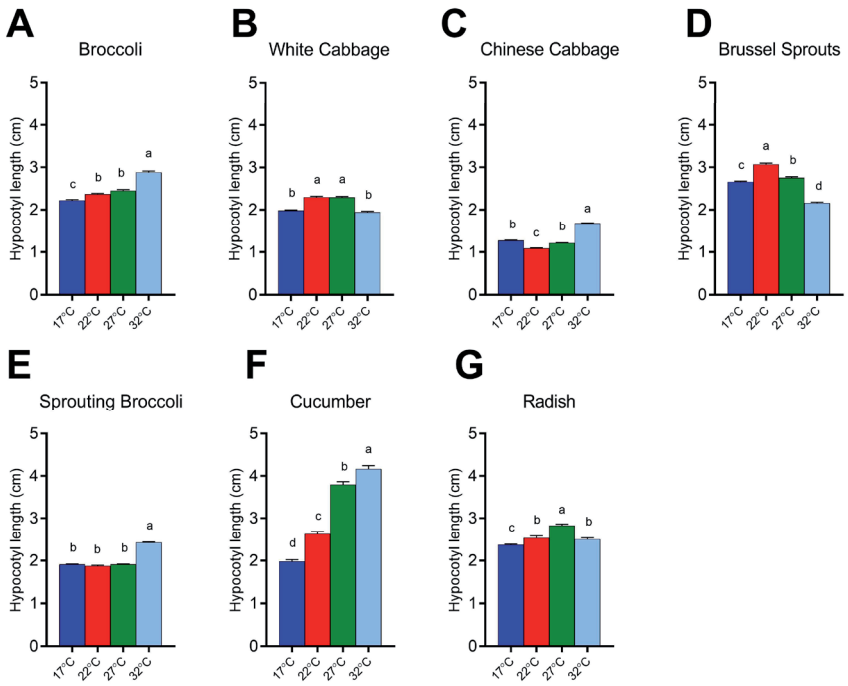

Figure 6.6: Different crops responses to differences in growth temperature.

The indicated crops were grown under 17°C (blue bars), 22°C (red bars), 27°C (green bars) and 32°C (light blue bars) conditions. Error bars indicate standard error of the mean. Values are averages of ~125 seedlings for cucumber and ~250 individual seedlings for the other crops. Averages were tested by ANOVA and Tukey's HSD post hoc tests. Different letters indicate significant differences.

We next tested Heatin sensitivity in the set of white cabbage varieties to assess if sensitivity to temperature is related to sensitivity to Heatin (**Fig. 6.7B**). In contrast to the temperature sensitivity assessment above, this experiment was performed *in vitro* on petri dishes containing MS-agar medium, with a DMSO mock control or 25µM Heatin dissolved in the medium. ANOVA analysis revealed significant interactions between hypocotyl length of the genotype (variety), the growth temperature or the addition of Heatin. As in the previous experiment we found a significant interaction between the varieties and growth temperature. No interaction was found between the compound and the variety. The interaction between the three factors (temperature, variety and compound) was significant (**Fig. 6.7B**). Together this is in line with previous findings of an interaction between temperature and the Heatin compound in Arabidopsis (**Chapter 3, 5**).

To further assess correlations between temperature sensitivity and Heatin sensitivity in the set varieties, Pearson's correlation coefficients were calculated for the hypocotyl lengths of the different experiments, as well as the relative effects of each treatment compared to control conditions (**Fig. 6.7C**). Surprisingly, this revealed no

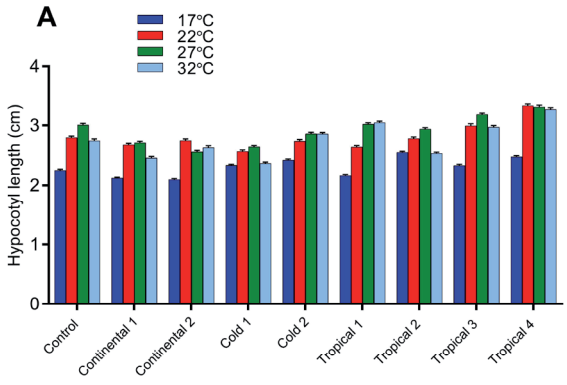

ANOVA results	P-value
variety	0
temperature	2,2E-297
var:temp	9,7E-118

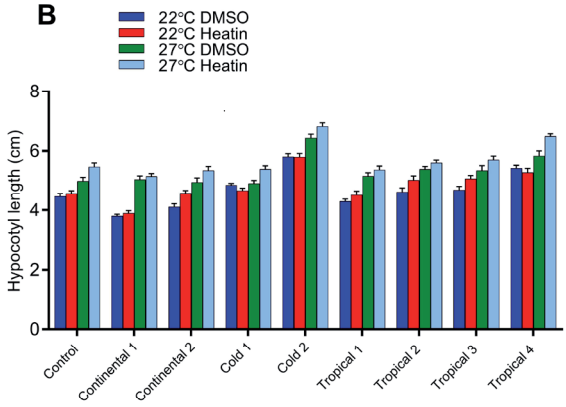

ANOVA results	P-value
variety	1,2E-134
compound	1,04E-11
temperature	1,24E-85
var:comp	0,525283
var:temp	2,81E-05
comp:temp	0,005879
var:comp:temp	0,020428

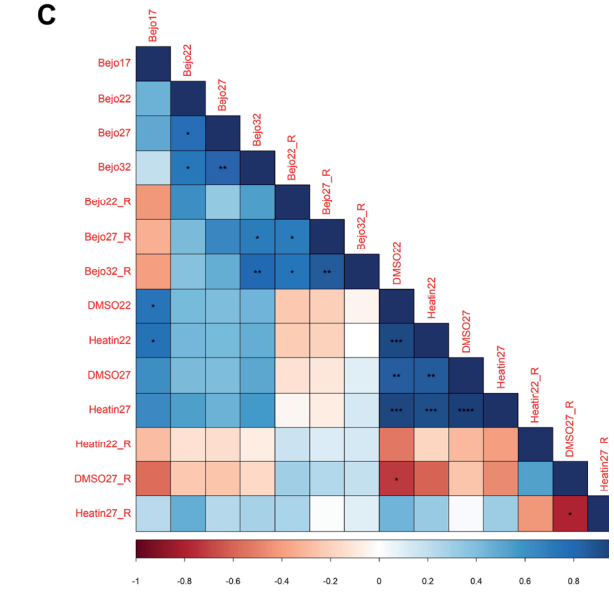

Figure 6.7: Different white cabbage varieties responses to differences in growth temperature.

(**A**) Hypocotyl lengths of white cabbage varieties which are bred for various geographical regions were grown under 17°C (blue bars), 22°C (red bars), 27°C (green bars) and 32°C (light blue bars) conditions. Values are averages of ~250 individual seedlings. (**B**) The same white cabbage varieties grown *in vitro* under 22°C (blue and red bars) and 27°C (green and light blue bars) conditions on medium containing a DMSO solvent mock (blue and green bars) or 25μM Heatin (red and light blue bars). Averages were tested by ANOVA and Tukey's HSD post hoc tests. Different letters indicate significant differences. Error bars indicate standard error of the mean. (**C**) Pearson correlation coefficient calculated between the hypocotyl lengths as shown in (**A**) and (**B**), and the relative effects of Temperature and Heatin. Colors represent correlation coefficient from -1 (dark red) over 0 (white) to 1 (dark blue). Asterisks indicate significance as $p<0.01$ (*), $p<0.001$ (**), $p<0.0001$ (***) and $p<0.00001$ (****). Graph was made using the R package "corrplot"

strong correlation between the absolute hypocotyl lengths of the two independent experiments. Nevertheless, a significant correlation was found between the soil experiment at 17°C and the plate experiments at 22°C independent of the presence of Heatin (**Fig. 6.7C**). This suggests that growth temperature effects on soil and *in vitro* affect the different genotypes differently and should therefore not be directly compared. A surprising significant correlation within the *in vitro* experiment was that responsiveness to temperature (DMSO27_R) negatively correlates to the Heatin responsiveness under high temperature (Heatin27_R). This suggests that Heatin had its biggest effects in varieties that show the smallest thermomorphogenic response.

Discussion

Heatin is a small molecule that phenocopies thermomorphogenesis in Arabidopsis (**Chapter 2, 3**). In this work, we determined natural variation in Heatin responses in Arabidopsis (**Fig. 6.2**), as well as its activity across species (**Fig. 6.4, 6.5, 6.7B**). We identified genes potentially involved in the Heatin response by GWAS (**Fig. 6.3, Table 6.1**), and assessed Heatin's potential for application in crops.

The GWAS revealed a locus on chromosome 1 that significantly associated with the response to Heatin and the SNP with the highest association to Heatin response was located in *ULP1D/OST1* (**Fig. 6.3**) *ULP1D/OST1* is the most likely candidate gene for being responsible for the association of this locus, however due to linkage disequilibrium the causative gene can actually be a considerable distance from the highest associated SNP[247,254]. To validate *ULP1D/OST1* as the responsible gene for the association, Heatin sensitivity will have to be tested in lines with altered in *ULP1D/OST1* expression or function. *ULP1D/OST1* affects PhytochromeB (PhyB) activity via deSUMOylation. PhyB functions both as a thermosensor in thermomorphogenesis[42,43] and as a red/far-red sensor in the shade avoidance response[43,129].

Another gene found in the genomic region of interest was *TPS10*. This gene is part of a family of genes encoding for Trehalose-6-Phosphate (T6P) producing proteins. T6P is an important signalling molecule in sugar signalling, a process with direct links to hypocotyl elongation[195,259]. Additionally, we previously identified HEXOKINASE1 and 2 in a pulldown experiment using a Heatin probe (**Chapter 5**). Together this supports the idea that sugar signalling could be involved in Heatin signalling.

It should be noted that an additional SNP significantly associated to Heatin response was identified more than 30kb downstream of the highest SNP mentioned above (**Fig. 6.3D**). Additionally, the highest associating SNPs for Picloram and high temperature treatment were found over 30kb upstream (**Fig. 6.3D**). Together, this argues for the assessment of the involvement of all genes in this genomic region (**Table 6.1**). Independent functions in Heatin, Picloram or high temperature signalling have to be considered for each gene separately.

None of the previously identified genomic loci was previously associated with thermomorphogenesis [248,260–263]. This can have several reasons. First, thermomorphogenesis phenotypes are strongly dependent on the light conditions[47,264]. Thus, small variations in light quantity, quality and daylengths between labs can impose relatively large differences in otherwise similar experimental setups between labs. Indeed, differences in light intensity and diurnal regime exist between growth conditions used in our lab and growth conditions as reported by several studies[248,261,262]. Differences in light quality are more difficult to compare between labs as these are rarely reported but, importantly, it has been shown that blue light can suppress thermomorphogenesis[265]. Second, the genetic structure of the used natural variation source (accessions, recombinant inbred lines) can be different and can cause different observations. Previous studies have worked with different RIL populations[248,262] or other sets of natural variants[263].

Large natural variation was found in the response to Heatin of the tested 321 accession, ranging from increases to decreases in hypocotyl length compared to the DMSO control (**Fig. 6.2**). A direct comparison between a strongly positive and strongly negative responding accession could provide mechanistic insight in Heatin signalling. A RIL population could, for example, allow for isolation of loci that contribute to the negative response. Strikingly, in the temperature response is more uniformly positive, as we identified only 2 accessions with a negative hypocotyl length response under high ambient temperature conditions. This is in line with previous studies that found a universal increase in hypocotyl length in response to high temperature[124,248]. The phenotypic window of natural variation in response to Picloram was comparable to Heatin, with 20 accessions having a negative difference between the treated and untreated hypocotyls, of which 8 also showed a negative response to Heatin and 2 responded negative to all treatments (**Fig. 6.2**). Together, this suggests that the genetic machinery underlying thermomorphogenesis is more conserved than the factors involved in response to Heatin or auxin. Furthermore,

distantly related species were shown to also display thermomorphogenesis[41] (**Fig. 6.4, 6.5**). Indeed, the first use of the term thermomorphogenesis was in a study using *Lilium longiflorum*, a monocot species, suggesting that the response is ancient[266].

As we have shown in previous chapters, a chemical compound such as Heatin can be used as a handle to identify novel genes and proteins that are required for a biological response under study; in our case hypocotyl elongation/thermomorphogenesis. One other advantage of chemical genetics is that the identified compounds can be applied directly to other species, next to being a tool for fundamental research[246]. Here we have shown that the Heatin effects on hypocotyl elongation is restricted to a subset of *Brassicaceae*-clade species (**Fig. 6.4, 6.5, 6.7B**). Heatin has a significant interaction with temperature (**Fig. 6.4, 6.7B**), which would potentially allow for the priming of these crops for high temperature by increasing thermomorphogenesis at the moment high temperature occurs in field conditions. Here, Heatin was applied exogenously to the plant by using a medium supplemented with this small molecule at a specific and controlled concentration. Large scale application in agriculture would have to be preceded by studies into the efficient and controlled application in a soil-based growth system as well as studies into the effects on the environment and its accumulation in the ecosystem.

Previously we identified the NIT1-subfamily of NITRILASE proteins (NIT1, 2 and 3) as direct targets of Heatin (**Chapter 5**). The *NIT1*-subfamily of genes are a *Brassicaceae* specific sub-family of the ubiquitous family of *NIT4*-like Nitrilases found in all plant species. Nitrilases of the *NIT1*-subfamily have been shown to function in secondary metabolite and auxin biosynthesis[61,62,232]. The findings presented here are in line with our previous identification of NITs as interactors with Heatin (**Chapter 5**), as only *Brassicaceae* clade plants are sensitive to Heatin (**Fig. 6.4, 6.5, 6.7B**). Although *Sorghum bicolor* and *Zea mays* do not contain NIT1-subfamily-like Nitrilases, they do have NIT4-like homologs that are enzymatically similar to the NIT1-subfamily[267,268]. Assessment of the Heatin sensitivity of these species could provide further insight into the role and function of Heatin.

We have shown here that hypocotyl length is a marker for the cultivation climate in white cabbage, without being purposely selected for. This indicates that sufficient genetic variation exist in the broccoli germplasm for breeding of thermotolerant white cabbage varieties if required[19]

Material and Methods

Plant material

Natural accessions used for the natural variation experiments and subsequent GWAS were previously described[250–253]. Accessions were grown on Primasta soil and seeds were harvested in parallel prior to the experiment in bulk to minimize environmental effects on *e.g.* seed

quality. The p*if4-2* mutant line used as control was previously described[53]. Crop seed batches were provided by Bejo Zaden BV and were samples of commercial batches of F1 hybrid seeds.

Growth conditions

Plants for hypocotyl length assays with Heatin were grown on sterile 0.8% plant agar (Duchefa P1001) 1x Murashige-Skoog medium (MS, including MES Buffer and vitamines, Duchefa M0255) without sucrose in petri-dishes. Seeds were surface sterilized by either a solution of 0.8% commercial bleach (Glorix) in ethanol for 10 minutes, followed by twice washing with ethanol for 10 minutes (GWAS), or by chlorine gas for 3 hours (Crop analyses). After sowing, seeds were stratified for 1 week (Arabidopsis) or 1 night (all crops) at 4°C in the dark to break dormancy. The petri-dishes containing the plants were subsequently grown vertically with slight tilt, under 100 µmol m^{-2} s^{-1} white light short day conditions (8 hours light/16 hours darkness) at 70% relative humidity in climate-controlled Microclima 1000 growth cabinets (Snijders) at either 22°C (control) or 27°C (high temperature).

For temperature range (17 - 32°C) responsive hypocotyl elongation assays with crops, two trays with coco mixture soil were sown with 80 (cucumber) or 150 (other crops) seeds per tray. The seedlings were grown under 300 µmol m^{-2} s^{-1} white light long day conditions (16 hours light/8 hours darkness). Seedlings were grown until cotyledons were completely opened and spread out.

Phenotyping

To measure hypocotyl lengths, petri-dishes with seedlings were pictured after 10 (bell pepper and chili pepper), 8 (all other crops/varieties) or 7 (GWAS) days using a flatbed scanner. Crop seedlings on soil were grown until the cotyledons were fully unfolded and spread out. Seedlings were cut on ground level and pictured using a flatbed scanner. Hypocotyl lengths were measured using ImageJ software (https://imagej.nih.gov/ij/).

Genome Wide Association Study

Arabidopsis seedlings of each accession were grown on medium with 0,1% dimethyl sulfoxide (DMSO, Sigma Aldrich) and a final concentration of 2,5µM Picloram or 8,5µM Heatin or 0,1% DMSO a solvent mock control in square petri dishes. Plates were divided into nine 4 cm x 4 cm squares. On each square one random accession was grown and hypocotyl lengths were assessed after 7 days as described above. In total 9 equal batches of plates were sown on different days, using Col-0 and*pif4-2* seedlings as controls in each batch (**Fig. S6.3**). Data was gathered and organized in spreadsheets and values over 2 times the standard deviation from the mean of each accession were removed.

The generated data was uploaded to the publicly available GWAP software (http://gwas.gmi.oeaw.ac.at[269]). The data was tested against the 250k SNP Dataset v3.06; TAIR9. This covered 97% (316/322) of the used accessions. Data was analysed without transforming

and as GWAS method, the Accelerated Mixed Model (AMM) was used. Default FDR thresholds were used.

Statistical analysis

Data was analyzed with R statistical software. Correlation analyses and graphing was done using the "corrplot" package using the default Pearson's method. The used script can be found in **supplemental file 6.3**. Statistical testing of averages of hypocotyls was done as described previously (**Supplemental file 3.1**).

Supplemental Figures

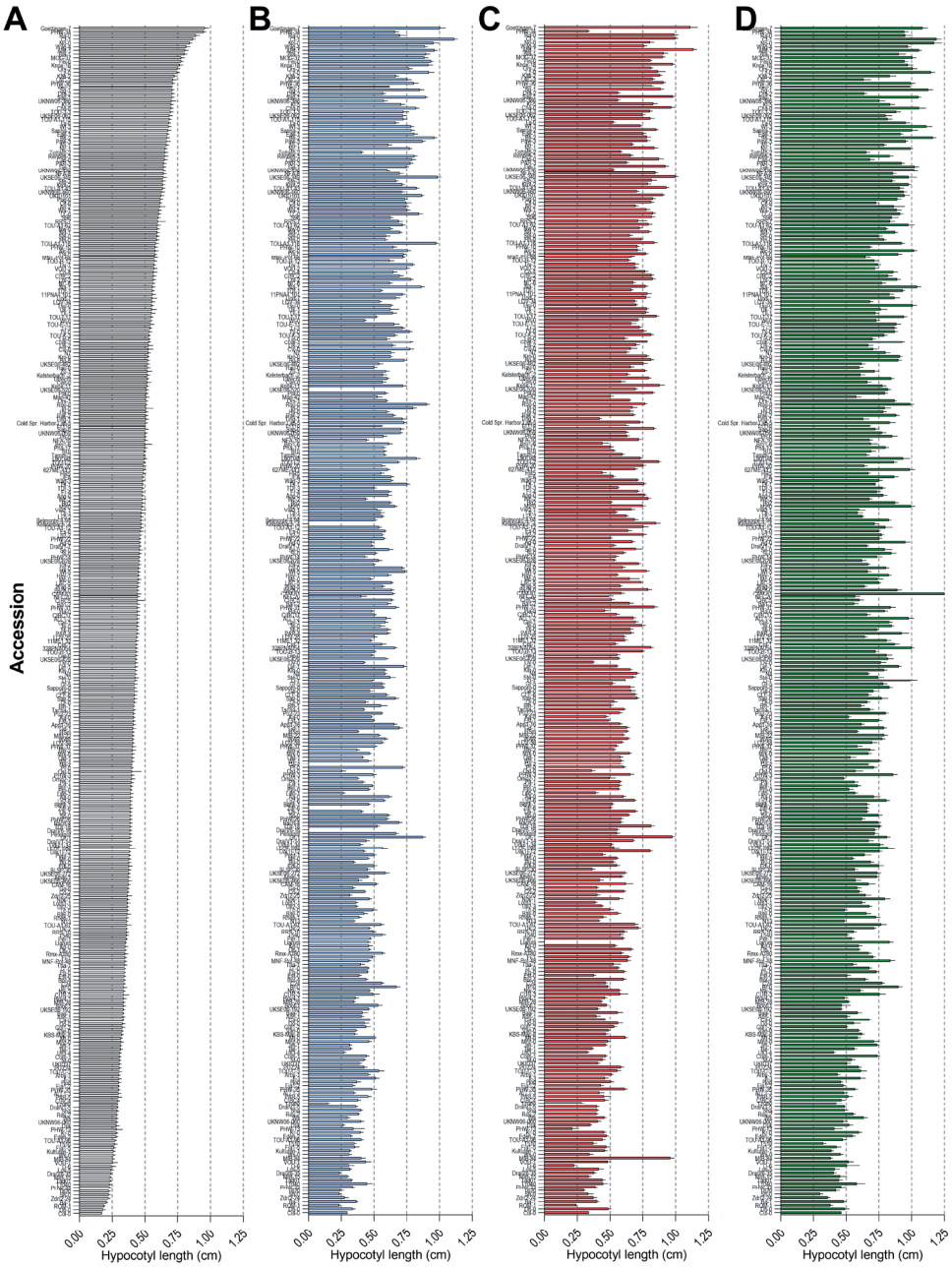

Supplemental Figure 6.1: Absolute hypocotyl lengths of treatments and control for 321 ecotypes.

Lengths in cm are shown for all tested ecotypes that grew to give a hypocotyl upon treatment with DMSO solvent mock (**A**) 8.5µM Heatin (**B**), 2.5µM Picloram (**C**) or 27°C (**D**). Ecotypes are sorted to length of the hypocotyl on DMSO mock medium. Error bars represent standard error of the mean.

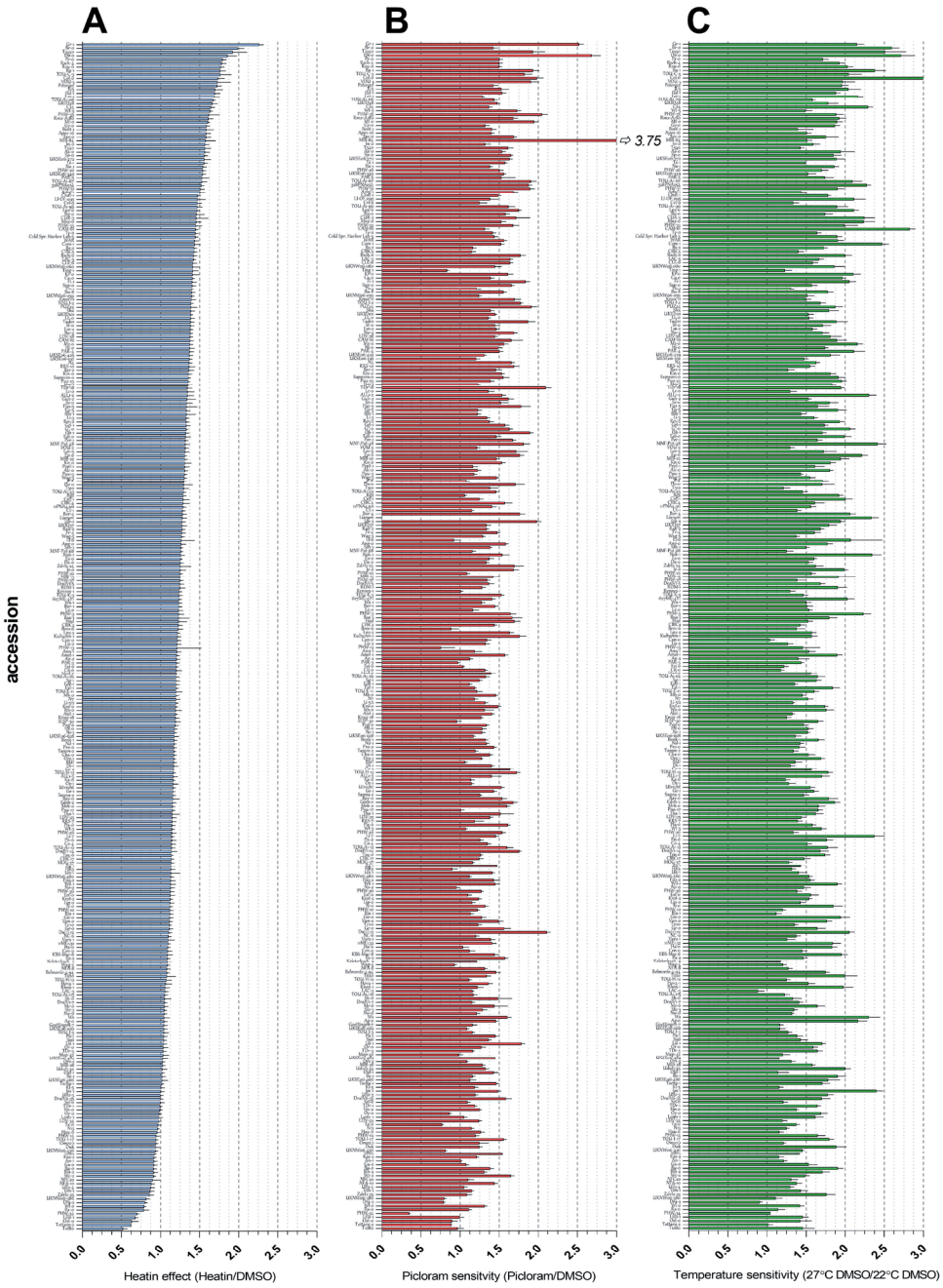

Supplemental Figure 6.2: Relative response of hypocotyl lengths to treatments for 321 ecotypes.

Relative responses are shown for all ecotypes that were used in the GWAS to treatment with 8.5µM Heatin (**A**), 2.5µM Picloram (**B**) or 27°C (**C**). Ecotypes are sorted to strength of the response to Heatin. Error bars represent standard error of the mean. Values exceeding the x-axis are indicated with an arrow and the actual value is shown.

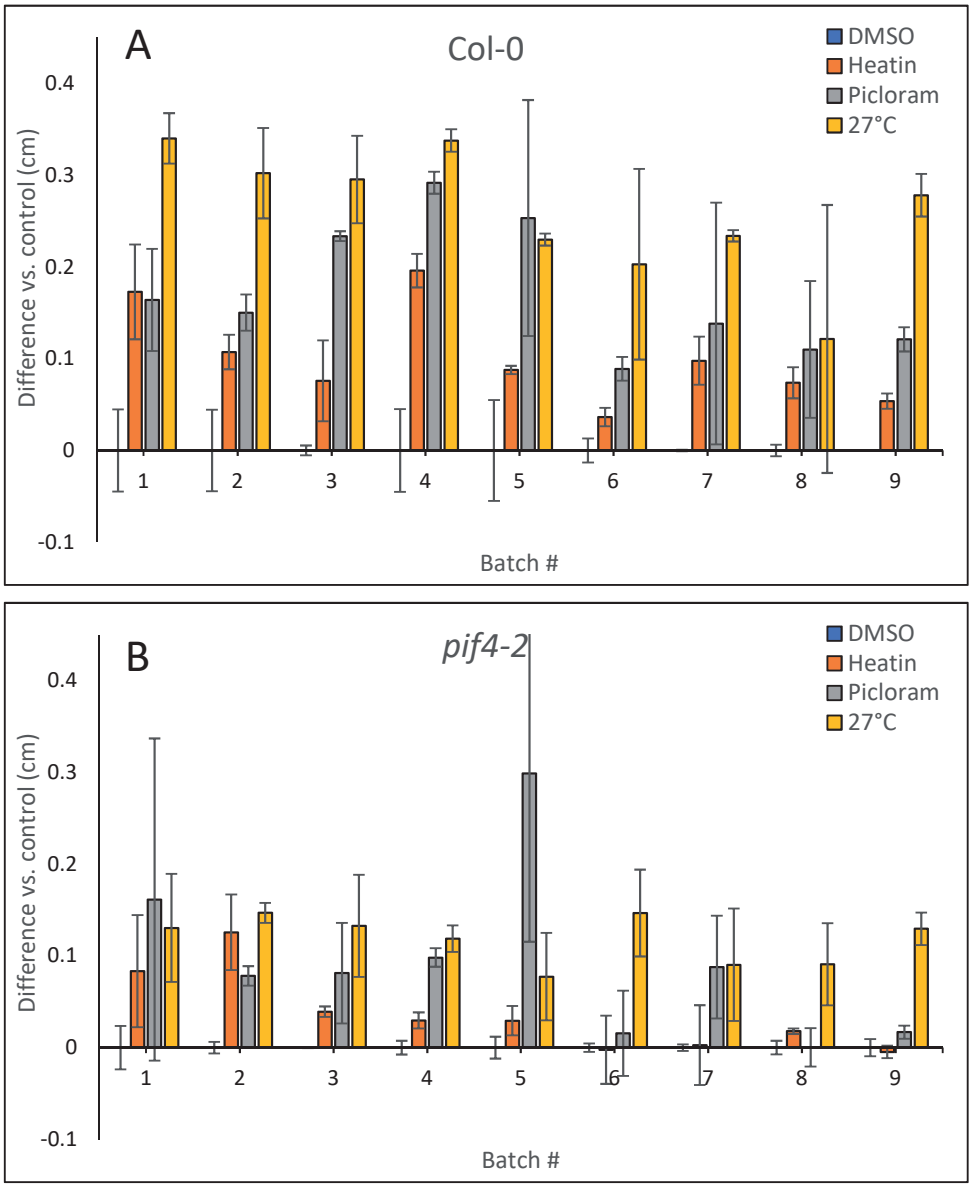

Supplemental Figure 6.3: Absolute differences in hypocotyl lengths between different treatments and the DMSO mock control for Col-0 and *pif4-2*.

Differences in cm are shown for the tested genotypes: Col-0 (**A**) and *pif4-2* (**B**) grown on DMSO mock (blue bars), Heatin (orange bars), Picloram (grey bars) or 27°C (yellow bars). Error bars represent standard deviation of 2 replicas of each ~20 seedlings. X-axis denotes in which time-separated batch the controls were grown.

Supplementary files

Supplemental files are available on request (lennardcasper@yahoo.com):

Supplemental file 6.1. List of Arabidopsis accessions used for the GWAS

Supplemental file 6.2. output of statistical analysis of different cabbage strains

Supplemental file 6.3. R script for correlation analysis and graph

CHAPTER 7

General Discussion

Lennard van der Woude[1] | Sjef Smeekens[1] | Martijn van Zanten[1]

[1] Molecular Plant Physiology, Institute of Environmental Biology, Utrecht University, the Netherlands

Heatin a as novel growth stimulator

Plants accurately monitor their environment and adjust their growth and development continuously to perform optimally under suboptimal conditions. One important external factors affecting plant growth, physiology, development and phenology is ambient temperature[41]. In Arabidopsis, the set of architectural growth adaptations induced in response to high temperature is collectively called thermomorphogenesis. Thermomorphogenesis consists among others of elongation of hypocotyls and petioles, as well as hyponasty. These phenotypes are controlled by a poorly understood temperature sensing and signaling network, relying at least in part on temperature perception by Phytochrome B (PhyB)[42,43]. Upon perception of high temperature, the suppression of PHYTOCHROME INTERACTING FACTOR 4 (PIF4) by PhyB is relieved. PIF4 subsequently stimulates the expression of auxin biosynthesis genes, which leads to accumulation of the bioactive auxin indole-3-acetic acid (IAA)[39,56]. Following the acid growth theory[77], cell elongation is subsequently stimulated, resulting in thermomorphogenesis (**Chapter 1**).

Temperature as a stimulus is easily applied to plants in an experimental setting. However, temperature is pervasive and affects almost every molecular process in the plant. Therefore, investigation into temperature sensing and signaling pathways are prone to a plethora of secondary (thermodynamic and homeostatic) effects, that are not necessarily the results of active temperature sensing and signaling. A further complication is the prevalence of genetic redundancy in plants[87]. To overcome these obstacles, we undertook a chemical genetic strategy to gain novel insights into the signaling networks underlying growth at high temperatures, and thermomorphogenesis in particular.

First, we performed a chemical genetic screen (**Chapter 2**). The screen was designed to identify compounds working downstream or parallel of PIF4, without being limited to discovering only auxin-like molecules. In short, we screened for chemical compounds that rescued impaired hypocotyl elongation of the *pif4-2* knock-out mutant under high ambient temperature conditions. In a following secondary selection, compounds were excluded that resembled picloram (a synthetic auxin) treatment. Doing so, we identified ten small molecules that restored thermomorphogenesis in the *pif4* mutant in a manner (partly) distinct from picloram addition. One of these compounds, Heatin is the subject of this thesis.

Heatin reliably and reproducibly mimics thermomorphogenesis in seedlings already under control temperature and stimulates thermomorphogenesis further under high ambient temperature conditions. Phenotypes of Heatin treatment are notably distinct from picloram treatment, as the latter also has profound effects on root growth, cotyledon curling and gravitropism, next to hypocotyl elongation[265,270] (**Fig. 3.1**). The remaining nine hit compounds identified in our screen displayed no obvious structural analogy to Heatin and do not contain Heatin's minimal active moiety. Therefore, these compounds can be useful additional tools to further investigate signaling pathways underlying thermomorphogenesis in follow-up studies. Such follow-up investigations

could be performed along the lines of research described in this thesis for Heatin. Thus, performing SAR studies and identification, confirmation and validation of the receptive proteins. To explore a possible overlap with Heatin's mode of action, a reverse genetic strategy could be undertaken, testing for example the *aao1 aao2* mutant or *nit* mutants for resistance to the nine compounds.

Mechanisms of Heatin-induced growth

One fundamental aspect that needed to be addressed to understand Heatin's mode of action was whether or not Heatin acts like a *bona fide* auxin; *i.e.* if Heatin activity relies on binding the TIR1/AFB receptor(s) causing the degradation of AUX/IAA proteins[271]. Although clearly distinct from picloram treatment effects on the organismal level, Heatin could still act as an auxin on the molecular level, as hypocotyl elongation in general and thermomorphogenesis specifically are auxin driven processes.

Whereas Heatin's effect on seedlings was restricted to the hypocotyl (**Fig. 3.1**) and no *DR5:LUC* induction was observed (**Fig. 3.5A**), other findings pointed towards Heatin acting as a *bona fide* auxin. We show for instance that both picloram and Heatin activity rely on functional auxin perception proteins, as *tir1/afb* mutants are resistant to Heatin and picloram (**Fig. 3.5B, C**). Strikingly however, whereas for picloram *AFB5* is the specific receptor[66,108], as the *afb5-5* mutant is insensitive to picloram but *afb5-5* mutant is still partially sensitive to Heatin. This again points to distinctive effects of Picloram and Heatin. However, we also demonstrate that a combination of picloram and Heatin can satiate the same auxin signaling system, as Picloram reaches supra-optimal concentrations at lower concentrations in the presence of Heatin (**Fig. 3.5E**). Moreover, the transcriptomic response of Heatin has a clear auxin fingerprint, as several well-known auxin responsive genes including *AUX/IAA*, *GH3* and *SAUR*s were upregulated in response to Heatin. Additionally, GO-term enrichment analysis also points towards similarities between the Heatin transcriptome and that in response to auxin (**Chapter 4**). Testing of mutants in the up-regulated *AUX/IAA* and *GH3* genes (*e.g. iaa5-1*[272] and higher order *gh3* family mutants[273]), however, did not uncover an essential role for the *GH3* family members, nor *IAA5*, in mediating Heatin responses (data not shown). As the upregulation of *GH3* and *AUX/IAA* genes is ascribed a function in feedback signaling[75], rather than having a mechanistic causal function, the absence of a phenotype in these mutants was not surprising. For SAUR genes no well characterized knock-out mutants are available, as these genes form a large family and are highly redundant[75]. Based on the recently discovered function of the *SAUR* gene family[76], the upregulated *SAUR* genes may nevertheless directly contribute to the Heatin-stimulated hypocotyl elongation phenotype. Further analyses using for example stabilized fusion protein overexpressors[274] of the upregulated SAUR gene family members might provide detailed knowledge on this proposed link.

Taken together, it is possible that Heatin acts as an auxin agonist that only affects the hypocotyl, or alternatively, Heatin acts by increasing auxin signaling via a mode

of action upstream of auxin perception. The latter could for example be achieved by stimulating IAA biosynthesis *in situ*. Last, these possible modes of action are not mutually exclusive, and could act in parallel.

Additional support for the hypothesis that Heatin acts as a *bona fide* auxin, is the close association between Heatin and another small bioactive molecule, Sirtinol (**Chapter 3**). Sirtinol was identified previously in a chemical genetics screen for compounds that induced the synthetic auxin promoter *DR5*. Sirtinol exerts suppression of hypocotyl elongation in the dark, a typical auxin-induced phenotype[93,105]. The strong similarity to Heatin was initially discovered when performing a structure-activity relationship analysis on the Heatin molecule. This revealed that the minimal active moieties of Heatin and Sirtinol are similar (**Fig. 3.3 and Table 3.1**). The association was further tested and confirmed by applying Heatin to Sirtinol resistant mutants and by the generation of dose response assays using the minimal active compound of Sirtinol, 2-Hydroxy-1-naphthaldehyde (HNA) in comparison with Heatin. This analysis indicated that Sirtinol-resistant mutants were also resistant to Heatin application, and moreover, that HNA was able to induce hypocotyl elongation, strictly at low concentrations (**Fig. 3.3**).

It is proposed that Sirtinol's mode of action relies on an unknown mechanism of hydrolyzation of Sirtinol's hydrazine bond, releasing HNA. Aldehyde Oxidase proteins then metabolize HNA into 2-Hydroxy-1-naphthoic acid (HNC). HNC is subsequently active as an auxin, binding the TIR1/AFB receptors and activating auxin signaling[93,105]. However, work by Kepinski and Leyser (2004), who tested the ability of Sirtinol to promote the interaction between the auxin binding domain II of AUX/IAA protein and TIR1, demonstrated that in contrast to the established synthetic auxin NAA, Sirtinol could not enhance the interacting, neither *in vitro*, nor *in vivo*[275]. This argues against Sirtinol acting as a *bona fide* auxin, and following that, argues against Heatin acting as auxin as well. We however clearly demonstrate that the Aldehyde Oxidases (AAO1 and AAO2) are required for Heatin activity (**Fig. 3.4**), possibly linking Heatin to Sirtinol signaling.

Arguing strongly in favor of Heatin acting upstream of auxin perception, is the observation that Heatin directly interacts with Nitrilase proteins (**Chapter 5**). Using a Heatin analogue modified with an alkyne mini-tag, we synthesized probe-covered magnetic beads, we pulled-down proteins interacting with this probe from a protein extract and subsequently, by eluting with the original Heatin molecule, Heatin interacting proteins were eluted and identified by mass spectrometry. This recovered the complete NIT1-subfamily of Nitrilases as targets of Heatin. Follow-up analysis showed that Heatin reduces NIT activity *in vitro* (**Fig. 5.5**). The functional relevance of the Heatin-NIT interaction was validated by analysis of the Heatin response in a selection of *nit* mutants. Indeed, *nit1* and *nit2* mutants responded less to Heatin concerning hypocotyl elongation (**Fig. 5.4**). Taken together, this suggests that Heatin, at least in part, cannot be considered a *bona fide* auxin.

Nitrilases of the NIT1 subfamily function in auxin biosynthesis[61,63] in a *Brassicaceae*-specific pathway parallel to the main auxin biosynthesis route[276]. In the

NIT-dependent pathway, L-tryptophan is metabolized into indole-3-acetaldoxime (IAOx) by the cytochrome P450 family member CYP79B2[60]. IAOx is subsequently converted into indole-3-acetonitrile (IAN) by CYP71A1 and then hydrolyzed by Nitrilases into bioactive IAA[61]. Strikingly, CYP79B2 is upregulated under high temperature conditions in a PIF4-dependent manner[56]. As we found a strong dependency on auxin signaling for the effects of Heatin, we tested whether Heatin affects auxin biosynthesis in a NIT1 subfamily dependent manner (**Fig. 5.6**). Indeed, we found higher IAA levels in Heatin-treated seedlings compared to the control treatment. Strikingly, in *nit* and *aao1 aao2* double mutants this increase was absent. Moreover, consistent with an inhibition of NIT1 subfamily function, Heatin causes a strong accumulation of IAN. Of note, in 2 day-old wild type seedlings, no clear effects on IAA were observed in the presence of Heatin (**Chapter 3**), while at that time point the effects of Heatin on hypocotyl elongation became visible (**Fig. 4.1**). Therefore, possibly the very early effects of Heatin on elongation growth do not require *de novo* auxin biosynthesis. Future work could focus on testing Heatin analogues, as well as Sirtinol, HNA and HNC in *in vitro* assays for modulating NIT enzyme activity as well. Furthermore, the effect of Heatin on *in vivo* Nitrilase activity should be assessed to confirm that the effects observed *in vitro* are translatable to the organism level.

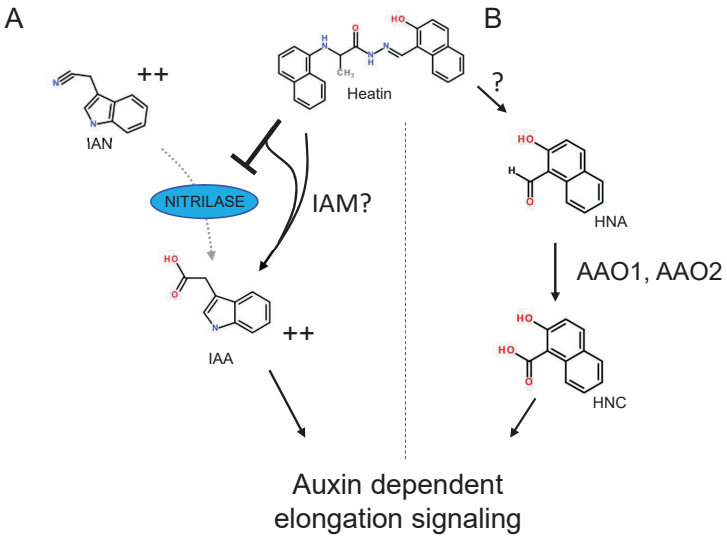

Figure 7.1: Models for Heatin's mode of action.

Two non-mutually exclusive models are proposed based on the data obtained in this thesis. (A) Heatin directly interacts with NIT proteins and inhibits their function, causing accumulation of IAN. Via an unknown pathway, this inhibition leads to IAA accumulation and subsequent downstream auxin signaling and elongation growth. (B) Heatin is hydrolyzed into HNA by an unknown mechanism and subsequently metabolized into HNC by AAO1 and AAO2. HNC then acts as auxin and activates downstream auxin signaling leading to elongation growth.

In conclusion, we propose a model where Heatin inhibits the function of the NIT1 subfamily. This leads to accumulation of IAN and potentially also accumulation of other IAA precursor molecules, eventually stimulation IAA production via an alternative route. Indeed, we found increased levels of indole-3-acetamide (IAM) in Heatin treated seedlings, that were absent in the *nit* and *aao* mutants (**Fig. 5.6**). The increase in IAA subsequently activates auxin signaling, leading to hypocotyl elongation (**Fig. 7.1A**). Additionally, Heatin can be metabolized via AAO enzymes into HNC, and thereby stimulate auxin signaling directly (**Fig. 7.1B**). This dual function could explain why *nit* mutants are still partially responsive to Heatin. Although *AAO* genes have been suggested[225], but also been questioned[226,227], to play a role in IAA biosynthesis, it is unlikely that a metabolic link between AAOs and NITs exists with a potential role in Heatin signaling. This is mainly due to the fact that the products of both families of enzymes in auxin biosynthesis are the same, *i.e.* bioactive IAA.

Future directions

We applied chemical genetics to unravel molecular signaling pathways mediating thermomorphogenesis. We conclude that Heatin functions as a specific agonist of thermomorphogenesis. Further investigations into Heatin's effects are necessary for a complete understanding of the mode of action. For example, using the Heatin SAR data, fluorescent analogues could be synthesized to visualize its localization on organ, cell and sub-cellular level. Overlap with possible activation of highly sensitive auxin signaling markers such as the R2D2 line[277] could confirm the activation of auxin signaling by Heatin. Moreover, probing possible derivatization of Heatin *in vivo* could further deepen knowledge on Heatin's mode of action.

Brassinosteroid (BR) signaling has been shown to act as a feedback mechanism controlling *PIF4* dependent stimulation thermomorphogenesis[74]. BR signaling acts both upstream of PIF4 and is simultaneously induced by auxin signaling. Moreover, BR promotes the expression of *SAUR* genes. It would be insightful to test for interactions between Heatin and BR signaling. This could be easily achieved by supplementing the growth medium with both Heatin and BR, or known disruptors of biosynthesis or signaling of BR such as brassinopride[95] or by testing available mutants in BR signaling. This could provide additional insight into where Heatin acts in the thermomorphogenesis signaling network.

Considering thermomorphogenesis signaling, we can ascribe a novel function to *NIT1* and *NIT2* in high temperature-induced hypocotyl elongation, as mutants for these genes are less responsive to increased temperature signals (**Fig. 5.4**). Additionally, our RNA-seq and proteomics analysis (**Chapter 4**) revealed dynamic regulation of the different NIT1-subfamily members. *NIT1* and *NIT3* exhibited reduced expression under high temperature conditions, whereas the expression of *NIT2* was increased. Because Heatin mimics thermomorphogenesis and inhibits Nitrilase function, we propose that high temperature also may lead to inhibition of NIT function. Previously it was shown for

NIT2 that the thermal optimum for enzymatic IAN substrate conversion is at the relatively low temperature of 12-15°C, decreasing rapidly at higher temperatures. This response is consistent with inhibition under high temperature conditions[232]. The atypical temperature sensitivity profile of NIT2 is striking, as it is not observed for NIT1 or NIT3, nor for other NIT2 substrates, and may play a specific role in thermomorphogenesis signaling. The reduction in enzymatic activity at high temperature seems to contrast with the stimulation of the expression under high temperature of the enzyme CYP79B2, operating upstream in the NIT dependent IAA biosynthesis pathway[56]. This involvement should be studied in more detail to reveal the exact function of the NIT1 subfamily in thermomorphogenesis. Additionally, as Nitrilases also have a function in defense against pathogens and herbivory[62,63,232], it would be insightful to test Heatin effects on plant defense. This consideration is strengthened by the notions that temperature-dependent modulation of defense occurs in a PIF4 dependent manner and that Heatin acts downstream of PIF4 effects.

Specificity and applicability of Heatin

In line with the observation that Heatin targets the *Brassicaceae* specific NIT1-subfamily[231], Heatin activity seems restricted to the *Brassicaceae* cabbage family (**Chapter 6**). Heatin could potentially be applied to modulate thermomorphogenesis/elongation growth traits in cabbages, protecting them from detrimental effects of high temperature by increasing their cooling capacity or stimulating the growth of young seedlings immediately after germination, thereby promoting seedling establishment. The effects observed in *Brassicaceae* crop species were however markedly smaller than in Arabidopsis. Prior to application of Heatin in *Brassicaceae* crops, the applied concentrations, compound delivery and perhaps the compound itself will have to be optimized. This can be achieved through testing of analogues, but also by targeted breeding for Heatin sensitivity. Extensive natural variation for Heatin sensitivity in Arabidopsis suggests such targeted breeding efforts to be successful (**Fig. 6.1**). Importantly, the molecular components of thermomorphogenesis identified in this study could enable breeding of thermotolerant crops with optimal performance by mediating elongation growth under suboptimal conditions.

References

1. IPCC. Climate Change 2014: Synthesis Report. Contribution of Working Groups I, II and III to the Fifth Assessment Report of the Intergovernmental Panel on Climate Change. (IPCC, 2014).
2. Wolff, E. et al. Climate updates: progress since the fifth Assessment Report (AR5) of the Intergovernmental Panel on Climate Change (IPCC). (The Royal Society, 2017).
3. Forster, P. M. Inference of Climate Sensitivity from Analysis of Earth's Energy Budget. Annu. Rev. Earth Planet. Sci. **44,** 85–106 (2016).
4. Proistosescu, C. & Huybers, P. J. Slow climate mode reconciles historical and model-based estimates of climate sensitivity. Sci. Adv. **3,** e1602821 (2017).
5. Fitter, A. H. & Fitter, R. S. R. Rapid changes in flowering time in British plants. Science **296,** 1689–1691 (2002).
6. Cook, B. I., Wolkovich, E. M. & Parmesan, C. Divergent responses to spring and winter warming drive community level flowering trends. Proc. Natl. Acad. Sci. U. S. A. **109,** 9000–9005 (2012).
7. Bertrand, R. et al. Changes in plant community composition lag behind climate warming in lowland forests. Nature **479,** 517–520 (2011).
8. Lamprecht, A., Semenchuk, P. R., Steinbauer, K., Winkler, M. & Pauli, H. Climate change leads to accelerated transformation of high-elevation vegetation in the central Alps. New Phytol. (2018). doi:10.1111/nph.15290
9. Craufurd, P. Q. & Wheeler, T. R. Climate change and the flowering time of annual crops. J. Exp. Bot. **60,** 2529–2539 (2009).
10. Asseng, S. et al. Rising temperatures reduce global wheat production. Nat. Clim. Change **5,** 143–147 (2015).
11. Chmielewski, F.-M., Müller, A. & Bruns, E. Climate changes and trends in phenology of fruit trees and field crops in Germany, 1961–2000. Agric. For. Meteorol. **121,** 69–78 (2004).
12. Tao, F., Yokozawa, M., Xu, Y., Hayashi, Y. & Zhang, Z. Climate changes and trends in phenology and yields of field crops in China, 1981–2000. Agric. For. Meteorol. **138,** 82–92 (2006).
13. Zhao, C. et al. Temperature increase reduces global yields of major crops in four independent estimates. Proc. Natl. Acad. Sci. **114,** 9326–9331 (2017).
14. Lobell, D. B. & Gourdji, S. M. The Influence of Climate Change on Global Crop Productivity. **160,** (2012).
15. Springmann, M. et al. Global and regional health effects of future food production under climate change: a modelling study. The Lancet **387,** 1937–1946 (2016).
16. Pilbeam, D. J. Breeding crops for improved mineral nutrition under climate change conditions. J. Exp. Bot. **66,** 3511–3521 (2015).
17. Smith, M. R., Golden, C. D. & Myers, S. S. Potential rise in iron deficiency due to future anthropogenic carbon dioxide emissions. GeoHealth **1,** 248–257
18. Myers, S. S., Wessells, K. R., Kloog, I., Zanobetti, A. & Schwartz, J. Effect of increased concentrations of atmospheric carbon dioxide on the global threat of zinc deficiency: a modelling study. Lancet Glob. Health **3,** e639–e645 (2015).

19. Atlin, G. N., Cairns, J. E. & Das, B. Rapid breeding and varietal replacement are critical to adaptation of cropping systems in the developing world to climate change. Glob. Food Secur. **12,** 31–37 (2017).
20. Challinor, A. J., Koehler, A.-K., Ramirez-Villegas, J., Whitfield, S. & Das, B. Current warming will reduce yields unless maize breeding and seed systems adapt immediately. Nat. Clim. Change **6,** 954–958 (2016).
21. Dwivedi, S. L. et al. Landrace Germplasm for Improving Yield and Abiotic Stress Adaptation. Trends Plant Sci. **21,** 31–42 (2016).
22. Barabaschi, D. et al. Next generation breeding. Plant Sci. **242,** 3–13 (2016).
23. Batley, J. & Edwards, D. The application of genomics and bioinformatics to accelerate crop improvement in a changing climate. Curr. Opin. Plant Biol. **30,** 78–81 (2016).
24. Parent, B. & Tardieu, F. Temperature responses of developmental processes have not been affected by breeding in different ecological areas for 17 crop species. New Phytol. **194,** 760–774 (2012).
25. Brutnell, T. P. Model grasses hold key to crop improvement. Nat. Plants (2015). doi:10.1038/nplants.2015.62
26. Argyris, J. et al. Quantitative trait loci associated with seed and seedling traits in Lactuca. Theor. Appl. Genet. **111,** 1365–1376 (2005).
27. Pimentel, I. & Contreras, S. Red and Far-red Light Treatments to Modify Thermoinhibition, Photoblasticity, and Longevity in Lettuce Seeds. HortTechnology **24,** 463–470 (2014).
28. Shimizu, H. et al. Decentralized circadian clocks process thermal and photoperiodic cues in specific tissues. Nat. Plants **1,** nplants2015163 (2015).
29. Penfield Steven. Temperature perception and signal transduction in plants. New Phytol. **179,** 615–628 (2008).
30. Yamori, W., Hikosaka, K. & Way, D. A. Temperature response of photosynthesis in C3, C4, and CAM plants: temperature acclimation and temperature adaptation. Photosynth. Res. **119,** 101–117 (2014).
31. Falcone, D. L., Ogas, J. P. & Somerville, C. R. Regulation of membrane fatty acid composition by temperature in mutants of Arabidopsis with alterations in membrane lipid composition. BMC Plant Biol. **4,** 17 (2004).
32. Gangappa, S. N., Berriri, S. & Kumar, S. V. PIF4 Coordinates Thermosensory Growth and Immunity in Arabidopsis. Curr. Biol. **27,** 243–249 (2017).
33. Cheng, C. et al. Plant immune response to pathogens differs with changing temperatures. Nat. Commun. **4,** 2530 (2013).
34. Gould, P. D. et al. The molecular basis of temperature compensation in the Arabidopsis circadian clock. Plant Cell **18,** 1177–1187 (2006).
35. Mizuno, T. et al. Ambient Temperature Signal Feeds into the Circadian Clock Transcriptional Circuitry Through the EC Night-Time Repressor in Arabidopsis thaliana. Plant Cell Physiol. **55,** 958–976 (2014).

36. Gray, W. M., Östin, A., Sandberg, G., Romano, C. P. & Estelle, M. .High temperature promotes auxin-mediated hypocotyl elongation in Arabidopsis. Proc. Natl. Acad. Sci. U. S. A. **95,** 7197–7202 (1998).
37. Koini, M. A. et al. High temperature-mediated adaptations in plant architecture require the bHLH transcription factor PIF4. Curr. Biol. CB **19,** 408–413 (2009).
38. Zanten, M. van, Voesenek, L. A. C. J., Peeters, A. J. M. & Millenaar, F. F. Hormone- and Light-Mediated Regulation of Heat-Induced Differential Petiole Growth in Arabidopsis. Plant Physiol. **151,** 1446–1458 (2009).
39. Sun, J., Qi, L., Li, Y., Chu, J. & Li, C. .PIF4–Mediated Activation of YUCCA8 Expression Integrates Temperature into the Auxin Pathway in Regulating Arabidopsis Hypocotyl Growth. PLOS Genet. **8,** e1002594 (2012).
40. Wang, R. et al. .HSP90 regulates temperature-dependent seedling growth in Arabidopsis by stabilizing the auxin co-receptor F-box protein TIR1. Nat. Commun. **7,** 10269 (2016).
41. Quint, M. et al. Molecular and genetic control of plant thermomorphogenesis. Nat. Plants **2,** 15190 (2016).
42. Jung, J.-H. et al. Phytochromes function as thermosensors in Arabidopsis. Science **354,** 886–889 (2016).
43. Legris, M. et al. Phytochrome B integrates light and temperature signals in Arabidopsis. Science **354,** 897–900 (2016).
44. Crawford, A. J., McLachlan, D. H., Hetherington, A. M. & Franklin, K. A. High temperature exposure increases plant cooling capacity. Curr. Biol. CB **22,** R396-397 (2012).
45. Bridge, L. J., Franklin, K. A. & Homer, M. E. Impact of plant shoot architecture on leaf cooling: a coupled heat and mass transfer model. J. R. Soc. Interface **10,** 20130326 (2013).
46. Vile, D. et al. Arabidopsis growth under prolonged high temperature and water deficit: independent or interactive effects? Plant Cell Environ. **35,** 702–718
47. Legris, M., Nieto, C., Sellaro, R., Prat, S. & Casal, J. J. Perception and signalling of light and temperature cues in plants. Plant J. **90,** 683–697 (2017).
48. Rockwell, N. C., Su, Y.-S. & Lagarias, J. C. PHYTOCHOME STRUCTURE AND SIGNALING MECHANISMS. Annu. Rev. Plant Biol. **57,** 837–858 (2006).
49. Jung, J.-H. et al. Phytochromes function as thermosensors in Arabidopsis. Science **354,** 886–889 (2016).
50. Ni, W. et al. A Mutually Assured Destruction Mechanism Attenuates Light Signaling in Arabidopsis. Science **344,** 1160–1164 (2014).
51. Delker, C., Zanten, M. van & Quint, M. Thermosensing Enlightened. Trends Plant Sci. **22,** 185–187 (2017).
52. Oh, E., Zhu, J.-Y. & Wang, Z.-Y. Interaction between BZR1 and PIF4 integrates brassinosteroid and environmental responses. Nat. Cell Biol. **14,** 802–809 (2012).
53. Leivar, P. et al. The Arabidopsis Phytochrome-Interacting Factor PIF7, Together with PIF3 and PIF4, Regulates Responses to Prolonged Red Light by Modulating phyB Levels. Plant Cell **20,** 337–352 (2008).

54. Sakuraba, Y. et al. Phytochrome-interacting transcription factors PIF4 and PIF5 induce leaf senescence in Arabidopsis. Nat. Commun. **5,** 4636 (2014).
55. Leivar, P. & Monte, E. PIFs: Systems Integrators in Plant Development. Plant Cell tpc.113.120857 (2014). doi:10.1105/tpc.113.120857
56. Franklin, K. A. et al. .PHYTOCHROME-INTERACTING FACTOR 4 (PIF4) regulates auxin biosynthesis at high temperature. Proc. Natl. Acad. Sci. U. S. A. **108,** 20231–20235 (2011).
57. Mano, Y. & Nemoto, K. The pathway of auxin biosynthesis in plants. J. Exp. Bot. **63,** 2853–2872 (2012).
58. Franklin, K. A. et al. PHYTOCHROME-INTERACTING FACTOR 4 (PIF4) regulates auxin biosynthesis at high temperature. Proc. Natl. Acad. Sci. U. S. A. **108,** 20231–20235 (2011).
59. Won, C. et al. Conversion of tryptophan to indole-3-acetic acid by TRYPTOPHAN AMINOTRANSFERASES OF ARABIDOPSIS and YUCCAs in Arabidopsis. Proc. Natl. Acad. Sci. U. S. A. **108,** 18518–18523 (2011).
60. Zhao, Y. et al. Trp-dependent auxin biosynthesis in Arabidopsis: involvement of cytochrome P450s CYP79B2 and CYP79B3. Genes Dev. **16,** 3100–3112 (2002).
61. Lehmann, T. et al. Arabidopsis NITRILASE 1 Contributes to the Regulation of Root Growth and Development through Modulation of Auxin Biosynthesis in Seedlings. Front. Plant Sci. **8,** (2017).
62. Piotrowski, M. Primary or secondary? Versatile nitrilases in plant metabolism. Phytochemistry **69,** 2655–2667 (2008).
63. Vik, D., Mitarai, N., Wulff, N., Halkier, B. A. & Burow, M. Dynamic Modeling of Indole Glucosinolate Hydrolysis and Its Impact on Auxin Signaling. Front. Plant Sci. **9,** (2018).
64. Pollmann, S., Düchting, P. & Weiler, E. W. Tryptophan-dependent indole-3-acetic acid biosynthesis by IAA-synthase proceeds via indole-3-acetamide. Phytochemistry **70,** 523–531 (2009).
65. Dharmasiri, N., Dharmasiri, S. & Estelle, M. The F-box protein TIR1 is an auxin receptor. Nature **435,** 441 (2005).
66. Calderón Villalobos, L. I. A. et al. .A combinatorial TIR1/AFB-Aux/IAA co-receptor system for differential sensing of auxin. Nat. Chem. Biol. **8,** 477–485 (2012).
67. Gray, W. M., Kepinski, S., Rouse, D., Leyser, O. & Estelle, M. Auxin regulates SCF^{TIR1}-dependent degradation of AUX/IAA proteins. Nature **414,** 271 (2001).
68. Finet, C., Berne-Dedieu, A., Scutt, C. P. & Marlétaz, F. Evolution of the ARF gene family in land plants: old domains, new tricks. Mol. Biol. Evol. **30,** 45–56 (2013).
69. Tiwari, S. B., Hagen, G. & Guilfoyle, T. The Roles of Auxin Response Factor Domains in Auxin-Responsive Transcription. Plant Cell **15,** 533–543 (2003).
70. Parry, G. et al. Complex regulation of the TIR1/AFB family of auxin receptors. Proc. Natl. Acad. Sci. **106,** 22540–22545 (2009).
71. Okushima, Y. et al. Functional Genomic Analysis of the AUXIN RESPONSE FACTOR Gene Family Members in Arabidopsis thaliana: Unique and Overlapping Functions of ARF7 and ARF19. Plant Cell **17,** 444–463 (2005).
72. Oh, E. et al. Cell elongation is regulated through a central circuit of interacting transcription factors in the Arabidopsis hypocotyl. eLife **3,** (2014).

73. Ma, D. et al. Cryptochrome 1 interacts with PIF4 to regulate high temperature-mediated hypocotyl elongation in response to blue light. Proc. Natl. Acad. Sci. U. S. A. **113,** 224–229 (2016).
74. Ibañez, C. et al. Brassinosteroids Dominate Hormonal Regulation of Plant Thermomorphogenesis via BZR1. Curr. Biol. **28,** 303-310.e3 (2018).
75. Hagen, G. & Guilfoyle, T. Auxin-responsive gene expression: genes, promoters and regulatory factors. Plant Mol. Biol. **49,** 373–385 (2002).
76. Spartz, A. K. et al. .SAUR Inhibition of PP2C-D Phosphatases Activates Plasma Membrane H+-ATPases to Promote Cell Expansion in Arabidopsis. Plant Cell **26,** 2129–2142 (2014).
77. Arsuffi, G. & Braybrook, S. A. Acid growth: an ongoing trip. J. Exp. Bot. **69,** 137–146 (2018).
78. Fendrych, M., Leung, J. & Friml, J. TIR1/AFB-Aux/IAA auxin perception mediates rapid cell wall acidification and growth of Arabidopsis hypocotyls. eLife **5,**
79. Cosgrove, D. J. Plant cell wall extensibility: connecting plant cell growth with cell wall structure, mechanics, and the action of wall-modifying enzymes. J. Exp. Bot. **67,** 463–476 (2016).
80. Dejonghe, W. & Russinova, E. Plant Chemical Genetics: From Phenotype-Based Screens to Synthetic Biology. Plant Physiol. **174,** 5–20 (2017).
81. McCourt, P. & Desveaux, D. Plant chemical genetics. New Phytol. **185,** 15–26 (2010).
82. Cong, F., Cheung, A. K. & Huang, S.-M. A. Chemical Genetics–Based Target Identification in Drug Discovery. Annu. Rev. Pharmacol. Toxicol. **52,** 57–78 (2012).
83. Ridley, S. M., Elliott, A. C., Yeung, M. & Youle, D. High-throughput screening as a tool for agrochemical discovery: automated synthesis, compound input, assay design and process management. Pestic. Sci. **54,** 327–337 (1998).
84. Plant Chemical Genomics: Methods and Protocols. **1795,** (Springer New York, 2018).
85. Hicks, G. R. & Raikhel, N. V. Plant chemical biology: are we meeting the promise? Front. Plant Sci. **5,** (2014).
86. Chen, H.-W., Bandyopadhyay, S., Shasha, D. E. & Birnbaum, K. D. Predicting genome-wide redundancy using machine learning. BMC Evol. Biol. **10,** 357 (2010).
87. Cutler, S. & McCourt, P. Dude, Where's My Phenotype? Dealing with Redundancy in Signaling Networks. Plant Physiol. **138,** 558–559 (2005).
88. Blackwell, H. E. & Zhao, Y. Chemical Genetic Approaches to Plant Biology. Plant Physiol. **133,** 448–455 (2003).
89. De Rybel, B. et al. Chemical Inhibition of a Subset of Arabidopsis thaliana GSK3-like Kinases Activates Brassinosteroid Signaling. Chem. Biol. **16,** 594–604 (2009).
90. Rigal, A., Ma, Q. & Robert, S. Unraveling plant hormone signaling through the use of small molecules. Front. Plant Sci. **5,** (2014).
91. Park, S.-Y. et al. Abscisic acid inhibits type 2C protein phosphatases via the PYR/PYL family of START proteins. Science **324,** 1068–1071 (2009).
92. Savaldi-Goldstein, S. et al. New auxin analogs with growth-promoting effects in intact plants reveal a chemical strategy to improve hormone delivery. Proc. Natl. Acad. Sci. U. S. A. **105,** 15190–15195 (2008).

93. Zhao, Y., Dai, X., Blackwell, H. E., Schreiber, S. L. & Chory, J. SIR1, an upstream component in auxin signaling identified by chemical genetics. Science **301,** 1107–1110 (2003).
94. Nishimura, T. et al. Yucasin is a potent inhibitor of YUCCA, a key enzyme in auxin biosynthesis. Plant J. **77,** 352–366 (2014).
95. Gendron, J. M. et al. Chemical Genetic Dissection of Brassinosteroid–Ethylene Interaction. Mol. Plant **1,** 368–379 (2008).
96. Tóth, R. & Hoorn, R. A. L. van der. Emerging principles in plant chemical genetics. Trends Plant Sci. **15,** 81–88 (2010).
97. Serrano, M., Kombrink, E. & Meesters, C. Considerations for designing chemical screening strategies in plant biology. Front. Plant Sci. **6,** (2015).
98. Lin, L.-C., Hsu, J.-H. & Wang, L.-C. Identification of novel inhibitors of ACC synthase by chemical screening in Arabidopsis thaliana. J. Biol. Chem. jbc.M110.132498 (2010). doi:10.1074/jbc.M110.132498
99. Christian, M., Hannah, W. B., Lüthen, H. & Jones, A. M. Identification of auxins by a chemical genomics approach. J. Exp. Bot. **59,** 2757–2767 (2008).
100. Fozard, S. & Forde, B. G. Novel Micro-Phenotyping Approach to Chemical Genetic Screening for Increased Plant Tolerance to Abiotic Stress. in Plant Chemical Genomics: Methods and Protocols (eds. Fauser, F. & Jonikas, M.) 9–25 (Springer New York, 2018). doi:10.1007/978-1-4939-7874-8_2
101. Meesters, C. & Kombrink, E. Screening for Bioactive Small Molecules by In Vivo Monitoring of Luciferase-Based Reporter Gene Expression in Arabidopsis thaliana. in Plant Chemical Genomics: Methods and Protocols (eds. Hicks, G. R. & Robert, S.) 19–31 (Humana Press, 2014). doi:10.1007/978-1-62703-592-7_3
102. Armstrong, R. W., Combs, A. P., Tempest, P. A., Brown, S. D. & Keating, T. A. Multiple-Component Condensation Strategies for Combinatorial Library Synthesis. Acc. Chem. Res. **29,** 123–131 (1996).
103. Lipinski, C. A., Lombardo, F., Dominy, B. W. & Feeney, P. J. Experimental and computational approaches to estimate solubility and permeability in drug discovery and development settings. Adv. Drug Deliv. Rev. **46,** 3–26 (2001).
104. Chow, F. LATCA : a library of biologically active small molecules for plant chemical genomics. 17th Int. Conf. Arab. Res. 2006 **11,** (2006).
105. Dai, X., Hayashi, K., Nozaki, H., Cheng, Y. & Zhao, Y. Genetic and chemical analyses of the action mechanisms of sirtinol in Arabidopsis. Proc. Natl. Acad. Sci. U. S. A. **102,** 3129–3134 (2005).
106. Sakai, Y. et al. The chemical compound bubblin induces stomatal mispatterning in Arabidopsis by disrupting the intrinsic polarity of stomatal lineage cells. Development **144,** 499–506 (2017).
107. Oh, K. et al. A Chemical Genetics Strategy That Identifies Small Molecules Which Induce the Triple Response in Arabidopsis. Molecules **22,** 2270 (2017).
108. Quareshy, M. et al. The Tetrazole Analogue of the Auxin Indole-3-acetic Acid Binds Preferentially to TIR1 and Not AFB5. ACS Chem. Biol. (2018). doi:10.1021/acschembio.8b00527
109. Shani, E. et al. Gibberellins accumulate in the elongating endodermal cells of Arabidopsis root. Proc. Natl. Acad. Sci. U. S. A. **110,** 4834–4839 (2013).

110. Kaschani, F. et al. Minitags for small molecules: detecting targets of reactive small molecules in living plant tissues using 'click chemistry'. Plant J. **57,** 373–385 (2009).
111. Dejonghe, W. & Russinova, E. Target identification strategies in plant chemical biology. Front. Plant Sci. **5,** (2014).
112. Kinoshita, T. et al. Binding of brassinosteroids to the extracellular domain of plant receptor kinase BRI1. Nature **433,** 167–171 (2005).
113. Pai, M. Y. et al. Drug Affinity Responsive Target Stability (DARTS) for Small Molecule Target Identification. Methods Mol. Biol. Clifton NJ **1263,** 287–298 (2015).
114. Jong, M. de & Leyser, O. Developmental Plasticity in Plants. Cold Spring Harb. Symp. Quant. Biol. **77,** 63–73 (2012).
115. Zanten, M., Bours, R., Pons, T. L. & Proveniers, M. C. G. Plant acclimation and adaptation to warm environments. in Temperature and Plant Development (eds. Franklin, K. & Wigge, P.) 49–78 (John Wiley & Sons, Inc, 2014). doi:10.1002/9781118308240.ch3
116. Balasubramanian, S., Sureshkumar, S., Lempe, J. & Weigel, D. Potent induction of Arabidopsis thaliana flowering by elevated growth temperature. PLoS Genet. **2,** e106 (2006).
117. Kumar, S. V. & Wigge, P. A. H2A.Z-Containing Nucleosomes Mediate the Thermosensory Response in Arabidopsis. Cell **140,** 136–147 (2010).
118. Huai, J. et al. SEUSS and PIF4 Coordinately Regulate Light and Temperature Signaling Pathways to Control Plant Growth. Mol. Plant (2018). doi:10.1016/j.molp.2018.04.005
119. Thomson, K.-S., Hertel, R., Müller, S. & Tavares, J. E. 1-N-naphthylphthalamic acid and 2,3,5-triiodobenzoic acid. Planta **109,** 337–352 (1973).
120. Nagashima, A., Uehara, Y. & Sakai, T. The ABC Subfamily B Auxin Transporter AtABCB19 is Involved in the Inhibitory Effects of N-1-Naphthyphthalamic Acid on the Phototropic and Gravitropic Responses of Arabidopsis Hypocotyls. Plant Cell Physiol. **49,** 1250–1255 (2008).
121. Noutoshi, Y. & Shirasu, K. A High-Throughput Chemical Screening Method for Inhibitors and Potentiators of Hypersensitive Cell Death Using Suspension Cell Culture of Arabidopsis thaliana. in Plant Chemical Genomics 39–47 (Humana Press, New York, NY, 2018). doi:10.1007/978-1-4939-7874-8_4
122. Drakakaki, G. et al. Clusters of bioactive compounds target dynamic endomembrane networks in vivo. Proc. Natl. Acad. Sci. U. S. A. **108,** 17850–17855 (2011).
123. Ibañez, C. et al. Ambient temperature and genotype differentially affect developmental and phenotypic plasticity in Arabidopsis thaliana. BMC Plant Biol. **17,** 114 (2017).
124. Delker, C. et al. Natural Variation of Transcriptional Auxin Response Networks in Arabidopsis thaliana. Plant Cell **22,** 2184–2200 (2010).
125. Oh, E. et al. Cell elongation is regulated through a central circuit of interacting transcription factors in the Arabidopsis hypocotyl. eLife **3,** (2014).
126. Sorin, C. et al. Auxin and Light Control of Adventitious Rooting in Arabidopsis Require ARGONAUTE1. Plant Cell **17,** 1343–1359 (2005).

127. Boonsirichai, K., Guan, C., Chen, R. & Masson, P. H. Root gravitropism: an experimental tool to investigate basic cellular and molecular processes underlying mechanosensing and signal transmission in plants. Annu. Rev. Plant Biol. **53,** 421–447 (2002).
128. Stavang, J. A. et al. Hormonal regulation of temperature-induced growth in Arabidopsis. Plant J. **60,** 589–601 (2009).
129. Leivar, P. et al. The Arabidopsis Phytochrome-Interacting Factor PIF7, Together with PIF3 and PIF4, Regulates Responses to Prolonged Red Light by Modulating phyB Levels. Plant Cell **20,** 337–352 (2008).
130. Sultan S E. Phenotypic plasticity for plant development, function and life history. Trends Plant Sci. **5,** 537–542 (2000).
131. Ibañez, C. et al. Ambient temperature and genotype differentially affect developmental and phenotypic plasticity in Arabidopsis thaliana. BMC Plant Biol. **17,** 114 (2017).
132. Moe, R. & Mortensen, L. M. THERMOMORPHOGENESIS IN POT PLANTS. Acta Hortic. 19–26 (1992). doi:10.17660/ActaHortic.1992.305.2
133. Zhao, C. et al. Temperature increase reduces global yields of major crops in four independent estimates. Proc. Natl. Acad. Sci. **114,** 9326–9331 (2017).
134. Stavang, J. A. et al. Hormonal regulation of temperature-induced growth in Arabidopsis. Plant J. **60,** 589–601 (2009).
135. Rayle, D. L. & Cleland, R. E. The Acid Growth Theory of auxin-induced cell elongation is alive and well. Plant Physiol. **99,** 1271–1274 (1992).
136. Hager, A. Role of the plasma membrane H+-ATPase in auxin-induced elongation growth: historical and new aspects. J. Plant Res. **116,** 483–505 (2003).
137. Kaschani, F. & Hoorn, R. Small molecule approaches in plants. Curr. Opin. Chem. Biol. **11,** 88–98 (2007).
138. Rakusová, H. et al. Polarization of PIN3-dependent auxin transport for hypocotyl gravitropic response in Arabidopsis thaliana. Plant J. **67,** 817–826 (2011).
139. Grieneisen, V. A., Xu, J., Marée, A. F. M., Hogeweg, P. & Scheres, B. Auxin transport is sufficient to generate a maximum and gradient guiding root growth. Nature **449,** 1008 (2007).
140. Martins, S. et al. Brassinosteroid signaling-dependent root responses to prolonged elevated ambient temperature. Nat. Commun. **8,** (2017).
141. Normanly, J., Grisafi, P., Fink, G. R. & Bartel, B. Arabidopsis mutants resistant to the auxin effects of indole-3-acetonitrile are defective in the nitrilase encoded by the NIT1 gene. Plant Cell **9,** 1781–1790 (1997).
142. Marlo, J. E. et al. Discovery and Characterization of Novel Allosteric Potentiators of M1 Muscarinic Receptors Reveals Multiple Modes of Activity. Mol. Pharmacol. **75,** 577–588 (2009).
143. Chen, J.-G., Gao, Y. & Jones, A. M. Differential Roles of Arabidopsis Heterotrimeric G-Protein Subunits in Modulating Cell Division in Roots. Plant Physiol. **141,** 887–897 (2006).
144. Grozinger, C. M., Chao, E. D., Blackwell, H. E., Moazed, D. & Schreiber, S. L. Identification of a class of small molecule inhibitors of the sirtuin family of NAD-dependent deacetylases by phenotypic screening. J. Biol. Chem. **276,** 38837–38843 (2001).

145. Zhao, Y., Dai, X., Blackwell, H. E., Schreiber, S. L. & Chory, J. SIR1, an upstream component in auxin signaling identified by chemical genetics. Science **301,** 1107–1110 (2003).
146. Dai, X., Hayashi, K., Nozaki, H., Cheng, Y. & Zhao, Y. Genetic and chemical analyses of the action mechanisms of sirtinol in Arabidopsis. Proc. Natl. Acad. Sci. U. S. A. **102,** 3129–3134 (2005).
147. Kaschani, F. & van der Hoorn, R. Small molecule approaches in plants. Curr. Opin. Chem. Biol. **11,** 88–98 (2007).
148. Cheng, Y., Dai, X. & Zhao, Y. AtCAND1, A HEAT-Repeat Protein That Participates in Auxin Signaling in Arabidopsis. Plant Physiol. **135,** 1020–1026 (2004).
149. Li, J., Dai, X. & Zhao, Y. A Role for Auxin Response Factor 19 in Auxin and Ethylene Signaling in Arabidopsis. Plant Physiol. **140,** 899–908 (2006).
150. Klepikova, A. V., Kasianov, A. S., Gerasimov, E. S., Logacheva, M. D. & Penin, A. A. A high resolution map of the Arabidopsis thaliana developmental transcriptome based on RNA-seq profiling. Plant J. **88,** 1058–1070 (2016).
151. Covington, M. F. & Harmer, S. L. The Circadian Clock Regulates Auxin Signaling and Responses in Arabidopsis. PLOS Biol. **5,** e222 (2007).
152. del Pozo, J. C. & Estelle, M. The Arabidopsis cullin AtCUL1 is modified by the ubiquitin-related protein RUB1. Proc. Natl. Acad. Sci. U. S. A. **96,** 15342–15347 (1999).
153. del Pozo, J. C. et al. AXR1-ECR1-dependent conjugation of RUB1 to the Arabidopsis Cullin AtCUL1 is required for auxin response. Plant Cell **14,** 421–433 (2002).
154. Greenham, K. et al. RETRACTED: The AFB4 Auxin Receptor Is a Negative Regulator of Auxin Signaling in Seedlings. Curr. Biol. **21,** 520–525 (2011).
155. Sun, J., Qi, L., Li, Y., Chu, J. & Li, C. PIF4–Mediated Activation of YUCCA8 Expression Integrates Temperature into the Auxin Pathway in Regulating Arabidopsis Hypocotyl Growth. PLOS Genet. **8,** e1002594 (2012).
156. Kepinski, S. & Leyser, O. Auxin-induced SCFTIR1–Aux/IAA interaction involves stable modification of the SCFTIR1 complex. Proc. Natl. Acad. Sci. U. S. A. **101,** 12381–12386 (2004).
157. Bours, R., Kohlen, W., Bouwmeester, H. J. & Krol, A. R. van der. Thermoperiodic control of hypocotyl elongation depends on auxin induced ethylene signaling which controls downstream PIF3 activity. Plant Physiol. pp.114.254425 (2014). doi:10.1104/pp.114.254425
158. Walsh, T. A. et al. Mutations in an Auxin Receptor Homolog AFB5 and in SGT1b Confer Resistance to Synthetic Picolinate Auxins and Not to 2,4-Dichlorophenoxyacetic Acid or Indole-3-Acetic Acid in Arabidopsis. Plant Physiol. **142,** 542–552 (2006).
159. Savaldi-Goldstein, S. et al. New auxin analogs with growth-promoting effects in intact plants reveal a chemical strategy to improve hormone delivery. Proc. Natl. Acad. Sci. U. S. A. **105,** 15190–15195 (2008).
160. Koiwai, H., Akaba, S., Seo, M., Komano, T. & Koshiba, T. Functional expression of two Arabidopsis aldehyde oxidases in the yeast Pichia pastoris. J. Biochem. (Tokyo) **127,** 659–664 (2000).
161. Böttcher, C. et al. The Biosynthetic Pathway of Indole-3-Carbaldehyde and Indole-3-Carboxylic Acid Derivatives in Arabidopsis1[W]. Plant Physiol. **165,** 841–853 (2014).

162. Seo, M. et al. Higher activity of an aldehyde oxidase in the auxin-overproducing superroot1 mutant of Arabidopsis thaliana. Plant Physiol. **116,** 687–693 (1998).
163. Seo, M. et al. Comparative studies on the Arabidopsis aldehyde oxidase (AAO) gene family revealed a major role of AAO3 in ABA biosynthesis in seeds. Plant Cell Physiol. **45,** 1694–1703 (2004).
164. Seo, M. et al. The Arabidopsis aldehyde oxidase 3 (AAO3) gene product catalyzes the final step in abscisic acid biosynthesis in leaves. Proc. Natl. Acad. Sci. U. S. A. **97,** 12908–12913 (2000).
165. Leivar, P. et al. The Arabidopsis Phytochrome-Interacting Factor PIF7, Together with PIF3 and PIF4, Regulates Responses to Prolonged Red Light by Modulating phyB Levels. Plant Cell **20,** 337–352 (2008).
166. Teschner, J. et al. A Novel Role for Arabidopsis Mitochondrial ABC Transporter ATM3 in Molybdenum Cofactor Biosynthesis[W][OA]. Plant Cell **22,** 468–480 (2010).
167. Ruegger, M. et al. The TIR1 protein of Arabidopsis functions in auxin response and is related to human SKP2 and yeast Grr1p. Genes Dev. **12,** 198–207 (1998).
168. Parry, G. et al. Complex regulation of the TIR1/AFB family of auxin receptors. Proc. Natl. Acad. Sci. **106,** 22540–22545 (2009).
169. Gleason, C., Foley, R. C. & Singh, K. B. Mutant Analysis in Arabidopsis Provides Insight into the Molecular Mode of Action of the Auxinic Herbicide Dicamba. PLoS ONE **6,** (2011).
170. Estelle, M. A. & Somerville, C. Auxin-resistant mutants of Arabidopsis thaliana with an altered morphology. Mol. Gen. Genet. MGG **206,** 200–206 (1987).
171. González-Guzmán, M., Abia, D., Salinas, J., Serrano, R. & Rodríguez, P. L. Two New Alleles of the abscisic aldehyde oxidase 3 Gene Reveal Its Role in Abscisic Acid Biosynthesis in Seeds. Plant Physiol. **135,** 325–333 (2004).
172. Ibdah, M., Chen, Y.-T., Wilkerson, C. G. & Pichersky, E. An Aldehyde Oxidase in Developing Seeds of Arabidopsis Converts Benzaldehyde to Benzoic Acid. Plant Physiol. **150,** 416–423 (2009).
173. Jones, A. M., Ecker, J. R. & Chen, J.-G. A Reevaluation of the Role of the Heterotrimeric G Protein in Coupling Light Responses in Arabidopsis. Plant Physiol. **131,** 1623–1627 (2003).
174. Ullah, H. et al. The β-Subunit of the Arabidopsis G Protein Negatively Regulates Auxin-Induced Cell Division and Affects Multiple Developmental Processes. Plant Cell **15,** 393–409 (2003).
175. Chen, J.-G. et al. GCR1 Can Act Independently of Heterotrimeric G-Protein in Response to Brassinosteroids and Gibberellins in Arabidopsis Seed Germination. Plant Physiol. **135,** 907–915 (2004).
176. Gao, Y. et al. Genetic characterization reveals no role for the reported ABA receptor, GCR2, in ABA control of seed germination and early seedling development in Arabidopsis. Plant J. Cell Mol. Biol. **52,** 1001–1013 (2007).
177. Trusov, Y. et al. Heterotrimeric G Protein γ Subunits Provide Functional Selectivity in Gβγ Dimer Signaling in Arabidopsis. Plant Cell **19,** 1235–1250 (2007).
178. Chen, J.-G. et al. A Seven-Transmembrane RGS Protein That Modulates Plant Cell Proliferation. Science **301,** 1728–1731 (2003).

179. Guo, J., Zeng, Q., Emami, M., Ellis, B. E. & Chen, J.-G. The GCR2 gene family is not required for ABA control of seed germination and early seedling development in Arabidopsis. PloS One **3,** e2982 (2008).
180. Okushima, Y. et al. Functional Genomic Analysis of the AUXIN RESPONSE FACTOR Gene Family Members in Arabidopsis thaliana: Unique and Overlapping Functions of ARF7 and ARF19. Plant Cell **17,** 444–463 (2005).
181. Alonso, J. M. et al. Genome-Wide Insertional Mutagenesis of Arabidopsis thaliana. Science **301,** 653–657 (2003).
182. Bradford, M. M. A rapid and sensitive method for the quantitation of microgram quantities of protein utilizing the principle of protein-dye binding. Anal. Biochem. **72,** 248–254 (1976).
183. Ruyter-Spira, C. et al. Physiological Effects of the Synthetic Strigolactone Analog GR24 on Root System Architecture in Arabidopsis: Another Belowground Role for Strigolactones? Plant Physiol. **155,** 721–734 (2011).
184. Oñate-Sánchez, L. & Vicente-Carbajosa, J. DNA-free RNA isolation protocols for Arabidopsis thaliana, including seeds and siliques. BMC Res. Notes **1,** 93 (2008).
185. van Zanten, M., Bours, R., Pons, T. L. & Proveniers, M. C. G. Plant acclimation and adaptation to warm environments. in Temperature and Plant Development (eds. Franklin, K. a & Wigge, P. a) 49–78 (John Wiley & Sons, Inc, 2014). doi:10.1002/9781118308240.ch3
186. Rayle, D. L. & Cleland, R. E. The Acid Growth Theory of auxin-induced cell elongation is alive and well. Plant Physiol. **99,** 1271–1274 (1992).
187. Balasubramanian, S., Sureshkumar, S., Lempe, J. & Weigel, D. Potent induction of Arabidopsis thaliana flowering by elevated growth temperature. PLoS Genet. **2,** e106 (2006).
188. Sidaway-Lee, K., Costa, M. J., Rand, D. A., Finkenstadt, B. & Penfield, S. Direct measurement of transcription rates reveals multiple mechanisms for configuration of the Arabidopsis ambient temperature response. Genome Biol. **15,** R45 (2014).
189. Kumar, S. V. & Wigge, P. A. H2A.Z-Containing Nucleosomes Mediate the Thermosensory Response in Arabidopsis. Cell **140,** 136–147 (2010).
190. Zhang, Y. et al. A Quartet of PIF bHLH Factors Provides a Transcriptionally Centered Signaling Hub That Regulates Seedling Morphogenesis through Differential Expression-Patterning of Shared Target Genes in Arabidopsis. PLOS Genet. **9,** e1003244 (2013).
191. Tasset, C. et al. POWERDRESS-mediated histone deacetylation is essential for thermomorphogenesis in Arabidopsis thaliana. PLOS Genet. **14,** e1007280 (2018).
192. Fernie, A. R. & Stitt, M. On the Discordance of Metabolomics with Proteomics and Transcriptomics: Coping with Increasing Complexity in Logic, Chemistry, and Network Interactions Scientific Correspondence. Plant Physiol. **158,** 1139–1145 (2012).
193. Vasseur, F., Pantin, F. & Vile, D. Changes in light intensity reveal a major role for carbon balance in Arabidopsis responses to high temperature. Plant Cell Environ. **34,** 1563–1576
194. Sairanen, I. et al. Soluble Carbohydrates Regulate Auxin Biosynthesis via PIF Proteins in Arabidopsis. Plant Cell **24,** 4907–4916 (2012).

195. Liu, Z. et al. Phytochrome interacting factors (PIFs) are essential regulators for sucrose-induced hypocotyl elongation in Arabidopsis. J. Plant Physiol. **168,** 1771–1779 (2011).
196. Palmblad, M., Mills, D. J. & Bindschedler, L. V. Heat-Shock Response in Arabidopsis thaliana Explored by Multiplexed Quantitative Proteomics Using Differential Metabolic Labeling. J. Proteome Res. **7,** 780–785 (2008).
197. Černy, M., Jedelsky, P. L., Novak, J., Schloseer, A. & Brzobohaty, B. Cytokinin modulates proteomic, transcriptomic and growth responses to temperature shocks in Arabidopsis. Plant Cell Environ. **37,** 1641–1655 (2014).
198. Rocco, M. et al. Proteomic analysis of temperature stress-responsive proteins in Arabidopsis thaliana rosette leaves. Mol BioSyst **9,** 1257–1267 (2013).
199. Kosová, K., Vítámvás, P., Prášil, I. T. & Renaut, J. Plant proteome changes under abiotic stress - Contribution of proteomics studies to understanding plant stress response. Plant Proteomics Eur. **74,** 1301–1322 (2011).
200. Neilson, K. A., Gammulla, C. G., Mirzaei, M., Imin, N. & Haynes, P. A. Proteomic analysis of temperature stress in plants. Proteomics **10,** 828–845 (2010).
201. Kaplan, F. et al. Exploring the Temperature-Stress Metabolome of Arabidopsis. Plant Physiol. **136,** 4159–4168 (2004).
202. Guy, C., Kaplan, F., Kopka, J., Selbig, J. & Hincha, D. K. Metabolomics of temperature stress. Physiol. Plant. **132,** 220–235 (2008).
203. Mittler, R., Finka, A. & Goloubinoff, P. How do plants feel the heat? Trends Biochem. Sci. **37,** 118–125 (2012).
204. Saidi, Y., Finka, A. & Goloubinoff, P. Heat perception and signalling in plants: a tortuous path to thermotolerance. New Phytol. **190,** 556–565 (2011).
205. Haslbeck, M. & Vierling, E. A First Line of Stress Defense: Small Heat Shock Proteins and Their Function in Protein Homeostasis. Mol. Chaperones Protein Qual. Control Part I **427,** 1537–1548 (2015).
206. Nusinow, D. A. et al. The ELF4-ELF3-LUX complex links the circadian clock to diurnal control of hypocotyl growth. Nature **475,** 398–402 (2011).
207. Zhu, J.-Y., Oh, E., Wang, T. & Wang, Z.-Y. TOC1–PIF4 interaction mediates the circadian gating of thermoresponsive growth in Arabidopsis. Nat. Commun. **7,** 13692 (2016).
208. Armijo, G. et al. A Salicylic Acid–Induced Lectin-Like Protein Plays a Positive Role in the Effector-Triggered Immunity Response of Arabidopsis thaliana to Pseudomonas syringae Avr-Rpm1. Mol. Plant. Microbe Interact. **26,** 1395–1406 (2013).
209. García-Olmedo, F., Molina, A., Alamillo, J. M. & Rodríguez-Palenzuéla, P. Plant defense peptides. Pept. Sci. **47,** 479–491 (1998).
210. Hernández-Blanco, C. et al. Impairment of Cellulose Synthases Required for Arabidopsis Secondary Cell Wall Formation Enhances Disease Resistance. Plant Cell **19,** 890–903 (2007).
211. Jülke, S. & Ludwig-Müller, J. Response of Arabidopsis thaliana Roots with Altered Lipid Transfer Protein (LTP) Gene Expression to the Clubroot Disease and Salt Stress. Plants **5,** 2 (2015).

212. Maharjan, P. M. & Choe, S. High Temperature Stimulates DWARF4 (DWF4) Expression to Increase Hypocotyl Elongation in Arabidopsis. J. Plant Biol. **54,** 425 (2011).
213. Chen, G. et al. Discordant protein and mRNA expression in lung adenocarcinomas. Mol. Cell. Proteomics MCP **1,** 304–313 (2002).
214. Gygi, S. P., Rochon, Y., Franza, B. R. & Aebersold, R. Correlation between protein and mRNA abundance in yeast. Mol. Cell. Biol. **19,** 1720–1730 (1999).
215. Dünser, K. & Kleine-Vehn, J. Differential growth regulation in plants-the acid growth balloon theory. Curr. Opin. Plant Biol. **28,** 55–59 (2015).
216. Park, Y.-J., Lee, H.-J., Ha, J.-H., Kim, J. Y. & Park, C.-M. COP1 conveys warm temperature information to hypocotyl thermomorphogenesis. New Phytol. **215,** 269–280 (2017).
217. Pufky, J., Qiu, Y., Rao, M. V., Hurban, P. & Jones, A. M. The auxin-induced transcriptome for etiolated Arabidopsis seedlings using a structure/function approach. Funct. Integr. Genomics **3,** 135–143 (2003).
218. Paponov, I. A. et al. Comprehensive Transcriptome Analysis of Auxin Responses in Arabidopsis. Mol. Plant **1,** 321–337 (2008).
219. Nijland, W. et al. Monitoring plant condition and phenology using infrared sensitive consumer grade digital cameras. Agric. For. Meteorol. **184,** 98–106 (2014).
220. Trapnell, C., Pachter, L. & Salzberg, S. L. TopHat: discovering splice junctions with RNA-Seq. Bioinformatics **25,** 1105–1111 (2009).
221. Anders, S., Pyl, P. T. & Huber, W. HTSeq—a Python framework to work with high-throughput sequencing data. Bioinformatics **31,** 166–169 (2014).
222. Anders, S. & Huber, W. Differential expression analysis for sequence count data. Genome Biol. **11,** R106 (2010).
223. Carvalho, M. T. V. et al. Gomphrena claussenii, a novel metal-hypertolerant bioindicator species, sequesters cadmium, but not zinc, in vacuolar oxalate crystals. New Phytol. **208,** 763–775 (2015).
224. Mann, M. E., Rahmstorf, S., Steinman, B. A., Tingley, M. & Miller, S. K. The Likelihood of Recent Record Warmth. Sci. Rep. **6,** 19831 (2016).
225. Seo, M. et al. Higher activity of an aldehyde oxidase in the auxin-overproducing superroot1 mutant of Arabidopsis thaliana. Plant Physiol. **116,** 687–693 (1998).
226. Mashiguchi, K. et al. The main auxin biosynthesis pathway in Arabidopsis. Proc. Natl. Acad. Sci. **108,** 18512–18517 (2011).
227. Seo, M. et al. Comparative studies on the Arabidopsis aldehyde oxidase (AAO) gene family revealed a major role of AAO3 in ABA biosynthesis in seeds. Plant Cell Physiol. **45,** 1694–1703 (2004).
228. Rix, U. & Superti-Furga, G. Target profiling of small molecules by chemical proteomics. Nat. Chem. Biol. **5,** 616–624 (2009).
229. Futamura, Y., Muroi, M. & Osada, H. Target identification of small molecules based on chemical biology approaches. Mol. Biosyst. **9,** 897–914 (2013).

230. Wang, P., Bouwman, F. G. & Mariman, E. C. M. Generally detected proteins in comparative proteomics--a matter of cellular stress response? Proteomics **9,** 2955–2966 (2009).
231. Trompetter, I. Untersuchungen zu den NIT1-homologen Nitrilasen der Brassicaceae. (Ruhr-Universität Bochum, 2010).
232. Vorwerk, S. et al. Enzymatic characterization of the recombinant Arabidopsis thaliana nitrilase subfamily encoded by the NIT2/NIT1/NIT3-gene cluster. Planta **212,** 508–516 (2001).
233. Piotrowski, M., Schönfelder, S. & Weiler, E. W. The Arabidopsis thaliana Isogene NIT4 and Its Orthologs in Tobacco Encode β-Cyano-l-alanine Hydratase/Nitrilase. J. Biol. Chem. **276,** 2616–2621 (2001).
234. Katz, E. et al. The glucosinolate breakdown product indole-3-carbinol acts as an auxin antagonist in roots of Arabidopsis thaliana. Plant J. **82,** 547–555
235. Michalski, A. et al. Ultra high resolution linear ion trap Orbitrap mass spectrometer (Orbitrap Elite) facilitates top down LC MS/MS and versatile peptide fragmentation modes. Mol. Cell. Proteomics MCP **11,** O111.013698 (2012).
236. Olsen, J. V. et al. Parts per million mass accuracy on an Orbitrap mass spectrometer via lock mass injection into a C-trap. Mol. Cell. Proteomics MCP **4,** 2010–2021 (2005).
237. Cox, J. et al. Andromeda: a peptide search engine integrated into the MaxQuant environment. J. Proteome Res. **10,** 1794–1805 (2011).
238. Cox, J. & Mann, M. MaxQuant enables high peptide identification rates, individualized p.p.b.-range mass accuracies and proteome-wide protein quantification. Nat. Biotechnol. **26,** 1367–1372 (2008).
239. Cox, J. et al. Accurate proteome-wide label-free quantification by delayed normalization and maximal peptide ratio extraction, termed MaxLFQ. Mol. Cell. Proteomics MCP **13,** 2513–2526 (2014).
240. Tyanova, S. et al. The Perseus computational platform for comprehensive analysis of (prote) omics data. Nat. Methods **13,** 731–740 (2016).
241. Slyke, D. D. V., Hiller, A. & Plazin, W. the technical assistance of J. Determination of Ammonia in Blood. J. Biol. Chem. **102,** 499–504 (1933).
242. Pencík, A. et al. Ultra-rapid auxin metabolite profiling for high-throughput mutant screening in Arabidopsis. J. Exp. Bot. **69,** 2569–2579 (2018).
243. Rappsilber, J., Ishihama, Y. & Mann, M. Stop and go extraction tips for matrix-assisted laser desorption/ionization, nanoelectrospray, and LC/MS sample pretreatment in proteomics. Anal. Chem. **75,** 663–670 (2003).
244. Novák, O. et al. Tissue-specific profiling of the Arabidopsis thaliana auxin metabolome. Plant J. Cell Mol. Biol. **72,** 523–536 (2012).
245. Rittenberg, D. & Foster, G. L. A New Procedure for Quantitative Analysis by Isotope Dilution, with Application to the Determination of Amino Acids and Fatty Acids. J. Biol. Chem. **133,** 737–744 (1940).

246. Schreiber, K. J. et al. Found in Translation: High-Throughput Chemical Screening in Arabidopsis thaliana Identifies Small Molecules That Reduce Fusarium Head Blight Disease in Wheat. Mol. Plant. Microbe Interact. **24,** 640–648 (2011).
247. The 1001 Genomes Consortium. 1,135 Genomes Reveal the Global Pattern of Polymorphism in Arabidopsis thaliana. Cell **166,** 481–491 (2016).
248. Box, M. S. et al. ELF3 Controls Thermoresponsive Growth in Arabidopsis. Curr. Biol. **25,** 194–199 (2015).
249. Atwell, S. et al. Genome-wide association study of 107 phenotypes in Arabidopsis thaliana inbred lines. Nature **465,** 627–631 (2010).
250. Baxter, I. et al. A coastal cline in sodium accumulation in Arabidopsis thaliana is driven by natural variation of the sodium transporter AtHKT1;1. PLoS Genet. **6,** e1001193 (2010).
251. Li, Y., Huang, Y., Bergelson, J., Nordborg, M. & Borevitz, J. O. Association mapping of local climate-sensitive quantitative trait loci in Arabidopsis thaliana. Proc. Natl. Acad. Sci. U. S. A. **107,** 21199–21204 (2010).
252. Platt, A. et al. The scale of population structure in Arabidopsis thaliana. PLoS Genet. **6,** e1000843 (2010).
253. Wintermans, P. C. A., Bakker, P. A. H. M. & Pieterse, C. M. J. Natural genetic variation in Arabidopsis for responsiveness to plant growth-promoting rhizobacteria. Plant Mol. Biol. **90,** 623–634 (2016).
254. Kim, S. et al. Recombination and linkage disequilibrium in Arabidopsis thaliana. Nat. Genet. **39,** 1151–1155 (2007).
255. Korte, A. & Farlow, A. The advantages and limitations of trait analysis with GWAS: a review. Plant Methods **9,** 29 (2013).
256. Conti, L. et al. Small Ubiquitin-Like Modifier Proteases OVERLY TOLERANT TO SALT1 and -2 Regulate Salt Stress Responses in Arabidopsis. Plant Cell **20,** 2894–2908 (2008).
257. Sadanandom, A. et al. SUMOylation of phytochrome-B negatively regulates light-induced signaling in Arabidopsis thaliana. Proc. Natl. Acad. Sci. **112,** 11108–11113 (2015).
258. Ramon, M. et al. Extensive expression regulation and lack of heterologous enzymatic activity of the Class II trehalose metabolism proteins from Arabidopsis thaliana. Plant Cell Environ. **32,** 1015–1032
259. Stewart, J. L., Maloof, J. N. & Nemhauser, J. L. PIF Genes Mediate the Effect of Sucrose on Seedling Growth Dynamics. PLOS ONE **6,** e19894 (2011).
260. Raschke, A. et al. Natural variants of ELF3 affect thermomorphogenesis by transcriptionally modulating PIF4-dependent auxin response genes. BMC Plant Biol. **15,** 197 (2015).
261. Delker, C. et al. The DET1-COP1-HY5 Pathway Constitutes a Multipurpose Signaling Module Regulating Plant Photomorphogenesis and Thermomorphogenesis. Cell Rep. **9,** 1983–1989 (2014).
262. Zhu, W. et al. Natural Variation Identifies ICARUS1, a Universal Gene Required for Cell Proliferation and Growth at High Temperatures in Arabidopsis thaliana. PLOS Genet. **11,** e1005085 (2015).

263. Sanchez-Bermajo, E. et al. Genetic architecture of natural variation in thermal responses of Arabidopsis thaliana. Plant Physiol. pp.00942.2015 (2015). doi:10.1104/pp.15.00942
264. Johansson, H. et al. Arabidopsis cell expansion is controlled by a photothermal switch. Nat. Commun. **5,** (2014).
265. Ma, D. et al. Cryptochrome 1 interacts with PIF4 to regulate high temperature-mediated hypocotyl elongation in response to blue light. Proc. Natl. Acad. Sci. U. S. A. **113,** 224–229 (2016).
266. Erwin, J. E., Heins, R. D. & Karlsson, M. G. Thermomorphogenesis in Lilium longiflorum. Am. J. Bot. **76,** 47–52 (1989).
267. Jenrich, R. et al. Evolution of heteromeric nitrilase complexes in Poaceae with new functions in nitrile metabolism. Proc. Natl. Acad. Sci. U. S. A. **104,** 18848–18853 (2007).
268. Kriechbaumer, V. et al. Maize nitrilases have a dual role in auxin homeostasis and β-cyanoalanine hydrolysis. J. Exp. Bot. **58,** 4225–4233 (2007).
269. Seren, Ü. et al. GWAPP: A Web Application for Genome-Wide Association Mapping in Arabidopsis. Plant Cell **24,** 4793–4805 (2012).
270. Prigge, M. J. et al. The Arabidopsis Auxin Receptor F-Box Proteins AFB4 and AFB5 Are Required for Response to the Synthetic Auxin Picloram. G3 Bethesda Md **6,** 1383–1390 (2016).
271. Lee, S. et al. Defining Binding Efficiency and Specificity of Auxins for SCFTIR1/AFB-Aux/IAA Co-receptor Complex Formation. ACS Chem. Biol. **9,** 673–682 (2014).
272. Overvoorde, P. J. et al. Functional Genomic Analysis of the AUXIN/INDOLE-3-ACETIC ACID Gene Family Members in Arabidopsis thaliana. Plant Cell **17,** 3282–3300 (2005).
273. Gutierrez, L. et al. Auxin Controls Arabidopsis Adventitious Root Initiation by Regulating Jasmonic Acid Homeostasis. Plant Cell tpc.112.099119 (2012). doi:10.1105/tpc.112.099119
274. Spartz, A. K. et al. The SAUR19 subfamily of SMALL AUXIN UP RNA genes promote cell expansion. Plant J. Cell Mol. Biol. **70,** 978–990 (2012).
275. Kepinski, S. & Leyser, O. Auxin-induced SCFTIR1–Aux/IAA interaction involves stable modification of the SCFTIR1 complex. Proc. Natl. Acad. Sci. U. S. A. **101,** 12381–12386 (2004).
276. Zhao, Y. Auxin Biosynthesis: A Simple Two-Step Pathway Converts Tryptophan to Indole-3-Acetic Acid in Plants. Mol. Plant **5,** 334–338 (2012).
277. Liao, C.-Y. et al. Reporters for sensitive and quantitative measurement of auxin response. Nat. Methods **12,** 207–210 (2015).

Samenvatting in het Nederlands

Planten zijn gebonden aan een vaste standplaats en kunnen niet weglopen van stressvolle condities. Om optimaal te kunnen groeien en voort te kunnen planten, passen planten zich daarom continu aan de veranderende omgeving aan. Hiervoor hebben planten zeer gevoelige moleculaire waarnemingsmechanismes ontwikkeld.

Een van de belangrijkste omgevingsfactoren is temperatuur. Temperatuur beïnvloed op ingrijpende wijze de fysiologie en ontwikkeling van planten. In *Arabidopsis thaliana* (de Zandraket), een van de meest gebruikte model organismes in de plantenbiologie, veroorzaakt een paar graden verhoging in de temperatuur een ingrijpende verandering in de architectuur van de plant. Onder andere strekken de embryonale stengel (hypocotyl) en de bladstelen (petiolen), en de bladeren bewegen omhoog (hyponastie). Deze combinatie van aanpassingen heten samen thermomorfogenese. Thermomorfogenese verminderd de warmte instraling van de zon, beweegt de gevoelige bladeren weg van de warme bodem en leidt tegelijkertijd tot een verhoogde luchtstroom om de bladeren. Hierdoor neemt de koelingscapaciteit van de plant toe en kan de plant optimaal groeien onder suboptimale omstandigheden.

Het moleculair signaleringsnetwerk dat thermomorfogenese aanstuurt is slechts gedeeltelijk bekend. Aangetoond is dat het rood/ver-rood licht sensoreiwit Fytochroom B ook functioneert als temperatuur sensor. Onder invloed van een toenemende temperatuur, valt de remming van Fytochroom B op het eiwit PHYTOCHROME INTERACTING FACTOR 4 (PIF4) weg. Actieve PIF4 eiwitten stimuleren de aanmaak van het fytohormoon auxine. Deze toename in het auxine niveau leidt tot verweking van de celwand, wat cel strekking door turgordruk (wateropname) mogelijk maakt. Het is deze celstrekking die ten grondslag ligt aan eerdergenoemde thermomorfogenese responsen. Ondanks een sterke toename in de kennis van de moleculaire factoren die thermomorfogenese aansturen de laatste jaren, ontbreken er nog veel puzzelstukken die nodig zijn voor een volledig begrip van deze belangrijke aanpassing aan hoge temperatuur.

Het in dit proefschrift beschreven onderzoek volgt een chemisch genetische strategie met als doel verdere inzichten in thermomorfogenese signaleringsmechanismes te verwerven. Een chemisch genetische onderzoeksstrategie berust op het gebruikt van chemische stoffen die een biologisch proces beïnvloeden. Door de exacte werking van de chemische stof te achterhalen, kunnen nieuwe inzichten worden verkregen over het verstoorde biologisch proces. Een groot voordeel van deze methode is dat eiwitten met overlappende functies door dezelfde chemische stof beïnvloed kunnen worden. Klassieke genetische methodes, zoals mutant screens, schieten in dit soort gevallen soms te kort, omdat dan slechts individuele eiwitten of genen beïnvloed worden en bij uitschakeling de partner(s) de rol geheel of gedeeltelijk kan overnemen.

Een chemisch genetisch onderzoek kan worden onderverdeeld in verschillende stadia. Als eerste wordt vaak een grote set (bibliotheek) van verschillende chemicaliën

getest op hun activiteit in het te onderzoeken biologisch systeem. Wanneer een aantal actieve stoffen wordt geïdentificeerd en de activiteit ervan bevestigd, moet het werkingsmechanisme van de stoffen achterhaald worden. Hiervoor wordt vaak als eerste gezocht naar interacties met bekende componenten (hormonen of eiwitten) uit de signalering van het biologisch proces. Ook kan in detail bepaald worden welke chemische groepen (on)belangrijk zijn voor de activiteit van de stoffen door middel van een zogenaamde 'structure activity relationship' (SAR) studie. Als volgende stap wordt vaak direct de receptor (of andere targets) van de chemische stof geïdentificeerd. Dit kan bijvoorbeeld worden gedaan door het chemisch isoleren en identificeren van eiwitten die een directe interactie met de chemische stof aangaan. Door deze gegevens te combineren kan een gedetailleerd beeld worden gevormd van het werkingsmechanisme van de chemische stoffen, en daarmee het bestudeerde biologische proces.

In **Hoofdstuk 2** van dit proefschrift wordt de screening van een bibliotheek van chemicaliën beschreven met als doel stoffen te identificeren die thermomorfogenese kunnen herstellen in *pif4-2* mutanten. Waar wild-type zaailingen een sterke elongatie respons van de hypocotyl laten zien onder hoge temperatuur, is deze afwezig in zaailingen die gemuteerd zijn in *PIF4*. Voor de screening is gebruik gemaakt van hypocotyl strekking in jonge zaailingen vanwege het kleine formaat van de planten en de mogelijkheid om daarom veel stoffen in parallel te kunnen testen. In totaal zijn 8360 stoffen getest en na onafhankelijke bevestiging van de effecten zijn negen stoffen geselecteerd voor verdere experimenten. Dit is exclusief kandidaatstoffen die fenotypes veroorzaken die overeenkomen met auxine behandeling, zoals agravitropische groei en korte wortels. Dit om de kans te vergroten dat er onbekende onderdelen van het signaleringsnetwerk zouden worden gevonden. Dosis-response experimenten lieten zien dat één van de stoffen, hierna 'Heatin' genoemd, een sterk en reproduceerbaar effect heeft op de hypocotyl elongatie. In de rest van dit proefschrift zijn experimenten beschreven met als doel het ophelderen van het moleculaire werkingsmechanisme van Heatin.

In **hoofdstuk 3** wordt de moleculaire werking van Heatin verder uitgediept en wordt er onderzocht waar in de bekende signaleringsmechanismes Heatin ingrijpt. Heatin bleek in zaailingen exclusief de hypocotyl te beïnvloeden, en niet de wortelgroei, agravitropisme, of het ombuigen van de cotylen (epinastie). Dit in tegenstelling tot Picloram, een synthetisch auxine. Daarnaast stimuleerde Heatin ook in volwassen rozetten thermomorfogenese. Een SAR-analyse is uitgevoerd waaruit door het testen van in totaal 24 stoffen die in meerdere of mindere mate op Heatin lijken, werd geconcludeerd dat 1-aminomethyl-naphthalen-2-ol de minimaal actieve component is van de Heatin structuur. De resultaten van de SAR-analyse komen sterk overeen met resultaten van onafhankelijke reeds gepubliceerde werk van Dai *et al.* (2008), waarin de auxine activiteit van het molecuul Sirtinol wordt onderzocht. Uit een vergelijking tussen Heatin en Sirtinol blijkt dat Sirtinol ook hypocotyl elongatie kan induceren en dat mutanten die eerder zijn omschreven als Sirtinol-resistent ook Heatin-resistent zijn. Het voorgestelde

werkingsmechanisme voor Sirtinol is dat het *in situ* wordt omgezet tot een auxine-achtige stof. Deze auxine analoog activeert auxine signalering en veroorzaakt zo de geobserveerde fenotypes. Om te testen of Heatin ook als auxine werkt zijn auxine receptor mutanten getest, die ook resistent bleken te zijn tegen Heatin. Echter, Heatin heeft geen invloed op de activiteit van de *DR5* promoter, een veelgebruikte auxine reporter. Dit onderscheidt Heatin van bekende auxine analogen zoals Picloram of Sirtinol.

De link met auxine wordt verder versterkt in **Hoofdstuk 4** door de transscriptoom analyse. Uit deze evaluatie, waarin de expressie van alle genen in de plant tegelijk is gemeten, blijkt dat Heatin in vergelijking met auxine slecht minimale transcriptionele veranderingen teweegbrengt, maar dat de genen die wel differentieel tot expressie komen voor een groot gedeelte overeenkomen met genen die door auxine worden gereguleerd. Door te kijken naar de overlap tussen de beperkte transcriptionele regulatie van Heatin, en de zeer uitgebreide regulatie door temperatuur, zijn genen gevonden die waarschijnlijk een rol spelen bij het hypocotyl elongatie gedeelte van de temperatuur response. In tegenstelling tot transcriptionele regulatie, blijkt regulatie op het niveau van het proteoom (alle eiwitten) en het metaboloom (alle producten van de stofwisseling) weinig overeenstemming te vertonen met temperatuur regulatie.

Om eiwitten te identificeren die een directe interactie aangaan met Heatin zijn in **Hoofdstuk 5** door middel van een zogenaamde 'pulldown' Heatin interacterende eiwitten geisoleerd en geidentificeerd. Om dit mogelijk te maken is een aangepaste versie van Heatin chemisch gesynthetiseerd en aan magnetische beads geklikt; de zogenaamde Heatin-probe. Op basis van de SAR-analyse uit hoofdstuk 3 is bekend welk gedeelte van de Heatin structuur verantwoordelijk is voor de activiteit en derhalve niet veranderd kan worden bij de synthese van de Heatin-probe. In de SAR-analyse kwam ook een analoge stof naar voren die dezelfde activiteit als Heatin liet zien, maar chemische stabieler was. Op basis van deze Heatin analoog is de Heatin-probe ontworpen en gesynthetiseerd. Door de eiwitten op de beads (die dus waarschijnlijk met Heatin interacteren) te vergelijken met de eiwitten in de fractie niet gebonden eiwitten konden Heatin-interacterende eiwitten worden geïdentificeerd. Omdat chemische stoffen mogelijk meerdere eiwitten met overlappende functies kunnen beïnvloeden, is binnen de 162 gevonden eiwitten vervolgens gezocht naar eiwitten met gelijke structuur (eiwitfamilies) die als gehele familie waarschijnlijk daarom een target van Heatin zijn.

Na uitsluiting van bekende vals positieve eiwitfamilies blijkt dat Heatin waarschijnlijk de gehele NIT1-subfamilie van Nitrilase eiwitten beïnvloed. Om dit te bevestigen zijn mutanten die verstoord zijn in de Nitrilase functie getest op gevoeligheid voor Heatin. Hieruit bleek dat deze mutanten een verminderde gevoeligheid voor Heatin hebben. Daarnaast is de temperatuur afhankelijke hypocotyl elongatie ook verminderd in sommige van deze mutanten. Uit verdere experimenten blijkt Heatin *in vitro* Nitrilase functioneren te remmen. Omdat de NIT1-subfamilie mogelijk functioneert in auxine biosynthese, en in voorgaande hoofdstukken is vastgesteld dat Heatin een duidelijke

link met auxine vertoond, is onderzocht of Heatin de biosynthese van auxine, beïnvloed. Niveaus van actief auxine en enkele precursors is gemeten onder invloed van Heatin, zowel in wildtype zaailingen als ook in zaailingen verstoord in Nitrilase functie. Hieruit bleek dat Heatin een sterk effect heeft op de auxine biosynthese, op een manier die afhankelijk is van NIT1-subfamilie functie. Onder andere blijkt Heatin te leiden tot een toename van auxine niveaus in de plant, wat waarschijnlijk tot hypocotyl elongatie leidt.

In **Hoofdstuk 6** wordt het effect Heatin onderzocht in andere accessies van Arabidopsis. In een zogenaamde GWAS-screening wordt natuurlijke variatie in de response op Heatin tussen verschillende accessies van Arabidopsis gebruikt om genetische regio's te ontdekken die betrokken zijn bij de Heatin response. Hieruit blijkt een locus op chromosoom 1 te liggen wat bijdraagt aan de Heatin response. Daarnaast blijkt controle over thermomorphogenese, als ook response op Picloram te worden beïnvloed door hetzelfde locus. Om mogelijke praktijk toepassing van Heatin te onderzoeken is naast het vaststellen van de verschillen in responsen in varianten van Arabidopsis, ook onderzocht of Heatin actief is buiten de soortsgrenzen, door te testen of Heatin hypocotyl elongatie veroorzaakt in enkele commerciële tuinbouw gewassen. Hieruit blijkt dat Heatin waarschijnlijk uitluitend actief is in de *Brassicaceae*, een familie planten waar naast Arabidopsis ook vele koolsoorten binnen vallen.

In conclusie wordt een werkingsmechanisme voorgesteld waarbij Heatin-behandeling leidt tot hypocotyl elongatie door een directe inhiberende interactie met Nitrilase eiwitten. Deze inhibitie veranderd auxine-biosynthese, wat leidt tot een toename in auxine niveaus en, daaruit volgend, een toename in strekkingsgroei en thermomorfogenese. Deze hypothese wordt ondersteund door het feit dat de Nitrilase familie exclusief aanwezig is in de Brassicaceae familie en dat Heatin exclusief actief lijkt te zijn in deze familie. Een alternatieve verklaring voor de activiteit van Heatin is dat het, als Sirtinol, wordt gemetaboliseerd tot een actief auxine.

Het in dit proefschrift uitgevoerde onderzoek naar de werking van Heatin heeft een functie voor Nitrilase eiwitten in hypocotyl elongatie blootgelegd. Ook lijken de Nitrilase eiwitten een rol te spelen bij thermomorfogenese. Verder onderzoek is nodig om de precieze rol van de Nitrilases binnen de thermomorfogenese op te helderen.

Curriculum vitae

Lennard Casper van der Woude was born in Rotterdam on December 19, 1988. In 2007 he received his VWO – Gymnasium diploma from the Marnix Gymnasium in Rotterdam. In the same year, he started his BSc Biology studies at Utrecht University in Utrecht, The Netherlands. As a final project for his BSc, Lennard wrote a thesis under the supervision of Dr. Marcel Proveniers titled: 'Thermoresponsen en sensoren in planten'. In 2011, Lennard received his BSc diploma and subsequently followed the MSc program Molecular Cellular Life Sciences at Utrecht University. During this program he performed two internships. The first was performed at the Molecular Plant Physiology group at Utrecht University under the supervision of Dr. Marcel Proveniers. During this 9-month internship, Lennard worked on a project titled: 'Control of meristem competence by environmental signals: defining a window of sensitivity to changing ambient temperature and day length'. The second, 6-month, internship was performed at the Umeå Plant Science Centre (UPSC) in Umeå, Sweden under the supervision of Dr. Martijn van Zanten and Dr. Stéphanie Robert. This project was titled 'Characterization of chemical compounds that affect the high temperature acclimation syndrome in *Arabidopsis thaliana*'. The findings of this project were used to write a PhD proposal as a Master thesis, which was funded as part of the EPS Graduate school starting materials program of NWO. With this personal grant, Lennard started working as a graduate student in May 2014, in the Molecular Plant Physiology group under the supervision of Dr. Martijn van Zanten and Prof. Dr. Sjef Smeekens on a project investigating the molecular mechanism by which one of the chemical compounds identified at the UPSC; called Heatin, stimulates thermomorphogenesis. The findings of this project are described in this thesis.

List of publications

Celine Tasset, Avilash Singh Yadav, Rupali Singh, **Lennard van der Woude**, Maxim Nekrasov, David Tremethick, Martijn van Zanten, Sureshkumar Balasubramanian. 2018. **POWERDRESS-mediated histone deacetylation is essential for thermomorphogenesis in Arabidopsis thaliana**. *PLOS Genetics* **14**, e1007280.

Lennard van der Woude, Giorgio Perrella, L. Basten Snoek, Mark van Hoogdalem, Ondřej Novák, Marcel van Verk, Heleen N. van Kooten, Lennert E. Zorn, Rolf Tonckens, Joram A. Dongus, Evelien A. Stouten, Marcel C.G. Proveniers, Wouter Kohlen, Sureshkumar Balasubramanian, Karin Ljung, Alexander R. van der Krol, Sjef Smeekens, Eirini Kaiserli, Martijn van Zanten. **Histone Deacetylase 9 defines a warm temperature acclimation pathway.** (Submitted)

Lennard van der Woude *et al*., **Studying thermomorphogenesis using the bio-active small molecule Heatin.** (In preparation)

Dankwoord

Mijn thesis is af, en daar ben ik best wel blij mee! Ik heb dit echter niet alleen gedaan. Zonder de hulp, ondersteuning en bijdrages in wat voor vorm dan ook van de volgende personen zou het schrijven van dit boekje niet gelukt zijn.

Allereerst, Martijn, ik beschouw mezelf erg gelukkig dat ik jou als co-promotor en begeleider tijdens mijn PhD heb gehad! Ik vond het erg stimulerend en tegelijkertijd relaxt om met jou samen te werken, en heb mede dankzij jouw stimulans heel erg veel geleerd tijdens mijn PhD. Van de praktische hulp in het lab tot je supersnelle feedback op mijn thesis manuscript, ik denk dat het moeilijk is jouw rol in het succes van mijn PhD te overschatten. Mega Bedankt!

Sjef, ik ben dankbaar voor jouw ondersteuning en support tijdens mijn PhD als mijn promotor. Met goed advies, al dan niet aan de koffietafel, wist je me te motiveren en te helpen het maximale uit het onderzoek en de data te halen.

Ik wil graag mijn leescommissie, Richard Immink, Sander van der Krol, Ronald Pierik, Ive de Smet en Kirsten ten Tusscher bedanken voor de tijd en energie die jullie hebben geïnvesteerd in het beoordelen van mijn thesis.

Veel dank voor alle betrokkenen bij alle wetenschappelijke samenwerkingen: Twan en Roland voor de Hotel projecten, Nathaniel, Kamal en Grusson voor de onmisbare hulp bij het chemische gedeelte van dit werk. Wouter Kohlen, Ondrej Novak, Karin Ljung and Marcel van Verk all the other experiments. Suzanne Bulder en Corine de Groot van Bejo, bedankt voor de prettige samenwerking en gastvrijheid en krokettenlunch in Warmenhuizen.

Thanks also to the groups that hosted me as guest in their labs outside of Utrecht: In Oxford, thanks to Renier, Judith and Daniel for the great help, which ensured the project was a success in the end. Also, thanks to the rest of the group for making me feel welcome, and ensuring I also had some fun. In Bochum, Thanks to Markus Piotrowski for hosting me in an excellent way, and the great scientific input while being there.

Iedereen bij MPF verdient een hele grote Bedankt! Met zijn allen vormen jullie een gezellige diverse groep, waar een ontspannende en stimulerende sfeer heerst, en waar ik voor plus-minus 7 jaar met veel plezier heb rondgelopen. Ga vooral door met de foodcourt Friday, kerstdiners en het taartenoverschot, en probeer dat paaseitjes record terug te krijgen! Ik begin op mijn kamer: Savani, onze PhD projecten liepen enigszins parallel, ik vond het super leuk om het hele traject zo met jou te delen. Tussen de onzin gesprekken tijdens koffie/thee pauzes en het mega drukke practicum geven was het altijd gezellig! Succes nog even met het afronden van je thesis en daarna je defence. Komt ongetwijfeld helemaal goed. Evelien, Ik heb ook intens genoten van jou als kamergenoot. Het was super handig om jou zo dichtbij te hebben, ik heb veel van je geleerd (ook van jouw uitleg aan anderen die het kantoor in kwamen..), en genoten van de gezelligheid op kantoor en in het lab. Jolanda, ook van jou heb ik veel geleerd. Bedankt voor het nemen

van de tijd om me te helpen met alle willekeurige dingen die ik aan je kwam vragen, en je kritische, opbouwende inzichten tijdens werkbesprekingen. En natuurlijk het gezelschap tijdens alle lunches en koffiepauzes! Marcel, door het schrijven van mijn bachelor thesis onder jouw begeleiding ben ik initieel geïnteresseerd geraakt in de moleculaire fysiologie van planten. Alle uitgebreide gesprekken tijdens pauzes (of daarna) hebben veel bijgedragen aan het actief houden van mijn fascinatie voor planten. Ook heb ik je input tijdens werkbesprekingen e.d. erg gewaardeerd, en alle over-de-top verhalen tijdens de pauzes! Sjors, ik heb genoten van jouw surrealistische, kritische, overmatige positieve instelling! Ik denk dat je met die instelling je PhD zeker tot een prachtig einde gaat brengen. Paul, natuurlijk super je collega PhD-er te zijn. Ik vond het een eer om je Paranimf te mogen zijn! Goed om een beetje te weten wat me te wachten staat bij mijn promotie. En nu nog meer eer dat je ook bij mij Paranimf wilt zijn. Daarna moeten we weer eens avocado's gaan enten, denk je niet? Laura, bedankt voor je hulp met alle random code/R/RNAseq/etc vragen die ik je kwam vragen. Veel succes met de rest van je PhD project. Henriette, bedankt voor je kritische input tijdens werkbesprekingen en de stimulatie om in de RNA-seq data te duiken! Veel plezier met zo veel mogelijk zeilen. Shahram, it was nice to work with you for a little while. Good luck on the rest of your project! Lazero an Badraldin, Thanks a lot for the discussions about science and life. Former PhD students at MPF: Jeroen, Nicole, Monika, Jeba, Wouter, Julia, and Post-doc: Magdalena, thanks a lot for all the fun and advice.

Thanks to all students that have done internships in the MPF group! Too many to name all, but a special mention for those who worked on the thermomorphogenesis project: Adrian, Joram, Heleen, Dorrit, Machiel, Bram, Kim, Rebecca, Molly, Koen and the other students that I am probably possibly forgetting. An even more special thanks to the student who I got to supervise: Colin, Jan en Lennert! Colin, je hebt superhard gewerkt aan de GWAS en zo een grote bijdrage geleverd aan mijn thesis. Er zijn weinig mensen die kunnen claimen dat ze 40(?) keer de hoogte van het Kruyt gebouw hebben gemeten aan hypocotylen tijdens hun stage! Jan, bedankt voor het werk dat je verzet hebt met de verschillende experimenten tijdens je stage. Ik heb genoten van het werken met jou, en die band die je steeds opzette die op led zeppelin lijkt. En natuurlijk de student met bijna dezelfde naam en kapsel als ik, Lennert! Ik vond het super leuk om je als student te begeleiden! Bedankt voor je inzet en succes met het vinden van werk en tot ziens!

Naast werk moet een persoon ook ontspannen, en dan liever niet alleen! Ik wil iedereen bedanken die me daarbij heeft geholpen. Niek, Ruud, Ruben, Sjoerd, Otters, Sandor, Steven, Joshua, Karel, Edwin, Ik ben blij dat ik jullie mijn vrienden mag noemen en mede daardoor een gelukkig mens. Jasper, speciale vermelding voor de Paranimf. Super bedankt!!

Mijn Familie, ik ben dankbaar voor jullie steun en liefde, begrip en interesse. Dat betekent erg veel voor mij. Ma belle-famille, je veux vous remercier de m'accueillir dans la famille, et de me donner la motivation d'apprendre le Français, à coté de ma thèse !

Het belangrijkste als laatste. Adeline, zonder jouw steun en liefde was er waarschijnlijk geen boekje geweest. Je was samen met mij van het begin tot het einde, en je hebt me ook tijdens de stressvolle periodes weten te motiveren en te ontspannen. Ik prijs mezelf een gelukkig persoon, om nu met zijn drieën verder te gaan.

En die derde is Lizon. Jij draaide alles op het laatste nog eens flink op de kop. Maar je bracht ook een flinke dosis motivatie en een nog flinkere dosis relativering met je mee. Om in je eigen woorden te spreken: haaaa giiiii goooee ggglllrrr grgrgr.